

2017

# Molecular Recognition Profiles of Molecular Cocrystals

Ian C. Tinsley

*Eastern Illinois University*


This research is a product of the graduate program in [Chemistry](#) at Eastern Illinois University. [Find out more](#) about the program.

---

## Recommended Citation

Tinsley, Ian C., "Molecular Recognition Profiles of Molecular Cocrystals" (2017). *Masters Theses*. 2745.  
<https://thekeep.eiu.edu/theses/2745>

This is brought to you for free and open access by the Student Theses & Publications at The Keep. It has been accepted for inclusion in Masters Theses by an authorized administrator of The Keep. For more information, please contact [tabruns@eiu.edu](mailto:tabruns@eiu.edu).

  
**The Graduate School**  
EASTERN ILLINOIS UNIVERSITY™  
**Thesis Maintenance and Reproduction Certificate**

FOR: Graduate Candidates Completing Theses in Partial Fulfillment of the Degree  
Graduate Faculty Advisors Directing the Theses

RE: Preservation, Reproduction, and Distribution of Thesis Research

---

Preserving, reproducing, and distributing thesis research is an important part of Booth Library's responsibility to provide access to scholarship. In order to further this goal, Booth Library makes all graduate theses completed as part of a degree program at Eastern Illinois University available for personal study, research, and other not-for-profit educational purposes. Under 17 U.S.C. § 108, the library may reproduce and distribute a copy without infringing on copyright; however, professional courtesy dictates that permission be requested from the author before doing so.

Your signatures affirm the following:

- The graduate candidate is the author of this thesis.
- The graduate candidate retains the copyright and intellectual property rights associated with the original research, creative activity, and intellectual or artistic content of the thesis.
- The graduate candidate certifies her/his compliance with federal copyright law (Title 17 of the U. S. Code) and her/his right to authorize reproduction and distribution of all copyrighted materials included in this thesis.
- The graduate candidate in consultation with the faculty advisor grants Booth Library the non-exclusive, perpetual right to make copies of the thesis freely and publicly available without restriction, by means of any current or successive technology, including by not limited to photocopying, microfilm, digitization, or internet.
- The graduate candidate acknowledges that by depositing her/his thesis with Booth Library, her/his work is available for viewing by the public and may be borrowed through the library's circulation and interlibrary loan departments, or accessed electronically.
- The graduate candidate waives the confidentiality provisions of the Family Educational Rights and Privacy Act (FERPA) (20 U. S. C. § 1232g; 34 CFR Part 99) with respect to the contents of the thesis and with respect to information concerning authorship of the thesis, including name and status as a student at Eastern Illinois University.

I have conferred with my graduate faculty advisor. My signature below indicates that I have read and agree with the above statements, and hereby give my permission to allow Booth Library to reproduce and distribute my thesis. My adviser's signature indicates concurrence to reproduce and distribute the thesis.

Graduate Candidate Signature \_\_\_\_\_

Faculty Adviser Signature \_\_\_\_\_

Printed Name \_\_\_\_\_

Printed Name \_\_\_\_\_

Chemistry

6-2-2017

Graduate Degree Program

Date

*Please submit in duplicate.*





## Abstract

The manner in which molecules recognize each other holds critical importance to nearly every area of science. This significance stems from the key underpinning of molecular assembly to our most basic understanding of chemical processes. Whether these interactions relate to small-molecule catalytic transformations or complex physiological processes, the structural features responsible for molecular association play into the well-known adage that *form follows function* where material property arises from the collective structural features of the molecular components. Because the *form* of chemical systems is derived from a complex blend of covalent and non-bonded contacts, codifying each contributor has become essential for recognizing the functions and potential applications of materials. While considerable progress in this area has been realized by isolating and identifying molecular contacts and the structural details of their conditional exceptions, insight to the entire landscape of molecular associations remains an ongoing effort. This thesis explores the molecular recognition process from two uniquely different perspectives. The first is from cocrystallizing a variety of benzoic acids with the pharmaceutical agent sulfamethazine and the second area investigates how molecular shape controls quasiracemate formation.

Sulfamethazine is an active pharmaceutical ingredient (API) with a strong ability to form hydrogen bonds due to its donor and acceptor groups. The chemical structure of this API allows it to exist in more than one tautomer. The cocrystallization of this molecule with a coformer has the ability to influence which tautomer is present in the crystal structure. This thesis provides data that defines the relationship of coformer acidity to tautomer formation in sulfamethazine. A

total of eighteen cocrystals of sulfamethazine with benzoic acid derivatives were synthesized and the tautomeric form to coformer acidity was analyzed.

The cocrystallization of APIs is a classic example of molecular recognition between two or more compounds. Studies that seek to design these materials and others often focus on strong non-bonded contacts (e.g. hydrogen bonds) as a means to generate desired supramolecular architectures. Less well studied, but no less important to the overall molecular recognition process, are chemical features that produce less manageable motifs via ill-defined or weak contacts. Molecular shape is one such feature. This thesis exploits quasiracemates – *i.e.*, near racemic materials – to probe the role molecular topology plays in the recognition process. A diverse set of diarylamide quasienantiomers that differ incrementally in substituent size and molecular framework has been prepared. Mixing of pairs of these quasienantiomers in the melt using video-assisted host stage microscopy provided a robust diagnostic tool for detecting new quasiracemic crystalline phases. Data retrieved using this virtual melting-point phase method not only draws considerable attention to the role of topological features to supramolecular assemblies, but also the structural boundaries of these co-crystalline systems. This investigation synthetically explores the broad structure space towards the identification of new isostructural building blocks and highlights important molecular relationships responsible for molecular recognition that may serve in the design of new functional materials.

## Acknowledgement

I would like to express my thanks to Dr. Kraig Wheeler for his guidance and support throughout my career at Eastern Illinois University. Dr. Wheeler had an infectious joy and adoration for research and the sciences which rubbed off on everyone around him. He had constant patience with students and was always available in a time of need. Dr. Wheeler was extremely perceptive to detail and has engraved its importance on me as a student and a researcher. I cannot thank him enough for his impact on my future.

I would like to thank my committee members, Drs. Mark McGuire, Radu Semeniuc, Daniel Sheeran and the Chemistry Departmental Graduate Coordinator Dr. Barbara Lawrence for their support and constant willingness to help me when needed. The office door to all these faculty members was always open and each were easily approachable. I must thank the Graduate School of Eastern Illinois University for allowing me the opportunity to continue my education. It provided me with countless memories that I will cherish forever. The Chemistry Department at Eastern Illinois University provided me the educational support and research experience in order to advance to Ph. D. program.

In addition, thank you to all the faculty members of the Chemistry Department for their academic contributions towards my degree. I thank the members of the Wheeler research group both past and present: Mikayla Grant, Emily Pinter, Jacqueline Spaniol, and Benjamin Wagner for their constant support and memories. I also wish to thank the National Science Foundation (DMR 1505717) for partial support of my thesis work. Last but not least; I would like to thank my family for their continuous support and motivation throughout my educational journey.

## TABLE OF CONTENTS

<u>ABSTRACT</u>	<u>I</u>
<u>ACKNOWLEDGEMENT</u>	<u>III</u>
<u>LIST OF FIGURES</u>	<u>VI</u>
<u>LIST OF TABLES</u>	<u>XIV</u>
<u>LIST OF ABBREVIATIONS</u>	<u>XV</u>
<u>CHAPTER 1: INTRODUCTION</u>	<u>1</u>
1.1 MOLECULAR RECOGNITION	1
1.2 IMPORTANCE OF MOLECULAR CHIRALITY	4
1.2.1 RACEMIC AND QUASIRACEMIC MIXTURES	9
1.3 ASSESSMENT OF MOLECULAR RECOGNITION AND NONCOVALENT INTERACTIONS	10
1.3.1 CRYSTAL STRUCTURES AND CRYSTAL FORMS	11
1.3.2 HOT-STAGE THERMOMICROSCOPY	13
1.4 THESIS OVERVIEW	14
1.4.1 SULFAMETHAZINE AS AN ACTIVE PHARMACEUTICAL INGREDIENT	15
1.4.2 SULFAMETHAZINE AND COCRYSTALLIZATION WITH SUBSTITUTED BENZOIC ACIDS	16
1.4.3 MOLECULAR RECOGNITION BOUNDARIES OF DIARYLAMIDE QUASIRACEMATES	17
1.5 REFERENCES	23
<u>CHAPTER 2: EXPERIMENTAL</u>	<u>27</u>
2.1 PREPARATION OF SULFAMETHAZINE COCRYSTALS	27
2.2 SYNTHESIS OF ( <i>S</i> )- AND ( <i>R</i> )- <i>N</i> -(2-SUBSTITUTEDBENZOYL)METHYLBENZYLAMINE	28
2.3 HOT-STAGE MICROSCOPY	35
2.4 X-RAY CRYSTALLOGRAPHY – POWDER DIFFRACTION	36
2.5 X-RAY CRYSTALLOGRAPHY – SINGLE CRYSTAL DIFFRACTION	36
2.6 <sup>1</sup> H NMR OVERLAYS	37
2.7 REFERENCES	38
<u>CHAPTER 3: SUPRAMOLECULAR TENDENCIES OF SULFAMETHAZINE COCRYSTALS</u>	<u>39</u>
3.1 SULFA DRUG DEVELOPMENT	39
3.2 SULFAMETHAZINE STRUCTURE AND TAUTOMERIZATION	44
3.3 STRUCTURAL TENDENCIES OF SULFAMETHAZINE AND BENZOIC ACIDS	46
3.4 REFERENCES	60

CHAPTER 4: MOLECULAR RECOGNITION BOUNDARIES OF DIARYLAMIDE  
QUASIRACEMATES 62

---

4.1	OVERVIEW OF MOLECULAR RECOGNITION	62
4.2	CRYSTAL PACKING OF RACEMATES AND QUASIRACEMATES	63
4.3	SUBSTITUENT SELECTION AND PROOF OF CONCEPT	65
4.4	ANALYZING THE MELT WITH POWDER X-RAY DIFFRACTION	68
4.5	TOPOLOGICAL DIFFERENCES OF SUBSTITUENTS	69
4.6	ANALYZING THE MELT WITH NUCLEAR MAGNETIC RESONANCE	73
4.7	INTRAMOLECULAR HYDROGEN BONDING OF SUBSTITUENTS	76
4.8	IMPORTANCE OF QUASIRACEMATE FRAMEWORK AND SUBSTITUENT POSITION	81
4.9	MOLECULAR RECOGNITION PROFILES OF SAME HANDED QUASISANTIOMERS	85
4.10	CONCLUSION	86
4.11	REFERENCES	89

SUPPLEMENTAL INFORMATION 92

---

S.1	COCRYSTALS OF SULFAMETHAZINE	93
S.2	HOT STAGE THERMOMICROSCOPY	209
S.3	X-RAY CRYSTALLOGRAPHY – POWDER DIFFRACTION	234
S.4	X-RAY CRYSTALLOGRAPHY – SINGLE-CRYSTAL DIFFRACTION	238
S.5	<sup>1</sup> H NMR OVERLAYS	244
S.6	FUNCTIONAL GROUP AND CHEMICAL FRAMEWORK VOLUME AND SURFACE AREA COMPARISONS	246
S.7	REFERENCES	248

## List of Figures

Figure 1.1: Hydrogen Bonding of Nitrogenous Bases.	3
Figure 1.2: Molecular Recognition in Deoxyribonucleic Acid.	3
Figure 1.3: Enantiomers of Thalidomide.	5
Figure 1.4: Stereoisomers of Labetalol.	7
Figure 1.5: Stereoisomers of Ibuprofen.	8
Figure 1.6: Types of Multicomponent Crystals.	11
Figure 1.7: Forms of Sulfamethazine	15
Figure 1.8: Substituted Benzoic Acids Utilized in Cocrystallization.	17
Figure 1.9: Quasiracemic Structure of N-(2-Chloro)/ N-2-(Bromobenzoyl)methylbenzylamine.	19
Figure 1.10: Diarylamide Molecular Frameworks Used in this Thesis Study.	19
Figure 1.11: Functional Group Volumes and Surface Areas.	20
Figure 1.12: Kofler Contact Method.	21
Figure 3.1: Domagk's Initial Sulfonamide Compounds for Antimicrobial Activity Testing.	40
Figure 3.2: Metabolic Breakdown of Protonsil Red to Sulfanilamide.	41
Figure 3.3: Molecular Structure of Folic Acid.	42
Figure 3.4: Molecular Structure of <i>p</i> -Aminobenzoic Acid and Sulfanilamide.	42
Figure 3.5: Amidine Tautomer of Sulfamethazine.	43
Figure 3.6: Forms of Sulfamethazine.	44
Figure 3.7: Substituted Benzoic Acid Cofomers.	46

Figure 3.8: $R_2^2(8)$ Hydrogen Bonding Ring Pattern For Carboxylic Acids Described by Etter.	46
Figure 3.9: Crystal Structure of the Cocrystal of Sulfamethazine and <i>p</i> -Hydroxybenzoic Acid Showing Thermal Parameters (50% Thermal Ellipsoids) and Hydrogen bonding.	48
Figure 3.10: Crystal Structure of the Cocrystal of Sulfamethazine and <i>p</i> -Hydroxybenzoic Acid Showing Thermal Parameters (50% Thermal Ellipsoids) and Hydrogen Bonding Scheme.	48
Figure 3.11: Crystal Structure of the Cocrystal of Sulfamethazine and <i>p</i> -Hydroxybenzoic Acid Showing Thermal Parameters (50% Thermal Ellipsoids), $\pi$ - $\pi$ Stacking, and Hydrogen Bond Scheme.	49
Figure 3.12: Crystal Structure of the Cocrystal of Sulfamethazine and <i>p</i> -Methoxybenzoic Acid Showing Thermal Parameters (50% Thermal Ellipsoids) and Hydrogen bonding.	51
Figure 3.13: Crystal Structure of the Cocrystal of Sulfamethazine and <i>p</i> -Methoxybenzoic Acid Showing Thermal Parameters (50% Thermal Ellipsoids) and Supramolecular Assembly.	51
Figure 3.14: Crystal Structure of Sulfamethazine and Benzoic Acid Showing Thermal Parameters (50% ellipsoids) and Labeling Scheme.	54
Figure 3.15: Plot Showing the Relationship between Benzoic Acid Strength and N3-O2 Hydrogen Bonding Distance.	54
Figure 3.16: Plot Showing Relationship between Benzoic Acid Strength and N2-O1 Hydrogen Bonding Distance.	55



Figure 3.17: Plot Showing Relationship between Benzoic Acid Strength and C14-N2 Bonding Distance.	55
Figure 3.18: Plot Showing Relationship between Benzoic Acid Strength and C14-N3 Bonding Distance.	56
Figure 3.19: Crystal Structure of the Cocrystal of Sulfamethazine and <i>p</i> -Dimethylaminobenzoic Acid Showing Thermal Parameters (50% Thermal Ellipsoids).	56
Figure 3.20: Crystal Structure of the Cocrystal of Sulfamethazine and <i>p</i> -Dimethylaminobenzoic Acid Showing Thermal Parameters (50% Thermal Ellipsoids) and $\pi$ - $\pi$ Stacking.	57
Figure 4.1: Chiral Diarylamides Used in the Present Study.	63
Figure 4.2: Crystal Packing Relationship between Racemic and Quasiracemic Compounds.	63
Figure 4.3: Melting Point Phase Diagrams of Idealized Racemic and Quasiracemic Mixtures.	65
Figure 4.4: Hot Stage Polarized Light Microscopy Using the A) ( <i>S</i> )-Br (left) and ( <i>R</i> )-Br (right) B) ( <i>S</i> )-Cl and ( <i>R</i> )-Br C) ( <i>S</i> )-I and ( <i>R</i> )-Br Pairs Showing the Emergence of New Racemic and Quasiracemic Crystalline Phases.	66
Figure 4.5: Powder XRD of ( <i>S</i> )-Cl/( <i>R</i> )-Br Quasiracemate and Related Components.	68
Figure 4.6: Hot Stage Microscopy Results from Combining Diarylamide A) Quasienantiomers B) Molecular Pairs with the Same Chirality [e.g. ( <i>R</i> )-X and ( <i>R</i> )-X'].	70
Figure 4.7: <sup>1</sup> H NMR Overlays of the <i>S</i> -CH <sub>3</sub> / <i>R</i> -CF <sub>3</sub> Quasiracemate System.	73

Figure 4.8: Crystal Structure of ( <i>S</i> )- <i>N</i> -(2-methoxybenzoyl)methylbenzylamine Showing Thermal Ellipsoids (50% Probability) and Intramolecular N- H···O Hydrogen Bonding.	75
Figure 4.9: Overlay of 2-Substituted Diarylamides Showing the Conformational Difference of the Methoxy Framework (Pink).	75
Figure 4.10: Search Criteria for Methoxy Group in CSD and Resulting Bonding Distances between “O” of Methoxy Functional Group and “N” of Amide Functional Group.	77
Figure 4.11: Graphical Search Criteria of the CDS for 2-hydroxyarylamides.	77
Figure 4.12: A CDS Search Showing O···N Intramolecular Bond Distances for 2-hydroxy Arylamides.	79
Figure 4.13: Results of CSD Search Showing Correlation of O···O Distance to O-H···O=C Hydrogen Bonding Angle.	79
Figure 4.14: Two Orientations for the Hydroxyl Group Observed from a CSD Search.	80
Figure 4.15: Substitution Patterns and Chemical Frameworks of Previously Investigated Quasiracemic Systems.	81
Figure 4.16: Chemical Frameworks Showing meta and para Substituted Diarylamides.	81
Figure 4.17: Hot Stage Polarized Light Microscopy Using the A) ( <i>S</i> )-2-Cl (left) and ( <i>R</i> )-3-Cl (right) B) ( <i>R</i> )-4-Cl and ( <i>S</i> )-3-Cl C) ( <i>S</i> )-2-Cl and ( <i>R</i> )-4-Cl Pairs.	82

Figure 4.18: Hot Stage Polarized Light Microscopy Using the A) ( <i>R</i> )-2-Br (left) and ( <i>S</i> )-3-Cl (right) B) ( <i>S</i> )-3-Cl and ( <i>R</i> )-4-Br C) ( <i>S</i> )-4-Cl and ( <i>S</i> )-2-Br Pairs.	83
Figure 4.19: Hot stage polarized light microscopy using the A) ( <i>R</i> )-Cl (left) and ( <i>R</i> )-Br (right) B) ( <i>R</i> )-I/( <i>R</i> )-Br Pairs and Showing the Characteristics of Solid Solution and Conglomerate Crystalline Phase Formation.	85
Figure S.1: Crystal Structure of the Cocrystal of Sulfamethazine and Benzoic Acid Showing Thermal Parameters (50% Thermal Ellipsoids) and Hydrogen Bonding.	93
Figure S.2: Crystal Structure of the Cocrystal of Sulfamethazine and <i>o</i> -Nitrobenzoic Acid Showing Thermal Parameters (50% Thermal Ellipsoids) and Hydrogen Bonding.	98
Figure S.3: Crystal Structure of the Cocrystal of Sulfamethazine and <i>m</i> -Nitrobenzoic Acid Showing Thermal Parameters (50% Thermal Ellipsoids) and Hydrogen Bonding.	103
Figure S.4: Crystal Structure of the Cocrystal of Sulfamethazine and <i>p</i> -Nitrobenzoic Acid Showing Thermal Parameters (50% Thermal Ellipsoids) and Hydrogen Bonding.	112
Figure S.5: Crystal Structure of the Cocrystal of Sulfamethazine and <i>o</i> -Methylbenzoic Acid Showing Thermal Parameters (50% Thermal Ellipsoids) and Hydrogen Bonding.	120

Figure S.6: Crystal Structure of the Cocrystal of Sulfamethazine and <i>m</i> -Methylbenzoic Acid Showing Thermal Parameters (50% Thermal Ellipsoids) and Hydrogen Bonding.	125
Figure S.7: Crystal Structure of the Cocrystal of Sulfamethazine and <i>p</i> -Methylbenzoic Acid Showing Thermal Parameters (50% Thermal Ellipsoids) and Hydrogen Bonding.	130
Figure S.8: Crystal Structure of the Cocrystal of Sulfamethazine and <i>o</i> - Fluorobenzoic Acid Showing Thermal Parameters (50% Thermal Ellipsoids) and Hydrogen Bonding.	135
Figure S.9: Crystal Structure of the Cocrystal of Sulfamethazine and <i>m</i> - Fluorobenzoic Acid Showing Thermal Parameters (50% Thermal Ellipsoids) and Hydrogen Bonding.	142
Figure S.10: Crystal Structure of the Cocrystal of Sulfamethazine and <i>p</i> -Fluorobenzoic Acid Showing Thermal Parameters (50% Thermal Ellipsoids) and Hydrogen Bonding.	148
Figure S.11: Crystal Structure of the Cocrystal of Sulfamethazine and <i>m</i> -Chlorobenzoic Acid Showing Thermal Parameters (50% Thermal Ellipsoids) and Hydrogen Bonding.	156
Figure S.12: Crystal Structure of the Cocrystal of Sulfamethazine and <i>p</i> -Chlorobenzoic Acid Showing Thermal Parameters (50% Thermal Ellipsoids) and Hydrogen Bonding.	161

Figure S.13: Crystal Structure of the Cocrystal of Sulfamethazine and <i>m</i> -Methoxybenzoic Acid Showing Thermal Parameters (50% Thermal Ellipsoids) and Hydrogen Bonding.	171
Figure S.14: Crystal Structure of the Cocrystal of Sulfamethazine and <i>p</i> -Methoxybenzoic Acid Showing Thermal Parameters (50% Thermal Ellipsoids) and Hydrogen Bonding.	179
Figure S.15: Crystal Structure of the Cocrystal of Sulfamethazine and <i>p</i> -Hydroxybenzoic Acid Showing Thermal Parameters (50% Thermal Ellipsoids) and Hydrogen Bonding.	185
Figure S.16: Crystal Structure of the Cocrystal of Sulfamethazine and <i>p</i> - Ethylbenzoic Acid Showing Thermal Parameters (50% Thermal Ellipsoids) and Hydrogen Bonding.	191
Figure S.17: Crystal Structure of the Cocrystal of Sulfamethazine and <i>p</i> -Dimethylaminobenzoic Acid Showing Thermal Parameters (50% Thermal Ellipsoids) and Hydrogen Bonding.	197
Figure S.18: Crystal Structure of the Cocrystal of Sulfamethazine and <i>o</i> -Acetyloxybenzoic Acid Showing Thermal Parameters (50% Thermal Ellipsoids) and Hydrogen Bonding.	203
Figure S.19: Powder XRD of ( <i>S</i> )-CH <sub>3</sub> / <i>(R)</i> -Br Quasiracemate and Related Components.	234
Figure S.20: Powder XRD of ( <i>S</i> )-Br/ <i>(R)</i> -CF <sub>3</sub> Quasiracemate and Related Components.	235

Figure S.21: Powder XRD of ( <i>S</i> )-Cl/( <i>R</i> )-NO <sub>2</sub> Quasiracemate and Related Components.	236
Figure S.22: Powder XRD of ( <i>S</i> )-Cl/( <i>R</i> )-I Quasiracemate and Related Components.	237
Figure S.23: Crystal Structure of <i>N</i> -(2-Fluoro)/ <i>N</i> -2-(benzoyl)methylbenzylamine Quasiracemate Showing Thermal Parameters (50% Thermal Ellipsoids).	238
Figure S.24: Crystal Structure of <i>N</i> -(2-Trifluoro)/ <i>N</i> -2-(Nitrobenzoyl)methylbenzylamine Quasiracemate Showing Thermal Parameters (50% Thermal Ellipsoids).	238
Figure S.25: Crystal Structure of <i>N</i> -(2-Trifluoro)/ <i>N</i> -2-(Methylbenzoyl)methylbenzylamine Quasiracemate Showing Thermal Parameters (50% Thermal Ellipsoids).	239
Figure S.26: Crystal Structure of <i>N</i> -(2-Nitro)/ <i>N</i> -2-(Bromobenzoyl)methylbenzylamine Quasiracemate Showing Thermal Parameters (50% Thermal Ellipsoids).	239
Figure S.27: Crystal Structure of <i>N</i> -(2-Trifluoro)/ <i>N</i> -2-(Iodobenzoyl)methylbenzylamine Quasiracemate Showing Thermal Parameters (50% Thermal Ellipsoids).	240
Figure S.28: <sup>1</sup> H NMR Overlays of the <i>S</i> -Cl/ <i>R</i> -Br Quasiracemate System.	244
Figure S.29: <sup>1</sup> H NMR Overlays of the <i>S</i> -NO <sub>2</sub> / <i>R</i> -CF <sub>3</sub> Quasiracemate System.	244
Figure S.30: <sup>1</sup> H NMR Overlays of the <i>S</i> -Br/ <i>R</i> -CF <sub>3</sub> Quasiracemate System.	245
Figure S.21: <sup>1</sup> H NMR Overlays of the <i>S</i> -Cl/ <i>R</i> -I Quasiracemate System.	245

## List of Tables

Table 3.1: Melting Point of Coformers and Sulfamethazine Cocrystals.	47
Table S1: Hot-Stage Images of Racemic and Quasiracemic Pairs.	209
Table S2: Hot Stage Images of Same Handed Homochiral Diarylamide Derivatives.	222
Table S3: Crystallographic Data for Diarylamide Quasiracemates.	241
Table S4: Hydrogen Bond Parameters for Diarylamide Quasiracemate Structures.	243
Table S5: Functional Group Volume Comparison.	246
Table S6: Diarylamide Molecular Volume Comparison.	246
Table S7: Functional Group Surface Area Comparison.	247
Table S8: Diarylamide Surface Area Comparison.	247

## List of Abbreviations

$F(000)$	The effective number of electrons in the crystal unit cell contributing to X-ray diffraction
$D_x$	Crystal density
$V$	Volume of a unit cell.
$Z$	Number of molecules per unit cell.
$R_{\text{int}}$	The residual electron density for symmetry-equivalent reflections used to calculate average diffraction intensities
$w$	Refinement weighting scheme as defined by : $w = q / [\sigma^2(F_0^2) + (aP)^2 + bP + d + e \sin \theta]$
$S$	The least-squares of goodness-of-fit parameter after the final cycle of least squares
$\Delta\rho$	The largest ratio of the final least-squares parameter shift divided by the final standard uncertainty
$R/R^2w$ (obs)	Residual Indices calculated for all observed reflections $>2\sigma$ .
$R/R^2w$ (all)	Residual Indices calculated for all reflections.
$\mu(\text{MoK}\alpha)$	The absorption coefficient as calculated from the atomic content of the cell, the density and the radiation wavelength.
NMR	Nuclear Magnetic Resonance
API	Active Pharmaceutical Ingredient
CSD	Cambridge Structural Database
$G_D^A(r)$	Graph Set Notation (G) Pattern Designation (R) Ring (C) Chain (A) Number of Acceptor Atoms (D) Number of Donor Atoms (r) Degree (Number of Atoms Involved in Pattern)



## Chapter 1: Introduction

### 1.1 Molecular Recognition

Molecular recognition can be best described as the ability of molecules to recognize one another that often results from specific molecular interaction features. A variety of materials in all fields of science undergo molecular association and transformations that involve molecular recognition. These types of interactions are commonly defined as non-covalent interactions involving two or more chemical components. Such close contacts may include hydrogen bonding,  $\pi$ - $\pi$  stacking, metal coordination, and halogen bonding. An understanding of molecular recognition is vital to the development of next generation materials that display advanced chemical functions. As stated by Feynman, *when we have some control of the arrangement of things on a molecular scale, we will get an enormously greater range of possible properties that substances can have.*<sup>1</sup> This idea directly extends to the field of *Crystal Engineering* where the focus is to organize and control the arrangement of molecules in crystalline materials for the optimization of a property to perform a specific function.<sup>2</sup> The activity of pharmaceutical materials relies on similar molecule...molecule interactions that in turn carries over to the molecular recognition process associated with active sites. Molecular recognition processes are far reaching and have played a role in such seminal science discoveries as the structure of deoxyribonucleic acid (DNA).<sup>3</sup> The structure of DNA contains several types of molecular associations such as hydrogen bonding and  $\pi$ - $\pi$  stacking. The nucleotide bases found in DNA effectively organize with complementary bases via hydrogen bonds. E. Chargaff is largely credited with determining the number of purines and pyrimidines in different species by examining and tabulating the

differences in concentration. Chargaff's investigations helped to establish the composition of DNA from equal numbers of purines and pyrimidines and also the association of adenine with thymine and guanine with cytosine. This discovery is now known as Chargaff's rule.<sup>4,5</sup> When analyzing the structures of purines and pyrimidines one can clearly see how recognition occurs through hydrogen bonding (Figure 1.1).<sup>6</sup> The chemical structures shown in Figure 1 demonstrate how adenine and thymine form two hydrogen bonds while guanine and cytosine form three hydrogen bonds. This type of recognition serves as the primary interactions that occurs in the structure originally proposed by Watson and Crick.<sup>3</sup> In addition to hydrogen bonding,  $\pi$ - $\pi$  stacking provides a necessary stabilization effect that is critical to the helical nature of the DNA structure (Figure 1.2).<sup>7</sup> It is worth noting that the complex blend of molecular associations found in DNA offer important insight to the unique functions of this important material. The non-covalent interactions observed in DNA are also found in a variety of other types of biological and chemical processes including protein folding and multi-protein systems such as enzyme receptor interactions.<sup>8</sup>

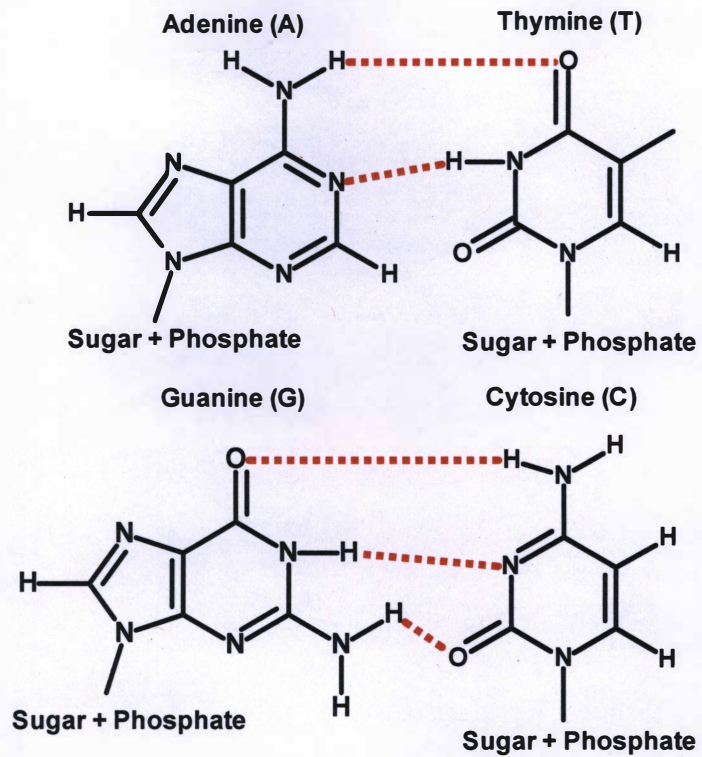


Figure 1.1: Hydrogen Bonding of Nitrogenous Bases.

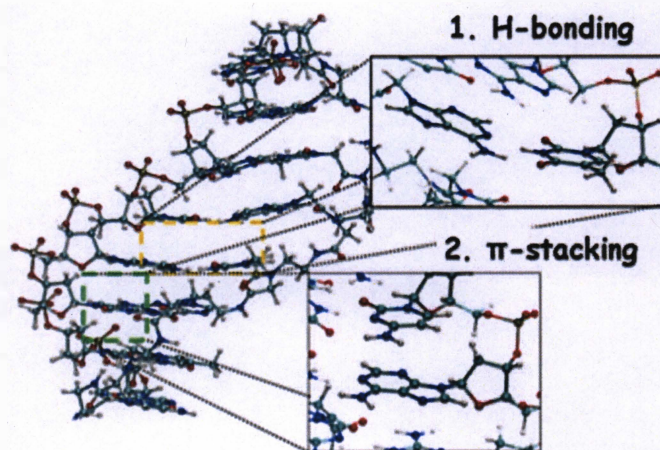


Figure 1.2: Molecular Recognition in Deoxyribonucleic Acid.

## 1.2 Importance of Molecular Chirality

As described in the preceding discussion, the fundamental structure of chemical compounds directly influences the properties of the materials that they make up. Pharmaceutical materials offer an important example of this area of science where the structure and organization of the building blocks greatly impact the physical and chemical properties of these materials.<sup>9</sup> The ability to control chemical properties such as solubility, toxicity, and lipophilicity are important ongoing themes with the development of pharmaceuticals that ultimately determines the marketability of targeted drugs. This same insight to the chemical structure also helps investigators determine the most suitable route for the formulation and delivery of potential therapeutic agents. Typical delivery methods include topical, oral, sublingual, inhalation, and injection. A clear view of the complete structural landscape of a pharmaceutical compound is thus vital when determining or producing specific structure-activity relationships. Molecular chirality – *i.e.* the handedness of molecules – and its use in pharmaceutical agents provides an important structural feature that can greatly effect physiochemical activity.<sup>9</sup>

In 1848, while working with sodium ammonium tartrate, Louis Pasteur showed for the first time that left and right-handed crystals could be isolated through spontaneous mechanical separation.<sup>10</sup> Though the importance of molecular chirality was not immediately understood by the science community, this molecular feature now provides a critical component of many science disciplines. For instance, the pharmaceutical industry now adopts molecular chirality as a key molecular feature into the design of many drug formulations. One indication of this importance is that 56% of drugs on the market today display chirality with 88% of the remaining compounds existing as racemic mixtures.<sup>10</sup> Despite stereoisomers containing the same molecular formula and differing

only in the spatial arrangement of their atoms to produce molecular handedness, such compounds as applied pharmaceutical formulations can exhibit very different properties. By exchanging one enantiomer for another the result can be a drastic difference in the pharmacology, pharmacokinetics, and pharmacodynamics of the material. Adverse side effects can develop by changing molecular chirality or by combining equimolar amounts of enantiomers to give racemic mixtures. One potential outcome from administering racemic mixtures includes elevated activity of one of the enantiomers as compared to the other stereoisomer. These enantiomeric compounds are known as the eutomer, more biologically active, and the distomer, less biologically active.<sup>10</sup> The activity of racemic mixtures does not always present a physiological drawback since enantiomers may exhibit similar pharmaceutical properties. Some racemic mixtures contain an inactive distomer that is effectively converted via enzymatic action to the needed eutomer.<sup>10</sup> Thalidomide, Labetalol, and Ibuprofen offer examples of pharmaceutical agents where the stereochemical features of the compounds effect activity, and where the activity of the enantiomers differ drastically.

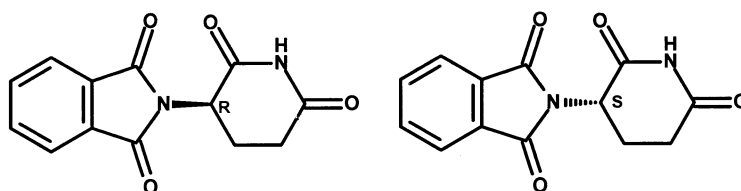


*Figure 1.3: Enantiomers of Thalidomide.*

The first synthetic investigations of thalidomide occurred in 1954 at the pharmaceutical company Chemie Grunenthal GmbH. Initial testing of thalidomide showed that this potential therapeutic exhibited antihistamine properties as well as

performing well as a sedative.<sup>11</sup> The drug was considered safe for mild sedation and introduced to the commercial market in 1957. By 1960 the drug was introduced to 20 different countries, but soon after several alarming side effects emerged prompting further investigations into its activity. By 1961 it was found that women exposed to thalidomide during their first trimester of pregnancy to combat morning sickness were in jeopardy of giving birth to children with defects. This discovery by Frances Kelsey, an FDA physician, prevented the introduction of the drug to the United States market.<sup>12</sup> These developments prompted the removal of the drug from the global market and by 1962 a complete removal occurred. The abnormalities observed during pregnancy included shortening and loss of limbs, but also these side effects extended to deformation of ears, eyes, and hearts of the children. The adverse impact of thalidomide to society was significant with nearly 10,000 cases of victims suffering from birth complications. The critical challenge of thalidomide's story is that drug administration occurred as the racemic form; a direct result from the single chiral center of the compound resulting in two enantiomers (Figure 1.3).<sup>11</sup> After the initial tragedy of thalidomide, more in-depth studies determined the origin of these birth defects. The teratogenic enantiomer, (*S*)-thalidomide, was the cause of abnormal development during pregnancy, while the *R* enantiomer provided beneficial therapeutic properties. Simply dispensing this isomer was hindered because of the challenges associated with solubility. The superior solubility of the racemic mixture as compared to its enantiopure components limited the availability of this therapeutic as a single enantiomer. In addition, administering only the *R* form did not alleviate the problem of teratogenicity since the drug can undergo an *in vivo* racemization via a bidirectional chiral inversion process.<sup>10-12</sup> The tragedy of thalidomide has been long

lasting with its effects still prevalent today. Many problems associated with this drug could have been prevented through a clear understanding of the relationship between thalidomide's molecular structure and the physicochemical activity of the therapeutic. Today, thalidomide has been developed as an effective treatment for leprosy and Myeloma.<sup>12</sup> This progress is the direct result of the science community's well-defined assessment of thalidomide's chemical structure, activity, and mechanistic action.

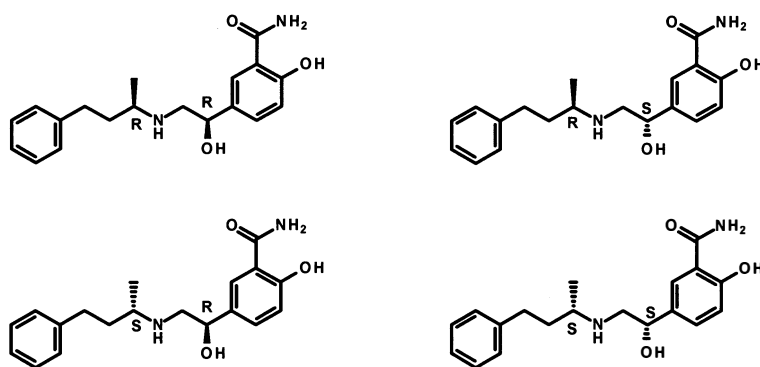
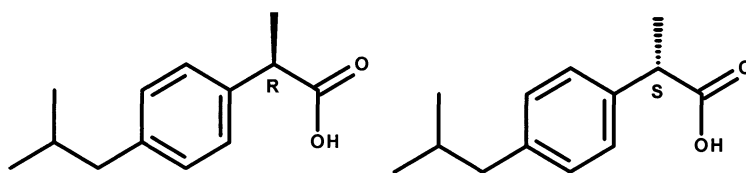


Figure 1.4: Stereoisomers of Labetalol.

Like thalidomide, Labetalol is another example of a pharmaceutical agent that exists with multiple stereoisomers. However, unlike thalidomide, labetalol contains two chiral carbon atoms that translates to four different stereoisomers (Figure 1.4).<sup>13</sup> Thalidomide offers an example where the properties of the stereoisomers are significantly different. The impact of labetalol's four stereoisomers is more subtle and relates to the location of activity. A full understanding of the structure activity relationship should occur prior to the introduction of a pharmaceutical compound to the general public. Labetalol shows both alpha and beta adrenergic properties that can be utilized as a treatment of high blood pressure and as an antihypertensive. The *R,R* isomer of labetalol behaves as a beta-blocker, but expresses little alpha-blocking activity. By changing the

first chiral center to give the *S,R* isomer, the beta-blocking activity vanishes and high alpha blocking activity develops. The two remaining isomers, *S,S* and *R,S* are inactive. When prescribing labetalol the drug will often be administered as mixture of the *R,R* and *S,R* diastereomers in order for both alpha and beta blocking to occur.<sup>13</sup> The case of labetalol and its four isomers further solidifies the importance of understanding structures of compounds as it plays a role in their activity and selectivity.



*Figure 1.5: Stereoisomers of Ibuprofen.*

Ibuprofen is a known nonsteroidal anti-inflammatory drug (NSAID) that inhibits cyclooxygenase 1 (COX 1). Ibuprofen, like the two previous examples, thalidomide and labetalol, contains a chiral carbon resulting in two stereoisomers (Figure 1.5). Ibuprofen is marketed as a racemic mixture, but its activity is largely dependent on the *S* isomer.<sup>10</sup> The *S* isomer is 100 times more effective as an inhibitor of COX1 than the *R*-isomer. The anti-inflammatory and analgesic properties of ibuprofen leads to its common use. Despite only one isomer being active, the compound undergoes a unidirectional inversion mediated by enzymatic action to give inversion of the *R* isomer to the *S* isomer. During this process only the *R* isomer can undergo this chemical change.<sup>10</sup> In the case of ibuprofen, neither of the isomers cause extreme or detrimental side effects similar to thalidomide nor is additional activity observed at multiple active sites. Ibuprofen provides



an example in which a beneficial inversion process occurs that results in an inactive form of a drug, *R*-isomer, becoming active, *S*-isomer, through the enzymatic activity.<sup>10</sup>

Thalidomide, Labetalol, and Ibuprofen highlight the importance of stereochemistry in the pharmaceutical industry. In the cases of Thalidomide and Labetalol the use of the wrong enantiomer can result in side effects ranging from birth defects to a lack of therapeutic activity. An understanding of structure activity relationships does not only apply to pharmaceuticals, but applies to nearly all functional materials. The control and optimization of properties to give a desired performance level is strongly dependent on an intimate understanding of the structure activity relationship of compounds and materials. Without a full understanding of molecular recognition, the ability to predict the activity of a specific material may not occur. This thesis explores the molecular recognition processes by use of racemic and quasiracemic materials, where molecular shape is exploited as a structural feature to understand the formation of supramolecular architectures.

### **1.2.1 Racemic and Quasiracemic Mixtures**

The ability of two molecular components to organize together in a crystal – *i.e.* a cocrystal - is dependent on the complementary features of the components for recognition to occur. The driving force for assembling the components of a cocrystalline system often relates to formation of such interactions as hydrogen bonds,  $\pi$  stacking, and metal coordination. Although less well studied, the topological features of the cocrystalline molecules can also have a drastic effect on molecular recognition. The analogy of the lock and key mechanism that corresponds to enzyme receptors speaks to the importance of the magnitude and profile of matching shapes to the molecular recognition process. For example, if the key is too large it will not fit in the lock and if the key is too small, it

will not release the lock. Investigations of molecular crystals most often focus on non-covalent interactions such as hydrogen bonding largely because such contacts can be quantified via various parameters (e.g. bond distances and angles). Though molecular shape is widely recognized as a key determinant in crystal organization, studies that focus on this structural feature are rare.<sup>14-18</sup> One such reason for the lack of attention to molecular shape is related to the challenge of quantifying molecular and functional group topology. Perhaps one approach to classify molecular shape is by use of the work of Gavezzotti from the 1980s.<sup>19,20</sup> Gavezzotti described the volume and surface of various functional groups. Though not a direct indicator of molecular shape this information has proven useful when comparing the spatial features of two or more substituents or chemical frameworks.

### **1.3 Assessment of Molecular Recognition and Noncovalent Interactions**

The assessment and determination of molecular recognition profiles can occur through a variety of techniques. X-ray crystallography is a non-destructive technique that provides critical information about the three-dimensional structure of chemical compounds. In addition to determining the fundamental aspects of chemical structure, X-ray diffraction patterns collected from crystallographic studies give insight to the contents of the crystal lattice such as non-covalent interactions and the symmetry that defines these molecular associations. By determining the molecular packing in crystals the properties that arise from these arrangements can also be identified.<sup>21</sup> A crystal can be defined as an ordered three-dimensional array of atoms, ions, or molecules within a solid. Some compounds, such as active pharmaceutical ingredients (APIs), can form more than one type of crystal structure. These crystal structures are known as polymorphs.<sup>22,23</sup> The

term polymorph was first introduced by Mitscherlich in 1820<sup>24</sup>, but the definition has changed slightly with more recent modifications. The original and frequently accepted definition of polymorphism, coined by McCrone, is *a solid crystalline phase of a given compound resulting from the possibility of at least two different arrangements of the molecules of that compound in the solid state.*<sup>25</sup> The technique of crystallography often looks at structures that do not contain only one component but contains an additional component.

### 1.3.1 Crystal Structures and Crystal Forms

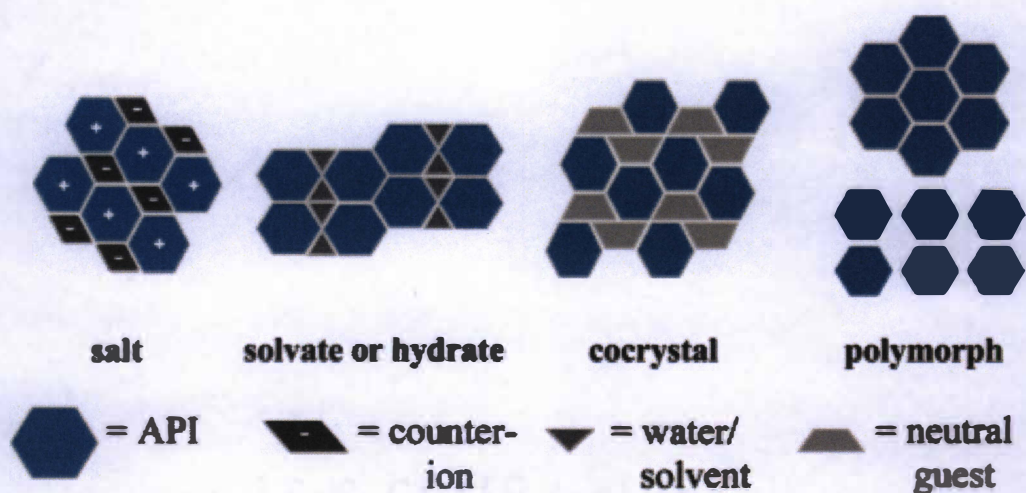


Figure 1.6: Types of Multicomponent Crystals.<sup>26</sup>

Some examples of compounds that frequently exist in polymorphic forms are APIs. For a drug to reach the market it must first undergo a variety of tests that include a formulation process. One solid form or polymorph must be selected for this process and is largely dependent on the properties of that crystalline phase. Many potential challenges associated with pharmaceuticals formulations include solubility, density, toxicity, and lipophilicity. One such way to reach the desired material properties is by administering an

amorphous form or a multi-component form consisting molecular salts or cocrystals (Figure 1.6).<sup>26</sup> Developing a language that effectively describes multicomponent crystals has been a topic of much recent debate.<sup>22,23,27</sup> As of 2011, the United States Food and Drug Administration (FDA) recommended a classification system for APIs; however, this attempt was not adequate for describing all formulations.<sup>22,23</sup>

Multicomponent crystals are a system in which two or more chemically different components are present in the crystal lattice. These components may include ions, solvents, or cofomers (Figure 1.6). When one of the components of a multicomponent crystal contains a nonzero formal charge, it is known as an ion. Components that are liquid while at room temperature are solvents. A residue that is neither a liquid nor a charged component of the crystal is considered a cofomer.<sup>23</sup> While multicomponent crystals containing APIs can exist in several polymorphic forms, they may also include salts, solvates/hydrates, or cocrystals. The benefit of multicomponent crystals is that material properties may be engineered by combining targeted components. This approach has been shown to be effective at increasing the overall usefulness of a therapeutic agent.<sup>23</sup> Multicomponent crystals fall under three classes of compounds: salts, solvates, and cocrystals. A salt, is a crystal system composed of at least two ions. Solvates include crystalline phases that incorporate solvent as well as a cofomer or at least two ions. The final class of multicomponent crystalline systems is a cocrystal which contains a crystal with a cofomer in addition to another cofomer or at least two ions. The classification of multicomponent crystals can be further divided into seven subclasses – *i.e.* true solvates, true salts, true cocrystals, salt solvates, cocrystal solvates, cocrystal salt, and cocrystal salt solvates.<sup>23</sup> Prior to analyzing crystals with the use of X-

ray diffraction other techniques may be utilized. The qualitative technique, hot-stage microscopy, helps to investigate molecular recognition without subjecting materials to experiments with uncontrollable variables such as single crystal growth.<sup>28</sup> This technique allows for the preparation of cocrystals by melting two coformers together with one another.<sup>29</sup> In addition to looking at molecular recognition and the ability of two substances to form cocrystals, this technique has a long history in describing the solid states of active pharmaceutical ingredients.

### **1.3.2 Hot-Stage Thermomicroscopy**

The technique of thermomicroscopy was developed by the early work of Otto Lehman, Ludwig and Adelheid Kofler, and Maria Kunhert Brandstatter.<sup>30</sup> This analytical technique allows the thermal characterization of a material's physical properties. The equipment consists of a temperature controlled hot stage equipped with a microscope and video capture. Some physical properties observed include physical and chemical decomposition as well as phase transitions.<sup>31</sup> A benefit from using this technique centers on its effective use with assessing the thermal properties of binary mixtures. With the use of known starting materials, one can determine the ratios of the starting components in new crystalline phases based on the melting temperature of mixture.<sup>28</sup> The work reported by Lehman highlighted that heating an organic compound leads to a unique thermal signature characteristic of the material. Work performed by Ludwig and Adelheid Kofler further helped in the identification of organic materials characteristics through analysis utilizing this technique.<sup>30</sup> During these early years, the available instrumentation for hot stage work was quite primitive that ultimately led to significant advances in instrumentation. The Kofler hot stage was one such piece of equipment developed by L. and A. Kofler to perform their experiments. This method utilized by the Koflers was later

termed the *contact method* by McCrone.<sup>31</sup> This method provides information on the formation of new crystalline phases as well as eutectic mixture formation. In addition to new crystalline phases being formed during the heating and cooling stages of this method, cocrystal screening of binary systems can occur rapidly. Maria Kunhert Brandstatter focused her work on organic compounds that would have a specific medical benefit. Today, the pharmaceutical industry utilizes hot-stage microscopy for the solid-state characterization of drugs. This is not limited to one crystal type but allows for the analysis of multiple polymorphs as well as solvates and hydrates.<sup>30</sup> Hot stage microscopy has been coined as *one of the oldest and simplest methods suitable for screen purposes*.<sup>31</sup> Today this technique continues to be used as a cocrystallization screening diagnostic tool. Through the study of cocrystallization of two or more molecules, one can determine the ability of molecules to recognize one another. One type of active pharmaceutical ingredient commonly studied in cocrystallization is the sulfonamide drugs.<sup>32</sup>

#### **1.4 Thesis Overview**

This thesis builds on previous work and the current understanding of the factors that affect the molecular recognition profiles of cocrystalline organic materials. This work primarily focuses on two areas with the first examining a family of benzoic acid and sulfamethazine cocrystalline systems. Important structural trends emerge from this study by combining sulfamethazine and a collection of benzoic acids that vary in structure and position of a pendant substituent. The second area studies the structural boundary of molecular shape to the molecular recognition process. This investigation more specifically aims to determine the role of topology to the molecular recognition process. While the shape space of molecules is known to contribute to crystal packing

and the recognition process in general, investigating this structural feature has attracted little attention. Efforts in these areas provide comprehensive investigations that highlight families of structurally related compounds and their role in the molecular recognition process.

#### 1.4.1 Sulfamethazine as an Active Pharmaceutical Ingredient

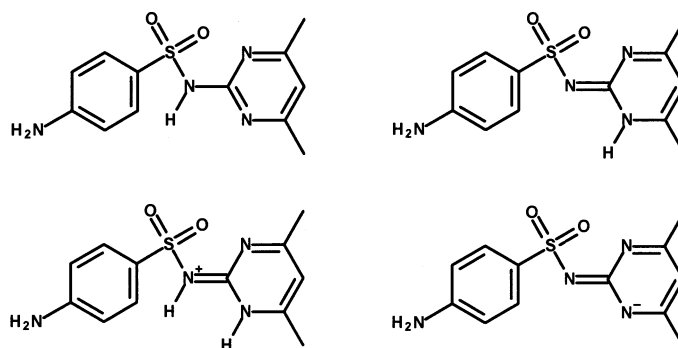


Figure 1.7: Forms of Sulfamethazine.

Sulfa drugs were developed as antimicrobial agents with uses in both veterinary and human applications. The core structure of sulfa drugs contains a sulfonamide group that often promotes a blend of hydrogen bond interactions. The outcome from hydrogen bond stabilization is that sulfa drugs readily assemble with secondary molecules (coformers) via complementary hydrogen-bond groups.<sup>32</sup> In addition to existing in more than one polymorph, some drugs in this family are capable of at least two tautomeric forms, an amidine or an imidine. One such example of a sulfa drug capable of existing in more than one tautomer is sulfamethazine (Figure 1.7)<sup>33</sup>, also reported under the names sulfadimidine and sulfadimethylpyridine.<sup>34</sup> The complexity of molecular assembly of sulfamethazine largely relates to the assortment of functional groups capable of hydrogen bonding. The amine and sulfonamide substituents provide three acidic NH protons. In

addition to these donor groups there are also five acceptor regions capable of hydrogen-bonding. These regions include the amine, two oxygen atoms of the sulfonamide group, and two hetrocyclic nitrogen atoms present in the pyrimidine ring.<sup>34</sup> Surprisingly, despite sulfamethazine containing many of the same structural elements as other sulfa drugs, only one polymorph is known to date.<sup>35</sup> Depending on the structural features of the cofomer assembled with sulfamethazine, these secondary molecules can greatly effect which tautomer is present. Sulfamethazine has been shown to form cocrystals with carboxylic acids, amides, saccharin, theophylline, and other molecular components.<sup>33,34,36-39</sup> In each case cocrystallization of sulfamethazine with these active pharmaceutical ingredients leads to the formation of  $R_2^2(8)$  hydrogen-bonded rings as previously defined by Etter.<sup>40,41</sup> This motif is identified by a ring (R) of eight atoms with two acceptor and two donor atoms assembling the pattern.

#### **1.4.2 Sulfamethazine and cocrystallization with substituted Benzoic Acids**

Many studies have explored the cocrystallization ability of sulfamethazine. While these investigations contribute to our current understanding of sulfamethazine's structural chemistry, no literature reports have attempted to correlate tautomer formation to the acidity of the cofomer.<sup>29,32-35,37,39</sup> Additionally, sulfamethazine has been shown to hydrogen bond with carboxylic acids and more specifically benzoic acids, but these studies seem to be isolated investigations with each reporting a limited number of crystal structures.<sup>29,32,34,36,38,39</sup> This investigation moves beyond these previous reports and examines a substantial set of sulfamethazine-benzoic acid cocrystalline systems. This is accomplished by introducing to the project benzoic acids that systematically differ in functional group composition and location. This design strategy allows for a wide array of substituents with electron donating and withdrawing groups that in turn, results in



range of pKa values for the cofomers. The strength of these donating and withdrawing properties affect hydrogen bond ability and the overall assembly of the cocrystalline motifs.<sup>42</sup>

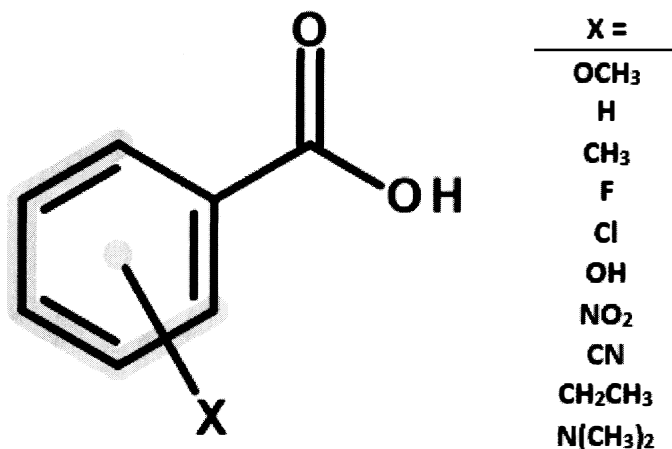


*Figure 1.8: Substituted Benzoic Acids Utilized in Cocrystallization.*

The cocrystallization of sulfamethazine occurred using various substituted benzoic acids (Figure 1.8). This study aimed to look at the molecular recognition process between this API and various benzoic acids in order to determine when each specific tautomer will occur in a cocrystal. The benzoic acids used in this study provided a range of acid strengths resulting in the formation of two different tautomers. Controlling which tautomer forms plays a large role in activity and location of activity as shown in the previously discussed pharmaceutical examples. This ability of sulfamethazine to cocrystallize in various tautomers suggests that optimization of specific properties may occur during a formulation process.

### **1.4.3 Molecular recognition boundaries of diarylamide quasiracemates**

The design of functional materials depends on a clear understanding of all factors responsible for the molecular assembly process. Although the design of functional

materials has advanced in the past few decades to give new materials of current importance, the construction of engineered supramolecular structures still remains at a primitive level.<sup>8</sup> Structural organization of solids is controlled through the interactions occurring within the solid including hydrogen bonding, electrostatic interactions, and  $\pi$ - $\pi$  stacking. The role and magnitude these interactions play determine the organization of these solids. Another such interaction recognized as a factor in organization is topology. Although this property is accepted as a factor in crystal organization the studies involving size and shape are often limited.<sup>14</sup>

Previous investigations in the Wheeler Lab have focused on synthesizing and combining pairs of isosteric compounds to form quasiracemic structures. Quasiracemates, or quasiracemic compounds, consist of 1:1 ratio of two chemically unique components of opposite handedness (*i.e.*,  $R$ - $X/S$ - $X'$ ). Studies in the area most often maximize success by combining structurally similar components. These studies have led to important discoveries and a deeper understanding of quasiracemic materials; even so, several critical questions still remain such as the comprehensive role of molecular shape to the molecular recognition process. Unlike other investigations in the field of supramolecular chemistry that focus on non-covalent interactions, our investigations focus on how molecular topology influences crystal packing.<sup>14-18</sup> The lack of clearly defined descriptors of molecular shape has limited the development of research programs in this area. Molecular volume and surface area calculations offer one approach to quantify the shape space of molecules.<sup>19,20</sup> A variety of quasiracemic scaffolds have been utilized to investigate molecular recognition and the formation of quasiracemic structures.<sup>16-18</sup> Despite previous studies, a defined structural boundary for quasiracemate formation has

yet to occur. Developing an understanding of the role topology plays in recognition processes coupled with other interactions would help in the design and development of new materials with a range of applications from biological functions to novel solids.<sup>43</sup>

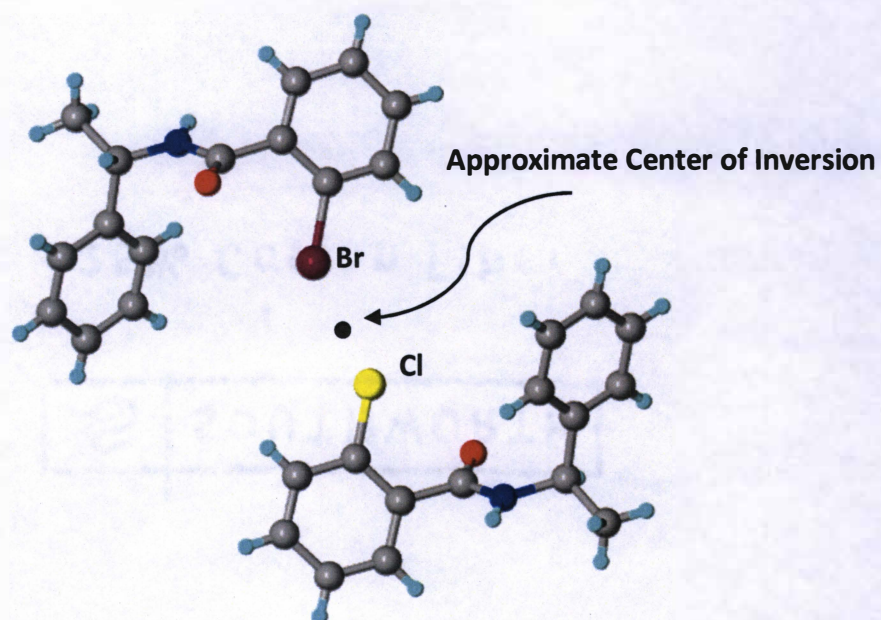


Figure 1.9: Quasicrystalline Structure of N-(2-Chloro)/N-(2-Bromobenzoyl)methylbenzylamine.

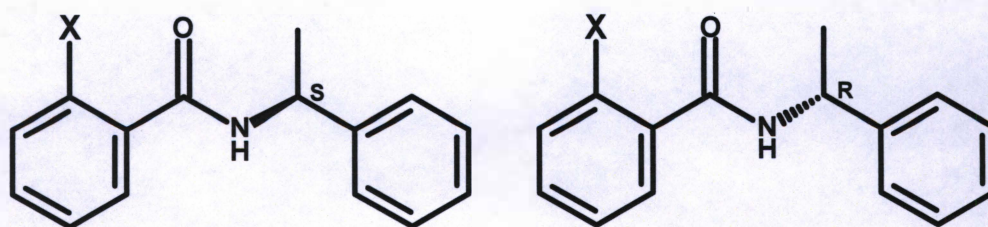


Figure 1.10: Diarylamide Molecular Frameworks Used in this Thesis Study.

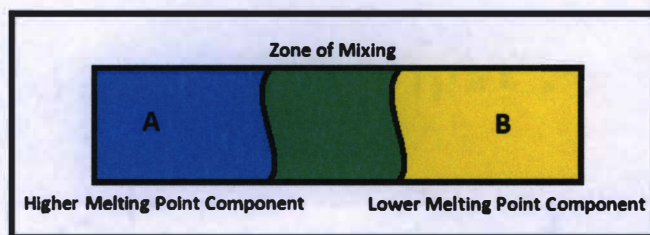
X =	Group	Group Surface
	Volume (Å <sup>3</sup> )	Area (Å <sup>2</sup> )
H	5.9	6.8
F	7.8	12.1
Cl	19.6	29.0
CN	21.0	32.2
CH <sub>3</sub>	23.3	33.4
NO <sub>2</sub>	23.2	37.0
Br	27.6	37.1
CF <sub>3</sub>	28.9	37.3
OCH <sub>3</sub>	32.6	40.1
I	34.6	45.0
C <sub>6</sub> H <sub>5</sub>	82.9	94.9

Figure 1.11: Functional Group Volumes and Surface Areas.<sup>19,20</sup>

The focus of this project lies with determining the influence of molecular shape to how molecules recognize each other. This investigation builds on a previously reported diarylamide quasiracemic material and extends this success to a family of diarylamides suitable for determining the structural boundaries of quasiracemate formation (Figure 1.9).<sup>15</sup> This study exploits the symmetry preference found in crystalline racemic compounds. It has been shown that 92% of racemic crystal structures form inversion related motifs.<sup>18</sup> This strong structural proclivity of racemates to form centrosymmetric assemblies also extends to quasiracemates such as that shown in Figure 1.9. This program aims to provide insight to the role topology plays in the recognition process through ortho-substituted diarylamide quasiracemic enantiomers. This study takes the molecular scaffold shown in Figure 1.10, both (*R*) and (*S*) enantiomers, and modifies the strategy to include a variety of substituents that vary in size and shape (Figure 1.11). The molecular volumes and surface areas of these diarylamide derivatives are provided in Figure 1.11.<sup>19,20</sup> These substituents differ incrementally in shape and size and increase the overall volume and surface area of the structure .



Previous experiments in the Wheeler Lab have utilized quasiracemic materials for studying molecular topology and its influence in generating supramolecular structures. Through these studies, it has been identified that quasiracemic structures organize in 1:1 ratios with one another of each handed component. These structures organize in a predictable manner, much like that of their racemic counterparts, with a pseudo-inversion center. Unlike racemates, these structures do not contain a true inversion center due to each handed molecule being chemically unique.<sup>14-18</sup>



*Figure 1.12: Kofler Contact Method.*

A family of compounds was synthesized from starting components varying in pendant substituent resulting in twenty-two compounds in total. The synthesis of these products occurred in a parallel fashion and chemical connectivity was determined via proton ( $^1\text{H}$ ) nuclear magnetic resonance (NMR) and carbon ( $^{13}\text{C}$ ) NMR. In order to purify and isolate the products, slow evaporation recrystallization techniques were used. Identification of the molecular recognition process occurred through hot-stage thermomicroscopy and the Kofler contact method (Figure 1.12). Racemic compounds were used as models to ensure this technique would apply to quasiracemic enantiomers. Under a controlled thermal environment, each compound was melted, and allowed to mix

with another of opposite handedness, to determine whether the two compounds would form a new crystalline phase.<sup>30,31</sup>

The contact method provided a visual phase diagram in which the identification of a new crystalline phase occurred through the presence of two eutectic points while identification of a conglomerate occurred through the presence of a single eutectic point. The presence of two eutectic points and a new crystalline phase suggested that a recognition process occurred and that the compounds associated with one another. The presence of a new crystalline phase resulted in further analysis of the solid through <sup>1</sup>H NMR, <sup>13</sup>C NMR, powder X-ray diffraction, and single crystal X-ray diffraction. Diffraction techniques provide information for the structural determination of these quasiracemic structures. Some quasienantiomeric pairs were unable to grow viable single crystals to be analyzed resulting in the need for powder X-ray diffraction. Powder X-ray diffraction provided the molecular fingerprint of the quasiracemic compound allowing for differentiation from the starting materials.

The thermal processing of these synthesized diarylamide starting materials resulted in virtual phase diagrams and molecular association profiles for each of the one hundred and ten experiments that were completed. This information provides a structural landscape of the effects of topology that vary incrementally in size and shape on this molecular scaffold. This analysis will result in defined shape space boundary for these diarylamide derivatives.

## 1.5 References

- (1) Balzani, Vincenzo; Credi, Alberto; Venturi, M. *Molecular Devices and Machines: Concepts and Perspectives for the Nanoworld*; WILEY-VCH: Federal Republic of Germany, 2008.
- (2) Tiekink, E. R. T. *Chem. Commun.* **2014**, 50 (76), 11079–11082.
- (3) Watson, J. D.; Crick, F. H. C. *Nature*. 1953, pp 737–738.
- (4) Chargaff, E. *Experientia* **1950**, 6, 201–209.
- (5) Chargaff, E.; Lipshitz, R. *J. Am. Chem. Soc.* **1953**, 75 (15), 3658–3661.
- (6) Genetics, C. for R. What is DNA?  
[http://www.councilforresponsiblegenetics.org/geneticprivacy/DNA\\_sci\\_1.html](http://www.councilforresponsiblegenetics.org/geneticprivacy/DNA_sci_1.html)  
(accessed Jan 1, 2017).
- (7) Krylov, A. Open-shell Species: A Challenge to Electronic Structure Theory  
<http://chem.usc.edu/faculty/Krylov.html> (accessed Jan 1, 2017).
- (8) Gellman, S. *Chem. Rev.* **1997**, 97 (5), 1231–1232.
- (9) Datta, S.; Grant, D. J. W. *Nat. Rev. Drug Discov.* **2004**, 3 (1), 42–57.
- (10) Nguyen, L. A.; He, H.; Pham-Huy, C. *Int. J. Biomed. Sci.* **2006**, 2 (2), 85–100.
- (11) Eriksson, T.; Björkman, S.; Höglund, P. *Eur. J. Clin. Pharmacol.* **2001**, 57 (5), 365–376.
- (12) Vargesson, N. *Birth Defects Res. Part C Embryo Today Rev.* **2015**, 105 (2), 140–156.
- (13) Gold, E. H.; Chang, W.; Cohen, M.; Baum, T.; Ehrreich, S.; Johnson, G.; Prioli, N.; Sybertz, E. J. *J. Med. Chem.* **1982**, 25 (11), 1363–1370.
- (14) Fomulu, S. L.; Hendi, M. S.; Davis, R. E.; Wheeler, K. A. *Cryst. Growth Des.*

- 2002, 2 (6), 637–644.
- (15) Fomulu, S. L.; Hendi, M. S.; Davis, R. E.; Wheeler, K. A. *Cryst. Growth Des.* 2002, 2 (6), 645–651.
- (16) Hendi, M. S.; Hooter, P.; Davis, R. E.; Lynch, V. M.; Wheeler, K. A. *Cryst. Growth Des.* 2004, 4 (1), 95–101.
- (17) Breen, M. E.; Tameze, S. L.; Dougherty, W. G.; Kassel, W. S.; Wheeler, K. A. *Cryst. Growth Des.* 2008, 8 (10), 3863–3870.
- (18) Lineberry, A. M.; Benjamin, E. T.; Davis, R. E.; Kassel, W. S.; Wheeler, K. A. *Cryst. Growth Des.* 2008, 8 (2), 612–619.
- (19) Gavezzotti, A. *J. Am. Chem. Soc.* 1983, 105 (16), 5220–5225.
- (20) Gavezzotti, A. *J. Am. Chem. Soc.* 1985, 107 (4), 962–967.
- (21) Smyth, M. S.; Martin, J. H. *J. Clin. Pathol. Mol. Pathol.* 2000, 53 (1), 8–14.
- (22) Aitipamula, S.; Banerjee, R.; Bansal, A. K.; Biradha, K.; Cheney, M. L.; Choudhury, A. R.; Desiraju, G. R.; Dikundwar, A. G.; Dubey, R.; Duggirala, N.; Ghogale, P. P.; Ghosh, S.; Goswami, P. K.; Goud, N. R.; Jetti, R. R. K. R.; Karpinski, P.; Kaushik, P.; Kumar, D.; Kumar, V.; Moulton, B.; Mukherjee, A.; Mukherjee, G.; Myerson, A. S.; Puri, V.; Ramanan, A.; Rajamannar, T.; Reddy, C. M.; Rodriguez-Hornedo, N.; Rogers, R. D.; Row, T. N. G.; Sanphui, P.; Shan, N.; Shete, G.; Singh, A.; Sun, C. C.; Swift, J. A.; Thaimattam, R.; Thakur, T. S.; Thaper, R. K.; Thomas, S. P.; Tothadi, S.; Vangala, V. R.; Variankaval, N.; Vishweshwar, P.; Weyna, D. R.; Zaworotko, M. J. *Cryst. Growth Des.* 2012, 12 (5), 2147–2152.
- (23) Grothe, E.; Meekes, H.; Vlieg, E.; Ter Horst, J. H.; De Gelder, R. *Cryst. Growth*



- Des.* **2016**, *16* (6), 3237–3243.
- (24) Desiraju, G. R. *Cryst. Growth Des.* **2008**, *8* (1), 3–5.
- (25) W. C. McCrone, in *Polymorphism in Physics and Chemistry of the Organic Solid State*; Fox, D.; Labes, M. M.; Weissberger, A., Eds. Wiley Interscience: New York, 1965; Vol. II, pp. 726.
- (26) Schultheiss, N.; Newman, A. *Cryst. Growth Des.* **2009**, *9* (6), 2950–2967.
- (27) Patrick Stahly, G. *Cryst. Growth Des.* **2009**, *9* (10), 4212–4229.
- (28) Berry, D. J.; Seaton, C. C.; Clegg, W.; Harrington, R. W.; Coles, S. J.; Horton, P. N.; Hursthouse, M. B.; Storey, R.; Jones, W.; Frišćić, T.; Blagden, N. *Cryst. Growth Des.* **2008**, *8* (5), 1697–1712.
- (29) Lu, J.; Li, Y. P.; Wang, J.; Li, Z.; Rohani, S.; Ching, C. B. *J. Cryst. Growth* **2011**, *335* (1), 110–114.
- (30) Vitez, I. M.; Newman, A. W.; Davidovich, M.; Kiesnowski, C. *Thermochim. Acta* **1998**, *324* (1–2), 187–196.
- (31) Lekšić, E.; Pavlović, G.; Meštrović, E. *Cryst. Growth Des.* **2012**, *12* (4), 1847–1858.
- (32) Caira, M. R. *Mol. Pharm.* **2007**, *4* (3), 310–316.
- (33) Fu, X.; Li, J.; Wang, L.; Wu, B.; Xu, X.; Deng, Z.; Zhang, H. *RSC Adv.* **2016**, *6* (31), 26474–26478.
- (34) Ghosh, S.; Bag, P. P.; Reddy, C. M. *Cryst. Growth Des.* **2011**, *11* (8), 3489–3503.
- (35) Maury, L.; Rambaud, J.; Pauvert, B.; Lasserre, Y.; Bergé, G.; Audran, M. *J. Pharm. Sci.* **1985**, *74* (4), 422–426.
- (36) Adsmund, D. A.; Grant, D. J. W. *J. Pharm. Sci.* **2001**, *90* (12), 2058–2077.

- (37) Lu, Jie; Rohani, S. *J. Pharm. Sci.* **2010**, *99* (9), 4042–4047.
- (38) Caira, M. R.; Nassimbeni, L. R.; Wildervanck, A. F. *J. Chem. Soc. Perkin Trans. 2* **1995**, No. 12, 2213–2216.
- (39) Patel, U.; Haridas, M.; Singh, T. P. *Acta Crystallogr. Sect. C Cryst. Struct. Commun.* **1988**, *44* (7), 1264–1267.
- (40) Etter, M. C.; MacDonald, J. C.; Bernstein, J. *Acta Crystallogr. Sect. B* **1990**, *46* (2), 256–262.
- (41) Etter, M. C. *Acc. Chem. Res.* **1990**, *23* (4), 120–126.
- (42) Seaton, C. C.; Chadwick, K.; Sadiq, G.; Guo, K.; Davey, R. J. *Cryst. Growth Des.* **2010**, *10* (2), 726–733.
- (43) Desiraju, G. R. *J. Chem. Sci.* **2010**, *122* (5), 667–675.

## Chapter 2: Experimental Details

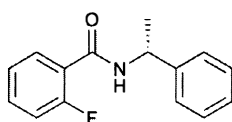
**General Considerations.** All chemicals and solvents were purchased from the Aldrich Chemical Co. or Acros Chemicals and used as received without further purification unless stated otherwise.  $^1\text{H}$  NMR and  $^{13}\text{C}$  NMR spectral data were recorded with a 400 MHz Bruker Avance spectrometer using TopSpin v.3.2. They were referenced using the solvent residual signal as internal standard. The chemical shift values are expressed as  $\delta$  values (ppm) and the value of coupling constants ( $J$ ) in Hertz (Hz). The following abbreviations were used for signal multiplicities: s, singlet; d, doublet; dd, doublet of doublets; t, triplet; q, quartet; m, multiplet; and br, broad. Melting point data were determined using a Melt-Temp apparatus and are uncorrected. The 2-substituted diarylamide derivatives for this study were prepared using a previously reported method starting from either the carboxylic acid or acid chloride.<sup>1</sup> The following general procedure, as described for (*R*)-*N*-(2-fluorobenzoyl)methylbenzylamine, was used to generate the homologous series of diarylamides.

### 2.1 Preparation of Sulfamethazine Cocrystals

Crystalline materials prepared for this study were grown in solution using equimolar amounts of sulfamethazine and the benzoic acid derivative. These mixtures were dissolved in a solvent system consisting of 1:1  $\text{CH}_3\text{CN}:\text{MeOH}$ . The solution was left partially covered and allowed to evaporate slowly at room temperature until crystals appeared typically after 2-4 days. Crystallographic assessment was carried out as

described in section 2.5 with full crystal structure details provided in section S1 of the Supplementary Information.

## 2.2 Synthesis of (*S*)- and (*R*)-*N*-(2-substitutedbenzoyl)methylbenzylamine



### (*R*)-*N*-(2-Fluorobenzoyl)methylbenzylamine

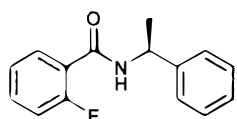
To a nitrogen purged 100-mL round-bottom flask containing a stir bar and 2-fluorobenzoic acid (0.8469 g, 6.00 mmol) at 0°C was added 2.2 mL of thionyl chloride (30.0 mmol). The reaction mixture was allowed to warm to room temperature and then refluxed for 2.5 hours to give a homogeneous yellow solution. Excess thionyl chloride was removed by washing the mixture with 15 mL of hexanes and the mixture was reduced using a mechanical diffusion pump to give a yellow solution. Without further purification, the acid chloride was treated with (*R*)-(+)- $\alpha$ -methylbenzylamine (1.7993 g, 14.8 mmol) dissolved in 5 mL dichloromethane and stirred overnight at room temperature. The reaction mixture was then extracted in succession with 25 mL H<sub>2</sub>O, 10 mL saturated NaHCO<sub>3</sub>, 10 mL 4 M HCl, and 10 mL H<sub>2</sub>O. The organic layer was dried using anhydrous magnesium sulfate and reduced under *vacuo* to give a solid colorless product (0.6413 g, 43.93% yield).

X-ray quality crystals were obtained *via* slow evaporation at room temperature using a 1:1 hexanes:dichloromethane solution.

Melting point 108-110°C.

<sup>1</sup>H NMR (400 MHz, acetone-*d*<sub>6</sub>):  $\delta$  8.80 (br s, 1H, N-H), 7.57-7.24 (m, 9H, C<sub>Ar</sub>-H), 5.12 (dq, *J* = 6.4 and 6.6 Hz, 1H, C<sub>sp3</sub>-H), 1.43 (d, *J* = 6.4 Hz, 3H, CH<sub>3</sub>)

$^{13}\text{C}$  NMR (100 MHz, acetone- $d_6$ ):  $\delta$  163.1, 160.2-157.8 (d,  $J = 247.1$  Hz), 144.6, 132.1-132.0 (d,  $J = 8.2$  Hz), 129.9, 128.3, 126.7, 126.0, 124.8-124.6 (d,  $J = 15.3$  Hz), 124.4-124.3 (d,  $J = 15.1$  Hz), 116.1- 115.9 (d,  $J = 21.9$  Hz), 48.6, 22.5.

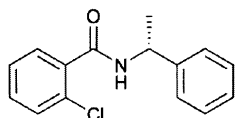


**(S)-N-(2-Fluorobenzoyl)methylbenzylamine**

Melting point 108-110°C, 85.89% yield.

$^1\text{H}$  NMR (400 MHz, acetone- $d_6$ ):  $\delta$  7.81-7.19 (m, 10H, N-H,  $\text{C}_{\text{Ar}}\text{-H}$ ), 5.32 (dq,  $J = 7.1$  and 7.2 Hz, 1H,  $\text{C}_{\text{sp}^3}\text{-H}$ ), 1.58 (d,  $J = 7.1$  Hz, 3H,  $\text{CH}_3$ ).

$^{13}\text{C}$  NMR (100 MHz, acetone- $d_6$ ):  $\delta$  162.6, 161.2-158.8(d,  $J = 246.3$  Hz), 144.4, 132.6-132.5 (d,  $J = 8.7$  Hz), 130.8, 128.4, 126.8, 126.1, 124.5-124.4 (d,  $J = 3.4$  Hz), 123.7-123.6 (d,  $J = 13.9$  Hz), 116.0-115.8 (d,  $J = 23.3$  Hz), 49.2, 21.8.

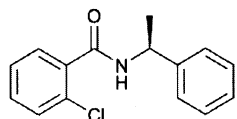


**(R)-N-(2-Chlorobenzoyl)methylbenzylamine**

Melting point 110-112°C, 68.25% yield.

$^1\text{H}$  NMR (400 MHz, acetone- $d_6$ ):  $\delta$  7.92 (br s, 1H, N-H), 7.52-7.24 (m, 9H,  $\text{C}_{\text{Ar}}\text{-H}$ ), 5.29 (dq,  $J = 7.1$  and 7.1 Hz, 1H,  $\text{C}_{\text{sp}^3}\text{-H}$ ), 1.57 (d,  $J = 7.1$  Hz, 3H,  $\text{CH}_3$ )

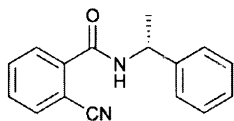
$^{13}\text{C}$  NMR (100 MHz, acetone- $d_6$ ):  $\delta$  165.5, 144.4, 137.3, 130.6, 130.5, 129.7, 129.0, 128.3, 126.9, 126.8, 126.2, 49.0, 21.7.



**(S)-N-(2-Chlorobenzoyl)methylbenzylamine**

Previously prepared by S. Fomulu with spectroscopic data provided in reference 1.

Melting point 110-112°C

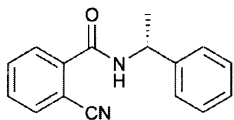


**(R)-N-(2-Cyanobenzoyl)methylbenzylamine**

Melting point 138-140°C, 84.11% yield.

$^1\text{H}$  NMR (400 MHz, acetone- $d_6$ ):  $\delta$  8.28 (br s, 1H, N-H), 7.87-7.22 (m, 9H,  $\text{C}_{\text{Ar}}\text{-H}$ ), 5.31 (dq,  $J = 7.1$  and 7.1 Hz, 1H,  $\text{C}_{\text{sp}^3}\text{-H}$ ), 1.59 (d,  $J = 7.1$  Hz, 3H,  $\text{CH}_3$ ).

$^{13}\text{C}$  NMR (100 MHz, acetone- $d_6$ ):  $\delta$  164.5, 144.1, 139.6, 133.9, 132.6, 130.7, 128.4, 126.9, 126.2, 122.9, 117.3, 111.1, 49.2, 21.5.

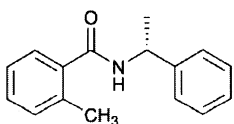


**(S)-N-(2-Cyanobenzoyl)methylbenzylamine**

Melting point 138-140°C, 34.58% yield.

$^1\text{H}$  NMR (400 MHz, acetone- $d_6$ ):  $\delta$  8.23 (br s, 1H, N-H), 7.87-7.24 (m, 9H,  $\text{C}_{\text{Ar}}\text{-H}$ ), 5.31 (dq,  $J = 7.1$  and 7.1 Hz, 1H,  $\text{C}_{\text{sp}^3}\text{-H}$ ), 1.59 (d,  $J = 7.0$  Hz, 3H,  $\text{CH}_3$ ).

$^{13}\text{C}$  NMR (100 MHz, acetone- $d_6$ ):  $\delta$  164.6, 144.1, 139.6, 133.9, 132.6, 130.7, 128.4, 126.9, 126.3, 122.5, 117.3, 111.1, 49.3, 21.6.

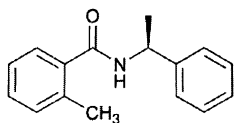


**(R)-N-(2-Methylbenzoyl)methylbenzylamine**

Melting point 110-112°C, 53.24% yield.

$^1\text{H}$  NMR (400 MHz, acetone- $d_6$ ):  $\delta$  7.82 (br s, 1H, N-H), 7.50-7.12 (m, 9H,  $\text{C}_{\text{Ar}}\text{-H}$ ), 5.29 (dq,  $J = 7.0$  and 7.3 Hz, 1H,  $\text{C}_{\text{sp}^3}\text{-H}$ ), 2.36 (s, 3H,  $\text{CH}_3$ ), 1.56 (d,  $J = 7.0$  Hz, 3H,  $\text{CH}_3$ ).

$^{13}\text{C}$  NMR (100 MHz, acetone- $d_6$ ):  $\delta$  168.5, 144.9, 137.4, 135.7, 130.4, 129.2, 128.3, 126.9, 126.7, 126.2, 125.4, 48.7, 21.8, 19.0.

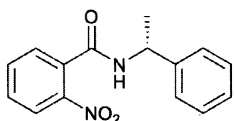


**(S)-N-(2-Methylbenzoyl)methylbenzylamine**

Melting point 110-112°C, 89.23% yield.

$^1\text{H NMR}$  (400 MHz, acetone- $d_6$ ):  $\delta$  7.77 (br s, 1H, N-H), 7.50-7.17 (m, 9H,  $\text{C}_{\text{Ar}}\text{-H}$ ), 5.30 (dq,  $J = 7.5$  and 7.5 Hz, 1H,  $\text{C}_{\text{sp}^3}\text{-H}$ ), 2.36 (s, 3H,  $\text{CH}_3$ ), 1.56 (d,  $J = 7.5$  Hz, 3H,  $\text{CH}_3$ ).

$^{13}\text{C NMR}$  (100 MHz, acetone- $d_6$ ):  $\delta$  168.3, 144.8, 137.4, 135.7, 130.4, 129.2, 128.3, 126.9, 126.7, 126.2, 125.4, 48.6, 21.7, 18.9.

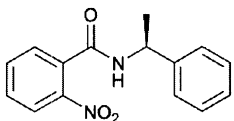


**(R)-N-(2-Nitrobenzoyl)methylbenzylamine**

Melting point 168-171°C, 30.44% yield.

$^1\text{H NMR}$  (400 MHz, acetone- $d_6$ ):  $\delta$  8.17 (br s, 1H, N-H), 8.03-7.25 (m, 9H,  $\text{C}_{\text{Ar}}\text{-H}$ ), 5.28 (dq,  $J = 7.0$  and 7.2 Hz, 1H,  $\text{C}_{\text{sp}^3}\text{-H}$ ), 1.58 (d,  $J = 7.0$  Hz, 3H,  $\text{CH}_3$ ).

$^{13}\text{C NMR}$  (100 MHz, acetone- $d_6$ ):  $\delta$  164.9, 147.4, 144.0, 142.2, 133.3, 130.4, 129.0, 128.3, 126.9, 126.2, 124.0, 49.0, 21.4.

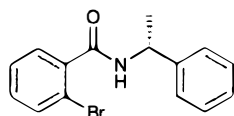


**(S)-N-(2-Nitrobenzoyl)methylbenzylamine**

Melting point 168-171°C, 82.78% yield.

$^1\text{H NMR}$  (400 MHz, acetone- $d_6$ ):  $\delta$  8.19 (br s, 1H, N-H), 8.03-7.25 (m, 9H,  $\text{C}_{\text{Ar}}\text{-H}$ ), 5.28 (q,  $J = 7.0$  and 7.2 Hz, 1H,  $\text{C}_{\text{sp}^3}\text{-H}$ ), 1.58 (d,  $J = 7.0$  Hz, 3H,  $\text{CH}_3$ ).

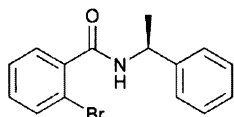
$^{13}\text{C NMR}$  (100 MHz, acetone- $d_6$ ):  $\delta$  164.9, 148.0, 147.4, 144.0, 133.3, 130.4, 129.0, 128.3, 126.9, 126.3, 124.0, 49.0, 21.4.



**(R)-N-(2-Bromobenzoyl)methylbenzylamine**

Previously prepared by S. Fomulu with spectroscopic data provided in reference 1.

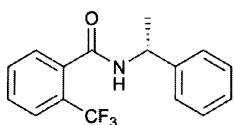
Melting point 117-121°C



**(S)-N-(2-Bromobenzoyl)methylbenzylamine**

Previously prepared by S. Fomulu with spectroscopic data provided in reference 1.

Melting point 117-121°C

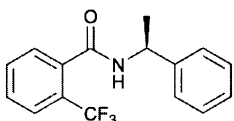


**(R)-N-(2-Trifluorobenzoyl)methylbenzylamine**

Melting point 140-143°C, 64.71% yield.

$^1\text{H}$  NMR (400 MHz, acetone- $d_6$ ):  $\delta$  8.00 (br s, 1H, N-H), 7.77-7.25 (m, 9H,  $\text{C}_{\text{Ar}}\text{-H}$ ), 5.29 (q,  $J = 7.0$  and 7.0 Hz, 1H,  $\text{C}_{\text{sp}^3}\text{-H}$ ), 1.56 (d,  $J = 7.0$  Hz, 3H,  $\text{CH}_3$ )

$^{13}\text{C}$  NMR (100 MHz, acetone- $d_6$ ):  $\delta$  166.3, 144.2, 137.0, 132.1, 129.4, 128.5, 128.3, 126.9, 126.2, 126.1, 125.4, 122.7, 49.0, 21.5.



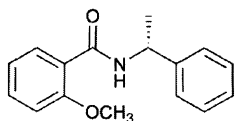
**(S)-N-(2-Trifluorobenzoyl)methylbenzylamine**

Melting point 140-143°C, 84.13% yield.

$^1\text{H}$  NMR (400 MHz, acetone- $d_6$ ):  $\delta$  8.00 (br s, 1H, N-H), 7.77-7.25 (m, 9H,  $\text{C}_{\text{Ar}}\text{-H}$ ), 5.30 (q,  $J = 7.0$  and 7.0 Hz, 1H,  $\text{C}_{\text{sp}^3}\text{-H}$ ), 1.56 (d,  $J = 7.0$  Hz, 3H,  $\text{CH}_3$ ).

$^{13}\text{C}$  NMR (100 MHz, acetone- $d_6$ ):  $\delta$  166.3, 144.2, 137.0, 132.1, 129.4, 128.5, 128.3, 127.2, 126.9, 126.2, 125.4, 122.7, 48.6, 21.5.



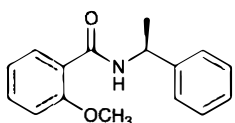


**(R)-N-(2-Methoxybenzoyl)methylbenzylamine**

Melting point 78-81°C, 86.85% yield.

$^1\text{H NMR}$  (400 MHz, acetone- $d_6$ ):  $\delta$  8.34 (br s, 1H, N-H), 8.06-7.05 (m, 9H,  $\text{C}_{\text{Ar}}\text{-H}$ ), 5.32 (dq,  $J = 7.0$  and 7.5 Hz, 1H,  $\text{C}_{\text{sp}^3}\text{-H}$ ), 4.00 (s, 3H, O- $\text{CH}_3$ ), 1.56 (d,  $J = 7.0$  Hz, 3H,  $\text{CH}_3$ ).

$^{13}\text{C NMR}$  (100 MHz, acetone- $d_6$ ):  $\delta$  163.8, 157.7, 144.8, 132.5, 131.5, 128.4, 126.8, 126.0, 122.4, 120.8, 111.9, 55.7, 48.9, 22.2.

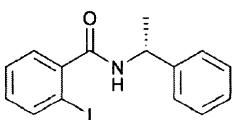


**(S)-N-(2-Methoxybenzoyl)methylbenzylamine**

Melting point 78-81°C, 75.82% yield.

$^1\text{H NMR}$  (400 MHz, acetone- $d_6$ ):  $\delta$  8.42 (br d,  $J=6.72$ , N-H), 8.18-7.06 (m, 9H,  $\text{C}_{\text{Ar}}\text{-H}$ ), 5.40 (dq,  $J = 7.0$  and 7.1 Hz, 1H,  $\text{C}_{\text{sp}^3}\text{-H}$ ), 3.93 (s, 3H, O- $\text{CH}_3$ ), 1.61 (d,  $J = 7.0$  Hz, 3H,  $\text{CH}_3$ ).

$^{13}\text{C NMR}$  (100 MHz, acetone- $d_6$ ):  $\delta$  163.7, 157.7, 144.8, 132.5, 131.5, 128.4, 126.8, 126.1, 122.4, 120.8, 111.8, 55.6, 48.9, 22.2.

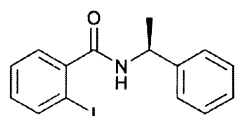


**(R)-N-(2-Iodobenzoyl)methylbenzylamine**

Melting point 137-140°C, 66.17% yield.

$^1\text{H NMR}$  (400 MHz, acetone- $d_6$ ):  $\delta$  7.88-7.14 (m, 10H, N-H,  $\text{C}_{\text{Ar}}\text{-H}$ ), 5.28 (dq,  $J = 7.0$  and 7.5 Hz, 1H,  $\text{C}_{\text{sp}^3}\text{-H}$ ), 1.59 (d,  $J = 7.0$  Hz, 3H,  $\text{CH}_3$ ).

$^{13}\text{C NMR}$  (100 MHz, acetone- $d_6$ ):  $\delta$  167.9, 144.1, 143.4, 139.4, 132.5, 130.4, 127.9, 127.8, 126.7, 126.3, 92.3, 48.8, 21.5.

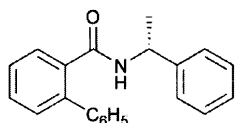


**(S)-N-(2-Iodobenzoyl)methylbenzylamine**

Melting point 137-140°C, 42.20% yield.

$^1\text{H}$  NMR (400 MHz, acetone- $d_6$ ):  $\delta$  7.88-7.16 (m, 10H, N-H,  $\text{C}_{\text{Ar}}\text{-H}$ ), 5.28 (dq,  $J=7.0$  and 7.1 Hz, 1H), 1.59 (d,  $J=7.0$ , 3H,  $\text{CH}_3$ ).

$^{13}\text{C}$  NMR (100 MHz, acetone- $d_6$ ):  $\delta$  168.0, 144.2, 143.5, 139.5, 132.6, 130.5, 128.3, 128.0, 126.8, 126.3, 92.3, 48.9, 21.6.

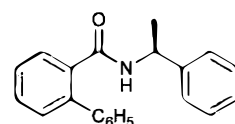


**(R)-N-(2-Phenylbenzoyl)methylbenzylamine**

Further purification of (R)- $\text{C}_6\text{H}_5$  was achieved by washing the sample with hexanes. Melting point 110-114°C, 63.24% yield.

$^1\text{H}$  NMR (400 MHz, acetone- $d_6$ ):  $\delta$  7.52-7.16 (m, 13H,  $\text{C}_{\text{Ar}}\text{-H}$ ), 5.07 (dq,  $J = 7.0$  and 7.5 Hz, 1H,  $\text{C}_{\text{sp}^3}\text{-H}$ ), 1.27 (d,  $J = 7.0$  Hz, 3H,  $\text{CH}_3$ ).

$^{13}\text{C}$  NMR (100 MHz, acetone- $d_6$ ):  $\delta$  168.2, 144.2, 140.6, 139.6, 137.5, 129.8, 129.3, 128.7, 128.1, 128.0, 127.2, 127.0, 126.5, 126.1, 48.6, 21.3, 13.4.

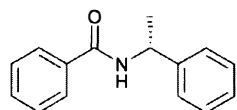


**(S)-N-(2-Phenylbenzoyl)methylbenzylamine**

Further purification of (S)- $\text{C}_6\text{H}_5$  was achieved by washing the sample with hexanes. Melting point 110-114°C, 19.78% yield.

$^1\text{H}$  NMR (400 MHz, acetone- $d_6$ ):  $\delta$  7.52-7.16 (m, 13H,  $\text{C}_{\text{Ar}}\text{-H}$ ), 5.07 (dq,  $J = 7.0$  and 7.2 Hz, 1H,  $\text{C}_{\text{sp}^3}\text{-H}$ ), 1.27 (d,  $J = 7.0$  Hz, 3H,  $\text{CH}_3$ ).

$^{13}\text{C}$  NMR (100 MHz, acetone- $d_6$ ):  $\delta$  168.2, 144.2, 140.7, 139.6, 137.5, 129.8, 129.3, 128.7, 128.2, 128.0, 127.2, 127.0, 126.6, 126.1, 48.6, 21.3, 13.4.

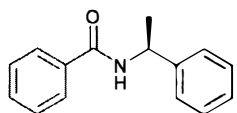


**(R)-N-(Benzoyl)methylbenzylamine**

Melting point 132-136°C, 68.38% yield.

$^1\text{H}$  NMR (400 MHz, acetone- $d_6$ ):  $\delta$  7.80-7.75 (m, 2H,  $\text{C}_{\text{Ar}}\text{-H}$ ), 7.53-7.26 (m, 8H,  $\text{C}_{\text{Ar}}\text{-H}$ ), 5.35 (dq,  $J = 6.9$  and  $7.1$  Hz, 1H,  $\text{C}_{\text{sp}^3}\text{-H}$ ), 1.62 (d,  $J = 7.1$  Hz, 3H,  $\text{CH}_3$ ).

$^{13}\text{C}$  NMR (100 MHz, acetone- $d_6$ ):  $\delta$  168.2, 141.6, 134.6, 131.5, 128.8, 128.6, 127.5, 126.9, 126.3, 48.2, 21.7.



**(S)-N-(Benzoyl)methylbenzylamine**

Melting point 132-136°C, 70.03% yield.

$^1\text{H}$  NMR (400 MHz, acetone- $d_6$ ):  $\delta$  7.81-7.76 (m, 2H,  $\text{C}_{\text{Ar}}\text{-H}$ ), 7.53-7.25 (m, 8H,  $\text{C}_{\text{Ar}}\text{-H}$ ), 5.34 (dq,  $J = 7.0$  and  $7.1$  Hz, 1H,  $\text{C}_{\text{sp}^3}\text{-H}$ ), 1.62 (d,  $J = 7.1$  Hz, 3H,  $\text{CH}_3$ ).

$^{13}\text{C}$  NMR (100 MHz, acetone- $d_6$ ):  $\delta$  168.2, 141.5, 134.6, 131.3, 128.7, 128.5, 127.5, 126.9, 126.3, 48.4, 21.7.

### 2.3 Hot-Stage Microscopy

The hot-stage microscopy experiments were performed using an optical polarizing microscope (*Olympus SZX10*) equipped with an *Instec HCS 302* hot-stage connected to an *Instec mK2000* temperature controller. Micrographs were collected under a range of magnifications (3.0-6.3x) using an attached video camera. The hot-stage was controlled by the WINDV software package (V1.0.120820). Pairs of diarylamide components were analyzed for cocrystallization behavior. Samples were prepared using standard glass microscope slides and cover slips. The higher melting point component was delivered first by heating the sample to the melting point temperature drawing the

sample under the cover slip. Upon cooling, the lower melting point component was then delivered in a similar fashion to create a contact interface between the two samples. These bimolecular samples were heated at a ramp rate of 2-5°C/min until complete melting of the sample occurred. All combinations (11 racemates and 55 quasiracemates) were processed using the video-assisted hot stage technique. Complete sets of hot-stage micrographs are included in section S2 of the Supplementary Information.

## 2.4 X-ray Crystallography - Powder Diffraction

Powder X-ray diffraction data were collected on a Bruker APEX II CCD diffractometer using phi and omega scans with graphite monochromatic Cu Mo  $K\alpha$  ( $\lambda = 1.54178 \text{ \AA}$ ) radiation. Data sets were collected at a detector distance of 15 cm using 4 Phi scans with 10° increments in  $2\theta$  ( $-20^\circ \rightarrow -50^\circ$ ) and omega ( $170^\circ \rightarrow 140^\circ$ ). The images were integrated using the APEX II XRD<sup>2</sup> plugin. Overlays of powder X-ray diffraction patterns are provided in section S3 of the Supplementary Information.

## 2.5 X-ray Crystallography – Single Crystal Diffraction

Crystallographic details for each diarylamide quasiracemate are summarized in Table S1. X-ray data were collected on a Bruker APEX II CCD diffractometer using phi and omega scans with graphite monochromatic Cu Mo  $K\alpha$  ( $\lambda = 1.54178 \text{ \AA}$ ) radiation. Data sets were corrected for Lorentz and polarization effects as well as absorption. The criterion for observed reflections is  $I > 2\sigma(I)$ . Lattice parameters were determined from least-squares analysis and reflection data. Empirical absorption corrections were applied using SADABS.<sup>2</sup> Structures were solved by direct methods and refined by full-matrix least-

squares analysis on  $F^2$  using X-SEED<sup>3</sup> equipped with SHELXS<sup>4</sup>. All non-hydrogen atoms were refined anisotropically by full-matrix least-squares on  $F^2$  using the SHELX<sup>4</sup> program. H atoms (for OH and NH) were located in difference Fourier synthesis and refined isotropically with independent O/N-H distances or restrained to 0.85(2) Å. The remaining H atoms were included in idealized geometric positions with  $U_{iso}=1.2U_{eq}$  of the atom to which they were attached ( $U_{iso}=1.5U_{eq}$  for methyl groups). Molecular configurations were compared to both the known chirality of the methylbenzylamine and estimated Flack parameters<sup>5</sup> and where applicable, atomic coordinates were inverted to achieve correct structural configurations. Crystallographic details are provided in section S4 of the Supplementary Information.

## 2.6 <sup>1</sup>H NMR Overlays

<sup>1</sup>H-NMR (acetone-*d*<sub>6</sub>) spectra collected on quasiracemic samples were retrieved from the melt. Overlays of <sup>1</sup>H NMR are provided in the Supplementary Information in section S5.

## 2.7 References

- 1) S. L. Fomulu, M. S. Hendi, R. E. Davis and K. A. Wheeler, *Cryst. Growth Des.*, 2002, **2**, 637.
- 2) G. M. Sheldrick, SADABS and TWINABS—Program for Area Detector Absorption Corrections, University of Göttingen, Göttingen, Germany, 2010.
- 3) L. J. Barbour, *J. Supramol. Chem.*, 2001, **1**, 189.
- 4) G. M. Sheldrick, *Acta Crystallogr., Sect. A: Fundam. Crystallogr.*, 2008, **64**, 112.
- 5) H. D. Flack, *Acta Crystallogr.*, 1983, **39**, 876-881.

## Chapter Three: Supramolecular Tendencies of Sulfamethazine Cocrystals

### 3.1 Sulfa Drug Development

Often in battles such as war, injuries and wounds worsen from bacterial infection. In early conflicts, such as World War I, a lack of modern medicine often led to increased mortality rates because of the inability to effectively treat wounds and the onset of serious conditions such as gangrene. Despite the best efforts by doctors and surgeons in the field many injuries sustained in the field resulted in amputations or even death. With the advance of wound care technology, wartime casualty rates due to bacterial infections nearly disappeared. Gerhard Domagk is generally credited with advancing treatments for infectious diseases that are embraced by modern medicine today.<sup>1</sup> Though now largely overlooked, Domagk's contributions to the field of antibiotics were significant and based on his service in the German Army during World War I. It was at that time he gained critical experience with wound care and the struggles involved with bacterial infection. Following Domagk's time in the military he later pursued and graduated from medical school where his investigations in medicine formally began.<sup>1</sup>

The idea of treating bacterial infections and diseases with the use of synthetic chemicals was a focal point of the Friedrich Bayer Company, a division of IG Farben, in the late 1920s. Following his recruitment, Domagk began working with the Bayer Company in 1927 and focused his efforts on the production of new pharmaceutical drugs. The thrust of Domagk's investigations examined the pharmacology of synthetic drugs using both animals and in vitro studies with a particular emphasis on the extremely contagious strain of Streptococcus, *Streptococcus hemolyticus*.<sup>1</sup>

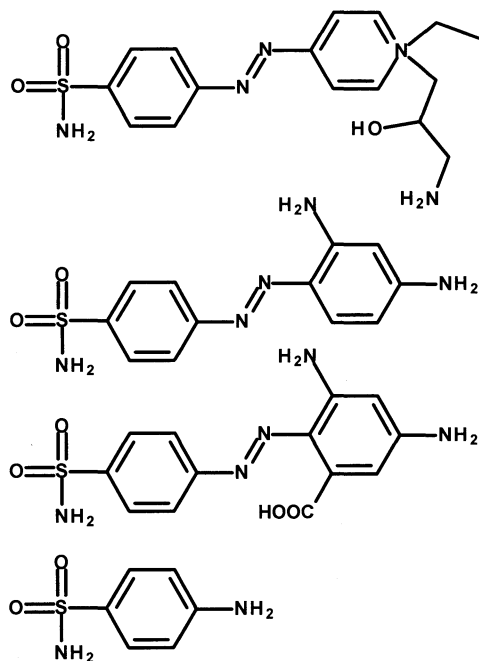


*Figure 3.1: Domagk's Initial Sulfonamide Compounds for Antimicrobial Activity Testing.*

The Bayer Company's initial investigations to obtain antibacterial agents were mostly unsuccessful, however, their efforts eventually resulted in several positive outcomes. While working on a sulfur containing azo dye in 1932, Domagk found this material lacked activity against bacteria *in vitro*, but was successful in protecting mice. Based on these results further synthetic methods optimized the activity of this dye (Figure 3.1). By 1936, the dye, at that time named Protonsil Red, was utilized as an effective treatment for streptococcus in humans.<sup>1</sup>

One of the first uses of Protonsil Red could be defined as unethical, but proved to be of importance in the investigations of its antimicrobial activity. Due to a pinprick Domagk's daughter, had become extremely sick. Through some simple investigation, Domagk was able to determine that her illness was due to a streptococcal infection. Based on his research in the laboratory and the conclusion that the illness derived from



the streptococcus bacteria, Domagk tested the experimental dye on his daughter to determine its effectiveness against bacteria in humans. Though this treatment may have been questionable due to a lack of previous human trials, it resulted in a quick and effective recovery.<sup>2</sup>

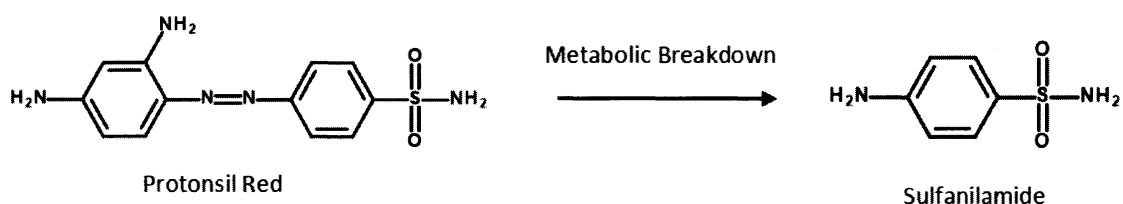


*Figure 3.2: Metabolic Breakdown of Protonsil Red to Sulfanilamide*

Understanding the antimicrobial activity seen in the dye did not occur immediately, but through further investigations evidence suggested that Protonsil Red underwent enzymatic activation in the body resulting in the production of sulfanilamide (Figure 3.2). The conclusion that production of sulfanilamide occurred through a metabolic process helped to explain the initial results that Domagk obtained. In vitro studies suggested that the dye lacked an observable antimicrobial activity, but in living specimen, mice, antimicrobial activity occurred.<sup>2</sup> Building on the discovery of sulfanilamide's antimicrobial activity chemists began developing this newly found therapeutic by synthesizing derivatives that eliminated side effects while at the same time increased drug potency. From the initial discovery in 1935, by 1946 more than 5,000 different variants of sulfa drugs were synthesized.<sup>1,2</sup> The most effective compounds prepared occurred through the modification of the single hydrogen atom located on the SO<sub>2</sub>NH<sub>2</sub> group (Figure 3.2). The synthesized derivatives of sulfanilamide became known as a new family of drugs, the sulfadugs.<sup>2</sup> At the time of their synthesis, the activity of

the sulfa drugs was not completely understood, but their development played a vital role during World War II in fighting the bacterial infections that plagued injuries in prior wars.

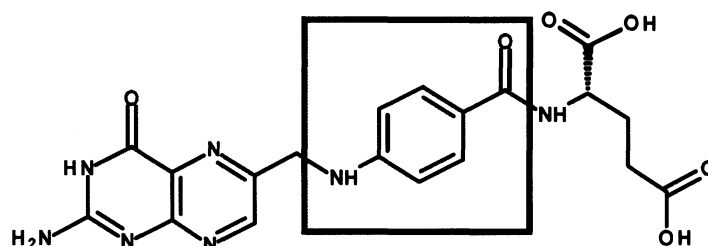


Figure 3.3: Folic Acid.

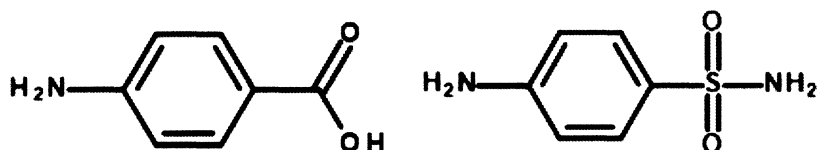
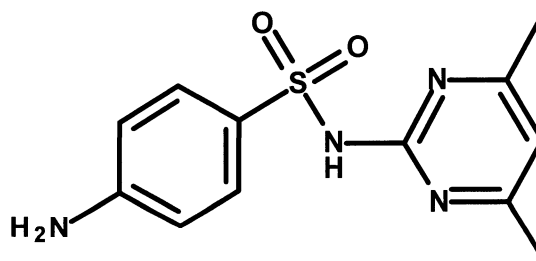


Figure 3.4: *p*-Aminobenzoic Acid and Sulfanilamide.

Today, the factors responsible for the activity of these drugs are known more completely. The enzymatic activity of these drugs is influenced by their molecular topology and the resulting ability to inhibit folic acid production. The production of folic acid (Figure 3.3) by bacteria occurs in bacterial cells by using *p*-aminobenzoic acid.<sup>3,4</sup> When viewing the structure of folic acid, one can see the similarity of *p*-aminobenzoic acid (Figure 3.4) to the portion highlighted in Figure 3.3. The topologies of *p*-aminobenzoic acid and sulfanilamide are remarkably similar to one another. When measuring the steric properties of these two molecules their size varies only by 3% from one another (Figure 3.4). The similar topologies of these two molecules results in the

inability of bacteria to distinguish between sulfanilamide and *p*-aminobenzoic acid that ultimately leads to bacterial death from a lack of folic acid production. These drugs are effective for human consumption due to folic acid being absorbed through food intake and it is not produced in our bodies.<sup>2,3,5</sup> Despite the effectiveness of the sulfa drugs, their use today has decreased significantly due in part to their long-lasting side effects and the development of antibiotic resistant bacteria. Perhaps more importantly is that the investigation of new sulfa antibiotics is largely an area not being explored by the pharmaceutical industry due to other therapeutics showing higher activity with less side effects. Despite lower use rates of these drugs, their study is no less important as their ability to cocrystallize provides insight in to how cofomers can be utilized to optimize the properties of a pharmaceutical. Herein we aim to determine the structural variations that occur within sulfamethazine, a sulfa drug, through the cocrystallization with various substituted benzoic acids.



*Figure 3.5: Amidine Tautomer of Sulfamethazine.*

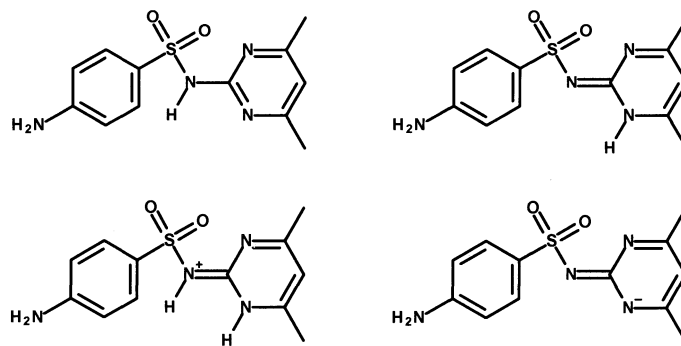


*Figure 3.6: Forms of Sulfamethazine.*

### 3.2 Sulfamethazine Structure and Tautomerization

Sulfamethazine, also known as sulfadimidine or sulfadimethylpyrimidine (Figure 3.5), is a sulfa drug that is used in both human and veterinary medicine for the treatment of bacterial diseases.<sup>6</sup> The structure of sulfamethazine is of particular interest in cocrystallization studies because the pendant functional groups allow for the construction of multiple hydrogen bond interactions. Three acidic protons and five possible acceptor groups provides opportunities for the construction of both intramolecular and intermolecular contacts. The acidic hydrogen atoms present in the structure of sulfamethazine are associated with amine (NH<sub>2</sub>) and the sulfonamide (NH). The acceptor groups are located on the sulfoxy oxygen atoms (SO), the amine (NH<sub>2</sub>), and the two nitrogen atoms found on the pyrimidine ring. Given the strong tendency of these groups to form hydrogen bonds, it is not surprising that sulfamethazine is capable of forming cocrystals with a variety of secondary molecules (coformers). The importance of using coformers is that while the chemical properties of these multicomponent materials can be effectively altered, the pharmacology of the sulfa drug remains intact.<sup>6</sup> Though these investigations commonly cocrystallize the API with benzoic acids and benzamides, there

has been no report on the systematic use of changing coformer acidity to the observed hydrogen bond patterns of the pharmaceutical.<sup>4,6-13</sup>

Despite the strong possibility for variations in hydrogen bonding, sulfamethazine is only known to exist in one polymorphic form.<sup>11</sup> The ability for a pharmaceutical to crystallize as polymorphs is known to have an effect on the chemical properties and bioavailability of the therapeutic agent.<sup>14,15</sup> Due to the presence of the sulfonamide and pyrimidyl groups in the structure of sulfamethazine there is a distinct possibility for tautomerization to occur (Figure 3.6).<sup>6,10,4</sup> Tautomers are isomeric structures that differ in the placement one hydrogen atom and organization of  $\pi$  electrons.<sup>16</sup> The amidine tautomer can be found in the top left of Figure 3.6 while the imidine tautomer is found in the top right. The two remaining tautomers are ions formed from protonation or deprotonation processes. Tautomerization has been shown to be common in compounds containing pyrimidine rings and sulfonamides.<sup>16,17</sup> The ability to control tautomer formation through cocrystallization can greatly impact properties such as lipophilicity, solubility, and bioavailability. The use of coformers has been shown to effect properties of APIs. It has been stated that many molecules of commercial importance are capable of cocrystallizing, but the selection of coformers is of critical importance.<sup>18-21</sup>

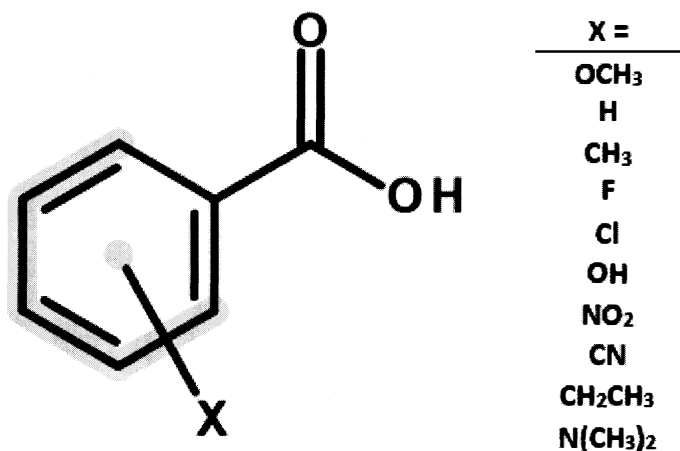


Figure 3.7: Substituted Benzoic Acid Coformers.

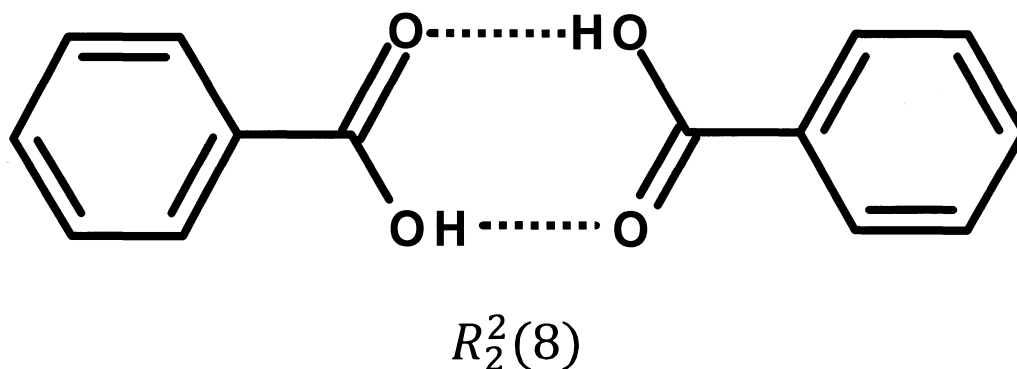


Figure 3.8:  $R_2^2(8)$  Hydrogen Bonding Ring Pattern For Carboxylic Acids Described by Etter.<sup>22,23</sup>

### 3.3 Structural Tendencies of Sulfamethazine and Benzoic Acids

Here we report the investigation of the relationship between coformer acidity and the tautomer form of the active pharmaceutical ingredient, sulfamethazine. We hypothesized that tautomer formation is largely dependent on the acidity of the coformer present in the cocrystallization process. Utilizing single substituted benzoic acids (Figure 3.7), a pKa ranging from 2-5 was obtained for this cocrystallization study. The cocrystallization of these coformers and this active pharmaceutical ingredient resulted in

the formation of intermolecular contacts in the shape of a rings,  $R_2^2(8)$ , as described by Etter (Figure 3.8).<sup>22,23</sup>

Table 3.1: Melting Point of Coformers and Sulfamethazine Cocrystals

<b>Coformer</b>	<b>Acid pK<sub>a</sub></b>	<b>Tautomer Formed</b>	<b>Coformer Melting Point (°C)</b>	<b>Cocrystal Melting Point (°C)</b>
Benzoic Acid	4.19	Amidine	121-122	216-222
<i>o</i> -Nitrobenzoic acid	2.16	Amidine	147-148	166-168
<i>m</i> -Nitrobenzoic acid	3.47	Amidine	140-141	201-204
<i>p</i> -Nitrobenzoic acid	3.41	Amidine	236-238	207-209
<i>o</i> -Methylbenzoic acid	3.91	Amidine	104-105	158-162
<i>m</i> -Methylbenzoic acid	4.27	Amidine	110-112	163-165
<i>p</i> -Methylbenzoic acid	4.35	Amidine	180-181	208-210
<i>o</i> -Fluorobenzoic acid	3.27	Amidine	122-125	187-196
<i>m</i> -Fluorobenzoic acid	3.86	Amidine	122-125	200-204
<i>p</i> -Fluorobenzoic acid	4.14	Amidine	182-184	215-222
<i>m</i> -Chlorobenzoic acid	3.83	Amidine	92-94	173-175
<i>p</i> -Chlorobenzoic acid	3.97	Amidine	242-244	205-208
<i>m</i> -Methoxybenzoic acid	4.09	Amidine	182-184	193-196
<i>p</i> -Methoxybenzoic acid	4.47	Imidine	184-186	174-178
<i>p</i> -Hydroxybenzoic acid	4.57	Imidine	213-215	219-221
<i>p</i> -Ethylbenzoic acid	4.35	Amidine	105-107	195-198
<i>p</i> -Dimethylaminobenzoic acid	4.98	Amidine	241-244	179-183
<i>o</i> -Acetyloxybenzoic acid (Aspirin)	3.49	Amidine	132-135	138-142

A total of 18 sulfamethazine crystallizations were performed using benzoic acid and benzoic acid derivatives to determine the role acidity plays in controlling which tautomer of sulfamethazine is present. To first ensure that the crystals obtained were not starting materials, their melting points were compared to those reported in the literature for sulfamethazine, 198-200°C, and the coformer of the crystal (Table 3.1). Further investigations were performed to determine the identity of the tautomer occurred using single-crystal X-ray diffraction. Of the 18 cocrystal systems surveyed, only two contained the imidine tautomer (*p*-hydroxy and *p*-methoxybenzoic acid).

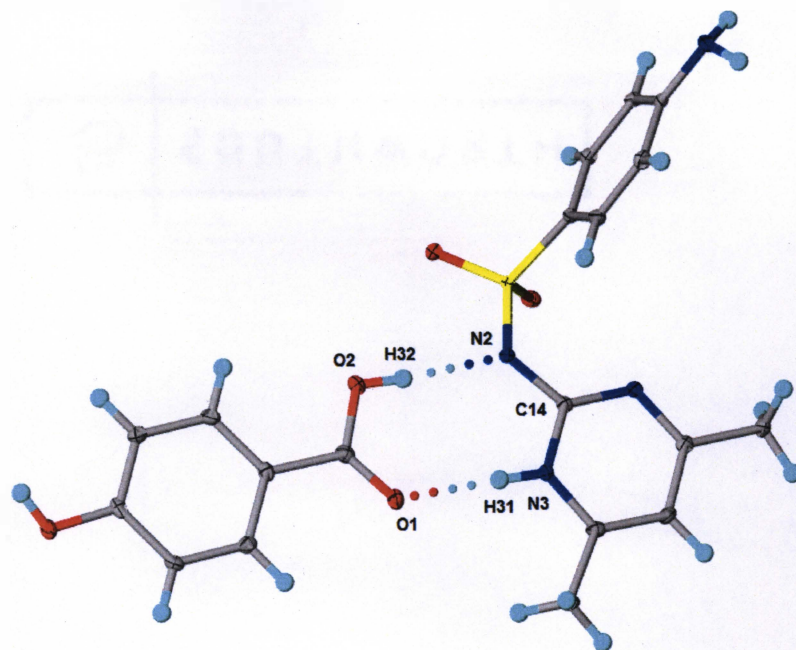


*Figure 3.9: Crystal Structure of the Cocrystal of Sulfamethazine and p-Hydroxybenzoic Acid Showing Thermal Parameters (50% Thermal Ellipsoids) and Hydrogen Bonding.*

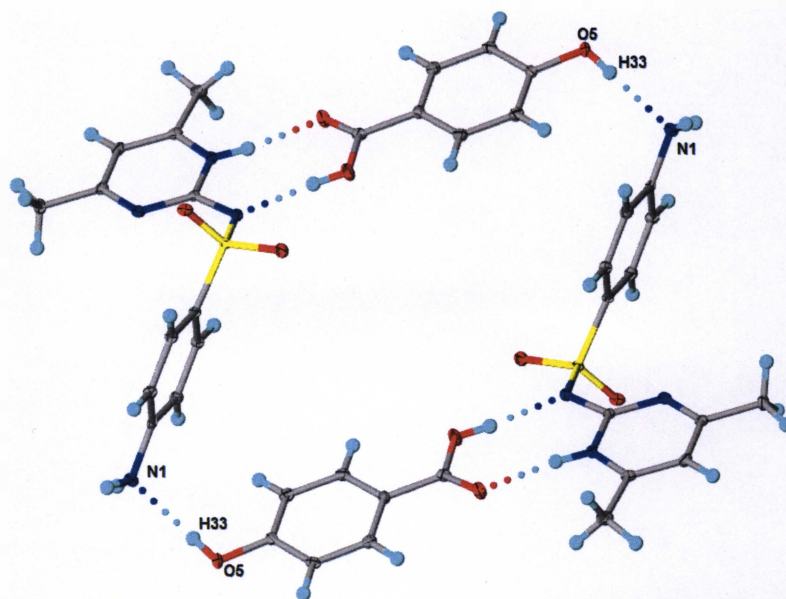


*Figure 3.10: Crystal Structure of the Cocrystal of Sulfamethazine and p-Hydroxybenzoic Acid Showing Thermal Parameters (50% Thermal Ellipsoids) and Hydrogen Bonding Scheme.*



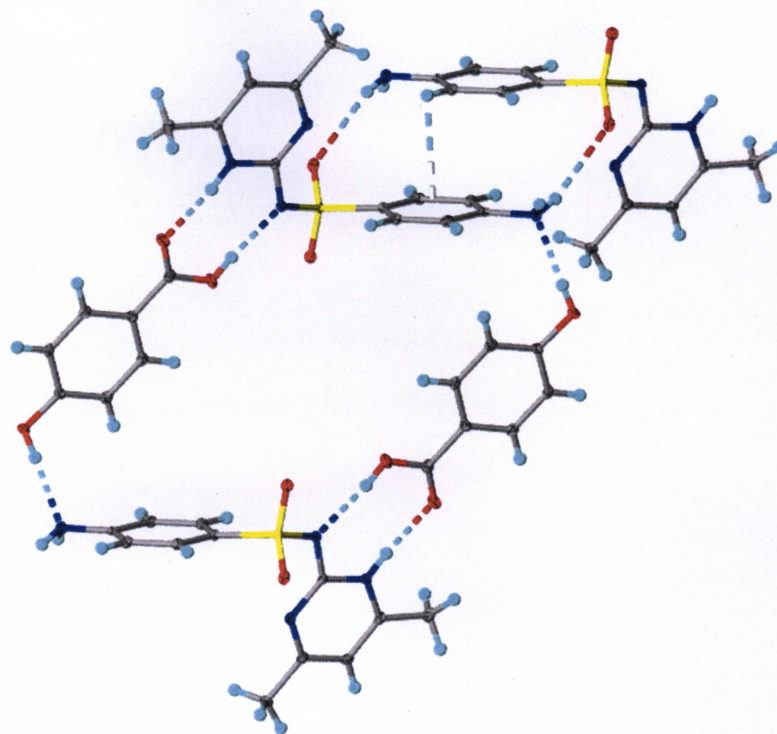


*Figure 3.11: Crystal Structure of the Cocrystal of Sulfamethazine and *p*-Hydroxybenzoic Acid Showing Thermal Parameters (50% Thermal Ellipsoids),  $\pi$ - $\pi$  Stacking, and Hydrogen Bond Scheme.*

The two crystal structures containing the imidine tautomer are of particular interest because of the lack of examples reported in the literature. The cocrystal of sulfamethazine and *p*-hydroxybenzoic acid (Figures 3.9 - 11) had previously been reported.<sup>6</sup> One can observe the presence of the imidine tautomer as well as a  $R_2^2(8)$  hydrogen bond motif involving the carboxylic acid and 2-aminopyrimidine fragment. In addition to this interaction, a  $R_2^2(16)$  hydrogen bond pattern is also observed between two adjacent inversion related sulfamethazine molecules. Due to the presence of the imidine tautomer, bond lengths between C14-N3 and C14-N2 should have distinct distances corresponding to single and double bond lengths of 1.28 and 1.47 Å,

respectively (atom labels shown in Figure 3.9).<sup>24</sup> Analyzing the distances of the C14-N3 and C14-N2 bonds resulted in bond lengths of 1.370 and 1.355 Å, respectively. The bond length between C14-N2 suggests the formation of a double bond and the presence of a single bond between C14-N3. This bonding pattern directly relates to the expected structure of the imidine tautomer (Figure 3.6). In addition to the intermolecular contact involving the carboxylic acid with the sulfonamide nitrogen and the nitrogen of the pyrimidine ring, the hydroxyl group located in the para position also forms a hydrogen bond to N1 of sulfamethazine. This hydrogen bond pattern is shown in Figure 3.10 and extends to neighboring motifs to give a cyclic tetramer. In addition to these hydrogen bonding motifs the packing of this crystal structure involves  $\pi$ - $\pi$  stacking using the aromatic rings of sulfamethazine (Figure 3.11). This intermolecular contact occurs at a centroid...centroid distance of 3.770 Å and an interplanar distance of 3.232 Å for sulfamethazine aromatic groups related by centers of inversion. These combined intermolecular contacts provide a driving force for cocrystal formation that help to stabilize the imidine tautomer.<sup>6</sup>



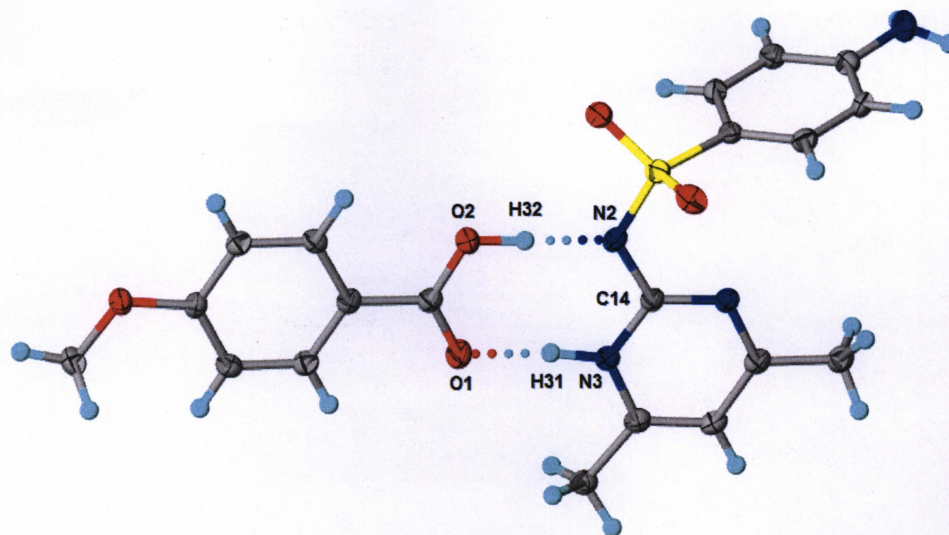


*Figure 3.12: Crystal Structure of the Cocrystal of Sulfamethazine and p-Methoxybenzoic Acid Showing Thermal Parameters (50% Thermal Ellipsoids) and Hydrogen Bonding.*

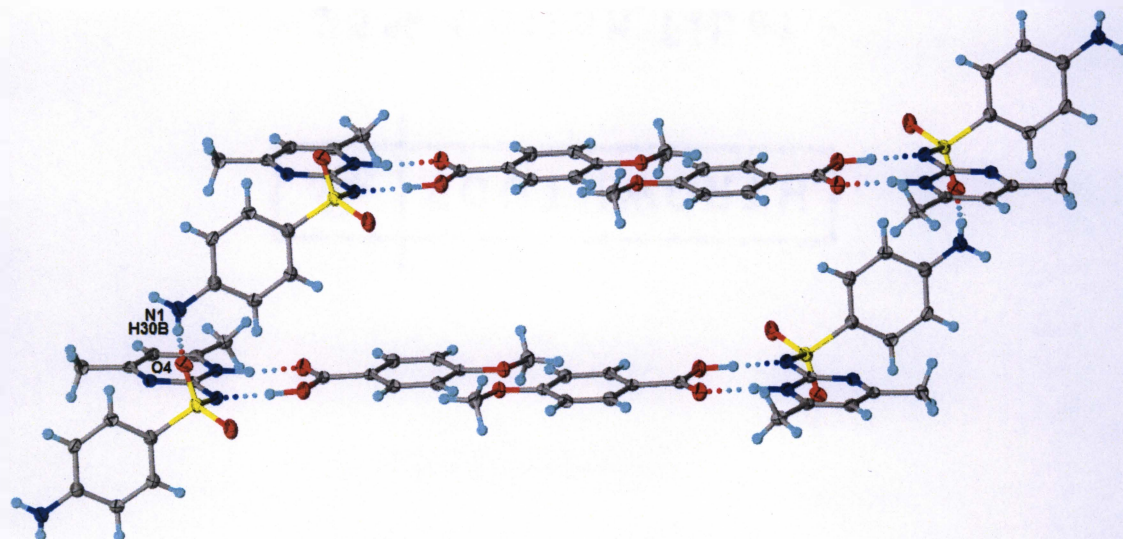


*Figure 3.13: Crystal Structure of the Cocrystal of Sulfamethazine and p-Methoxybenzoic Acid Showing Thermal Parameters (50% Thermal Ellipsoids) and Supramolecular Assembly.*

When comparing the cocrystal structure of *p*-methoxybenzoic acid determined for this thesis work to that of the previously discussed cocrystal structure containing *p*-hydroxybenzoic acid, it is clear they have similar crystal packing patterns with a few

distinct differences (Figure 3.12 and 3.13). This structure contains the same  $R_2^2(8)$ , N2...H32-O2 and N3-H31...O1, hydrogen bonding found in the previous structure, but by replacing the hydroxyl substituent with a methoxy group, the result is the lack of hydrogen bonding at this site. Despite the absence of hydrogen bonding with the methoxy group of the benzoic acid, other molecular associations occur such as a N1-H...O4 C (8) hydrogen-bonded chain that links neighboring sulfamethazine molecules. This intermolecular contact results in a new hydrogen bonding motif that when combined with the  $R_2^2(8)$  contact forms a supramolecular macrocycle consisting of four sulfamethazine and four *p*-methoxybenzoic acid components (Figure 3.13). The overall morphologies of the *p*-hydroxybenzoic acid (cyclic tetramer) and *p*-methoxybenzoic acid (cyclic octamer) cocrystals are similar. One interesting aspect of the *p*-methoxybenzoic acid structure is related to the assembly of adjacent benzoic acids. These molecules serve as a molecular linker for the sulfamethazine components. Though not formally associated by strong hydrogen bonds, these benzoic acid components assemble by use of complementary shapes and close packing directed by inversion symmetry (Figure 3.13). The bridges do not participate in  $\pi$  -  $\pi$  stacking since the closest intermolecular contact is 6.320 Å away. This is also true for the aromatic rings of sulfamethazine. As previously discussed, the imidine tautomer results in differing lengths for the C14-N3 and C14-N2 amidine tautomer bonds and should result in distances consistent with C-N and C=N bonds. The C14-N3 bond length was measured and found to be 1.359 Å, while the C14-N2 bond was 1.356 Å. Though the C14-N2 bond is slightly shorter than the C14-N3 bond, these distances are shorter than that expected for a C-N bond, but longer than a C=N bond. This finding suggests that resonance stabilization impacts the bond

parameters observed in the crystal structure and is due to a mixture of tautomeric forms present in the structure.

Sulfamethazine is not the only sulfa drug capable of existing in more than one tautomeric form. Adsmund and co-workers have shown that a majority of sulfa drugs exist in the amidine tautomer; even so, there are several reported as imidine structures.<sup>4</sup> Their search of the Cambridge Structural Database (CSD) revealed that 39 sulfonamide structures form C (8), N1-H30B...O4, chains. Five of these crystal structures exist with the sulfamethazine component in the amidine tautomeric form. This trend was supported by data generated during this thesis work as 16 of the 18 structures display the amidine tautomer. Additional investigations utilizing the CSD have aimed to determine the preference of the amino and imino tautomer for the API moxonidine. The imino tautomer of moxonidine was found to be lower in energy than the amine tautomer, differing in energy by 5.74 kcal mol<sup>-1</sup>.<sup>16</sup> Interestingly, the tautomer that predominates with moxonidine does not correspond to the dominant tautomer found in sulfamethazine. From the analysis of 180 crystal structures containing (imidazole)imidazolidine-N-alkyl(aryl) fragments, it was found that tautomer stability was dependent on the environment, intra- and intermolecular contacts, and conjugation.<sup>16</sup>

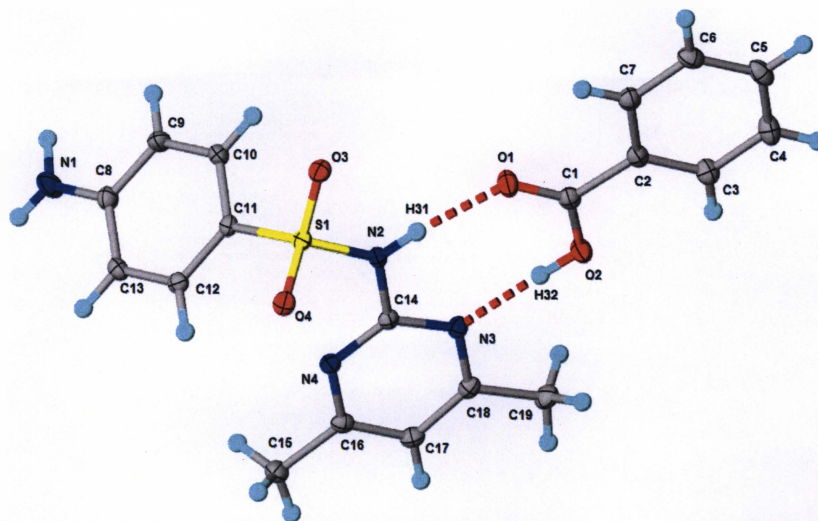


Figure 3.14: Crystal Structure of Sulfamethazine and Benzoic Acid Showing Thermal Parameters (50% ellipsoids) and Labeling Scheme.

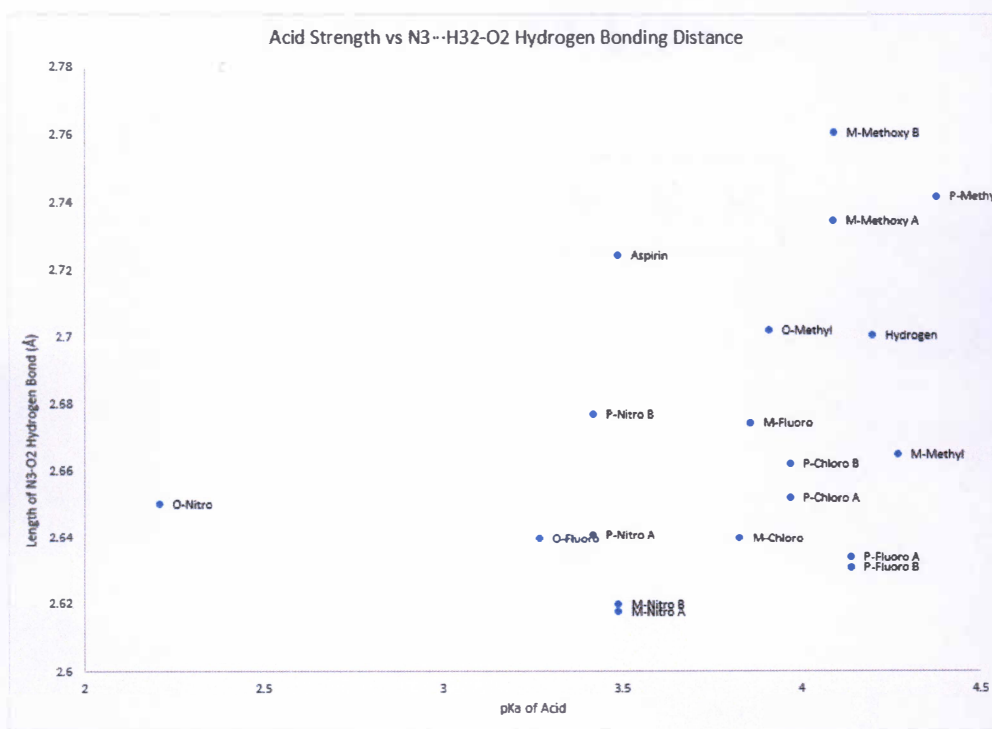


Figure 3.15: Plot Showing the Relationship between Benzoic Acid Strength and N3-O2 Hydrogen Bonding Distance.

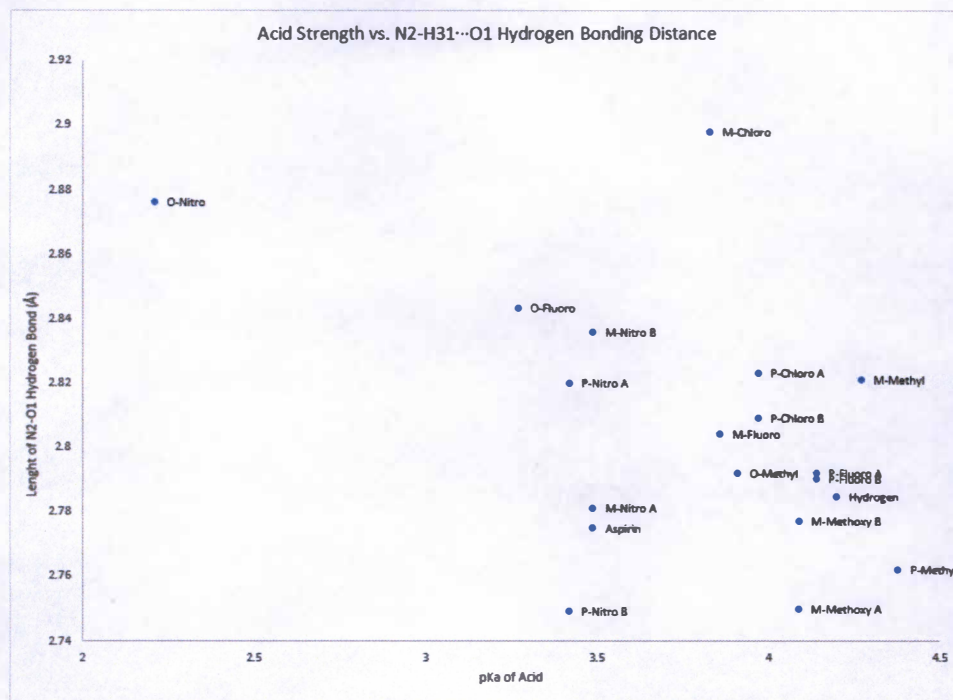


Figure 3.16: Plot Showing Relationship between Benzoic Acid Strength and N2-O1 Hydrogen Bonding Distance.

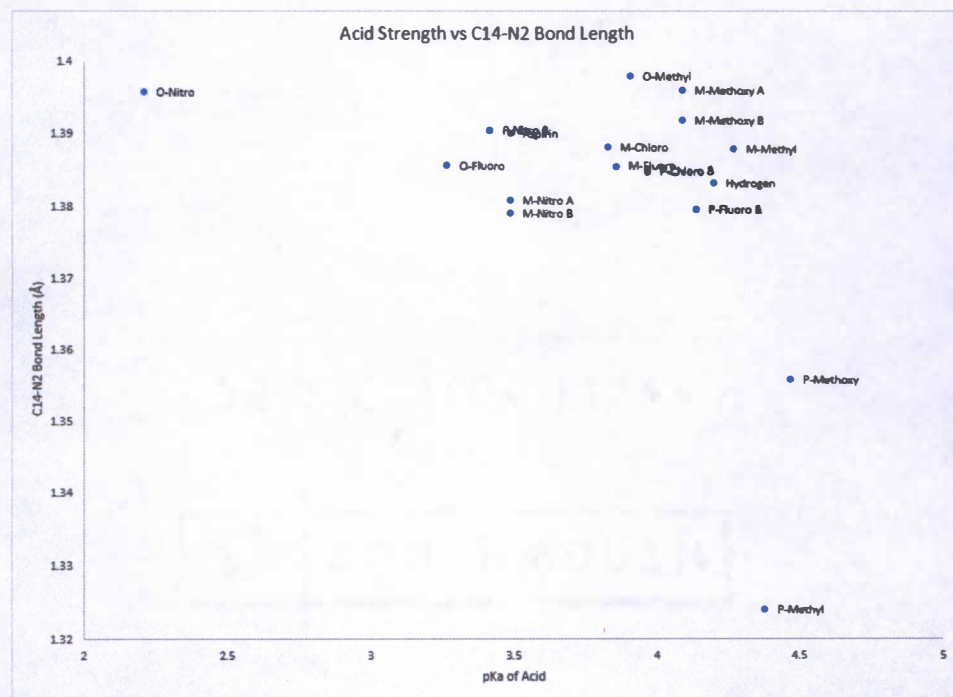


Figure 3.17: Plot Showing Relationship between Benzoic Acid Strength and C14-N2 Bonding Distance.



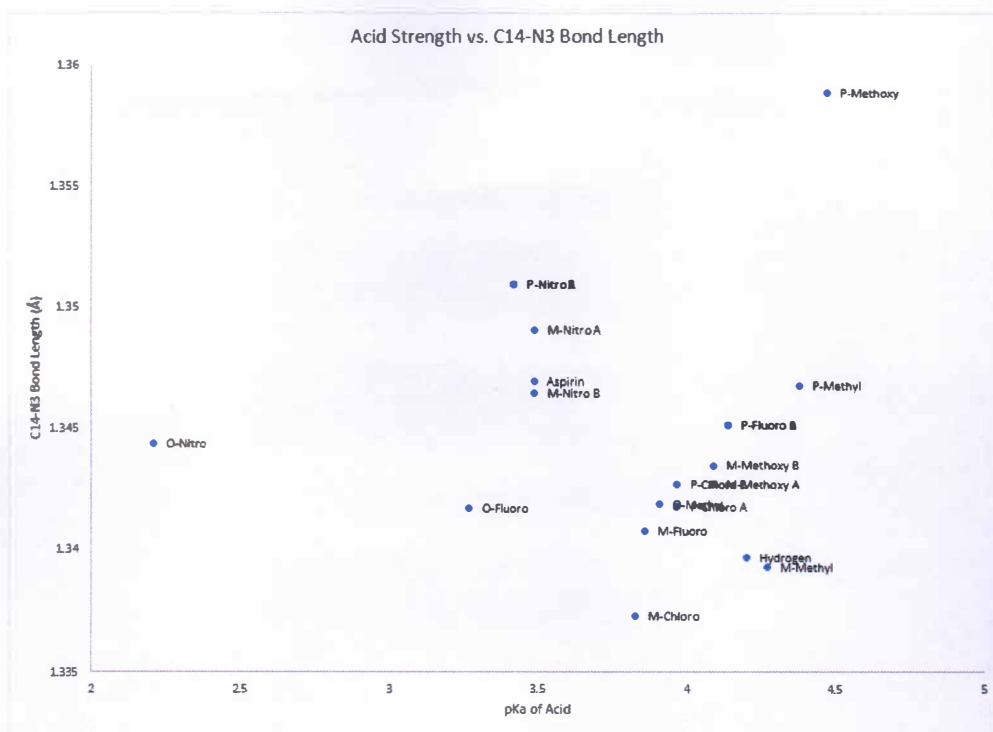


Figure 3.18: Plot Showing Relationship between Benzoic Acid Strength and C14-N3 Bonding Distance.

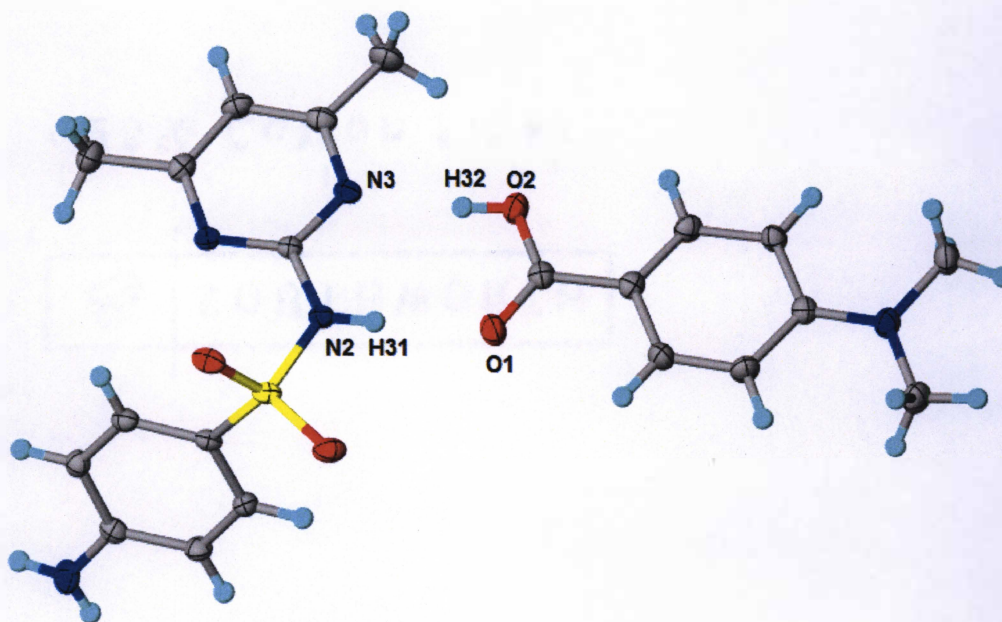
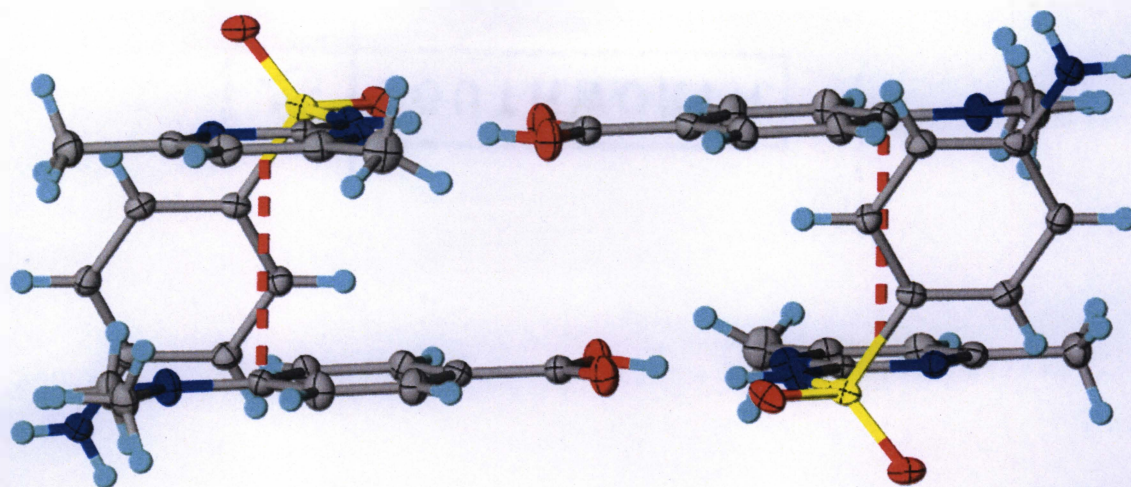


Figure 3.19: Crystal Structure of the Cocrystal of Sulfamethazine and p-Dimethylaminobenzoic Acid Showing Thermal Parameters (50% Thermal Ellipsoids).





*Figure 3.20: Crystal Structure of the Cocrystal of Sulfamethazine and p-Dimethylaminobenzoic Acid Showing Thermal Parameters (50% Thermal Ellipsoids) and  $\pi$  -  $\pi$  Stacking.*

As previously stated, sulfamethazine shows a preference for the amidine tautomer as evidenced by previous studies and data reported in this thesis work.<sup>4</sup> In order to understand how the benzoic acid affects the tautomeric structure of sulfamethazine, an investigation directed at studying a sizable collection of cocrystalline structures was performed. The benzoic acids selected for this investigation are shown in Table 3.1 and differ in substitution pattern (e.g. ortho, meta, para) and functional group properties. By including this diverse set of 18 benzoic acid cofomers, the structural landscape from cocrystallizing these components with sulfamethazine should offer important insight to the structural trends of these bimolecular systems. In addition to understanding the conditions that favor amidine or imidine tautomer formation, this study is also interested in the supramolecular patterns and intermolecular contacts that emerge from investigating sets of related crystal structures

Similar to the imidine tautomer found in the structures containing 4-hydroxy and 4-methoxy benzoic acids, the amidine tautomer was assessed using the N2-H31...O1, N3...H32-O2, C14-N2, and C14-N3 bond lengths (Figure 3.14). This data clearly showed how the acidity of the benzoic acid cofomers effects the molecular structure of sulfamethazine. When first analyzing the  $R_2^2(8)$  hydrogen bonding motif, a clear relationship between the cofomer acidity and sulfamethazine was observed. The N3...H32-O2 contact showed shorter hydrogen bonding distances for more acidic benzoic acids and longer bonds for benzoic acids with lower acidity (Figure 3.15). A similar relationship was found when looking at the other portion of this hydrogen bonding motif. The N2-H31...O1 hydrogen bond showed a similar correlation of intermolecular contact length and benzoic acid acidity (Figure 3.16).

The amidine/imidine tautomerization process is dependent on the placement of electrons, in the form of a double bond, as well as a hydrogen atom. In order to determine the role of the benzoic acid on this process, it is helpful to compare the adjacent C14-N2 and C14-N3 bonds. In the presence of a strongly acidic benzoic acid, the length of the C14-N2 bond was found to be the longest, while this length shortened as the acidity of the benzoic acid decreased (Figure 3.17). A similar relationship occurred through the analysis of the C14-N3 bond. Short bonding distances were found with highly acidic benzoic acids while this bond lengthened as the acidity decreased (Figure 3.18). Inspection of Figures 3.15-18 shows the function of benzoic acid acidity to amidine/imidine tautomer formation that is underscored by assessment of the hydrogen bond and aminopyrimide bond parameters. Two of the least acidic benzoic acids used in this study were the *p*-methoxy ( $pK_a = 4.47$ ) and *p*-hydroxybenzoic ( $pK_a = 4.57$ ) acids.

Both of these conformers produce the imidine tautomer which follows the trend seen with bond lengthening and shortening with acidity. One exception to this structural trend was the structure of *p*-dimethylaminobenzoic Acid ( $pK_a = 4.98$ ) (Figure 3.19 and 3.20).

Despite an elevated  $pK_a$  value, the predominant driving forces responsible for crystal packing is  $\pi - \pi$  stacking (centroid $\cdots$ centroid, 3.683 Å; interplanar distance, 3.477 Å) and the carboxyl $\cdots$ pyrimidyl  $R_2^2(8)$  hydrogen bond (Figure 3.20). Unlike the structures of the hydroxyl and methoxy derivatives that are stabilized by additional hydrogen bonding, this structure does not contain hydrogen bonding that involves the dimethyl amine group.

Other literature reports support the idea that imidine tautomer formation most likely occurs from the use of less acidic conformers with the greatest attention given to benzamide cocrystalline systems.

This study has shown a general structural relationship between acidity of the benzoic acid conformer and tautomer formation. While component acidity and the formation of  $R_2^2(8)$  hydrogen bonds linking the benzoic acid and sulfamethazine are important, they are not the only factors responsible for cocrystal formation. The reported crystal structures are also stabilized by additional intra- and intermolecular contact. It was seen in two cases that the imidine tautomer was stabilized by additional hydrogen bonding of the conformer as well as the sulfamethazine molecule. The structure of the *p*-dimethylaminobenzoic acid cocrystal exists in the amidine form despite an elevated  $pK_a$  and supports the idea that additional contacts are required for the stabilization of the imidine tautomer. Further investigations are needed in order to fully understand the complex interplay of molecular features responsible for amidine/imidine tautomer formation and their role when placed in competitive hydrogen bond environments.

### 3.4 References

- (1) Bentley, R. *J. Ind. Microbiol. Biotechnol.* **2009**, *36* (6), 775–786.
- (2) Le Couteur, P.; Burreson, J. *Napoleon's Buttons: 17 Molecules that Changed History*; Jeremy P. Tarcher/Putnam: New York, 2003.
- (3) Brown, G. *J. Biol. Chem.* **1962**, *237* (2), 536–540.
- (4) Adsmund, D. A.; Grant, D. J. W. *J. Pharm. Sci.* **2001**, *90* (12), 2058–2077.
- (5) Bermingham, A.; Derrick, J. P. *BioEssays* **2002**, *24* (7), 637–648.
- (6) Ghosh, S.; Bag, P. P.; Reddy, C. M. *Cryst. Growth Des.* **2011**, *11* (8), 3489–3503.
- (7) Lu, Jie; Rohani, S. *J. Pharm. Sci.* **2010**, *99* (9), 4042–4047.
- (8) Caira, M. R. *Mol. Pharm.* **2007**, *4* (3), 310–316.
- (9) Caira, M. R.; Nassimbeni, L. R.; Wildervanck, A. F. *J. Chem. Soc. Perkin Trans. 2* **1995**, No. 12, 2213–2216.
- (10) Fu, X.; Li, J.; Wang, L.; Wu, B.; Xu, X.; Deng, Z.; Zhang, H. *RSC Adv.* **2016**, *6* (31), 26474–26478.
- (11) Maury, L.; Rambaud, J.; Pauvert, B.; Lasserre, Y.; Bergé, G.; Audran, M. *J. Pharm. Sci.* **1985**, *74* (4), 422–426.
- (12) Patel, U.; Haridas, M.; Singh, T. P. *Acta Crystallogr. Sect. C Cryst. Struct. Commun.* **1988**, *44* (7), 1264–1267.
- (13) Ucaciuc, R. L.; Onescu, C. I.; Ildervanck, A. W.; Aira, M. R. *C. Anal. Sci.* **2008**, *24*, 87–88.
- (14) Lu, J.; Rohani, S. *Curr. Med. Chem.* **2009**, *16* (7), 884–905.
- (15) Haleblan, J. K.; Borcka, L. *Acta Pharm. Jugosl.* **1990**, *40*, 71–94.
- (16) Babu Nanubolu, J.; Sridhar, B.; Ravikumar, K. *CrystEngComm* **2014**, *16* (46), 10602–10617.

- (17) Yanachkov, I. B.; Wright, G. E. *J. Org. Chem* **1994**, *59* (22), 6739–6743.
- (18) Datta, S.; Grant, D. J. W. *Nat. Rev. Drug Discov.* **2004**, *3* (1), 42–57.
- (19) Patrick Stahly, G. *Cryst. Growth Des.* **2009**, *9* (10), 4212–4229.
- (20) Tiekink, E. R. T. *Chem. Commun.* **2014**, *50* (76), 11079–11082.
- (21) Int, J.; Life, P. *Int. J. Pharm. Life Sci.* **2015**, *6* (3), 4324–4333.
- (22) Etter, M. C.; MacDonald, J. C.; Bernstein, J. *Acta Crystallogr. Sect. B* **1990**, *46* (2), 256–262.
- (23) Etter, M. C. *Acc. Chem. Res.* **1990**, *23* (4), 120–126.
- (24) Kiralj, R.; Ferreira, M. M. C. *J. Chem. Inf. Comput. Sci.* **2003**, *43* (3), 787–809.

## Chapter Four: Molecular Recognition Boundaries of Diarylamide Quasiracemates

### 4.1 Overview of Molecular Recognition

The manner in which molecules recognize each other holds critical importance to nearly every area of science.<sup>1-3</sup> This significance stems from the key underpinning of molecular assembly to our most basic understanding of chemical processes. Whether these interactions relate to small molecule catalytic transformations or complex physiological processes, the structural features responsible for molecular association play into the well-known adage that *form follows function* where material property arises from the collective structural features of the molecular components.<sup>4,5</sup> Because the *form* of chemical systems is derived from a complex blend of covalent and non-bonded contacts, codifying each contributor has become essential for recognizing the functions and potential applications of materials.<sup>6-8</sup> While considerable progress in this area has been realized by isolating and identifying molecular contacts and the structural details of their conditional exceptions, insight to the entire landscape of molecular associations remains an ongoing effort. Some of this challenge rests with chemical features that produce less manageable motifs via ill-defined or weak contacts. Molecular shape is one such feature. Although generally recognized as an important contributor to molecular assembly, the systematic use of topological features as a design element for supramolecular synthesis remains a relatively unexplored area.<sup>9-11</sup> The lack of direct attention to molecular shape largely relates to the intractable nature of this structural feature. To date, virtual screening based on molecular shape similarity has been widely used in drug discovery<sup>12</sup>;

however, surprisingly, no practically useful set of parameters or experiments for probing supramolecular synthesis via topological features exist.

	Group Volume ( $\text{\AA}^3$ )	Group Surface Area ( $\text{\AA}^2$ )
X = H	5.9	6.8
F	7.8	12.1
Cl	19.6	29.0
CN	21.0	32.2
CH <sub>3</sub>	22.3	33.4
NO <sub>2</sub>	23.2	37.0
Br	27.6	37.1
CF <sub>3</sub>	28.9	37.3
OCH <sub>3</sub>	32.6	40.1
I	34.6	45.0
C <sub>6</sub> H <sub>5</sub>	82.9	94.9

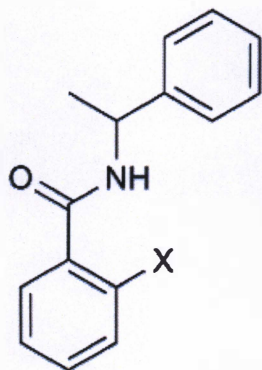


Figure 4.1: Chiral diarylamides Used in the Present Study.

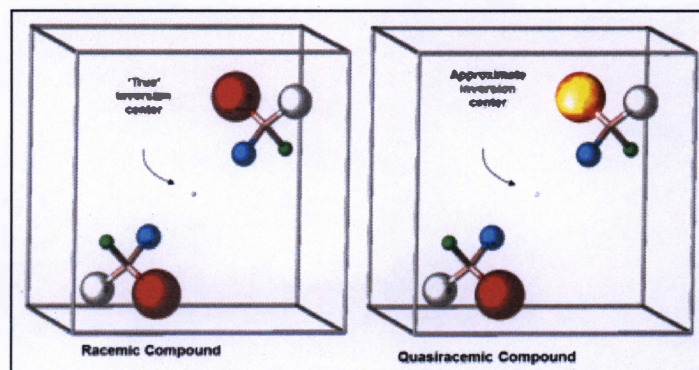


Figure 4.2: Crystal Packing Relationship between Racemic and Quasiracemic Compounds.

## 4.2 Crystal Packing of Racemates and Quasiracemates

Here we report the systematic investigation of the relationship between molecular shape and molecular recognition. We find that an understanding can be effectively achieved by mapping the shape space of quasiracemate fractional crystallization using



structurally simple chiral diarylamides precursors (Figure 4.1). Quasiracemates – pairs of chemically distinct molecules of opposite handedness [*e.g.*, (*R*)-*X* and (*S*)-*X'*]<sup>13</sup> – without exception, cocrystallize with component alignment that mimic the centrosymmetric patterns observed in their analogous racemic counterparts (Figure 4.2).<sup>9,10,14</sup>

This thermodynamic preference provides a key entry point for this thesis study since the complementary shapes of the quasienantiomeric building blocks serve as the primary driving force for these assemblies. The tendency for racemic molecules to assemble with inversion symmetry occurs approximately 92 percent of the time.<sup>15</sup> Such a notion is supported by the diversity of molecular architectures and functional groups represented by the collection of racemic and quasiracemic crystal structures. Using this approach, this program probes the role of molecular shape to the recognition process by surveying the cocrystallization behavior of pairs of quasienantiomeric compounds. It should also be noted that non-bonded contacts (*e.g.*, hydrogen bonds), while often important to the overall molecular recognition process, cannot explain the crystal growth events of racemates or quasiracemates from this study since comparable stabilization may be achieved from homomeric [(*R*)-*X*⋯(*R*)-*X*] or heteromeric [(*S*)-*X*⋯(*R*)-*X* or (*S*)-*X*⋯(*R*)-*X'*] contacts.

Moving beyond the current collection of known quasiracemic systems where component selection often follows pairs of closely related quasienantiomers, our investigation examined a topologically diverse set of related compounds to understand the structural boundaries of quasiracemate formation. A homologous family of *R* and *S* diarylamides that differ incrementally in the size and shape of the pendant substituents was selected for this study – a total of 22 compounds (Figure 4.1). The collection of 2-



substituted components range from  $X = H$  to  $C_6H_5$  with the topological features of these groups approximated using their volumes and surface areas.<sup>16,17</sup>

### 4.3 Substituent Selection and Proof of Concept

The substituents selected and utilized in this study systematically differ in both volume and surface area. In addition to substituent size, the electronic properties of the groups, electron donating and withdrawing abilities, were also considered when selecting the library of compounds for this investigation. Though some substituents included are capable of undergoing non-covalent intra- and intermolecular interactions, the overall strategy of substituent selection targeted groups that minimized such interactions. By excluding groups that have a high likelihood of forming contacts (e.g.  $CO_2H$  and  $OH$ ), the current program offers greater opportunities to define the boundaries of molecular topology to the organization of quasiracemic materials.

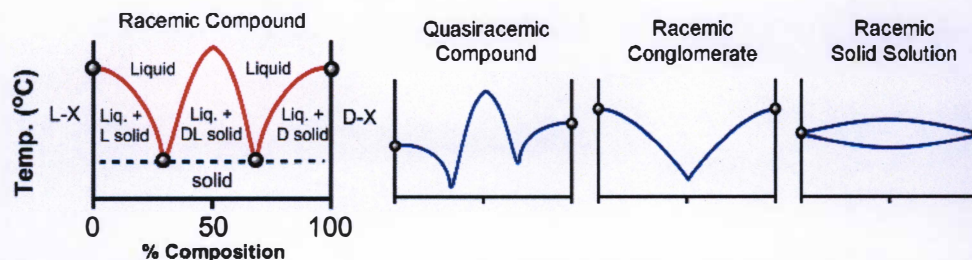
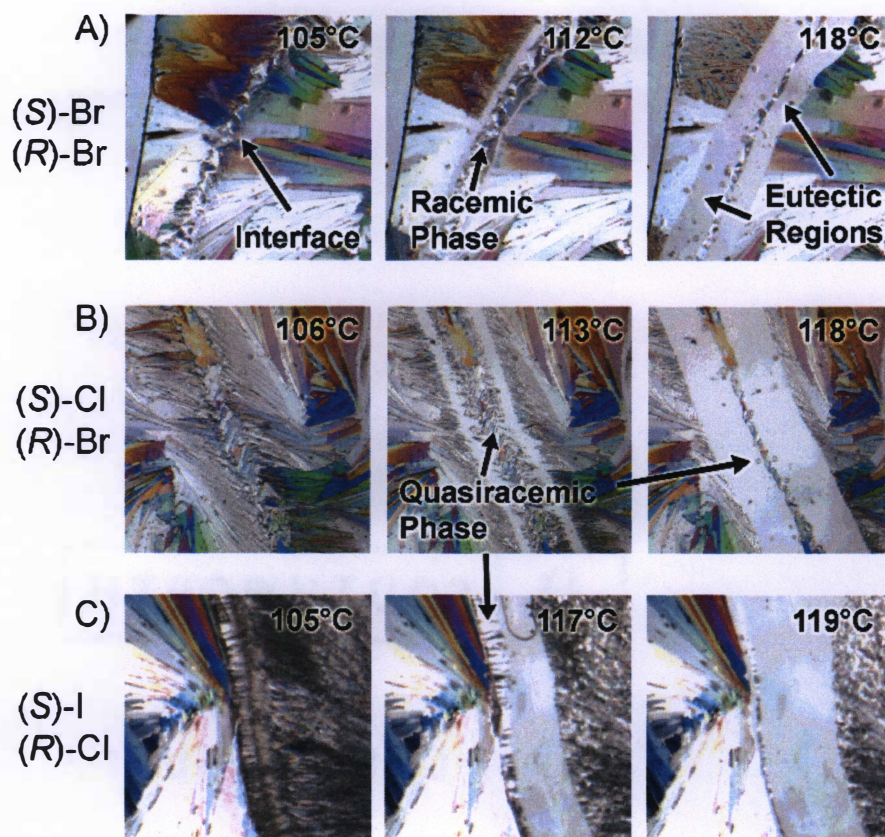


Figure 4.3: Melting Point Phase Diagrams of Idealized Racemic and Quasiracemic Mixtures.



*Figure 4.4: Hot Stage Polarized Light Microscopy Using the A) (S)-Br (left) and (R)-Br (right), B) (S)-Cl and (R)-Br and C) (S)-I and (R)-Br Pairs Showing the Emergence of New Racemic and Quasiracemic Crystalline Phases.*

To exclude the challenges that arise from solvent-assisted crystal growth processes, cocrystallization of pairs of quasisenantiomers was pursued from the melt using the Kofler contact fusion method.<sup>18-20</sup> A utility of this technique draws attention to the formation of new crystalline phases during the heating cycle as indicated by the emergence of melting regions (eutectic regions) in the viewing area. In the case of racemic and quasiracemic mixtures, distinguishing between the various modes of crystallization is possible given the unique thermal signature of each phase (Figure 4.3). For example, the thermal signature of racemic and quasiracemic materials should give way to two eutectic points. This arises since the affinity of enantiomers (or quasisenantiomers) is greater for molecules of opposite handedness than for the same



enantiomer. By contrast, the molecular components of racemic conglomerates have a greater affinity for the same enantiomer, whereas racemic solid solutions have no significant preference for the same enantiomer or the opposite one. The result is that conglomerates and solid solutions give one and no eutectic points, respectively. Figure 4.4A demonstrates the proof-of-concept of this method as applied to the ( $\pm$ )-*N*-(2-bromobenzoyl)methylbenzylamine system. The first snapshot indicates the two racemic components [(*S*)-Br (left), (*R*)-Br (right)] with a distinct interface between the crystalline phases. Video recording with increasing temperature provided an opportunity to view the thermal behaviour of cocrystallization in real-time. The onset of melting of the (*S*)-Br and (*R*)-Br adducts occurs at 112°C with the emergence of the racemic phase at the component interface (Figure 4.4A, center and right micrographs). The identity of this racemic phase was further supported by comparing its X-ray powder pattern to those calculated from the known crystal structures of (*S*)-Br and ( $\pm$ )-Br.<sup>21</sup>

The success of this method as applied to racemic Br suggests that the strategy could also be amenable to probing the molecular recognition profiles of quasiracemic systems. Similar to enantiomers (*S*)-Br and (*R*)-Br, quasienantiomers (*S*)-Cl and (*R*)-Br were thermally processed with video capture using the hot stage technique. Several micrographs of this process are provided in Figure 4.4B with results showing the onset of melting near 113°C for both the (*S*)-Cl (left) and (*R*)-Br (right) components. The complete thermal signature of this process offers an important glimpse into the molecular assembly of this material and highlights the formation of the (*S*)-Cl/(*R*)-Br quasiracemic phase at the interface region.

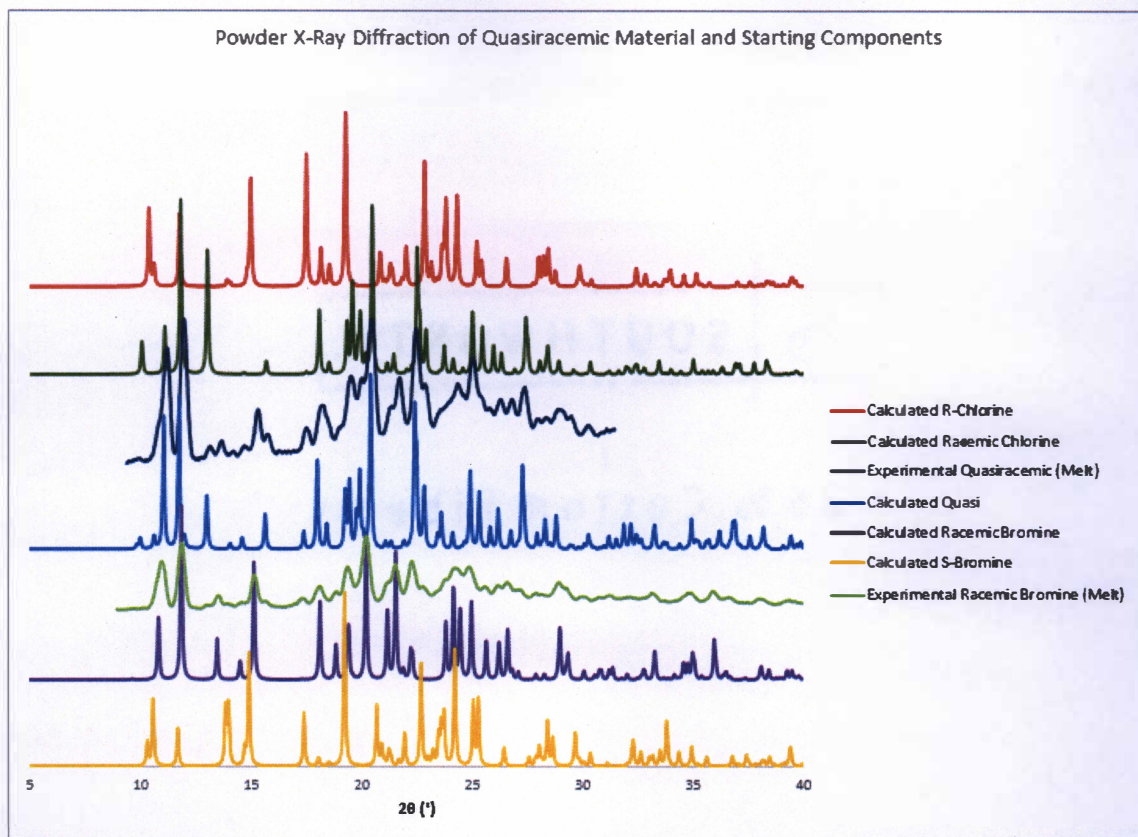


Figure 4.5: Powder XRD of (S)-Cl/(R)-Br Quasiracemate and Related Components.

#### 4.4 Analysing the Melt with Powder X-Ray Diffraction

In addition to utilizing Kofler's contact method, applying the technique of powder X-ray diffraction (PXRD) to this study provided an opportunity to compare the newly obtained crystalline phases from the melt to those simulated using reported crystal structures. The utility of this technique rests with how subtle variations in chemical and crystal structures translate to noticeable differences in the PXRD patterns (Figure 4.5). A comparison of the calculated ( $\pm$ )-bromine powder pattern (purple) determined from the previously reported crystal structure<sup>21</sup> to that of the experimentally derived PXRD data (lime green) shows a close match. The most intense peaks in the purple and lime green



powder patterns can be found at the  $2\theta$  values of 10.9, 11.8, 15.2, 18.1, 20.2, 22.2, 24.2, 28.9, and 35.9°. The (*S*)-Cl/(*R*)-Br quasiracemic phase (navy blue) obtained from the melt was also analysed using powder X-ray diffraction and evaluated in comparison to the calculated powder pattern (royal blue) in Figure 4.5. Like that of the bromine racemate, the Cl/Br quasiracemate showed intense peaks similar to that of the calculated values. Peaks were observed at  $2\theta = 11.0, 11.7, 15.6, 17.9, 20.4, 22.4, 24.9,$  and 27.3°. The similarity between the calculated data and the pattern obtained from the melt supports the formation of this quasiracemic phase using the hot stage microscopy technique. Furthermore, results from these two focused studies show that thermomicroscopy can be used as a viable tool to explore the role topology plays in molecular recognition.

#### 4.5 Topological Differences of Substituents

The appearance of the Cl/Br diarylamide quasiracemic phase was largely anticipated given the crystal structure was previously reported.<sup>21</sup> Furthermore, combining quasienantiomers that differ in Cl and Br substitutions has provided a common theme for other quasiracemate studies.<sup>9,21-23</sup> Though similar in topological features (spherical), a change from Cl to Br represents a 41% increase in substituent volume and an overall increase in diarylamide framework volume of 3%. Evidently, the structural difference imposed by the Cl and Br substituents does not present a sufficient deterrent to quasiracemate formation. Even so, we wondered if expanding the margin of shape space using the Cl/I pair would also achieve similar molecular recognition. The absence of reports featuring Cl/I quasiracemates, significantly different volumes (77% increase for Cl/I and 6% when considering the entire diarylamide framework), and our lack of success



with growing single crystals of  $(S)$ -I/ $(R)$ -Cl *via* solution methods initially suggested that the spatial difference of this substituent pair was beyond the structural boundary for quasiracemate formation. However, pursuing recognition behaviour of the  $(S)$ -I/ $(R)$ -Cl quasienantiomeric pair from the melt yielded key insight to the recognition profile of this system. Inspection of Figure 4.4C reveals a small, but distinct quasiracemic phase appearing at the boundary of the starting materials. This result, like that for the  $(S)$ -Cl/ $(R)$ -Br quasiracemic phase, underscores the importance of the recognition profile of quasienantiomers in forming quasiracemates from the melt.

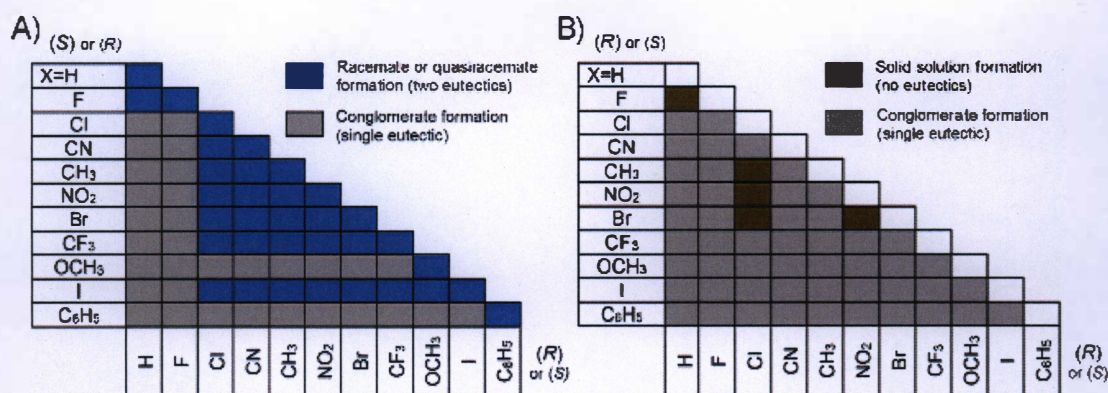


Figure 4.6: Hot Stage Microscopy Results from Combining Diarylamide A) Quasienantiomers and B) Molecular Pairs with the Same Chirality [e.g.  $(R)$ -X and  $(R)$ -X'].

Considering the success of the  $(S)$ -Cl/ $(R)$ -Br and  $(S)$ -I/ $(R)$ -Cl systems, could our hot stage approach be broadly applied as a diagnostic tool for mapping the shape space of quasiracemate assemblies? The collection of diarylamides selected for this study differ incrementally in size and shape and provided 55 unique bimolecular combinations (Figures 4.1 and 6A). Thermally processing all possible sets as before and tabulating these results provided a comprehensive view of the topological landscape for this diarylamide family. It is initially worth noting that heating each enantiomeric pair

resulted in, without exception, the growth of racemic phases where similar shapes of opposing chirality influence crystal formation. Such a structural bias during the heating stage is significant and indicates the relative thermodynamic stability of the racemic phase compared to that of the starting components. This same structural preference should also apply to the formation of the diarylamide quasiracemates. The remaining entries in Figure 4.6A correspond to the thermal signatures of each quasienantiomeric pair. This data is provided in the Supplementary Information (S2) and offers critical insight to those systems where quasiracemic phases form, but also highlights unsuccessful instances as indicated by the appearance of a single eutectic region. Several important trends emerge from this data. Combining (*S*)-H and (*R*)-F diarylamides produced a quasiracemic phase, but conglomerates form from thermal processing other building blocks in the series, presumably owing to a greater difference in the spatial properties of the functional group. It is not surprising the Cl/Br, Cl/CH<sub>3</sub>, Br/CH<sub>3</sub>, NO<sub>2</sub>/CH<sub>3</sub> pairs gave new quasiracemic phases since these sets are topologically similar and have been successfully used with other quasiracemic systems.<sup>9,15,21,22,24</sup> Of interest are also pairs that result in quasiracemates, but are less prevalent in the literature or consist of significantly different shape spaces (*e.g.* Cl/I, CN/CF<sub>3</sub>).

The crystal structures of several (*R*)-X and (*S*)-X' quasienantiomeric pairs that showed quasiracemate formation using the Kofler contact method were pursued. Of particular interest are diarylamide quasiracemic phases containing the trifluoromethyl functional group (Figure 4.6A) such as the NO<sub>2</sub>/CF<sub>3</sub>, CH<sub>3</sub>/CF<sub>3</sub>, and CF<sub>3</sub>/I systems. The significance of these materials is that quasiracemates containing the trifluoromethyl functional group are unknown in the literature. In addition, unlike the Cl/Br combination,

each of the NO<sub>2</sub> (trigonal planar) CH<sub>3</sub>, (tetrahedral), and I (spherical) groups paired with CF<sub>3</sub> correspond to significantly different shapes. The use of the NO<sub>2</sub>/CF<sub>3</sub> quasienantiomers represents a 25% increase in substituent volume and an overall increase in diarylamide framework volume of 2%. Similar to that of the Cl/Br quasiracemate, the CH<sub>3</sub>/CF<sub>3</sub> quasiracemate contain functional groups with nearly identical topologies. Also, the increase in substituent volume (and structural framework) from CH<sub>3</sub> to CF<sub>3</sub> represents a 30% (3%) increase and that for CF<sub>3</sub>/I is 20% (2%). Though the use of group volume information offers a quantitative method for the comparison of substituents and for the prediction of quasiracemate formation, this metric does not provide a direct measure of molecular shape. For example, while the CH<sub>3</sub> (22.3 Å<sup>3</sup>) and NO<sub>2</sub> (23.2 Å<sup>3</sup>) groups have similar volumes their shapes are very different. Though beyond the scope of the current study, mathematical descriptors that allow for easy evaluation of molecular shape are needed to understand the spatial relationship of the groups depicted in Figure 4.6A.

It is worth noting that the phenyl group included in this study provides an important benchmark for quasiracemate assessment. The large substituent volume (96.0 Å<sup>3</sup>) and surface area (94.9 Å<sup>2</sup>) of the C<sub>6</sub>H<sub>5</sub> group should result in conglomerate formation when combined the H → I substituted quasienantiomers. The hot stage micrographs found in the Supplementary Information (S2) corresponding to the phenyl enantiomer clearly show the lack of quasiracemate formation and suggest the spatial properties of phenyl and the other substituents are too great for molecular recognition to occur.



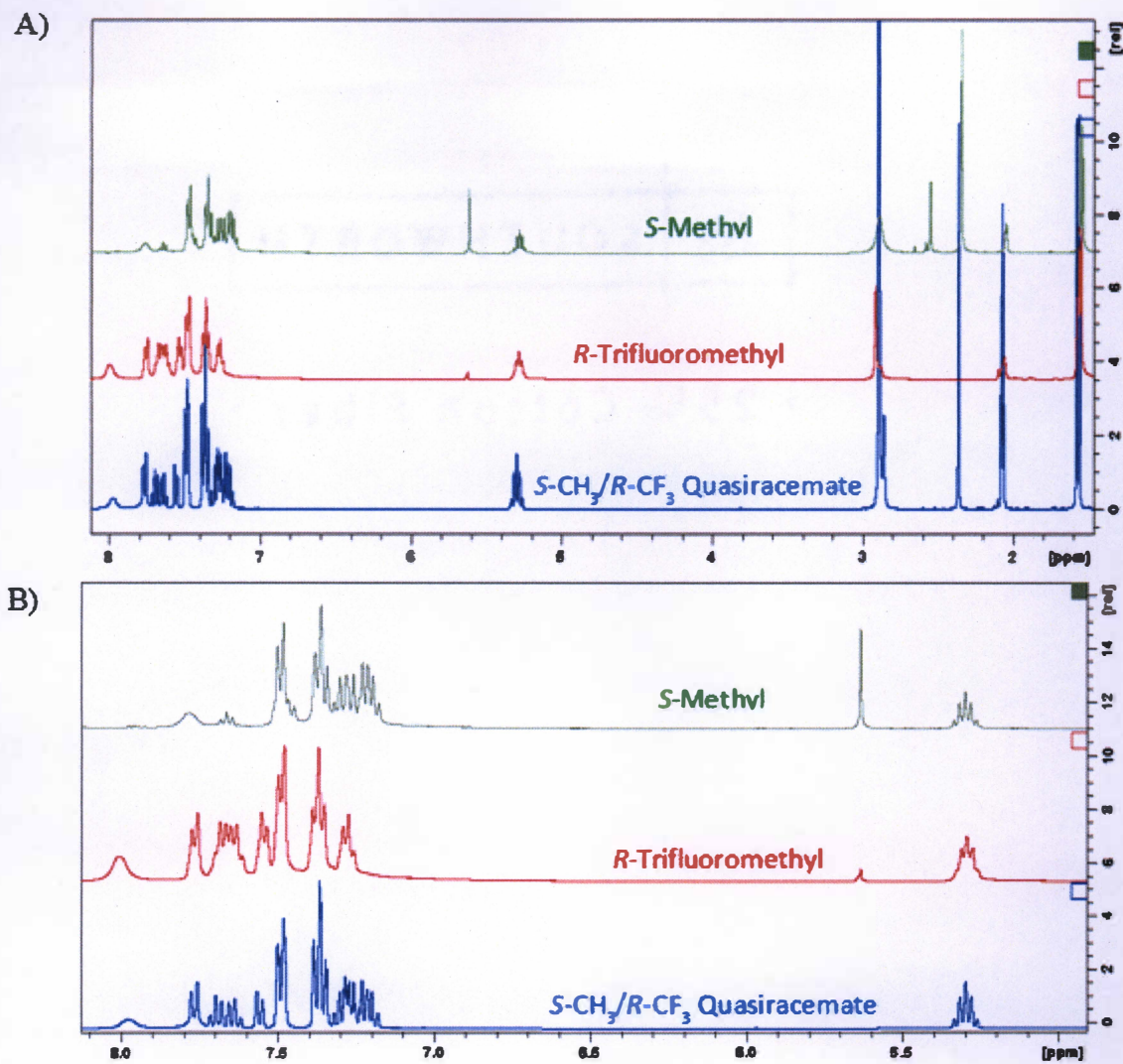


Figure 4.7:  $^1\text{H}$  NMR Overlays of the  $\text{S-CH}_3/\text{R-CF}_3$  Quasiracemate System.

#### 4.6 Analysing the Melt with Nuclear Magnetic Resonance

Since the formation of new crystalline phases does not necessarily signify quasiracemate formation, additional information was also retrieved for several sets of these thermally processed systems. Data retrieved from Nuclear Magnetic Resonance (NMR) studies were utilized to determine the ratios of quasienantiomeric components for several new crystalline phases formed from the melt. This was possible since each

quasienantiomer has a unique spectral signature. One such example was the (*S*)-CH<sub>3</sub>/*(R)*-CF<sub>3</sub> quasiracemic system (Figure 4.7). When comparing the spectral data of the starting components to that of the quasiracemate, one can visually differentiate the signals that correspond to each starting material found in the final quasiracemic product. When comparing the aromatic regions of the starting components to that of the quasiracemate both aromatic regions begin at 7.77 ppm, but the aromatic region corresponding to (*S*)-Methyl terminates at 7.17 ppm while the (*R*)-trifluoromethyl region ends at 7.25 ppm. When comparing the quasiracemate to these regions the aromatic region contains a signal that span 7.77-7.17 ppm. This spectral information supports the quasiracemate phase contains both starting components. More definitive is the signal found at 2.36 ppm (s, 3H, CH<sub>3</sub>). This peak is indicative of the 2-methyl substituent that is not found in the (*R*)-*N*-(2-trifluorobenzoyl)methylbenzylamine component. Peak integrations of this quasiracemic spectral data also helped to determine the 1:1 ratio of these two starting components. The techniques of NMR and powder X-ray diffraction (PXRD) data were also applied to the Cl/Br, CH<sub>3</sub>/CF<sub>3</sub>, NO<sub>2</sub>/CF<sub>3</sub>, Br/CF<sub>3</sub>, and Cl/I pairs and crystal structures were determined or retrieved from the extant database for the H/F, Cl/Br, NO<sub>2</sub>/CF<sub>3</sub>, NO<sub>2</sub>/Br, CH<sub>3</sub>/CF<sub>3</sub>, and CF<sub>3</sub>/I quasiracemates. This data is found in the Supplementary Information (S3-5). This collective information offers key support for the assignment of the quasiracemic phases generated from these hot stage experiments. Additionally, the crystal structures confirmed the role of approximate inversion symmetry (Figure 4.2) in these systems and in several cases provided calculated PXRD patterns for comparison with the hot stage samples. These structures are found in the Supplementary Information (S4). Attempts to grow crystals of other quasiracemic systems using various crystallization techniques and

solvent systems were unsuccessful presumably due to the non-complementary shape features of the components. Other methods for their assessment could be utilized including nuclear magnetic resonance (NMR) and powder X-ray diffraction as previously stated.

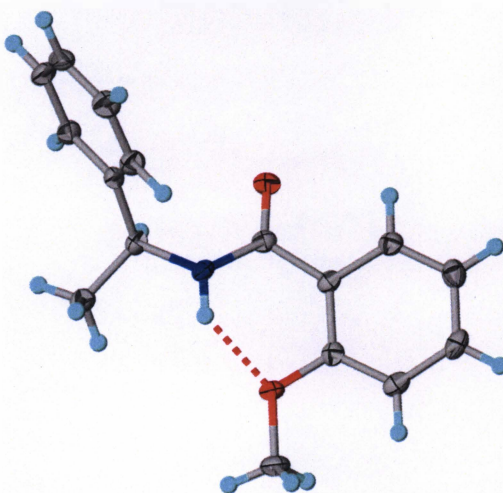


*Figure 4.8: Crystal Structure of (S)-N-(2-methoxybenzoyl)methylbenzylamine Showing Thermal Ellipsoids (50% Probability) and Intramolecular N-H...O Hydrogen Bond.*

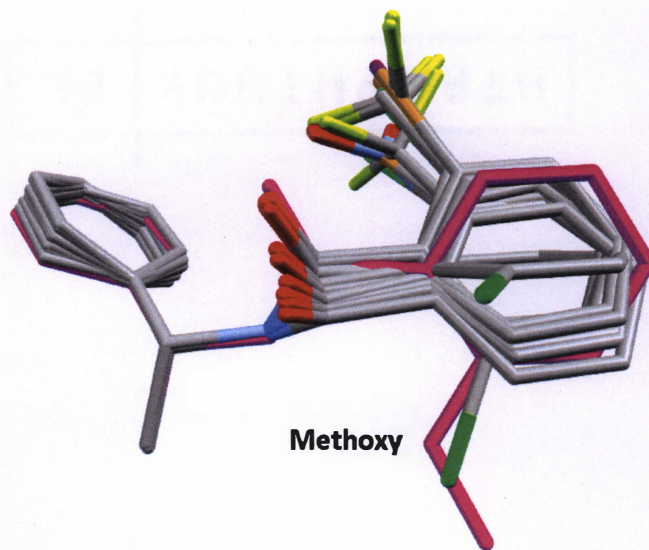


*Figure 4.9: Overlay of 2-Substituted Diarylamides Showing the Conformational Difference of the Methoxy Framework (Pink).*



#### 4.7 Intramolecular Hydrogen Bonding of Substituents

One outlier found in this study was the OCH<sub>3</sub> substituted diarylamide derivative where molecular assembly with the second component only occurs with its enantiomer (Figure 4.8). The only successful cocrystallization occurs with the racemate and suggests the likelihood of this derivative to also form new quasiracemic phases similar to the patterns observed with the other the entries provided in Figure 4.1. Even so, the distinct hot stage signatures corresponding to OCH<sub>3</sub> paired with other quasienantiomers support conglomerate formation likely due to the conformational features of the OCH<sub>3</sub> adduct. Unlike other crystal structures of 2-substituted diarylamides, the structure of (*S*)-OCH<sub>3</sub> is stabilized by an intramolecular N-H $\cdots$ OCH<sub>3</sub> contact (N $\cdots$ O, 2.669(3) Å; N-H $\cdots$ O, 139(3)°). This interaction controls the conformation, and thus topological features of (*S*)-OCH<sub>3</sub> as indicated by a significantly smaller N-C(=O)-C<sub>Ar</sub>-C<sub>Ar</sub> torsion angle (18.4°) compared to other 2-substituted diarylamides (47.5 – 79.9°) (Figure 4.9). N-C(=O)-C<sub>Ar</sub>-C<sub>Ar</sub> torsion angles were retrieved from the Cambridge Structural Database (CSD, Version 1.19) entries LUNPOZ, LUNPOZ01, LUNPUF, LUNQAM, LUNQEQ, LUNQIU and crystal structures of quasiracemates NO<sub>2</sub>/CF<sub>3</sub>, NO<sub>2</sub>/Br, CH<sub>3</sub>/CF<sub>3</sub>, and CF<sub>3</sub>/I.<sup>25</sup> The diarylamide framework with this substituent is unique in comparison to the other entries in Figure 4.6A since the OCH<sub>3</sub> group is capable of forming an intramolecular hydrogen bond. This non-bonded contact changed the outcome of the hot stage experiments by limiting rotation around the amide bond. In the other systems, this same amide torsion angle is likely controlled by crystal packing. The influence of the intramolecular N-H $\cdots$ OCH<sub>3</sub> contact results in the OCH<sub>3</sub> quasienantiomer no longer having a complementary shape to the other quasienantiomers.

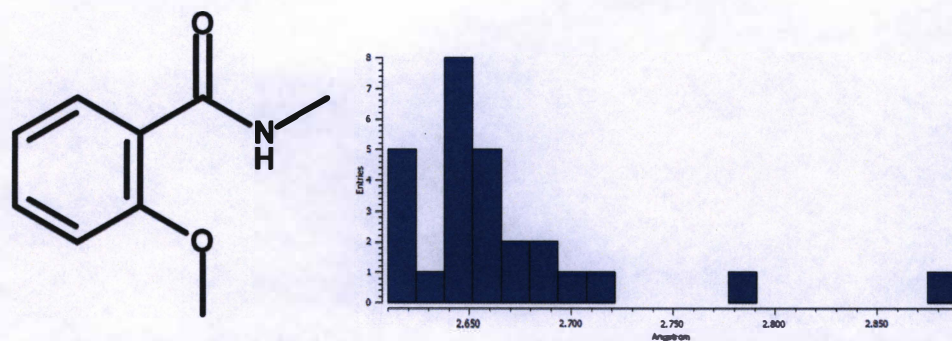


*Figure 4.10: Search Criteria for Methoxy Group in CSD and Resulting Bonding Distances between "O" of Methoxy Functional Group and "N" of Amide Functional Group.*

A search utilizing the CSD for 2-methoxy arylamides resulted in 21 entries using the search query found in Figure 4.10. The N $\cdots$ O bond distances were plotted with the data clustered between 2.60 – 2.70 Å (Figure 4.10). This collection of structural information correlated well with our OCH<sub>3</sub> entry where this same interaction is 2.669(3) Å. This data supports the notion that 2-methoxy diarylamides have a propensity to form intramolecular hydrogen bonds that ultimately control the conformational features of the molecules.

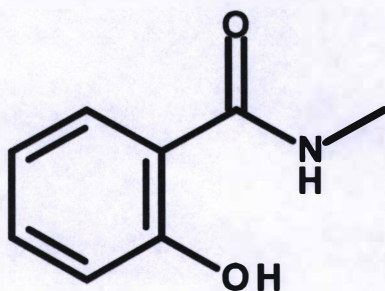


*Figure 4.11: Graphical search criteria of the CSD for 2-hydroxyarylamides.*

The results obtained from this search as well as those collected from our hot stage experiments helped to inform the selection process of substituents as the research program progressed. The inability of the methoxy substituent to form new crystalline phases provided evidence that functional groups capable of intramolecular interactions would likely not promote the formation of quasiracemic phases. One such example of a functional group capable of forming an intramolecular hydrogen bond is an alcohol group (Figure 4.11). Like the  $\text{OCH}_3$  derivative, OH can form intramolecular contacts, but can also serve as a hydrogen bond donor group. For this reason, groups known to form strong hydrogen bonds such as  $\text{NH}_2$  and  $\text{CO}_2\text{H}$  were excluded from this study. A search of the CSD for 2-hydroxy arylamides (Figure 4.11) resulted in 50 entries. The observed orientation of the hydroxyl groups show that additional intramolecular contacts similar to the methoxy adducts is very likely. While investigating the CSD, it was also found that the orientation of the OH substituent has a drastic effect on the formation of intermolecular non-covalent contacts. Analyzing the results of the search in the CSD shows that the formation of a hydrogen bond dictates the orientation of the alcohol group.



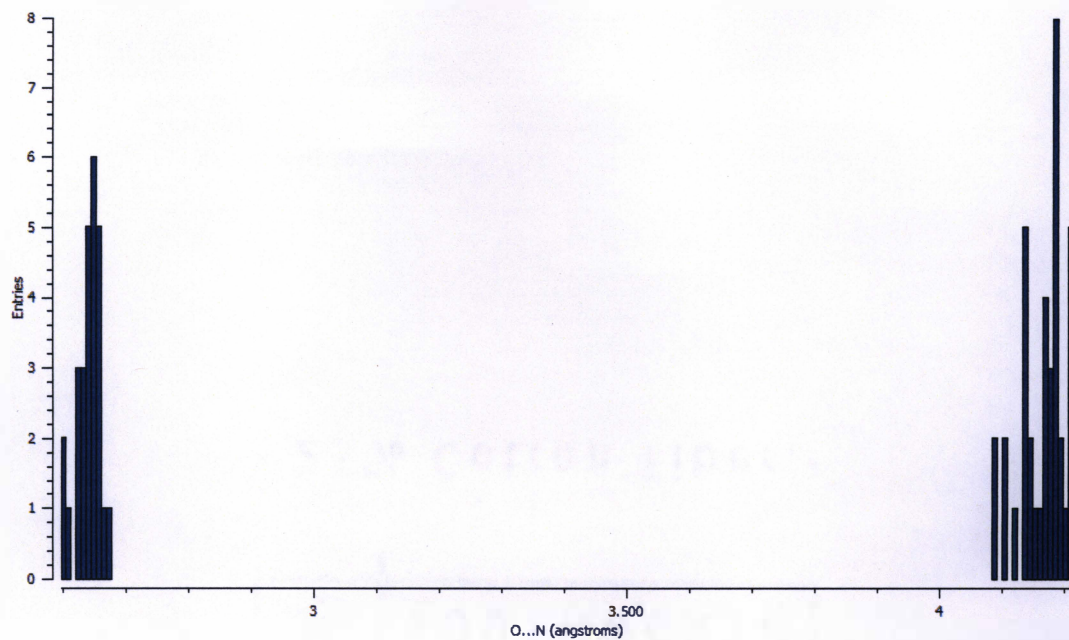


Figure 4.12: A CSD Search Showing O...N Intramolecular Bond Distances for 2-HydroxyArylamides.

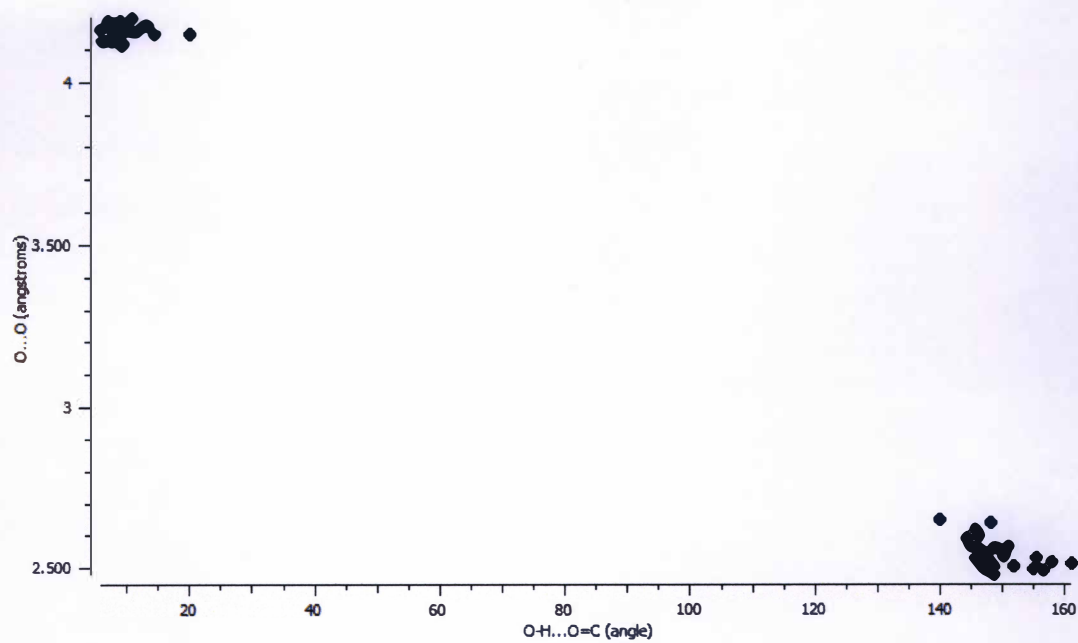
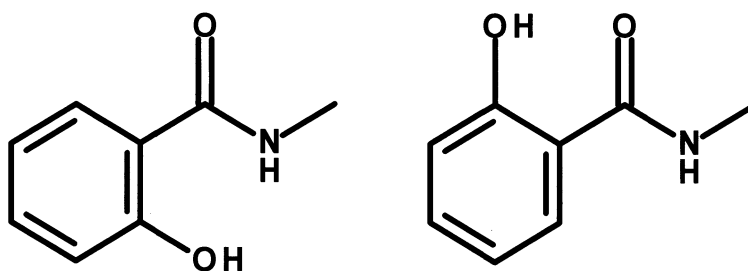


Figure 4.13: Results of CSD Search Showing Correlation of O...O Distance to O-H...O=C Hydrogen Bonding Angle.



*Figure 4.14: Two Orientations for the Hydroxyl Group Observed from a CSD Search.*

The two distinct clusters of entries shown in Figure 4.12 support the idea that intramolecular hydrogen bond formation controls the orientation of the functional group. Twenty-seven entries were found with  $O \cdots N$  distances near 2.6 Å and were in close proximity for hydrogen bond formation to occur while entries at distances greater than 4.0 Å were not involved in intramolecular contacts with the nitrogen of the amide. The remaining 23 entries found as a result of our search contained  $O \cdots O$  distances near 2.5 Å. These findings correlated to hydrogen bonding between the alcohol (-OH) and carbonyl (O=C) with a hydrogen bonding angle of approximately 150° (Figure 4.13). The two orientations of this functional group found from the CSD search are depicted in Figure 4.14. Orientation parallel to the carbonyl results in an  $OH \cdots O$  hydrogen bond while the other orientation results in an  $O \cdots HN$  hydrogen bond. The two orientations of the hydroxyl group are related by a rotation around the single bond between the carbonyl carbon of the amide and the benzene ring. This rotation directly influences intramolecular hydrogen bond formation.



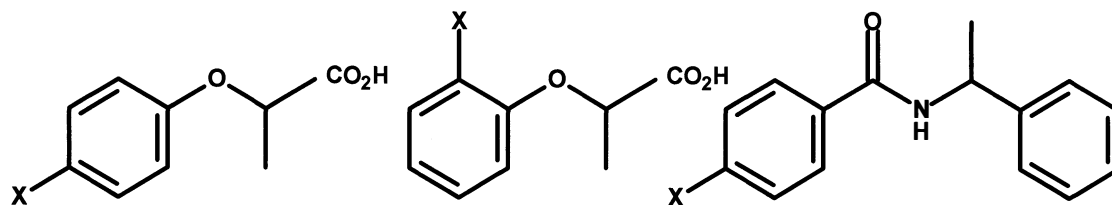


Figure 4.15: Substitution Patterns and Chemical Frameworks of Previously Investigated Quasiracemic Systems.

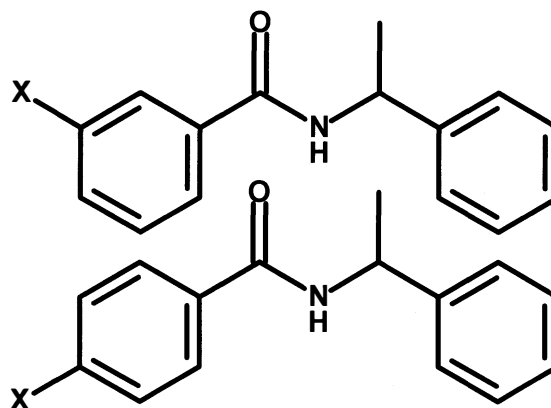


Figure 4.16: Chemical Frameworks Showing meta and para Substituted Diarylamides.

#### 4.8 Importance of Quasiracemate Framework and Substituent Position

Previous investigations of quasiracemic materials have utilized ortho substituted frameworks to generate the desired cocrystalline materials (Figure 4.15).<sup>22</sup> Several of these prior studies also examined meta and para substituted frameworks (Figure 4.15).<sup>26-27</sup> Molecular scaffolds containing hydrogen bond donor and/or acceptor groups are able to influence formation of intra- and intermolecular contacts. Previous investigations in to quasiracemic systems utilizing this scaffold placed the substituents in the para position.<sup>26</sup> However, unlike the current study of ortho substituted arylamides, analogous systems with groups located in the para position are incapable of forming intramolecular contacts with the amide group. The investigation of quasiracemic materials have also utilized substituents placed in the meta position, but this scaffold utilizes oxygen in the backbone

of the scaffold (Figure 4.15).<sup>27</sup> Each of these quasiracemate studies utilized pairs of quasienantiomers with the same substitution pattern – *i.e.*, ortho, meta, or para positions. In an attempt to further define the structural boundaries of molecular recognition for these diarylamide quasiracemic materials, several preliminary investigations showed the results from pairing quasienantiomers that differ in substitution pattern [e.g. 2-(*S*)-X···3-(*R*)-X or 3-(*S*)-X···4-(*R*)-X']. Probing systems in this manner resulted in ortho/meta, ortho/para, and meta/para combinations of substituent positions (Figure 4.16).

*Topologically dissimilar quasiracemates with the same substituent*

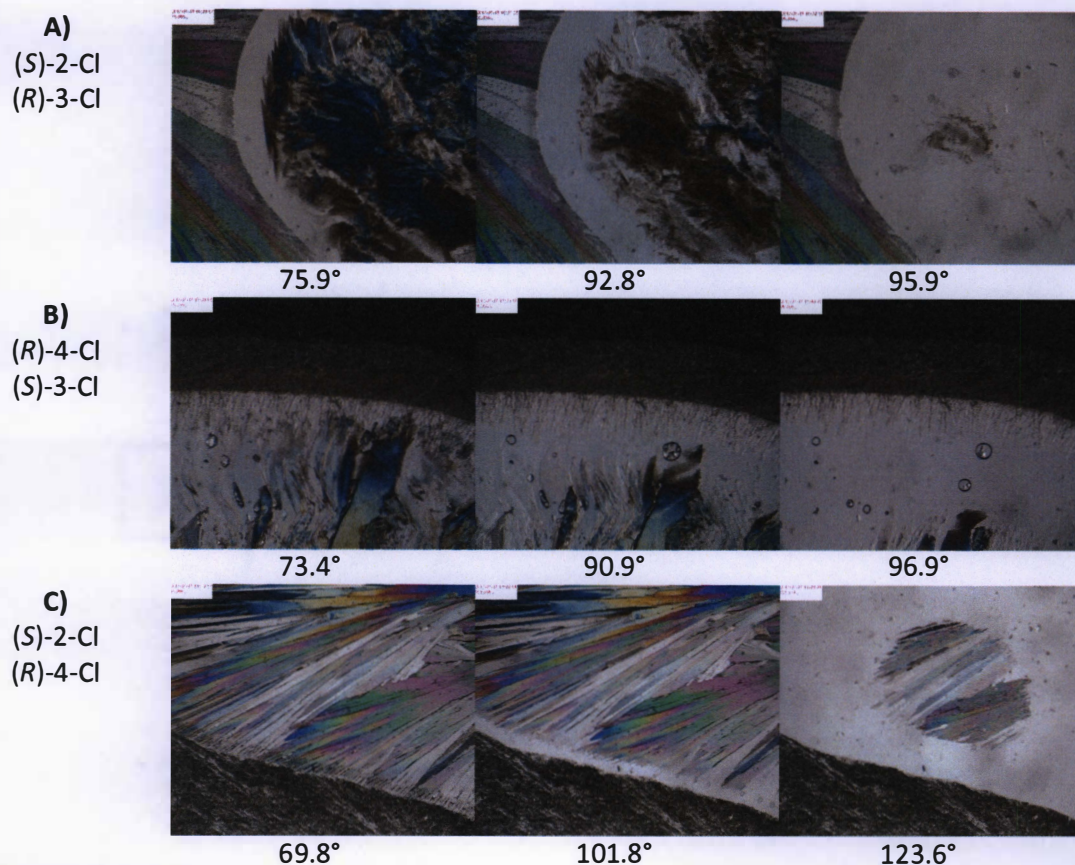
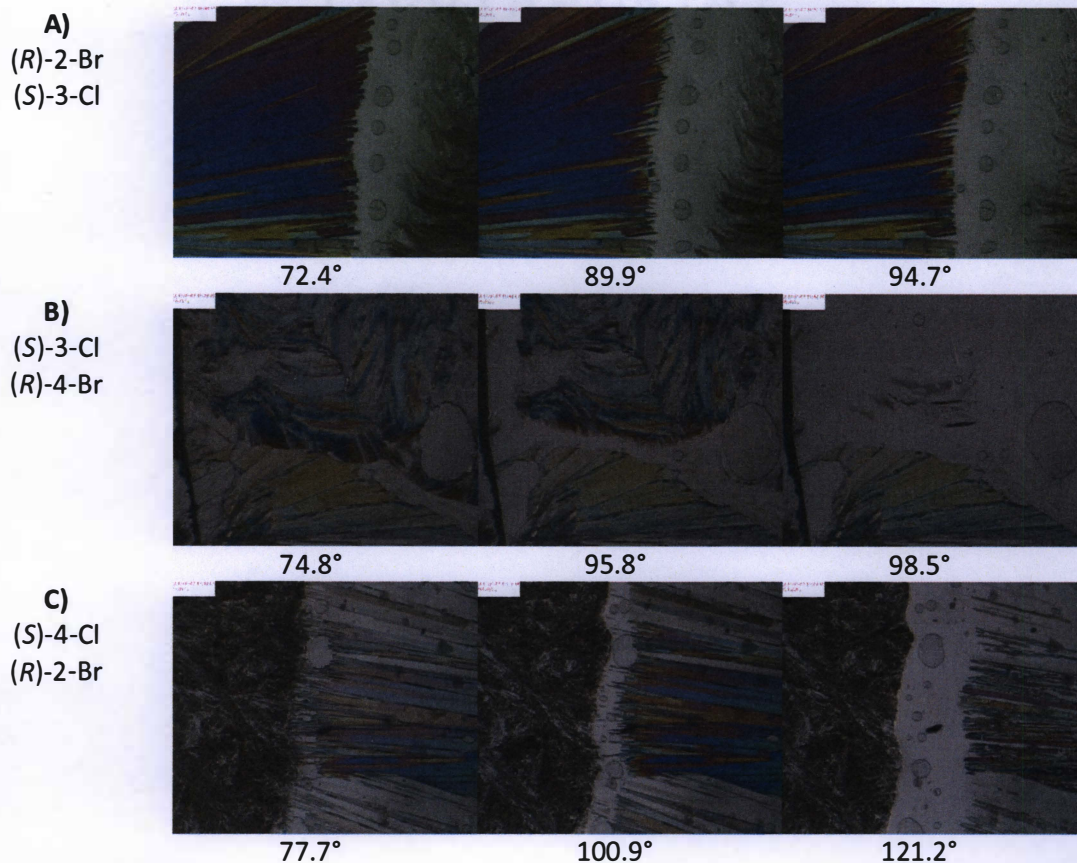


Figure 4.17: Hot Stage Polarized Light Microscopy Using the A) (*S*)-2-Cl (left) and (*R*)-3-Cl (right), B) (*R*)-4-Cl and (*S*)-3-Cl and C) (*S*)-2-Cl and (*R*)-4-Cl Pairs.

*Topologically dissimilar quasiracemates with the differing substituents*



*Figure 4.18: Hot Stage Polarized Light Microscopy Using the A) (R)-2-Br (left) and (S)-3-Cl (right), B) (S)-3-Cl and (R)-4-Br and C) (S)-4-Cl and (S)-2-Br Pairs.*

Initial investigations into these quasiracemic systems began by using the same molecular scaffold with differing substitution patterns; e.g. (-)-*N*-(2-chlorobenzoyl)methylbenzylamine and (+)-*N*-(3-chlorobenzoyl)methylbenzylamine system (Figure 4.17). In addition to looking at materials with the same substituent at different positions, preliminary studies compared systems in which both the functional group identity and position on the scaffold are different. The results of these investigations are provided in Figures 4.17 and 4.18. When comparing the thermal signatures of these hot stage investigations, clear observations are able to be made. In



systems containing both 2-substituted 3-substituted quasienantiomers (Figure 4.17A and 4.18A) a conglomerate is formed with these two components suggesting a lack of molecular recognition. In this case, loading the starting materials on the glass slide with the aid of heat and then cooling the system did not result in contact of the two crystalline phases as with other quasienantiomeric pairs in this study. Rather, these materials formed an amorphous region at the contact interface suggesting these materials are wholly incapable of cocrystal formation. Processing the remaining systems shown in Figures 4.17B-C and 4.18B-C in a similar manner resulted in distinct interfaces between the two crystalline phases. The interface between these two quasienantiomeric components suggests that no recognition occurred and a conglomerate formed. As heat is applied to these systems one can observe the clear development of a single eutectic point. Such thermal behaviour corresponds to a phase diagram of a quasiracemic conglomerate (Figure 4.3).

The inability of the above quasienantiomeric systems to form a new crystalline phase results from the contrasting molecular shapes of the components. Pairing building blocks that differ in substitution pattern evidently provides too large of a spatial variation for quasiracemate formation to occur. The lack of observed recognition extends to molecular pairs constructed using chemically same or different functional groups. Unlike quasienantiomeric systems containing molecular framework with the same substitution patterns, these investigations attempted to determine if a new quasiracemic phase would form between frameworks in which the positioning of the substituent changes. By referring to Figures 4.1 and 4.16, one can see how changing the substituent position greatly modifies the overall shape of the molecules. While this aspect of our hot stage

studies did not produce quasiracemate phases, the outcomes are critical to understanding the structural boundaries of the shape spaces that produce molecular associations. In the context of complementary molecular shapes, pairing components of opposite chirality that differ in substitution patterns exceeds the topological limit needed for cocrystallization to occur with these systems.

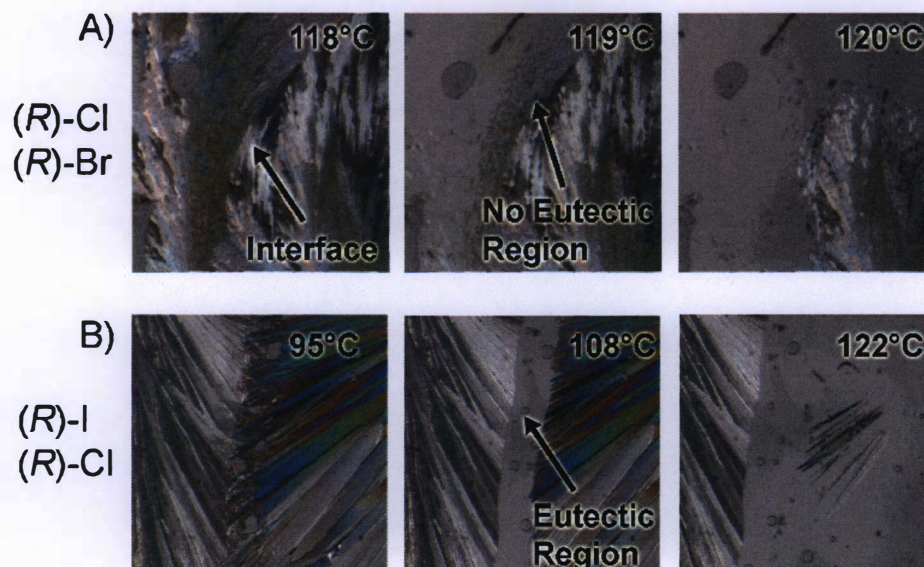


*Figure 4.19: Hot Stage Polarized Light Microscopy Using the A) (R)-Cl (left) and (R)-Br (right) and B) (R)-I/(R)-Br Pairs and Showing the Characteristics of Solid Solution and Conglomerate Crystalline Phase Formation.*

#### 4.9 Molecular Recognition Profiles of Same Handed Quasienantiomers

As shown, the attraction between pairs of quasienantiomers results from their complementary topologies and the thermodynamic consequence of constructing approximate inversion related motifs. Close packing arrangements achieved from these near inversion symmetry motifs are significant and provide sufficient incentive for quasiracemate formation. Even so, what would be the impact by exchanging the handedness of one component of a quasiracemate to give (R)-X and (R)-X' pair [or (S)-X

and (*S*)-X'] and then assessed using the hot stage method? If the pairs were altogether incompatible, then a thermal signature corresponding to a conglomerate should result. However, if comparable affinities of the (*R*)-X or (*R*)-X' molecules exist for the same compound and the other component then the hot stage event will reflect that of a solid solution. Figure 4.19 shows the results from thermally processing the (*R*)-Cl/(*R*)-Br and (*R*)-I/(*R*)-Cl systems. The lack of eutectic region for (*R*)-Cl/(*R*)-Br (Figure 4.19A, solid solution), but its presence in (*R*)-I/(*R*)-Cl (Figure 4.19B, conglomerate) clearly shows the variation with these thermal signatures. Figure 4.6B provides the hot stage results from processing the entire diarylamide family using pairs of components of the same chirality. Interestingly, only five of these entries - H/F, Cl/CH<sub>3</sub>, Cl/NO<sub>2</sub>, Cl/Br, and NO<sub>2</sub>/Br - exhibit solid solution behaviour. Because the structural principles that govern quasisracemic materials do not apply with these systems, hot stage results from (*R*)-X/(*R*)-X' binary mixtures offer a subtler assessment tool of molecular topology.

#### 4.10 Conclusion

In summary, we have developed experimental methods for assessing the structural boundary of molecular shape to molecular recognition. This strategy probes the complementary spatial features of a sizable family of diarylamide (*R*)-X/(*S*)-X' and (*R*)-X/(*R*)-X' pairs *via* hot stage microscopy. The aim of this study established the boundaries of quasisracemate formation. Within this study, the role of topology was defined and its role in molecular recognition highlighted. Compounds capable of undergoing intramolecular interactions resulted in a change of molecular shape and inhibited the formation of new crystalline phases from the melt as shown by our methoxy substituted

system. Results from our study with this substituent influenced the selection of additional compounds included in the library of compounds. One such substituent originally intended to be added to the library of compounds was the hydroxyl (-OH) group. Though the hydroxyl group has a surface area ( $19.3 \text{ \AA}^2$ ) and volume ( $12.6 \text{ \AA}^3$ ) incrementally different from the values reported for fluorine to chlorine, its potential role in intra- and intermolecular hydrogen bonding would obstruct quasiracemate formation.<sup>16,17</sup> A search of the CSD provided information related to the structural conformations of related materials. This exercise showed that hydroxyl groups placed in the ortho position results in the formation of intramolecular hydrogen bonds (Figure 4.14). The ability to form intramolecular contacts with donor/acceptor groups as part of the molecular framework changes the overall topology of the molecule resulting in a lack of molecular association with other quasienantiomers.

The importance of complementary shape was further reinforced by changing the substituent position in this study (Figure 4.16). The results of this study were found in Figure 4.17 and 4.18 in which the thermal behaviour of these systems showed that of a conglomerate system and no observable molecular recognition occurred between the components. Further investigations may contribute to the current understanding of the boundaries of quasiracemate formation by exploring the complete library of meta and para substituted diarylamide frameworks. Such results may prove important since such systems would lack intramolecular hydrogen bonds present in the current study. Moving beyond these systems, the use of multiple substituents attached to the aromatic ring may also prove useful for understanding the impact of systematically changing pendant substituents to molecular recognition.

Without access to effective methods for evaluating molecular shape, this study represents a step forward in determining the role of topology features to molecules assembly. This investigation highlighted the importance of topology in molecular recognition processes. These processes range from small-molecule catalytic transformations to protein-protein interactions in a substrate enzyme complex.<sup>28</sup> Through the use of Kofler's Contact Method a systematic investigation to determine structural boundaries of quasiracemate formation was able to occur. The phenyl substituted system was used as a baseline in this study in which no recognition would occur. A more definitive structural boundary of quasiracemate formation may be defined for each substituent through the addition of other functional groups to the scaffold in this study. The role of topology was exploited and the effect of changing the substituent topology was clearly shown with our methoxy substituted entry. The ability to form intramolecular contacts resulted in an overall change in the topology of the system and impeded the molecular recognition process. The current ability to approximate molecular shape and volume has limitations and new methods must be developed in order to more accurately describe the shape of molecules as previously discussed. Our current ability to approximate volumes does not include a descriptor to shape as shown with the nitro and methyl functional groups. This investigation is an initial step in understanding the role of topology in crystal packing and has been featured in a recent 2017, *Chemical Communications* article.<sup>29</sup> Further investigations must occur for a more complete understanding of this role. Despite this non-covalent interaction being less studied than its counterparts, it is no less important in how molecules recognize one another.



#### 4.11 References

- (1) E. Persch, O. Dumele and F. Diederich, *Angew. Chem, Int. Ed.* **2015**, *54*, 3290.
- (2) E. Mattia and S. Otto, *Nat. Nanotechnol.* **2015**, *10*, 111–119.
- (3) J.-M. Lehn, *Angew. Chem., Int. Ed.* **2013**, *52*, 2836.
- (4) R. Merindola and A. Walther, *Chem. Soc. Rev.* **2017**, DOI: 10.1039/C6CS00738D.
- (5) J.-M. Lehn, *Angew. Chem., Int. Ed.* **1990**, *29*, 1304.
- (6) T. S. Thakur, R. Dubey and G. R. Desiraju, *IUCrJ.* **2015**, *2*, 159.
- (7) G. R. Desiraju, *J. Am. Chem. Soc.* **2013**, *135*, 9952.
- (8) D. B. Varshey, J. R. G. Sander, T. Frišćić and L. R. MacGillivray in *Supramolecular Chemistry: From Molecules to Nanomaterials*, ed. J. W. Steed and P. A. Gale, John Wiley & Sons, Chichester, 2012, vol. 1, p 10-24.
- (9) J. M. Spaniol and K. A. Wheeler, *RSC Adv.* **2016**, *6*, 64921.
- (10) Q. Zhang and D. P. Curran, *Chem. Eur. J.* **2005**, *11*, 4866.
- (11) R. E. Davis, J. K. Whitesell, M.-S. Wong and N. –L. Chang, in *Perspectives in Supramolecular Chemistry: The Crystal as a Supramolecular Entity*, ed. G. R. Desiraju, John Wiley & Sons, Chichester, 1996, vol. 2, chpt. 3.
- (12) A. Nicholls, G. B. McGaughey, R. P. Sheridan, A. C. Good, G. Warren, M. Mathieu, S. W. Muchmore, S. P. Brown, J. A. Grant, J. A. Haigh, N. Nevins, A. N. Jain and B. Kelley, *J. Med. Chem.* **2010**, *53*, 3862.
- (13) A. Fredga, *Bull. Soc. Chim. Fr.* **1973**, *1*, 173.
- (14) S. P. Kelley, L. Fábíán and C. P. Brock, *Acta Crystallogr., Sect. B: Struct. Sci.* **2011**, *B67*, 79.

- (15) M. S. Hendi, P. Hooter, R. E. Davis, V. M. Lynch and K. A. Wheeler, *Cryst. Growth Des.* **2004**, *4*, 95.
- (16) A. Gavezzotti, *J. Am. Chem. Soc.* **1985**, *107*, 962.
- (17) A. Gavezzotti, *J. Am. Chem. Soc.* **1983**, *105*, 5220.
- (18) A. Lemmerer, J. Bernstein, U. J. Griesser, V. Kahlenberg, D. M. Tobbens, S. H. Lapidus, P. W. Stephens and C. Esterhuysen, *Chem. Eur. J.* **2011**, *17*, 13445.
- (19) D. J. Berry, C. C. Seaton, W. Clegg, R. W. Harrington, S. J. Coles, P. N. Horton, M. B. Hursthouse, R. Storey, W. Jones, T. Frišćić and N. Blagden, *Cryst. Growth Des.* **2008**, *8*, 1697.
- (20) L. Kofler and A. Kofler, *Thermal Micromethods for the Study of Organic Compounds and Their Mixtures*; Wagner: Innsbruck, 1952; translated by McCrone, W. C. McCrone Research Institute, Chicago, 1980.
- (21) S. L. Fomulu, M. S. Hendi, R. E. Davis and K. A. Wheeler, *Cryst. Growth Des.* **2005**, *5*, 727.
- (22) A. M. Lineberry, E. T. Benjamin, R. E. Davis, W. S. Kassel and K. A. Wheeler *Cryst. Growth Des.* **2008**, *8*, 612.
- (23) F. Toda, K. Tanaka, H. Miyamoto, H. Koshima, I. Miyahara and K. Hirotsu, *J. Chem. Soc., Perkin Trans. 2*, **1997**, 1877.
- (24) J. T. Cross, N. A. Rossi, M. Serafin and K. A. Wheeler, *CrystEngComm.* **2014**, *16*, 7251.

- (25) The Cambridge Structural Database  
C. R. Groom, I. J. Bruno, M. P. Lightfoot and S. C. Ward, *Acta Cryst.* **2016**, *B72*, 171-179.
- (26) Hendi, M. S.; Hooter, P.; Davis, R. E.; Lynch, V. N.; Wheeler, K. A. *Cryst. Growth Des.* **2004**, *4* (1), 95-101.
- (27) Breen, M. E.; Tameze, S. L.; Dougherty, W.G.; Kassel, W. S.; Wheeler, K. A. *Cryst. Growth Des.* **2008**, *8* (2), 3863-3870.
- (28) Coleman, R. G.; Sharp, K. A. *J. Chem. Inf. Model.* **2010**, *50*, 589-603.
- (29) Tinsley, I. C.; Spaniol, J. M.; Wheeler, K. A. *Chem. Commun.* **2017**, *53* (33), 4601–4604.

## Supplementary Information

<b>Table of Contents</b>	<b>Page</b>
<b>S1</b> - Cocrystals of Sulfamethazine	93
<b>S2</b> - Hot Stage Thermomicroscopy	209
<b>S3</b> - X-ray Crystallography – Powder Diffraction	234
<b>S4</b> - X-ray Crystallography – Single-Crystal Diffraction	238
<b>S5</b> - <sup>1</sup> H NMR Overlays	244
<b>S6</b> - Functional Group and Chemical Framework Volume and Surface Area Comparisons	246
<b>S7</b> – References	248

## S1. Cocrystals of Sulfamethazine

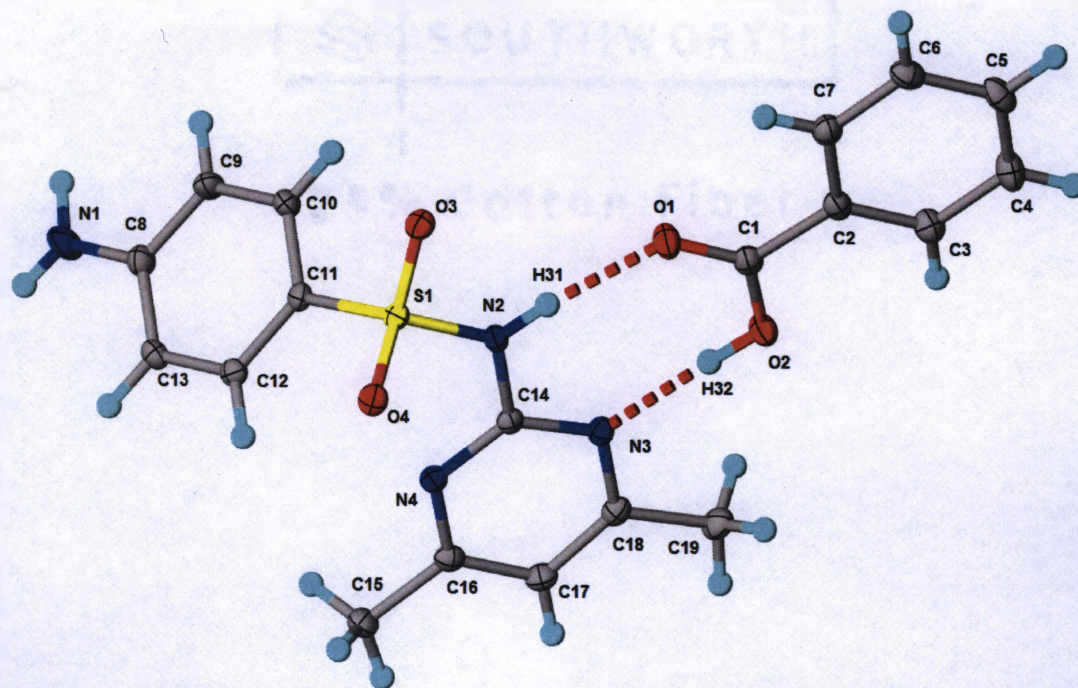


Figure S.1: Crystal Structure of the Cocrystal of Sulfamethazine and Benzoic Acid Showing Thermal Parameters (50% Thermal Ellipsoids) and Hydrogen Bonding.

### Crystal data

$C_{19}H_{20}N_4O_4S$

$M_r = 400.45$

Orthorhombic, *Pbca*

$a = 9.6808(4) \text{ \AA}$

$b = 15.6559(7) \text{ \AA}$

$c = 25.3269(11) \text{ \AA}$

$V = 3838.6(3) \text{ \AA}^3$

$Z = 8$

$F(000) = 1680$

$D_x = 1.386 \text{ Mg m}^{-3}$

Melting point: 489-495 K

Cu  $K\alpha$  radiation,  $\lambda = 1.54178 \text{ \AA}$

Cell parameters from 9967 reflections

$\theta = 2.8\text{--}68.2^\circ$

$\mu = 1.79 \text{ mm}^{-1}$

$T = 100 \text{ K}$

Blocks/Plates, colourless

$0.40 \times 0.24 \times 0.24 \text{ mm}$

Bruker APEXII CCD  
 diffractometer  
 Radiation source: fine-focus sealed tube  
 Detector resolution: 8.33 pixels mm<sup>-1</sup>  
 phi and omega scans  
 Absorption correction: multi-scan  
 SADABS2014/7, Bruker AXS  
 $T_{\min} = 0.640$ ,  $T_{\max} = 0.753$   
 54728 measured reflections

3513 independent reflections  
 3247 reflections with  $I > 2\sigma(I)$   
 $R_{\text{int}} = 0.049$   
 $\theta_{\max} = 68.2^\circ$ ,  $\theta_{\min} = 3.5^\circ$   
 $h = -11 \ 11$   
 $k = -18 \ 18$   
 $l = -30 \ 30$

## Refinement

Refinement on  $F^2$

Least-squares matrix: full

$$R[F^2 > 2\sigma(F^2)] = 0.031$$

$$wR(F^2) = 0.084$$

$$S = 1.07$$

3513 reflections

271 parameters

4 restraints

0 constraints

Hydrogen site location: mixed

H atoms treated by a mixture of independent and constrained refinement

$$w = 1/[\sigma^2(F_o^2) + (0.0376P)^2 + 2.7022P]$$

$$\text{where } P = (F_o^2 + 2F_c^2)/3$$

$$(\Delta/\sigma)_{\max} = 0.001$$

$$\Delta\rho_{\max} = 0.35 \text{ e } \text{\AA}^{-3}$$

$$\Delta\rho_{\min} = -0.43 \text{ e } \text{\AA}^{-3}$$

Extinction correction: none

## Fractional atomic coordinates and isotropic or equivalent isotropic displacement parameters ( $\text{\AA}^2$ )

	x	y	z	$U_{\text{iso}}^*/U_{\text{eq}}$
S1	0.34937 (4)	0.48543 (2)	0.34325 (2)	0.01544 (11)
O1	0.28955 (12)	0.37770 (7)	0.47690 (4)	0.0254 (3)
O2	0.47629 (12)	0.36057 (7)	0.52793 (4)	0.0225 (2)
H32	0.517 (3)	0.3845 (15)	0.5020 (8)	0.062 (8)*
O3	0.20724 (11)	0.47422 (7)	0.35829 (4)	0.0199 (2)
O4	0.40224 (11)	0.43144 (7)	0.30213 (4)	0.0207 (2)
N1	0.42642 (18)	0.84446 (9)	0.28043 (6)	0.0338 (4)
H30A	0.4847 (19)	0.8604 (12)	0.2579 (7)	0.032 (5)*
H30B	0.379 (2)	0.8843 (11)	0.2975 (7)	0.032 (5)*
N2	0.43169 (13)	0.46710 (8)	0.39891 (5)	0.0170 (3)
H31	0.3839 (19)	0.4425 (12)	0.4230 (7)	0.034 (5)*
N3	0.62053 (13)	0.44154 (8)	0.45161 (5)	0.0171 (3)
N4	0.64793 (13)	0.49792 (8)	0.36457 (5)	0.0172 (3)
C1	0.34461 (16)	0.35113 (9)	0.51747 (6)	0.0194 (3)
C2	0.26427 (16)	0.30532 (9)	0.55888 (6)	0.0187 (3)
C3	0.32589 (17)	0.27620 (10)	0.60510 (6)	0.0232 (3)
H3	0.4221	0.2841	0.6107	0.028*
C4	0.24552 (19)	0.23531 (10)	0.64303 (6)	0.0267 (4)
H4	0.2872	0.2145	0.6744	0.032*
C5	0.10513 (18)	0.22497 (10)	0.63513 (6)	0.0247 (4)
H5	0.0505	0.1979	0.6614	0.030*
C6	0.04380 (17)	0.25402 (10)	0.58891 (6)	0.0238 (3)
H6	-0.0526	0.2468	0.5836	0.029*
C7	0.12334 (17)	0.29344 (10)	0.55076 (6)	0.0221 (3)
H7	0.0818	0.3125	0.5189	0.026*

C8	0.40984 (17)	0.76154 (10)	0.29461 (6)	0.0214 (3)
C9	0.30990 (17)	0.73869 (10)	0.33243 (6)	0.0233 (3)
H9	0.2535	0.7816	0.3478	0.028*
C10	0.29299 (16)	0.65463 (10)	0.34741 (6)	0.0200 (3)
H10	0.2245	0.6398	0.3727	0.024*
C11	0.37659 (15)	0.59142 (9)	0.32540 (6)	0.0161 (3)
C12	0.47611 (16)	0.61271 (10)	0.28796 (6)	0.0173 (3)
H12	0.5333	0.5696	0.2732	0.021*
C13	0.49154 (16)	0.69659 (10)	0.27231 (6)	0.0192 (3)
H13	0.5581	0.7106	0.2462	0.023*
C14	0.57371 (15)	0.46886 (9)	0.40478 (6)	0.0154 (3)
C15	0.86838 (17)	0.53290 (11)	0.32639 (6)	0.0235 (3)
H15A	0.8522	0.4976	0.2950	0.035*
H15B	0.9667	0.5314	0.3355	0.035*
H15C	0.8407	0.5919	0.3190	0.035*
C16	0.78544 (15)	0.49901 (9)	0.37146 (6)	0.0181 (3)
C17	0.84506 (16)	0.47044 (10)	0.41807 (6)	0.0203 (3)
H17	0.9425	0.4704	0.4225	0.024*
C18	0.75894 (16)	0.44206 (9)	0.45793 (6)	0.0185 (3)
C19	0.81233 (17)	0.41122 (11)	0.51013 (6)	0.0246 (3)
H19A	0.7744	0.4468	0.5385	0.037*
H19B	0.9134	0.4149	0.5105	0.037*
H19C	0.7841	0.3518	0.5156	0.037*

Atomic displacement parameters ( $\text{\AA}^2$ )

	$U^{11}$	$U^{22}$	$U^{33}$	$U^{12}$	$U^{13}$	$U^{23}$
S1	0.01596 (19)	0.01455 (19)	0.01581 (19)	-0.00025 (13)	-0.00155 (13)	0.00020 (13)
O1	0.0241 (6)	0.0313 (6)	0.0208 (6)	-0.0030 (5)	-0.0002 (5)	0.0078 (5)
O2	0.0219 (6)	0.0258 (6)	0.0198 (5)	-0.0032 (5)	0.0019 (4)	0.0039 (5)
O3	0.0167 (5)	0.0194 (5)	0.0236 (6)	-0.0015 (4)	-0.0016 (4)	0.0021 (4)
O4	0.0256 (6)	0.0179 (5)	0.0185 (5)	0.0009 (4)	-0.0015 (4)	-0.0021 (4)
N1	0.0455 (10)	0.0182 (7)	0.0376 (9)	0.0031 (7)	0.0234 (7)	0.0053 (6)
N2	0.0155 (6)	0.0198 (6)	0.0156 (6)	-0.0004 (5)	0.0007 (5)	0.0038 (5)
N3	0.0200 (6)	0.0162 (6)	0.0152 (6)	0.0008 (5)	-0.0014 (5)	-0.0005 (5)
N4	0.0180 (6)	0.0156 (6)	0.0180 (7)	0.0013 (5)	0.0010 (5)	0.0000 (5)
C1	0.0241 (8)	0.0151 (7)	0.0188 (8)	0.0009 (6)	0.0019 (6)	-0.0026 (6)
C2	0.0243 (8)	0.0133 (7)	0.0186 (7)	-0.0004 (6)	0.0030 (6)	-0.0017 (6)
C3	0.0256 (8)	0.0222 (8)	0.0216 (8)	-0.0041 (7)	-0.0002 (6)	-0.0005 (6)
C4	0.0370 (10)	0.0247 (8)	0.0183 (8)	-0.0068 (7)	-0.0012 (7)	0.0020 (6)
C5	0.0330 (9)	0.0195 (8)	0.0215 (8)	-0.0075 (7)	0.0086 (7)	-0.0033 (6)
C6	0.0227 (8)	0.0208 (8)	0.0279 (8)	-0.0023 (6)	0.0057 (7)	-0.0026 (6)
C7	0.0258 (8)	0.0192 (8)	0.0211 (8)	0.0025 (6)	0.0013 (6)	-0.0002 (6)
C8	0.0249 (8)	0.0185 (8)	0.0208 (8)	0.0001 (6)	0.0020 (6)	0.0019 (6)
C9	0.0267 (8)	0.0183 (8)	0.0249 (8)	0.0058 (7)	0.0073 (7)	0.0010 (6)
C10	0.0201 (8)	0.0213 (8)	0.0187 (7)	0.0013 (6)	0.0037 (6)	0.0029 (6)
C11	0.0185 (7)	0.0151 (7)	0.0148 (7)	0.0002 (6)	-0.0025 (6)	0.0013 (5)
C12	0.0183 (7)	0.0197 (7)	0.0141 (7)	0.0014 (6)	-0.0013 (6)	-0.0018 (6)
C13	0.0208 (8)	0.0223 (8)	0.0145 (7)	-0.0015 (6)	0.0019 (6)	0.0002 (6)
C14	0.0170 (7)	0.0121 (6)	0.0171 (7)	0.0002 (6)	0.0000 (6)	-0.0015 (5)
C15	0.0205 (8)	0.0251 (8)	0.0248 (8)	0.0002 (7)	0.0041 (6)	0.0033 (7)
C16	0.0180 (8)	0.0148 (7)	0.0217 (8)	0.0001 (6)	0.0017 (6)	-0.0029 (6)
C17	0.0167 (7)	0.0208 (8)	0.0235 (8)	0.0011 (6)	-0.0014 (6)	-0.0027 (6)
C18	0.0213 (7)	0.0157 (7)	0.0184 (7)	0.0023 (6)	-0.0031 (6)	-0.0034 (6)
C19	0.0230 (8)	0.0295 (8)	0.0213 (8)	0.0050 (7)	-0.0051 (6)	-0.0001 (7)

Geometric parameters (Å, °)

S1—O4	1.4356 (11)	C6—C7	1.381 (2)
S1—O3	1.4384 (11)	C6—H6	0.9500
S1—N2	1.6446 (12)	C7—H7	0.9500
S1—C11	1.7399 (15)	C8—C13	1.407 (2)
O1—C1	1.2300 (19)	C8—C9	1.408 (2)
O2—C1	1.310 (2)	C9—C10	1.379 (2)
O2—H32	0.855 (17)	C9—H9	0.9500
N1—C8	1.357 (2)	C10—C11	1.395 (2)
N1—H30A	0.841 (15)	C10—H10	0.9500
N1—H30B	0.888 (15)	C11—C12	1.392 (2)
N2—C14	1.383 (2)	C12—C13	1.380 (2)
N2—H31	0.857 (15)	C12—H12	0.9500
N3—C14	1.3397 (19)	C13—H13	0.9500
N3—C18	1.350 (2)	C15—C16	1.493 (2)
N4—C14	1.3267 (19)	C15—H15A	0.9800
N4—C16	1.343 (2)	C15—H15B	0.9800
C1—C2	1.490 (2)	C15—H15C	0.9800
C2—C3	1.391 (2)	C16—C17	1.388 (2)
C2—C7	1.392 (2)	C17—C18	1.382 (2)
C3—C4	1.392 (2)	C17—H17	0.9500
C3—H3	0.9500	C18—C19	1.499 (2)
C4—C5	1.383 (3)	C19—H19A	0.9800
C4—H4	0.9500	C19—H19B	0.9800
C5—C6	1.389 (2)	C19—H19C	0.9800
C5—H5	0.9500		
O4—S1—O3	117.47 (7)	C10—C9—C8	120.74 (14)
O4—S1—N2	110.26 (6)	C10—C9—H9	119.6
O3—S1—N2	102.43 (6)	C8—C9—H9	119.6
O4—S1—C11	108.60 (7)	C9—C10—C11	119.88 (14)
O3—S1—C11	109.27 (7)	C9—C10—H10	120.1
N2—S1—C11	108.40 (7)	C11—C10—H10	120.1
C1—O2—H32	110.2 (18)	C12—C11—C10	120.26 (14)
C8—N1—H30A	122.9 (14)	C12—C11—S1	120.67 (11)
C8—N1—H30B	118.8 (13)	C10—C11—S1	119.01 (11)
H30A—N1—H30B	118.2 (19)	C13—C12—C11	119.90 (14)
C14—N2—S1	124.78 (11)	C13—C12—H12	120.1
C14—N2—H31	118.0 (14)	C11—C12—H12	120.1
S1—N2—H31	115.3 (14)	C12—C13—C8	120.78 (14)
C14—N3—C18	116.04 (13)	C12—C13—H13	119.6
C14—N4—C16	116.20 (13)	C8—C13—H13	119.6
O1—C1—O2	123.52 (14)	N4—C14—N3	127.29 (14)
O1—C1—C2	121.65 (14)	N4—C14—N2	117.55 (13)
O2—C1—C2	114.83 (13)	N3—C14—N2	115.15 (13)
C3—C2—C7	120.07 (14)	C16—C15—H15A	109.5
C3—C2—C1	121.77 (14)	C16—C15—H15B	109.5
C7—C2—C1	118.15 (14)	H15A—C15—H15B	109.5
C2—C3—C4	119.46 (15)	C16—C15—H15C	109.5
C2—C3—H3	120.3	H15A—C15—H15C	109.5
C4—C3—H3	120.3	H15B—C15—H15C	109.5
C5—C4—C3	120.21 (16)	N4—C16—C17	121.25 (14)
C5—C4—H4	119.9	N4—C16—C15	115.99 (14)
C3—C4—H4	119.9	C17—C16—C15	122.76 (14)
C4—C5—C6	120.22 (15)	C18—C17—C16	118.27 (14)



C4—C5—H5	119.9	C18—C17—H17	120.9
C6—C5—H5	119.9	C16—C17—H17	120.9
C7—C6—C5	119.84 (15)	N3—C18—C17	120.94 (14)
C7—C6—H6	120.1	N3—C18—C19	116.41 (14)
C5—C6—H6	120.1	C17—C18—C19	122.64 (14)
C6—C7—C2	120.17 (15)	C18—C19—H19A	109.5
C6—C7—H7	119.9	C18—C19—H19B	109.5
C2—C7—H7	119.9	H19A—C19—H19B	109.5
N1—C8—C13	121.27 (15)	C18—C19—H19C	109.5
N1—C8—C9	120.31 (15)	H19A—C19—H19C	109.5
C13—C8—C9	118.42 (14)	H19B—C19—H19C	109.5
O4—S1—N2—C14	53.14 (14)	O4—S1—C11—C10	156.47 (12)
O3—S1—N2—C14	178.94 (12)	O3—S1—C11—C10	27.18 (14)
C11—S1—N2—C14	-65.63 (14)	N2—S1—C11—C10	-83.72 (13)
O1—C1—C2—C3	-179.15 (14)	C10—C11—C12—C13	-0.4 (2)
O2—C1—C2—C3	0.7 (2)	S1—C11—C12—C13	176.72 (11)
O1—C1—C2—C7	-0.4 (2)	C11—C12—C13—C8	1.4 (2)
O2—C1—C2—C7	179.50 (13)	N1—C8—C13—C12	178.41 (16)
C7—C2—C3—C4	-0.1 (2)	C9—C8—C13—C12	-1.4 (2)
C1—C2—C3—C4	178.67 (14)	C16—N4—C14—N3	0.9 (2)
C2—C3—C4—C5	-1.0 (2)	C16—N4—C14—N2	179.89 (13)
C3—C4—C5—C6	1.1 (2)	C18—N3—C14—N4	-1.6 (2)
C4—C5—C6—C7	-0.1 (2)	C18—N3—C14—N2	179.43 (13)
C5—C6—C7—C2	-1.0 (2)	S1—N2—C14—N4	9.04 (19)
C3—C2—C7—C6	1.1 (2)	S1—N2—C14—N3	-171.85 (10)
C1—C2—C7—C6	-177.70 (14)	C14—N4—C16—C17	0.5 (2)
N1—C8—C9—C10	-179.49 (17)	C14—N4—C16—C15	-179.18 (13)
C13—C8—C9—C10	0.3 (2)	N4—C16—C17—C18	-1.2 (2)
C8—C9—C10—C11	0.7 (2)	C15—C16—C17—C18	178.53 (14)
C9—C10—C11—C12	-0.7 (2)	C14—N3—C18—C17	0.8 (2)
C9—C10—C11—S1	-177.84 (13)	C14—N3—C18—C19	-179.73 (13)
O4—S1—C11—C12	-20.70 (14)	C16—C17—C18—N3	0.5 (2)
O3—S1—C11—C12	-150.00 (12)	C16—C17—C18—C19	-178.99 (14)
N2—S1—C11—C12	99.11 (13)		

Hydrogen-bond geometry (Å, °)

<i>D</i> —H··· <i>A</i>	<i>D</i> —H	H··· <i>A</i>	<i>D</i> ··· <i>A</i>	<i>D</i> —H··· <i>A</i>
N1—H30 <i>A</i> ···O4 <sup>i</sup>	0.84 (2)	2.18 (2)	2.9964 (18)	164 (2)
N1—H30 <i>B</i> ···O3 <sup>ii</sup>	0.89 (2)	2.25 (2)	3.1127 (19)	165 (2)
N2—H31···O1	0.86 (2)	1.93 (2)	2.7847 (16)	174 (2)
O2—H32···N3	0.86 (2)	1.85 (2)	2.7006 (16)	173 (3)

Symmetry codes: (i)  $-x+1, y+1/2, -z+1/2$ ; (ii)  $-x+1/2, y+1/2, z$ .

All esds (except the esd in the dihedral angle between two l.s. planes) are estimated using the full covariance matrix. The cell esds are taken into account individually in the estimation of esds in distances, angles and torsion angles; correlations between esds in cell parameters are only used when they are defined by crystal symmetry. An approximate (isotropic) treatment of cell esds is used for estimating esds involving l.s. planes.

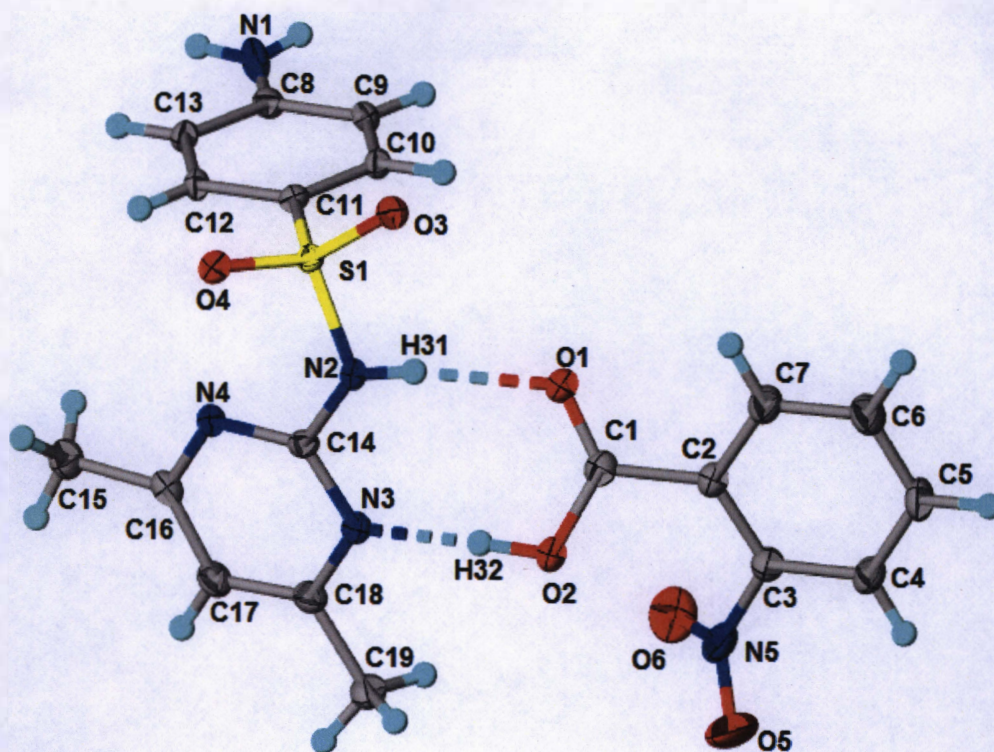


Figure S.2: Crystal Structure of the Cocrystal of Sulfamethazine and *o*-Nitrobenzoic Acid Showing Thermal Parameters (50% Thermal Ellipsoids) and Hydrogen Bonding.

#### Crystal data

$C_{12}H_{14}N_4O_2S \cdot C_7H_5NO_4$

$M_r = 445.45$

Orthorhombic,  $Pna2_1$

$a = 14.2344$  (7) Å

$b = 7.9707$  (4) Å

$c = 18.9829$  (9) Å

$V = 2153.76$  (18) Å<sup>3</sup>

$Z = 4$

$F(000) = 928$

$D_x = 1.374$  Mg m<sup>-3</sup>

Melting point: 439-441 K

Cu  $K\alpha$  radiation,  $\lambda = 1.54178$  Å

Cell parameters from 9905 reflections

$\theta = 4.7$ – $68.3^\circ$

$\mu = 1.74$  mm<sup>-1</sup>

$T = 100$  K

Plates, colourless

$0.33 \times 0.29 \times 0.06$  mm

Radiation source: fine-focus sealed tube  
 Detector resolution: 8.33 pixels mm<sup>-1</sup>  
 phi and  $\omega$  scans  
 Absorption correction: multi-scan  
 SADABS2014/7, Bruker AXS  
 $T_{\min} = 0.622$ ,  $T_{\max} = 0.753$   
 24432 measured reflections

3737 reflections with  $I > 2\sigma(I)$   
 $R_{\text{int}} = 0.041$   
 $\theta_{\max} = 68.2^\circ$ ,  $\theta_{\min} = 4.7^\circ$   
 $h = -15 \ 17$   
 $k = -9 \ 9$   
 $l = -22 \ 21$

### Refinement

Refinement on  $F^2$   
 Least-squares matrix: full  
 $R[F^2 > 2\sigma(F^2)] = 0.031$   
 $wR(F^2) = 0.081$   
 $S = 1.09$   
 3865 reflections  
 298 parameters  
 2 restraints  
 0 constraints

Hydrogen site location: mixed  
 H atoms treated by a mixture of independent and constrained refinement  
 $w = 1/[\sigma^2(F_o^2) + (0.0512P)^2 + 0.3396P]$   
 where  $P = (F_o^2 + 2F_c^2)/3$   
 $(\Delta/\sigma)_{\max} < 0.001$   
 $\Delta\rho_{\max} = 0.31 \text{ e } \text{\AA}^{-3}$   
 $\Delta\rho_{\min} = -0.22 \text{ e } \text{\AA}^{-3}$   
 Extinction correction: none  
 Absolute structure: Flack x determined using 1692 quotients  $[(I^+)-(I^-)]/[(I^+)+(I^-)]$  (Parsons, Flack and Wagner, Acta Cryst. B69 (2013) 249-259).  
 Absolute structure parameter: 0.028 (7)

### Fractional atomic coordinates and isotropic or equivalent isotropic displacement parameters ( $\text{\AA}^2$ )

	x	y	z	$U_{\text{iso}}^*/U_{\text{eq}}$
S1	0.94985 (4)	0.52343 (7)	1.00022 (4)	0.01658 (16)
O1	0.78700 (15)	0.3833 (3)	0.84647 (12)	0.0319 (5)
O2	0.79961 (16)	0.5570 (3)	0.75464 (11)	0.0281 (5)
O3	0.85657 (14)	0.4967 (2)	1.02650 (11)	0.0217 (4)
O4	1.00603 (14)	0.6517 (2)	1.03167 (10)	0.0213 (4)
O5	0.6893 (2)	0.5272 (6)	0.59377 (18)	0.0834 (13)
H31	0.885 (3)	0.524 (4)	0.9025 (18)	0.020 (9)*
H30B	1.135 (2)	-0.195 (5)	0.996 (2)	0.026 (9)*
H30A	1.215 (3)	-0.111 (5)	1.013 (2)	0.037 (11)*
H32	0.861 (3)	0.581 (5)	0.774 (2)	0.046 (11)*
O6	0.7759 (2)	0.3349 (4)	0.63996 (14)	0.0502 (7)
N1	1.16057 (19)	-0.1106 (3)	0.99839 (18)	0.0305 (6)
N2	0.93053 (17)	0.5749 (3)	0.91648 (12)	0.0195 (5)
N3	0.97302 (17)	0.6112 (3)	0.80024 (13)	0.0221 (5)
N4	1.09057 (17)	0.5907 (3)	0.89001 (12)	0.0209 (5)
N5	0.7060 (2)	0.4230 (4)	0.63854 (15)	0.0382 (7)
C1	0.7562 (2)	0.4429 (4)	0.79232 (15)	0.0237 (6)
C2	0.6611 (2)	0.3959 (3)	0.76502 (15)	0.0230 (6)
C3	0.6353 (2)	0.3989 (4)	0.69389 (15)	0.0252 (6)
C4	0.5444 (2)	0.3687 (4)	0.67207 (16)	0.0291 (7)
H4	0.5288	0.3726	0.6235	0.035*
C5	0.4763 (2)	0.3327 (4)	0.72186 (18)	0.0321 (7)
H5	0.4132	0.3129	0.7077	0.039*

C6	0.5004 (2)	0.3258 (4)	0.79230 (17)	0.0359 (8)
H6	0.4538	0.2998	0.8264	0.043*
C7	0.5923 (2)	0.3565 (4)	0.81381 (16)	0.0305 (7)
H7	0.6079	0.3503	0.8624	0.037*
C8	1.11096 (19)	0.0347 (3)	1.00072 (17)	0.0215 (5)
C9	1.0138 (2)	0.0374 (3)	0.98506 (14)	0.0208 (6)
H9	0.9821	-0.0642	0.9742	0.025*
C10	0.9651 (2)	0.1869 (3)	0.98549 (13)	0.0196 (6)
H10	0.8997	0.1880	0.9753	0.023*
C11	1.01151 (18)	0.3359 (3)	1.00078 (15)	0.0177 (5)
C12	1.10718 (19)	0.3365 (3)	1.01694 (13)	0.0188 (5)
H12	1.1384	0.4388	1.0274	0.023*
C13	1.15590 (19)	0.1869 (3)	1.01760 (14)	0.0201 (6)
H13	1.2207	0.1865	1.0296	0.024*
C14	1.0025 (2)	0.5929 (3)	0.86709 (14)	0.0193 (6)
C15	1.2568 (2)	0.5906 (4)	0.86552 (18)	0.0336 (7)
H15A	1.2664	0.6672	0.9052	0.050*
H15B	1.2997	0.6203	0.8271	0.050*
H15C	1.2692	0.4752	0.8807	0.050*
C16	1.1578 (2)	0.6041 (4)	0.84039 (16)	0.0247 (6)
C17	1.1345 (2)	0.6277 (4)	0.76975 (16)	0.0289 (7)
H17	1.1821	0.6416	0.7351	0.035*
C18	1.0407 (2)	0.6304 (4)	0.75123 (16)	0.0263 (6)
C19	1.0083 (2)	0.6521 (4)	0.67663 (16)	0.0344 (7)
H19A	0.9820	0.5461	0.6594	0.052*
H19B	1.0617	0.6848	0.6471	0.052*
H19C	0.9600	0.7396	0.6747	0.052*

### Atomic displacement parameters ( $\text{\AA}^2$ )

	$U^{11}$	$U^{22}$	$U^{33}$	$U^{12}$	$U^{13}$	$U^{23}$
S1	0.0150 (3)	0.0179 (3)	0.0168 (3)	0.0008 (2)	-0.0001 (3)	0.0001 (3)
O1	0.0269 (12)	0.0415 (12)	0.0274 (11)	-0.0078 (9)	-0.0078 (9)	0.0082 (9)
O2	0.0215 (12)	0.0351 (11)	0.0277 (11)	-0.0054 (9)	-0.0063 (9)	0.0058 (9)
O3	0.0166 (10)	0.0254 (9)	0.0230 (9)	0.0024 (7)	0.0031 (8)	0.0014 (8)
O4	0.0219 (11)	0.0208 (9)	0.0212 (9)	0.0019 (7)	-0.0016 (8)	-0.0018 (8)
O5	0.0333 (18)	0.163 (4)	0.054 (2)	-0.0089 (19)	-0.0061 (14)	0.067 (2)
O6	0.0383 (15)	0.0707 (18)	0.0416 (15)	0.0055 (13)	0.0116 (11)	-0.0172 (13)
N1	0.0182 (13)	0.0183 (11)	0.0552 (17)	-0.0020 (9)	-0.0052 (14)	-0.0003 (13)
N2	0.0154 (13)	0.0223 (11)	0.0207 (12)	-0.0018 (9)	-0.0027 (10)	0.0003 (9)
N3	0.0220 (13)	0.0238 (11)	0.0205 (12)	-0.0037 (9)	-0.0022 (10)	0.0003 (10)
N4	0.0178 (13)	0.0222 (11)	0.0228 (12)	-0.0023 (9)	-0.0013 (9)	0.0006 (9)
N5	0.0231 (15)	0.070 (2)	0.0216 (13)	-0.0034 (14)	-0.0025 (11)	0.0040 (14)
C1	0.0238 (16)	0.0242 (13)	0.0231 (15)	0.0018 (11)	-0.0015 (12)	-0.0037 (11)
C2	0.0215 (15)	0.0240 (14)	0.0236 (15)	0.0012 (11)	-0.0020 (11)	-0.0023 (11)
C3	0.0232 (16)	0.0292 (15)	0.0232 (15)	-0.0014 (12)	-0.0003 (12)	0.0000 (12)
C4	0.0292 (18)	0.0344 (16)	0.0236 (16)	-0.0032 (13)	-0.0061 (12)	-0.0035 (13)
C5	0.0204 (17)	0.0400 (17)	0.0358 (17)	-0.0050 (13)	-0.0044 (13)	-0.0033 (14)
C6	0.0269 (18)	0.0508 (19)	0.0300 (18)	-0.0087 (15)	0.0052 (13)	-0.0011 (15)
C7	0.0263 (17)	0.0426 (17)	0.0226 (15)	-0.0037 (13)	-0.0010 (12)	-0.0032 (13)
C8	0.0195 (13)	0.0216 (11)	0.0233 (12)	0.0010 (10)	0.0018 (13)	0.0022 (12)
C9	0.0203 (14)	0.0190 (12)	0.0231 (16)	-0.0051 (10)	-0.0006 (10)	0.0010 (10)
C10	0.0154 (13)	0.0250 (13)	0.0183 (14)	-0.0020 (10)	-0.0006 (9)	0.0002 (11)
C11	0.0188 (13)	0.0181 (11)	0.0163 (11)	0.0013 (9)	-0.0006 (11)	0.0010 (11)

C12	0.0147 (13)	0.0210 (12)	0.0207 (13)	-0.0017 (10)	-0.0013 (10)	-0.0007 (10)
C13	0.0154 (13)	0.0240 (13)	0.0211 (14)	-0.0001 (10)	-0.0019 (10)	0.0005 (10)
C14	0.0222 (15)	0.0168 (12)	0.0188 (14)	-0.0001 (10)	-0.0006 (10)	0.0015 (10)
C15	0.0222 (17)	0.0435 (18)	0.0351 (18)	-0.0029 (13)	0.0024 (13)	0.0020 (15)
C16	0.0231 (15)	0.0226 (13)	0.0284 (15)	-0.0035 (11)	0.0034 (12)	-0.0004 (11)
C17	0.0262 (17)	0.0360 (16)	0.0244 (15)	-0.0068 (13)	0.0058 (12)	-0.0009 (13)
C18	0.0303 (17)	0.0279 (15)	0.0206 (15)	-0.0063 (12)	0.0013 (12)	0.0004 (12)
C19	0.0336 (19)	0.049 (2)	0.0207 (16)	-0.0099 (15)	-0.0010 (13)	0.0026 (14)

### Geometric parameters (Å, °)

S1—O4	1.429 (2)	C5—H5	0.9500
S1—O3	1.434 (2)	C6—C7	1.392 (5)
S1—N2	1.665 (2)	C6—H6	0.9500
S1—C11	1.733 (2)	C7—H7	0.9500
O1—C1	1.214 (4)	C8—C13	1.408 (4)
O2—C1	1.311 (4)	C8—C9	1.414 (4)
O2—H32	0.97 (4)	C9—C10	1.379 (4)
O5—N5	1.212 (4)	C9—H9	0.9500
O6—N5	1.218 (4)	C10—C11	1.390 (4)
N1—C8	1.357 (4)	C10—H10	0.9500
N1—H30B	0.77 (4)	C11—C12	1.396 (4)
N1—H30A	0.83 (4)	C12—C13	1.380 (4)
N2—C14	1.396 (4)	C12—H12	0.9500
N2—H31	0.81 (4)	C13—H13	0.9500
N3—C14	1.344 (4)	C15—C16	1.491 (5)
N3—C18	1.348 (4)	C15—H15A	0.9800
N4—C14	1.327 (4)	C15—H15B	0.9800
N4—C16	1.347 (4)	C15—H15C	0.9800
N5—C3	1.468 (4)	C16—C17	1.394 (4)
C1—C2	1.497 (4)	C17—C18	1.381 (5)
C2—C7	1.385 (4)	C17—H17	0.9500
C2—C3	1.400 (4)	C18—C19	1.499 (4)
C3—C4	1.379 (4)	C19—H19A	0.9800
C4—C5	1.384 (5)	C19—H19B	0.9800
C4—H4	0.9500	C19—H19C	0.9800
C5—C6	1.382 (5)		
O4—S1—O3	118.62 (12)	C13—C8—C9	118.6 (2)
O4—S1—N2	108.36 (12)	C10—C9—C8	120.2 (2)
O3—S1—N2	102.46 (12)	C10—C9—H9	119.9
O4—S1—C11	109.34 (12)	C8—C9—H9	119.9
O3—S1—C11	109.80 (12)	C9—C10—C11	120.0 (3)
N2—S1—C11	107.59 (13)	C9—C10—H10	120.0
C1—O2—H32	111 (2)	C11—C10—H10	120.0
C8—N1—H30B	120 (3)	C10—C11—C12	120.8 (2)
C8—N1—H30A	119 (3)	C10—C11—S1	119.7 (2)
H30B—N1—H30A	118 (4)	C12—C11—S1	119.50 (19)
C14—N2—S1	123.1 (2)	C13—C12—C11	119.3 (2)
C14—N2—H31	115 (2)	C13—C12—H12	120.3
S1—N2—H31	109 (2)	C11—C12—H12	120.3
C14—N3—C18	116.2 (2)	C12—C13—C8	120.9 (2)
C14—N4—C16	116.2 (2)	C12—C13—H13	119.5
O5—N5—O6	124.8 (3)	C8—C13—H13	119.5
O5—N5—C3	117.2 (3)	N4—C14—N3	127.3 (3)

O6—N5—C3	118.0 (3)	N4—C14—N2	118.1 (2)
O1—C1—O2	124.3 (3)	N3—C14—N2	114.6 (3)
O1—C1—C2	121.4 (3)	C16—C15—H15A	109.5
O2—C1—C2	114.2 (2)	C16—C15—H15B	109.5
C7—C2—C3	117.6 (3)	H15A—C15—H15B	109.5
C7—C2—C1	117.7 (3)	C16—C15—H15C	109.5
C3—C2—C1	124.6 (3)	H15A—C15—H15C	109.5
C4—C3—C2	122.2 (3)	H15B—C15—H15C	109.5
C4—C3—N5	116.8 (3)	N4—C16—C17	121.0 (3)
C2—C3—N5	120.8 (3)	N4—C16—C15	116.2 (3)
C3—C4—C5	119.2 (3)	C17—C16—C15	122.8 (3)
C3—C4—H4	120.4	C18—C17—C16	118.5 (3)
C5—C4—H4	120.4	C18—C17—H17	120.8
C6—C5—C4	119.7 (3)	C16—C17—H17	120.8
C6—C5—H5	120.2	N3—C18—C17	120.9 (3)
C4—C5—H5	120.2	N3—C18—C19	116.4 (3)
C5—C6—C7	120.7 (3)	C17—C18—C19	122.7 (3)
C5—C6—H6	119.7	C18—C19—H19A	109.5
C7—C6—H6	119.7	C18—C19—H19B	109.5
C2—C7—C6	120.6 (3)	H19A—C19—H19B	109.5
C2—C7—H7	119.7	C18—C19—H19C	109.5
C6—C7—H7	119.7	H19A—C19—H19C	109.5
N1—C8—C13	120.4 (3)	H19B—C19—H19C	109.5
N1—C8—C9	121.0 (3)		
O4—S1—N2—C14	61.8 (2)	C9—C10—C11—S1	179.3 (2)
O3—S1—N2—C14	-172.0 (2)	O4—S1—C11—C10	167.7 (2)
C11—S1—N2—C14	-56.3 (2)	O3—S1—C11—C10	35.9 (3)
O1—C1—C2—C7	31.7 (4)	N2—S1—C11—C10	-74.8 (3)
O2—C1—C2—C7	-145.4 (3)	O4—S1—C11—C12	-12.0 (3)
O1—C1—C2—C3	-152.3 (3)	O3—S1—C11—C12	-143.8 (2)
O2—C1—C2—C3	30.5 (4)	N2—S1—C11—C12	105.5 (2)
C7—C2—C3—C4	1.8 (5)	C10—C11—C12—C13	0.1 (4)
C1—C2—C3—C4	-174.1 (3)	S1—C11—C12—C13	179.7 (2)
C7—C2—C3—N5	-173.9 (3)	C11—C12—C13—C8	1.4 (4)
C1—C2—C3—N5	10.2 (5)	N1—C8—C13—C12	177.0 (3)
O5—N5—C3—C4	52.6 (5)	C9—C8—C13—C12	-1.9 (4)
O6—N5—C3—C4	-125.7 (3)	C16—N4—C14—N3	-1.8 (4)
O5—N5—C3—C2	-131.5 (4)	C16—N4—C14—N2	178.4 (2)
O6—N5—C3—C2	50.2 (5)	C18—N3—C14—N4	-0.5 (4)
C2—C3—C4—C5	-0.6 (5)	C18—N3—C14—N2	179.4 (2)
N5—C3—C4—C5	175.2 (3)	S1—N2—C14—N4	-9.2 (3)
C3—C4—C5—C6	-0.7 (5)	S1—N2—C14—N3	170.94 (19)
C4—C5—C6—C7	0.7 (5)	C14—N4—C16—C17	3.2 (4)
C3—C2—C7—C6	-1.8 (4)	C14—N4—C16—C15	-176.2 (3)
C1—C2—C7—C6	174.5 (3)	N4—C16—C17—C18	-2.5 (5)
C5—C6—C7—C2	0.5 (5)	C15—C16—C17—C18	176.8 (3)
N1—C8—C9—C10	-177.9 (3)	C14—N3—C18—C17	1.2 (4)
C13—C8—C9—C10	0.9 (4)	C14—N3—C18—C19	-179.6 (3)
C8—C9—C10—C11	0.5 (4)	C16—C17—C18—N3	0.2 (5)
C9—C10—C11—C12	-1.0 (4)	C16—C17—C18—C19	-179.0 (3)

### Hydrogen-bond geometry (Å, °)

<i>D</i> —H··· <i>A</i>	<i>D</i> —H	H··· <i>A</i>	<i>D</i> ··· <i>A</i>	<i>D</i> —H··· <i>A</i>
-------------------------	-------------	---------------	-----------------------	-------------------------



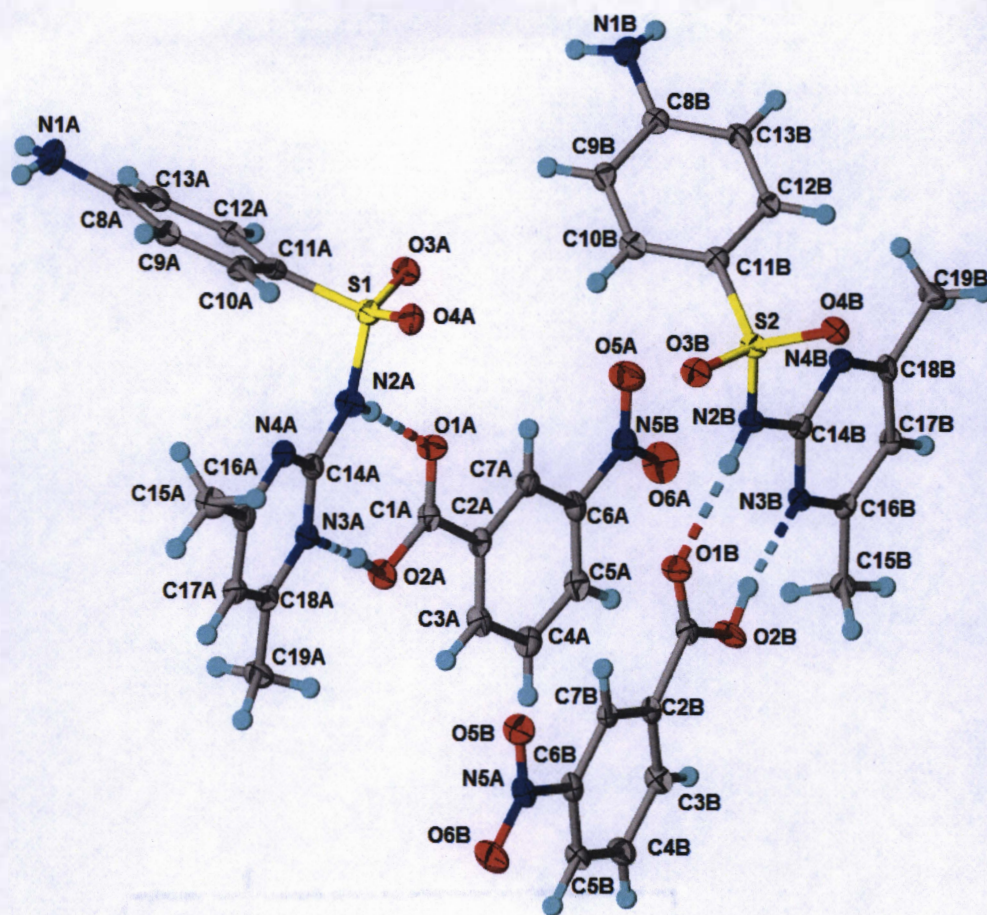


Figure S.3: Crystal Structure of the Cocrystal of Sulfamethazine and *m*-Nitrobenzoic Acid Showing Thermal Parameters (50% Thermal Ellipsoids) and Hydrogen Bonding.

#### Crystal data

$C_{12}H_{14}N_4O_2S \cdot C_{12}H_{13}N_4O_2S \cdot C_7H_5NO_4 \cdot C_7H_4NO_4$

$M_r = 445.45$

Triclinic, *P*

$a = 11.1257 (8) \text{ \AA}$

$b = 12.9928 (10) \text{ \AA}$

$c = 13.9550 (9) \text{ \AA}$

$\alpha = 93.079 (4)^\circ$

$\beta = 93.582 (4)^\circ$

$\gamma = 91.728 (5)^\circ$

$D_x = 1.473 \text{ Mg m}^{-3}$

Melting point: 474–477 K

Cu  $K\alpha$  radiation,  $\lambda = 1.54178 \text{ \AA}$

Cell parameters from 9958 reflections

$\theta = 3.2\text{--}68.4^\circ$

$\mu = 1.87 \text{ mm}^{-1}$

$T = 100 \text{ K}$



### Crystal data

$C_{12}H_{14}N_4O_2S \cdot C_{12}H_{13}N_4O_2S \cdot C_7H_5NO_4 \cdot C_7H_4NO_4$

$M_r = 445.45$

Triclinic,  $P$

$a = 11.1257$  (8) Å

$b = 12.9928$  (10) Å

$c = 13.9550$  (9) Å

$\alpha = 93.079$  (4)°

$\beta = 93.582$  (4)°

$\gamma = 91.728$  (5)°

$V = 2009.3$  (2) Å<sup>3</sup>

$Z = 4$

$F(000) = 928$

$D_x = 1.473$  Mg m<sup>-3</sup>

Melting point: 474-477 K

Cu  $K\alpha$  radiation,  $\lambda = 1.54178$  Å

Cell parameters from 9958 reflections

$\theta = 3.2$ – $68.4$ °

$\mu = 1.87$  mm<sup>-1</sup>

$T = 100$  K

Plates, colourless

$0.36 \times 0.09 \times 0.08$  mm

### Data collection

Radiation source: fine-focused sealed tube

Detector resolution: 8.33 pixels mm<sup>-1</sup>

$\phi$  and  $\omega$  scans

Absorption correction: multi-scan

SADABS2014/7, Bruker AXS

$T_{\min} = 0.572$ ,  $T_{\max} = 0.753$

7199 measured reflections

5182 reflections with  $I > 2\sigma(I)$

$R_{\text{int}} = ?$

$\theta_{\max} = 68.2$ °,  $\theta_{\min} = 3.2$ °

$h = -13$  13

$k = -15$  15

$l = 0$  16

### Refinement

Refinement on  $F^2$

Least-squares matrix: full

$R[F^2 > 2\sigma(F^2)] = 0.063$

$wR(F^2) = 0.158$

$S = 1.05$

7199 reflections

589 parameters

6 restraints

? constraints

Primary atom site location: ?

Secondary atom site location: ?

Hydrogen site location: mixed

H atoms treated by a mixture of independent and constrained refinement

$w = 1/[\sigma^2(F_o^2) + (0.0534P)^2 + 4.7677P]$

where  $P = (F_o^2 + 2F_c^2)/3$

$(\Delta/\sigma)_{\max} = 0.006$

$\Delta\rho_{\max} = 0.64$  e Å<sup>-3</sup>

$\Delta\rho_{\min} = -0.45$  e Å<sup>-3</sup>

Extinction correction: none

Extinction coefficient: ?

### Fractional atomic coordinates and isotropic or equivalent isotropic displacement parameters (Å<sup>2</sup>)

	$x$	$y$	$z$	$U_{\text{iso}}^*/U_{\text{eq}}$
S1	0.10838 (7)	0.58279 (6)	0.70341 (5)	0.02174 (18)
S2	0.11221 (7)	0.07055 (6)	0.80799 (5)	0.02098 (17)
O1A	0.40894 (19)	0.62524 (18)	0.85338 (15)	0.0251 (5)
O2A	0.5710 (2)	0.65004 (18)	0.76849 (15)	0.0270 (6)
H32A	0.518 (3)	0.646 (4)	0.7205 (18)	0.098 (19)*

O3A	0.09971 (19)	0.60254 (18)	0.80533 (16)	0.0274 (5)
O4A	0.0781 (2)	0.48192 (17)	0.66191 (16)	0.0264 (5)
O5A	0.4685 (2)	0.5964 (2)	1.19931 (17)	0.0377 (7)
O6A	0.6467 (2)	0.6143 (2)	1.27086 (17)	0.0437 (7)
O2B	0.57344 (19)	0.13288 (19)	0.79312 (15)	0.0279 (6)
O1B	0.41323 (19)	0.12138 (19)	0.68768 (15)	0.0283 (6)
O3B	0.10326 (19)	0.07928 (18)	0.70565 (16)	0.0262 (5)
O4B	0.08834 (19)	-0.02717 (17)	0.84653 (15)	0.0255 (5)
O5B	0.4868 (2)	0.10545 (19)	0.34541 (16)	0.0303 (6)
O6B	0.6675 (2)	0.1256 (2)	0.29770 (16)	0.0365 (6)
N1A	-0.1818 (3)	0.8865 (2)	0.4992 (2)	0.0346 (8)
H30A	-0.174 (3)	0.9484 (14)	0.525 (2)	0.030 (10)*
H30B	-0.185 (4)	0.887 (3)	0.4378 (12)	0.050 (12)*
N2A	0.2515 (2)	0.6125 (2)	0.69006 (18)	0.0237 (6)
H31A	0.292 (3)	0.623 (3)	0.7431 (15)	0.053 (13)*
N3A	0.4265 (2)	0.6338 (2)	0.61281 (18)	0.0203 (6)
N4A	0.2404 (2)	0.5850 (2)	0.52403 (18)	0.0215 (6)
N5A	0.5966 (2)	0.1192 (2)	0.36129 (19)	0.0254 (7)
N1B	-0.2049 (3)	0.3742 (2)	0.9833 (2)	0.0280 (7)
H30C	-0.206 (3)	0.378 (3)	1.0442 (11)	0.038 (11)*
H30D	-0.208 (4)	0.4330 (15)	0.958 (2)	0.052 (13)*
N2B	0.2544 (2)	0.1086 (2)	0.83717 (18)	0.0205 (6)
N3B	0.4302 (2)	0.1230 (2)	0.93368 (17)	0.0189 (6)
N4B	0.2410 (2)	0.0961 (2)	1.00219 (18)	0.0204 (6)
N5B	0.5781 (3)	0.6088 (2)	1.19868 (19)	0.0290 (7)
C1A	0.5185 (3)	0.6353 (2)	0.8485 (2)	0.0208 (7)
C2A	0.6025 (3)	0.6311 (2)	0.9353 (2)	0.0211 (7)
C3A	0.7267 (3)	0.6384 (3)	0.9303 (2)	0.0246 (8)
H3A	0.7602	0.6468	0.8701	0.030*
C4A	0.8023 (3)	0.6337 (3)	1.0132 (2)	0.0267 (8)
H4A	0.8872	0.6383	1.0091	0.032*
C5A	0.7547 (3)	0.6223 (3)	1.1015 (2)	0.0263 (8)
H5A	0.8057	0.6180	1.1582	0.032*
C6A	0.6304 (3)	0.6173 (2)	1.1044 (2)	0.0233 (7)
C7A	0.5524 (3)	0.6208 (2)	1.0234 (2)	0.0226 (7)
H7A	0.4676	0.6165	1.0278	0.027*
C8A	-0.1095 (3)	0.8173 (3)	0.5442 (2)	0.0234 (7)
C9A	-0.0935 (3)	0.7194 (3)	0.5020 (2)	0.0228 (7)
H9A	-0.1288	0.7018	0.4393	0.027*
C10A	-0.0275 (3)	0.6479 (3)	0.5495 (2)	0.0231 (7)
H10A	-0.0177	0.5814	0.5198	0.028*
C11A	0.0254 (3)	0.6732 (2)	0.6418 (2)	0.0202 (7)
C12A	0.0114 (3)	0.7709 (3)	0.6851 (2)	0.0235 (7)
H12A	0.0467	0.7881	0.7479	0.028*
C13A	-0.0538 (3)	0.8424 (3)	0.6366 (2)	0.0251 (8)
H13A	-0.0614	0.9095	0.6656	0.030*
C14A	0.3075 (3)	0.6091 (2)	0.6045 (2)	0.0202 (7)
C15A	0.2235 (3)	0.5607 (3)	0.3508 (2)	0.0304 (9)
H15A	0.2011	0.4869	0.3468	0.046*
H15B	0.2697	0.5769	0.2957	0.046*
H15C	0.1504	0.6009	0.3501	0.046*
C16A	0.2984 (3)	0.5868 (3)	0.4418 (2)	0.0242 (7)
C17A	0.4207 (3)	0.6121 (3)	0.4427 (2)	0.0235 (7)
H17A	0.4605	0.6132	0.3845	0.028*
C18A	0.4826 (3)	0.6354 (2)	0.5298 (2)	0.0230 (7)

C19A	0.6141 (3)	0.6660 (3)	0.5374 (2)	0.0285 (8)
H19A	0.6236	0.7408	0.5507	0.043*
H19B	0.6497	0.6468	0.4768	0.043*
H19C	0.6549	0.6306	0.5899	0.043*
C1B	0.5222 (3)	0.1278 (2)	0.7058 (2)	0.0219 (7)
C2B	0.6089 (3)	0.1314 (2)	0.6288 (2)	0.0206 (7)
C3B	0.7329 (3)	0.1475 (3)	0.6509 (2)	0.0251 (8)
H3B	0.7636	0.1540	0.7161	0.030*
C4B	0.8108 (3)	0.1541 (3)	0.5774 (2)	0.0278 (8)
H4B	0.8948	0.1654	0.5925	0.033*
C5B	0.7669 (3)	0.1444 (3)	0.4823 (2)	0.0253 (8)
H5B	0.8196	0.1488	0.4317	0.030*
C6B	0.6440 (3)	0.1279 (2)	0.4629 (2)	0.0223 (7)
C7B	0.5647 (3)	0.1210 (2)	0.5334 (2)	0.0212 (7)
H7B	0.4810	0.1093	0.5175	0.025*
C8B	-0.1280 (3)	0.3056 (2)	0.9441 (2)	0.0214 (7)
C9B	-0.0823 (3)	0.3202 (3)	0.8544 (2)	0.0230 (7)
H9B	-0.1021	0.3803	0.8217	0.028*
C10B	-0.0093 (3)	0.2495 (3)	0.8126 (2)	0.0226 (7)
H10B	0.0209	0.2605	0.7516	0.027*
C11B	0.0202 (3)	0.1607 (2)	0.8610 (2)	0.0197 (7)
C12B	-0.0232 (3)	0.1464 (2)	0.9512 (2)	0.0202 (7)
H12B	-0.0023	0.0869	0.9844	0.024*
C13B	-0.0958 (3)	0.2174 (3)	0.9924 (2)	0.0227 (7)
H13B	-0.1246	0.2069	1.0540	0.027*
C14B	0.3095 (3)	0.1085 (2)	0.9286 (2)	0.0194 (7)
C15B	0.6211 (3)	0.1446 (3)	1.0284 (2)	0.0222 (7)
H15D	0.6578	0.0981	0.9818	0.033*
H15E	0.6537	0.1320	1.0935	0.033*
H15F	0.6393	0.2163	1.0144	0.033*
C16B	0.4877 (3)	0.1253 (2)	1.0218 (2)	0.0182 (7)
C17B	0.4228 (3)	0.1115 (2)	1.1025 (2)	0.0202 (7)
H17B	0.4626	0.1113	1.1648	0.024*
C18B	0.2995 (3)	0.0982 (2)	1.0899 (2)	0.0215 (7)
C19B	0.2233 (3)	0.0849 (3)	1.1730 (2)	0.0303 (8)
H19D	0.1465	0.1185	1.1611	0.046*
H19E	0.2653	0.1163	1.2317	0.046*
H19F	0.2081	0.0112	1.1808	0.046*

Atomic displacement parameters ( $\text{\AA}^2$ )

	$U^{11}$	$U^{22}$	$U^{33}$	$U^{12}$	$U^{13}$	$U^{23}$
S1	0.0197 (3)	0.0269 (4)	0.0186 (4)	0.0000 (3)	-0.0007 (3)	0.0039 (3)
S2	0.0195 (3)	0.0262 (4)	0.0170 (3)	-0.0018 (3)	0.0006 (3)	0.0009 (3)
O1A	0.0196 (10)	0.0349 (13)	0.0205 (11)	0.0019 (9)	-0.0009 (9)	0.0004 (10)
O2A	0.0262 (11)	0.0363 (13)	0.0183 (11)	-0.0013 (10)	-0.0018 (9)	0.0047 (10)
O3A	0.0236 (11)	0.0377 (13)	0.0212 (11)	0.0005 (10)	0.0000 (9)	0.0067 (10)
O4A	0.0270 (11)	0.0241 (12)	0.0277 (12)	-0.0010 (9)	-0.0029 (9)	0.0049 (10)
O5A	0.0320 (13)	0.0546 (17)	0.0274 (13)	0.0037 (12)	0.0051 (11)	0.0041 (12)
O6A	0.0517 (16)	0.0597 (18)	0.0182 (12)	0.0026 (14)	-0.0101 (11)	0.0020 (12)
O2B	0.0248 (11)	0.0422 (14)	0.0166 (11)	-0.0047 (10)	0.0005 (9)	0.0043 (10)
O1B	0.0235 (11)	0.0447 (14)	0.0174 (11)	0.0027 (10)	0.0009 (9)	0.0075 (10)
O3B	0.0225 (11)	0.0336 (13)	0.0217 (11)	-0.0016 (10)	-0.0026 (9)	0.0007 (10)
O4B	0.0268 (11)	0.0263 (12)	0.0234 (11)	-0.0023 (10)	0.0040 (9)	0.0017 (10)

O5B	0.0284 (12)	0.0383 (14)	0.0236 (12)	-0.0007 (10)	-0.0022 (10)	0.0023 (11)
O6B	0.0412 (14)	0.0504 (16)	0.0190 (11)	-0.0021 (12)	0.0094 (10)	0.0039 (11)
N1A	0.0499 (18)	0.0327 (17)	0.0227 (15)	0.0182 (14)	0.0033 (13)	0.0057 (13)
N2A	0.0213 (13)	0.0326 (16)	0.0162 (13)	-0.0009 (11)	-0.0033 (11)	-0.0007 (12)
N3A	0.0200 (12)	0.0234 (14)	0.0176 (12)	0.0020 (11)	-0.0019 (10)	0.0041 (11)
N4A	0.0223 (13)	0.0247 (14)	0.0175 (12)	0.0023 (11)	-0.0016 (10)	0.0041 (11)
N5A	0.0327 (15)	0.0248 (15)	0.0191 (13)	-0.0020 (12)	0.0032 (12)	0.0044 (11)
N1B	0.0308 (14)	0.0297 (16)	0.0243 (14)	0.0072 (12)	0.0020 (12)	0.0040 (13)
N2B	0.0186 (12)	0.0271 (14)	0.0155 (12)	0.0018 (11)	-0.0027 (10)	0.0032 (11)
N3B	0.0199 (12)	0.0205 (13)	0.0169 (12)	0.0000 (10)	0.0030 (10)	0.0033 (11)
N4B	0.0200 (12)	0.0239 (14)	0.0181 (12)	0.0031 (11)	0.0028 (10)	0.0034 (11)
N5B	0.0405 (16)	0.0269 (15)	0.0195 (14)	0.0023 (13)	-0.0002 (12)	0.0032 (12)
C1A	0.0253 (15)	0.0184 (16)	0.0181 (15)	-0.0019 (12)	-0.0023 (13)	0.0020 (13)
C2A	0.0244 (15)	0.0195 (16)	0.0189 (15)	-0.0005 (13)	-0.0043 (12)	0.0024 (13)
C3A	0.0290 (16)	0.0238 (17)	0.0205 (16)	-0.0054 (14)	-0.0016 (13)	0.0029 (14)
C4A	0.0232 (16)	0.0252 (18)	0.0305 (18)	-0.0053 (13)	-0.0067 (14)	0.0024 (15)
C5A	0.0279 (16)	0.0269 (18)	0.0233 (16)	-0.0040 (14)	-0.0066 (13)	0.0041 (14)
C6A	0.0306 (16)	0.0220 (16)	0.0173 (15)	-0.0019 (13)	-0.0003 (13)	0.0043 (13)
C7A	0.0220 (15)	0.0227 (16)	0.0230 (16)	0.0007 (13)	-0.0021 (13)	0.0048 (13)
C8A	0.0242 (15)	0.0272 (17)	0.0199 (15)	-0.0024 (13)	0.0080 (13)	0.0068 (13)
C9A	0.0195 (15)	0.0305 (18)	0.0181 (15)	-0.0006 (13)	-0.0009 (12)	0.0028 (14)
C10A	0.0194 (15)	0.0248 (17)	0.0248 (16)	-0.0008 (13)	-0.0003 (13)	0.0005 (14)
C11A	0.0183 (14)	0.0217 (16)	0.0206 (15)	-0.0019 (12)	0.0052 (12)	-0.0005 (13)
C12A	0.0197 (14)	0.0318 (18)	0.0189 (15)	-0.0050 (13)	0.0027 (12)	0.0011 (14)
C13A	0.0255 (15)	0.0260 (17)	0.0245 (16)	-0.0005 (13)	0.0077 (13)	0.0030 (14)
C14A	0.0235 (15)	0.0210 (16)	0.0162 (14)	0.0020 (12)	0.0013 (12)	0.0024 (13)
C15A	0.0303 (17)	0.043 (2)	0.0170 (16)	0.0008 (16)	-0.0023 (14)	0.0032 (15)
C16A	0.0284 (16)	0.0247 (17)	0.0200 (15)	0.0053 (13)	-0.0011 (13)	0.0066 (13)
C17A	0.0241 (15)	0.0259 (17)	0.0213 (16)	0.0041 (13)	0.0025 (13)	0.0052 (13)
C18A	0.0259 (16)	0.0189 (16)	0.0248 (16)	0.0051 (13)	0.0023 (13)	0.0034 (13)
C19A	0.0257 (16)	0.037 (2)	0.0235 (16)	-0.0002 (15)	0.0048 (13)	0.0037 (15)
C1B	0.0250 (15)	0.0231 (17)	0.0179 (15)	-0.0004 (13)	0.0012 (12)	0.0047 (13)
C2B	0.0248 (15)	0.0150 (15)	0.0222 (15)	-0.0009 (12)	0.0016 (13)	0.0044 (13)
C3B	0.0264 (16)	0.0271 (18)	0.0214 (16)	-0.0039 (14)	0.0002 (13)	0.0007 (14)
C4B	0.0219 (15)	0.0344 (19)	0.0272 (17)	-0.0044 (14)	0.0007 (13)	0.0069 (15)
C5B	0.0252 (16)	0.0260 (17)	0.0257 (16)	-0.0005 (13)	0.0068 (13)	0.0062 (14)
C6B	0.0295 (16)	0.0186 (16)	0.0188 (15)	-0.0015 (13)	0.0013 (13)	0.0031 (13)
C7B	0.0206 (14)	0.0182 (15)	0.0256 (16)	0.0010 (12)	0.0028 (13)	0.0070 (13)
C8B	0.0180 (14)	0.0244 (17)	0.0209 (15)	-0.0033 (13)	-0.0037 (12)	-0.0009 (13)
C9B	0.0215 (15)	0.0267 (17)	0.0204 (15)	0.0009 (13)	-0.0052 (13)	0.0062 (13)
C10B	0.0218 (15)	0.0293 (18)	0.0159 (14)	-0.0028 (13)	-0.0035 (12)	0.0009 (13)
C11B	0.0183 (14)	0.0221 (16)	0.0180 (15)	-0.0025 (12)	-0.0023 (12)	-0.0003 (13)
C12B	0.0175 (14)	0.0256 (17)	0.0175 (14)	-0.0013 (12)	-0.0025 (12)	0.0056 (13)
C13B	0.0198 (15)	0.0293 (17)	0.0191 (15)	-0.0026 (13)	0.0010 (12)	0.0050 (14)
C14B	0.0210 (14)	0.0199 (16)	0.0171 (14)	0.0008 (12)	0.0009 (12)	-0.0001 (13)
C15B	0.0224 (15)	0.0247 (17)	0.0195 (15)	-0.0008 (13)	0.0012 (13)	0.0021 (13)
C16B	0.0188 (14)	0.0175 (15)	0.0179 (14)	0.0021 (12)	-0.0025 (12)	0.0003 (12)
C17B	0.0251 (15)	0.0216 (16)	0.0136 (14)	0.0005 (13)	-0.0019 (12)	0.0023 (12)
C18B	0.0286 (16)	0.0245 (16)	0.0121 (14)	0.0029 (13)	0.0020 (12)	0.0064 (13)
C19B	0.0283 (17)	0.045 (2)	0.0197 (16)	0.0038 (15)	0.0059 (13)	0.0108 (15)

Geometric parameters (Å, °)

S1—O4A	1.426 (2)	C9A—H9A	0.9500
S1—O3A	1.441 (2)	C10A—C11A	1.401 (4)
S1—N2A	1.652 (3)	C10A—H10A	0.9500

S1—C11A	1.746 (3)	C11A—C12A	1.393 (5)
S2—O4B	1.429 (2)	C12A—C13A	1.377 (5)
S2—O3B	1.436 (2)	C12A—H12A	0.9500
S2—N2B	1.662 (3)	C13A—H13A	0.9500
S2—C11B	1.744 (3)	C15A—C16A	1.492 (4)
O1A—C1A	1.228 (4)	C15A—H15A	0.9800
O2A—C1A	1.313 (4)	C15A—H15B	0.9800
O2A—H32A	0.860 (18)	C15A—H15C	0.9800
O5A—N5B	1.227 (4)	C16A—C17A	1.389 (4)
O6A—N5B	1.222 (4)	C17A—C18A	1.374 (4)
O2B—C1B	1.310 (4)	C17A—H17A	0.9500
O1B—C1B	1.222 (4)	C18A—C19A	1.501 (4)
O5B—N5A	1.234 (3)	C19A—H19A	0.9800
O6B—N5A	1.228 (3)	C19A—H19B	0.9800
N1A—C8A	1.376 (4)	C19A—H19C	0.9800
N1A—H30A	0.861 (16)	C1B—C2B	1.489 (4)
N1A—H30B	0.855 (16)	C2B—C7B	1.388 (4)
N2A—C14A	1.380 (4)	C2B—C3B	1.403 (4)
N2A—H31A	0.846 (17)	C3B—C4B	1.388 (5)
N3A—C18A	1.351 (4)	C3B—H3B	0.9500
N3A—C14A	1.349 (4)	C4B—C5B	1.383 (5)
N4A—C14A	1.327 (4)	C4B—H4B	0.9500
N4A—C16A	1.352 (4)	C5B—C6B	1.385 (4)
N5A—C6B	1.479 (4)	C5B—H5B	0.9500
N1B—C8B	1.369 (4)	C6B—C7B	1.367 (4)
N1B—H30C	0.851 (15)	C7B—H7B	0.9500
N1B—H30D	0.861 (17)	C8B—C9B	1.401 (4)
N2B—C14B	1.381 (4)	C8B—C13B	1.405 (4)
N3B—C14B	1.347 (4)	C9B—C10B	1.375 (5)
N3B—C16B	1.349 (4)	C9B—H9B	0.9500
N4B—C14B	1.331 (4)	C10B—C11B	1.404 (4)
N4B—C18B	1.348 (4)	C10B—H10B	0.9500
N5B—C6A	1.479 (4)	C11B—C12B	1.397 (4)
C1A—C2A	1.488 (4)	C12B—C13B	1.371 (4)
C2A—C3A	1.388 (4)	C12B—H12B	0.9500
C2A—C7A	1.392 (4)	C13B—H13B	0.9500
C3A—C4A	1.393 (4)	C15B—C16B	1.494 (4)
C3A—H3A	0.9500	C15B—H15D	0.9800
C4A—C5A	1.384 (5)	C15B—H15E	0.9800
C4A—H4A	0.9500	C15B—H15F	0.9800
C5A—C6A	1.386 (5)	C16B—C17B	1.392 (4)
C5A—H5A	0.9500	C17B—C18B	1.377 (4)
C6A—C7A	1.385 (4)	C17B—H17B	0.9500
C7A—H7A	0.9500	C18B—C19B	1.494 (4)
C8A—C9A	1.394 (5)	C19B—H19D	0.9800
C8A—C13A	1.412 (4)	C19B—H19E	0.9800
C9A—C10A	1.374 (4)	C19B—H19F	0.9800
O4A—S1—O3A	118.93 (14)	H15B—C15A—H15C	109.5
O4A—S1—N2A	110.26 (14)	N4A—C16A—C17A	121.5 (3)
O3A—S1—N2A	102.13 (13)	N4A—C16A—C15A	116.2 (3)
O4A—S1—C11A	109.50 (14)	C17A—C16A—C15A	122.3 (3)
O3A—S1—C11A	109.07 (14)	C18A—C17A—C16A	118.4 (3)
N2A—S1—C11A	106.05 (14)	C18A—C17A—H17A	120.8
O4B—S2—O3B	119.46 (14)	C16A—C17A—H17A	120.8
O4B—S2—N2B	109.61 (13)	N3A—C18A—C17A	121.1 (3)

O3B—S2—N2B	102.28 (13)	N3A—C18A—C19A	116.8 (3)
O4B—S2—C11B	108.36 (14)	C17A—C18A—C19A	122.0 (3)
O3B—S2—C11B	109.01 (14)	C18A—C19A—H19A	109.5
N2B—S2—C11B	107.48 (14)	C18A—C19A—H19B	109.5
C1A—O2A—H32A	110 (2)	H19A—C19A—H19B	109.5
C8A—N1A—H30A	114 (2)	C18A—C19A—H19C	109.5
C8A—N1A—H30B	119 (3)	H19A—C19A—H19C	109.5
H30A—N1A—H30B	111 (3)	H19B—C19A—H19C	109.5
C14A—N2A—S1	126.1 (2)	O1B—C1B—O2B	123.9 (3)
C14A—N2A—H31A	121 (2)	O1B—C1B—C2B	122.1 (3)
S1—N2A—H31A	113 (2)	O2B—C1B—C2B	114.0 (3)
C18A—N3A—C14A	116.2 (3)	C7B—C2B—C3B	119.8 (3)
C14A—N4A—C16A	115.8 (3)	C7B—C2B—C1B	118.9 (3)
O6B—N5A—O5B	123.6 (3)	C3B—C2B—C1B	121.4 (3)
O6B—N5A—C6B	118.9 (3)	C4B—C3B—C2B	119.9 (3)
O5B—N5A—C6B	117.5 (3)	C4B—C3B—H3B	120.1
C8B—N1B—H30C	117 (3)	C2B—C3B—H3B	120.1
C8B—N1B—H30D	116 (3)	C5B—C4B—C3B	120.4 (3)
H30C—N1B—H30D	114 (3)	C5B—C4B—H4B	119.8
C14B—N2B—S2	124.7 (2)	C3B—C4B—H4B	119.8
C14B—N3B—C16B	117.1 (3)	C4B—C5B—C6B	118.3 (3)
C14B—N4B—C18B	116.0 (3)	C4B—C5B—H5B	120.8
O6A—N5B—O5A	124.2 (3)	C6B—C5B—H5B	120.8
O6A—N5B—C6A	118.1 (3)	C7B—C6B—C5B	122.9 (3)
O5A—N5B—C6A	117.7 (3)	C7B—C6B—N5A	118.7 (3)
O1A—C1A—O2A	123.9 (3)	C5B—C6B—N5A	118.4 (3)
O1A—C1A—C2A	121.4 (3)	C6B—C7B—C2B	118.8 (3)
O2A—C1A—C2A	114.7 (3)	C6B—C7B—H7B	120.6
C3A—C2A—C7A	120.4 (3)	C2B—C7B—H7B	120.6
C3A—C2A—C1A	122.0 (3)	N1B—C8B—C9B	121.0 (3)
C7A—C2A—C1A	117.6 (3)	N1B—C8B—C13B	120.4 (3)
C2A—C3A—C4A	120.2 (3)	C9B—C8B—C13B	118.6 (3)
C2A—C3A—H3A	119.9	C10B—C9B—C8B	121.4 (3)
C4A—C3A—H3A	119.9	C10B—C9B—H9B	119.3
C5A—C4A—C3A	120.5 (3)	C8B—C9B—H9B	119.3
C5A—C4A—H4A	119.8	C9B—C10B—C11B	119.3 (3)
C3A—C4A—H4A	119.8	C9B—C10B—H10B	120.3
C6A—C5A—C4A	117.9 (3)	C11B—C10B—H10B	120.3
C6A—C5A—H5A	121.0	C12B—C11B—C10B	119.7 (3)
C4A—C5A—H5A	121.0	C12B—C11B—S2	120.9 (2)
C5A—C6A—C7A	123.2 (3)	C10B—C11B—S2	119.4 (2)
C5A—C6A—N5B	118.6 (3)	C13B—C12B—C11B	120.6 (3)
C7A—C6A—N5B	118.2 (3)	C13B—C12B—H12B	119.7
C6A—C7A—C2A	117.8 (3)	C11B—C12B—H12B	119.7
C6A—C7A—H7A	121.1	C12B—C13B—C8B	120.3 (3)
C2A—C7A—H7A	121.1	C12B—C13B—H13B	119.8
N1A—C8A—C9A	121.0 (3)	C8B—C13B—H13B	119.8
N1A—C8A—C13A	120.5 (3)	N4B—C14B—N3B	126.4 (3)
C9A—C8A—C13A	118.4 (3)	N4B—C14B—N2B	118.5 (3)
C10A—C9A—C8A	121.1 (3)	N3B—C14B—N2B	115.1 (3)
C10A—C9A—H9A	119.4	C16B—C15B—H15D	109.5
C8A—C9A—H9A	119.4	C16B—C15B—H15E	109.5
C9A—C10A—C11A	119.8 (3)	H15D—C15B—H15E	109.5
C9A—C10A—H10A	120.1	C16B—C15B—H15F	109.5
C11A—C10A—H10A	120.1	H15D—C15B—H15F	109.5

C12A—C11A—C10A	120.0 (3)	H15E—C15B—H15F	109.5
C12A—C11A—S1	119.6 (2)	N3B—C16B—C17B	120.2 (3)
C10A—C11A—S1	120.3 (2)	N3B—C16B—C15B	117.5 (3)
C13A—C12A—C11A	119.7 (3)	C17B—C16B—C15B	122.4 (3)
C13A—C12A—H12A	120.1	C18B—C17B—C16B	118.3 (3)
C11A—C12A—H12A	120.1	C18B—C17B—H17B	120.8
C12A—C13A—C8A	120.9 (3)	C16B—C17B—H17B	120.8
C12A—C13A—H13A	119.6	N4B—C18B—C17B	122.1 (3)
C8A—C13A—H13A	119.6	N4B—C18B—C19B	116.4 (3)
N4A—C14A—N3A	127.1 (3)	C17B—C18B—C19B	121.6 (3)
N4A—C14A—N2A	118.0 (3)	C18B—C19B—H19D	109.5
N3A—C14A—N2A	114.9 (3)	C18B—C19B—H19E	109.5
C16A—C15A—H15A	109.5	H19D—C19B—H19E	109.5
C16A—C15A—H15B	109.5	C18B—C19B—H19F	109.5
H15A—C15A—H15B	109.5	H19D—C19B—H19F	109.5
C16A—C15A—H15C	109.5	H19E—C19B—H19F	109.5
H15A—C15A—H15C	109.5		
O4A—S1—N2A—C14A	54.0 (3)	C14A—N3A—C18A— C19A	178.1 (3)
O3A—S1—N2A—C14A	-178.7 (3)	C16A—C17A—C18A— N3A	0.1 (5)
C11A—S1—N2A—C14A	-64.5 (3)	C16A—C17A—C18A— C19A	-178.5 (3)
O4B—S2—N2B—C14B	-48.5 (3)	O1B—C1B—C2B—C7B	-4.0 (5)
O3B—S2—N2B—C14B	-176.2 (3)	O2B—C1B—C2B—C7B	176.6 (3)
C11B—S2—N2B—C14B	69.1 (3)	O1B—C1B—C2B—C3B	174.5 (3)
O1A—C1A—C2A—C3A	177.5 (3)	O2B—C1B—C2B—C3B	-4.9 (4)
O2A—C1A—C2A—C3A	-2.3 (4)	C7B—C2B—C3B—C4B	0.7 (5)
O1A—C1A—C2A—C7A	-3.4 (5)	C1B—C2B—C3B—C4B	-177.8 (3)
O2A—C1A—C2A—C7A	176.8 (3)	C2B—C3B—C4B—C5B	-0.3 (5)
C7A—C2A—C3A—C4A	1.2 (5)	C3B—C4B—C5B—C6B	-0.1 (5)
C1A—C2A—C3A—C4A	-179.7 (3)	C4B—C5B—C6B—C7B	0.1 (5)
C2A—C3A—C4A—C5A	-0.4 (5)	C4B—C5B—C6B—N5A	179.0 (3)
C3A—C4A—C5A—C6A	-0.9 (5)	O6B—N5A—C6B—C7B	179.8 (3)
C4A—C5A—C6A—C7A	1.5 (5)	O5B—N5A—C6B—C7B	-0.4 (4)
C4A—C5A—C6A—N5B	-177.9 (3)	O6B—N5A—C6B—C5B	0.9 (4)
O6A—N5B—C6A—C5A	5.4 (5)	O5B—N5A—C6B—C5B	-179.4 (3)
O5A—N5B—C6A—C5A	-174.4 (3)	C5B—C6B—C7B—C2B	0.3 (5)
O6A—N5B—C6A—C7A	-174.0 (3)	N5A—C6B—C7B—C2B	-178.6 (3)
O5A—N5B—C6A—C7A	6.2 (4)	C3B—C2B—C7B—C6B	-0.7 (5)
C5A—C6A—C7A—C2A	-0.7 (5)	C1B—C2B—C7B—C6B	177.8 (3)
N5B—C6A—C7A—C2A	178.7 (3)	N1B—C8B—C9B—C10B	-177.1 (3)
C3A—C2A—C7A—C6A	-0.7 (5)	C13B—C8B—C9B—C10B	1.3 (5)
C1A—C2A—C7A—C6A	-179.8 (3)	C8B—C9B—C10B—C11B	-0.1 (5)
N1A—C8A—C9A—C10A	-175.9 (3)	C9B—C10B—C11B—C12B	-1.0 (4)
C13A—C8A—C9A—C10A	1.5 (5)	C9B—C10B—C11B—S2	179.7 (2)
C8A—C9A—C10A—C11A	-0.3 (5)	O4B—S2—C11B—C12B	25.0 (3)
C9A—C10A—C11A—C12A	-0.2 (5)	O3B—S2—C11B—C12B	156.5 (2)
C9A—C10A—C11A—S1	179.4 (2)	N2B—S2—C11B—C12B	-93.4 (3)
O4A—S1—C11A—C12A	160.7 (2)	O4B—S2—C11B—C10B	-155.7 (2)
O3A—S1—C11A—C12A	29.0 (3)	O3B—S2—C11B—C10B	-24.2 (3)
N2A—S1—C11A—C12A	-80.3 (3)	N2B—S2—C11B—C10B	85.9 (3)
O4A—S1—C11A—C10A	-18.9 (3)	C10B—C11B—C12B— C13B	0.9 (4)
O3A—S1—C11A—C10A	-150.7 (2)	S2—C11B—C12B—C13B	-179.8 (2)



N2A—S1—C11A—C10A	100.0 (3)	C11B—C12B—C13B—C8B	0.3 (5)
C10A—C11A—C12A— C13A	-0.4 (5)	N1B—C8B—C13B—C12B	177.0 (3)
S1—C11A—C12A—C13A	179.9 (2)	C9B—C8B—C13B—C12B	-1.3 (5)
C11A—C12A—C13A—C8A	1.7 (5)	C18B—N4B—C14B—N3B	-0.2 (5)
N1A—C8A—C13A—C12A	175.2 (3)	C18B—N4B—C14B—N2B	-179.0 (3)
C9A—C8A—C13A—C12A	-2.1 (5)	C16B—N3B—C14B—N4B	0.0 (5)
C16A—N4A—C14A—N3A	-0.9 (5)	C16B—N3B—C14B—N2B	178.8 (3)
C16A—N4A—C14A—N2A	177.4 (3)	S2—N2B—C14B—N4B	-13.4 (4)
C18A—N3A—C14A—N4A	1.0 (5)	S2—N2B—C14B—N3B	167.7 (2)
C18A—N3A—C14A—N2A	-177.3 (3)	C14B—N3B—C16B—C17B	0.9 (4)
S1—N2A—C14A—N4A	3.7 (4)	C14B—N3B—C16B—C15B	-178.1 (3)
S1—N2A—C14A—N3A	-177.8 (2)	N3B—C16B—C17B—C18B	-1.5 (5)
C14A—N4A—C16A— C17A	0.3 (5)	C15B—C16B—C17B— C18B	177.5 (3)
C14A—N4A—C16A— C15A	-179.5 (3)	C14B—N4B—C18B—C17B	-0.4 (5)
N4A—C16A—C17A— C18A	0.0 (5)	C14B—N4B—C18B—C19B	179.7 (3)
C15A—C16A—C17A— C18A	179.8 (3)	C16B—C17B—C18B—N4B	1.3 (5)
C14A—N3A—C18A— C17A	-0.6 (4)	C16B—C17B—C18B— C19B	-178.8 (3)

#### Hydrogen-bond geometry (Å, °)

<i>D</i> —H··· <i>A</i>	<i>D</i> —H	H··· <i>A</i>	<i>D</i> ··· <i>A</i>	<i>D</i> —H··· <i>A</i>
N1A—H30B···O3B <sup>i</sup>	0.86 (2)	2.31 (2)	3.091 (4)	152 (4)
N1B—H30C···O3A <sup>ii</sup>	0.85 (2)	2.34 (2)	3.101 (4)	149 (3)
N2A—H31A···O1A	0.85 (2)	1.95 (2)	2.781 (3)	167 (4)
O2A—H32A···N3A	0.86 (2)	1.76 (2)	2.616 (3)	172 (4)

Symmetry codes: (i)  $-x, -y+1, -z+1$ ; (ii)  $-x, -y+1, -z+2$ .

All esds (except the esd in the dihedral angle between two l.s. planes) are estimated using the full covariance matrix. The cell esds are taken into account individually in the estimation of esds in distances, angles and torsion angles; correlations between esds in cell parameters are only used when they are defined by crystal symmetry. An approximate (isotropic) treatment of cell esds is used for estimating esds involving l.s. planes.

S1—N2A—C14A—N3A	-177.8 (2)	N3B—C16B—C17B—C18B	-1.5 (5)
C14A—N4A—C16A—C17A	0.3 (5)	C15B—C16B—C17B—C18B	177.5 (3)
C14A—N4A—C16A—C15A	-179.5 (3)	C14B—N4B—C18B—C17B	-0.4 (5)
N4A—C16A—C17A—C18A	0.0 (5)	C14B—N4B—C18B—C19B	179.7 (3)
C15A—C16A—C17A—C18A	179.8 (3)	C16B—C17B—C18B—N4B	1.3 (5)
C14A—N3A—C18A—C17A	-0.6 (4)	C16B—C17B—C18B—C19B	-178.8 (3)

#### Hydrogen-bond geometry (Å, °)

<i>D</i> —H··· <i>A</i>	<i>D</i> —H	H··· <i>A</i>	<i>D</i> ··· <i>A</i>	<i>D</i> —H··· <i>A</i>
N1A—H30B···O3B <sup>i</sup>	0.86 (2)	2.31 (2)	3.091 (4)	152 (4)
N1B—H30C···O3A <sup>ii</sup>	0.85 (2)	2.34 (2)	3.101 (4)	149 (3)
N2A—H31A···O1A	0.85 (2)	1.95 (2)	2.781 (3)	167 (4)
O2A—H32A···N3A	0.86 (2)	1.76 (2)	2.616 (3)	172 (4)

Symmetry codes: (i)  $-x, -y+1, -z+1$ ; (ii)  $-x, -y+1, -z+2$ .

All esds (except the esd in the dihedral angle between two l.s. planes) are estimated using the full covariance matrix. The cell esds are taken into account individually in the estimation of esds in distances, angles and torsion angles; correlations between esds in cell parameters are only used when they are defined by crystal symmetry. An approximate (isotropic) treatment of cell esds is used for estimating esds involving l.s. planes.

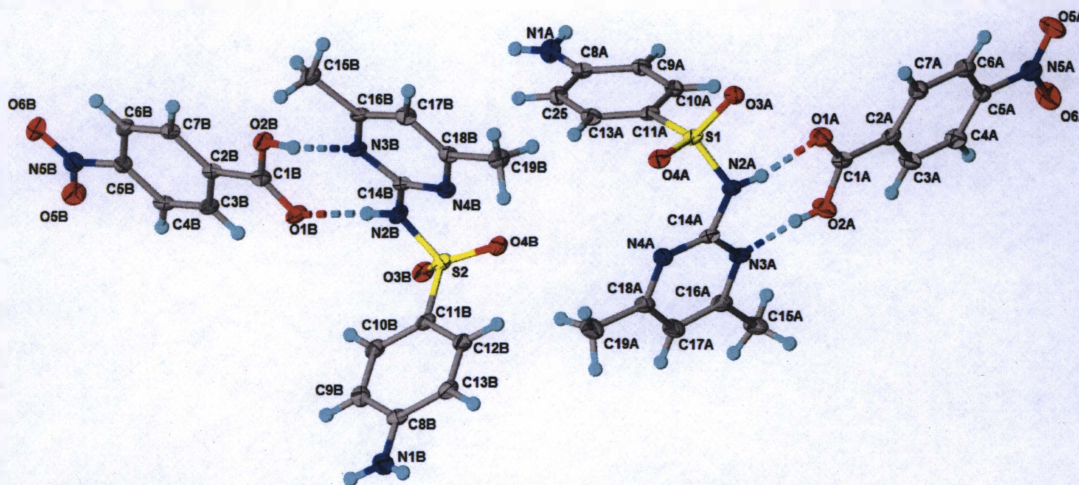


Figure S.4: Crystal Structure of the Cocrystal of Sulfamethazine and *p*-Nitrobenzoic Acid Showing Thermal Parameters (50% Thermal Ellipsoids) and Hydrogen Bonding.

#### Crystal data

$C_{12}H_{14}N_4O_2S \cdot C_7H_5NO_4$   
 $M_r = 445.45$

## Refinement

Refinement on  $F^2$   
Least-squares matrix: full  
 $R[F^2 > 2\sigma(F^2)] = 0.053$   
 $wR(F^2) = 0.136$   
 $S = 1.02$   
7240 reflections  
595 parameters  
8 restraints  
0 constraints

Hydrogen site location: mixed  
H atoms treated by a mixture of independent and  
constrained refinement  
 $w = 1/[\sigma^2(F_o^2) + (0.0602P)^2 + 0.0756P]$   
where  $P = (F_o^2 + 2F_c^2)/3$   
 $(\Delta/\sigma)_{\max} < 0.001$   
 $\Delta\rho_{\max} = 0.37 \text{ e } \text{\AA}^{-3}$   
 $\Delta\rho_{\min} = -0.39 \text{ e } \text{\AA}^{-3}$   
Extinction correction: none

## Fractional atomic coordinates and isotropic or equivalent isotropic displacement parameters ( $\text{\AA}^2$ )

	<i>x</i>	<i>y</i>	<i>z</i>	$U_{\text{iso}}^*/U_{\text{eq}}$
S1	0.31286 (10)	0.68243 (6)	0.26743 (4)	0.0224 (2)
O3A	0.3546 (3)	0.78173 (16)	0.24695 (12)	0.0265 (5)
N4A	0.1863 (4)	0.5347 (2)	0.38181 (15)	0.0288 (7)
O4A	0.1679 (3)	0.62923 (17)	0.23415 (12)	0.0258 (5)
N3A	0.3459 (3)	0.6329 (2)	0.47574 (15)	0.0259 (6)
N2A	0.2971 (4)	0.6943 (2)	0.35936 (15)	0.0233 (6)
H31A	0.362 (5)	0.743 (2)	0.380 (2)	0.071 (16)*
C10A	0.6318 (4)	0.6584 (2)	0.28031 (18)	0.0244 (7)
H10A	0.6445	0.7200	0.3061	0.029*
C25	0.5911 (4)	0.4784 (2)	0.20485 (18)	0.0251 (7)
H25	0.5774	0.4171	0.1786	0.030*
C8A	0.7485 (4)	0.5187 (2)	0.23076 (18)	0.0252 (7)
C14A	0.2740 (4)	0.6156 (2)	0.40654 (18)	0.0238 (7)
C13A	0.4584 (4)	0.5260 (2)	0.21693 (17)	0.0244 (7)
H13A	0.3533	0.4972	0.1999	0.029*
N1A	0.8813 (4)	0.4710 (2)	0.22156 (18)	0.0318 (7)
H30A	0.975 (3)	0.500 (3)	0.232 (2)	0.037 (12)*
H30B	0.877 (5)	0.420 (2)	0.1944 (19)	0.042 (12)*
C11A	0.4772 (4)	0.6170 (2)	0.25431 (17)	0.0228 (7)
C9A	0.7654 (4)	0.6104 (2)	0.26876 (19)	0.0252 (7)
H9A	0.8700	0.6391	0.2865	0.030*
C16A	0.3231 (4)	0.5608 (3)	0.52535 (19)	0.0294 (8)
C18A	0.1646 (5)	0.4622 (3)	0.43138 (19)	0.0316 (8)
C17A	0.2324 (5)	0.4738 (3)	0.5040 (2)	0.0348 (9)
H17A	0.2164	0.4227	0.5386	0.042*
C15A	0.4010 (5)	0.5799 (3)	0.60249 (19)	0.0362 (9)
H15A	0.5121	0.6115	0.5987	0.054*
H15B	0.4039	0.5181	0.6282	0.054*
H15C	0.3381	0.6227	0.6310	0.054*
C19A	0.0680 (6)	0.3704 (3)	0.4031 (2)	0.0463 (11)
H19A	0.0035	0.3835	0.3578	0.069*
H19B	-0.0045	0.3452	0.4417	0.069*
H19C	0.1415	0.3219	0.3911	0.069*
S2	0.07016 (10)	0.20503 (6)	0.21325 (4)	0.0244 (2)
O3B	0.1874 (3)	0.15073 (17)	0.24991 (12)	0.0280 (6)
N3B	0.0615 (3)	0.18954 (19)	-0.00353 (14)	0.0213 (6)

N34B	-0.0590 (3)	0.30249 (19)	0.07464 (15)	0.0220 (6)
O2A	0.5542 (3)	0.78286 (19)	0.52323 (14)	0.0357 (6)
H32A	0.492 (5)	0.733 (2)	0.504 (2)	0.065 (16)*
O4B	0.0788 (3)	0.30693 (17)	0.22815 (12)	0.0272 (5)
N2B	0.0950 (3)	0.1840 (2)	0.12404 (15)	0.0241 (6)
H31B	0.137 (5)	0.131 (2)	0.115 (2)	0.057 (14)*
O1A	0.5238 (3)	0.85150 (18)	0.41155 (13)	0.0338 (6)
O6A	1.0702 (3)	1.1703 (2)	0.66044 (15)	0.0466 (7)
O5A	1.0428 (4)	1.2476 (2)	0.55789 (15)	0.0492 (8)
C18B	-0.1084 (4)	0.3468 (2)	0.01249 (18)	0.0223 (7)
N1B	-0.5752 (4)	0.0046 (2)	0.27207 (18)	0.0337 (7)
H30D	-0.590 (4)	-0.0581 (14)	0.268 (2)	0.030 (11)*
H30C	-0.655 (4)	0.038 (3)	0.273 (2)	0.060 (15)*
C14B	0.0267 (4)	0.2285 (2)	0.06311 (17)	0.0199 (7)
C17B	-0.0732 (4)	0.3149 (2)	-0.05858 (18)	0.0248 (7)
H17B	-0.1059	0.3481	-0.1019	0.030*
C11B	-0.1222 (4)	0.1479 (2)	0.23141 (17)	0.0240 (7)
C8B	-0.4274 (4)	0.0519 (3)	0.25820 (17)	0.0246 (7)
C13B	-0.4012 (4)	0.1536 (3)	0.25954 (18)	0.0279 (8)
H13B	-0.4882	0.1904	0.2699	0.033*
C1A	0.5835 (4)	0.8530 (3)	0.47521 (19)	0.0270 (8)
C9B	-0.2969 (4)	-0.0018 (3)	0.24409 (18)	0.0269 (8)
H9B	-0.3121	-0.0710	0.2439	0.032*
C2A	0.6969 (4)	0.9367 (3)	0.50684 (18)	0.0260 (8)
N5A	1.0131 (4)	1.1763 (2)	0.59629 (17)	0.0318 (7)
C12B	-0.2509 (4)	0.2015 (3)	0.24611 (18)	0.0262 (8)
H12B	-0.2350	0.2708	0.2469	0.031*
C7A	0.7234 (4)	1.0210 (3)	0.46608 (19)	0.0288 (8)
H7A	0.6711	1.0239	0.4178	0.035*
C16B	0.0102 (4)	0.2341 (2)	-0.06519 (18)	0.0232 (7)
C5A	0.9017 (4)	1.0929 (2)	0.56388 (19)	0.0259 (8)
C10B	-0.1463 (4)	0.0466 (3)	0.23048 (18)	0.0256 (8)
H10B	-0.0587	0.0102	0.2204	0.031*
C19B	-0.1994 (4)	0.4330 (3)	0.02352 (19)	0.0282 (8)
H19D	-0.2923	0.4149	0.0543	0.042*
H19E	-0.2382	0.4546	-0.0254	0.042*
H19F	-0.1274	0.4860	0.0489	0.042*
C6A	0.8248 (4)	1.1008 (3)	0.49482 (19)	0.0314 (8)
H6A	0.8408	1.1592	0.4676	0.038*
C15B	0.0468 (4)	0.1922 (3)	-0.14024 (18)	0.0279 (8)
H15D	0.1545	0.1693	-0.1370	0.042*
H15E	0.0447	0.2426	-0.1780	0.042*
H15F	-0.0351	0.1373	-0.1546	0.042*
C3A	0.7754 (4)	0.9319 (3)	0.57632 (19)	0.0296 (8)
H3A	0.7573	0.8743	0.6043	0.035*
C4A	0.8802 (4)	1.0100 (3)	0.60577 (19)	0.0303 (8)
H4A	0.9355	1.0066	0.6533	0.036*
O2B	0.2121 (3)	0.03128 (17)	-0.02982 (12)	0.0259 (5)
H32B	0.159 (6)	0.080 (3)	-0.018 (3)	0.087 (19)*
O1B	0.2151 (3)	0.01007 (17)	0.09437 (12)	0.0288 (6)
O6B	0.6436 (3)	-0.36537 (18)	-0.06644 (13)	0.0335 (6)
O5B	0.6630 (3)	-0.37401 (18)	0.05452 (14)	0.0369 (6)
C2B	0.3518 (4)	-0.0957 (2)	0.01966 (17)	0.0212 (7)
N5B	0.6176 (3)	-0.3364 (2)	-0.00318 (16)	0.0266 (7)
C3B	0.4047 (4)	-0.1425 (2)	0.08291 (18)	0.0244 (7)

H3B	0.3794	-0.1207	0.1314	0.029*
C5B	0.5287 (4)	-0.2504 (2)	0.00488 (18)	0.0216 (7)
C4B	0.4937 (4)	-0.2206 (2)	0.07553 (18)	0.0245 (7)
H4B	0.5299	-0.2530	0.1185	0.029*
C6B	0.4799 (4)	-0.2040 (2)	-0.05954 (18)	0.0246 (7)
H6B	0.5073	-0.2256	-0.1077	0.029*
C1B	0.2532 (4)	-0.0132 (2)	0.03155 (18)	0.0233 (7)
C7B	0.3907 (4)	-0.1258 (2)	-0.05167 (18)	0.0227 (7)
H7B	0.3562	-0.0928	-0.0947	0.027*

Atomic displacement parameters (Å<sup>2</sup>)

	$U^{11}$	$U^{22}$	$U^{33}$	$U^{12}$	$U^{13}$	$U^{23}$
S1	0.0240 (4)	0.0289 (5)	0.0144 (4)	0.0022 (3)	0.0015 (3)	0.0038 (3)
O3A	0.0333 (14)	0.0248 (13)	0.0214 (12)	0.0022 (11)	0.0018 (10)	0.0057 (9)
N4A	0.0389 (18)	0.0263 (16)	0.0198 (15)	-0.0032 (14)	0.0037 (13)	0.0010 (12)
O4A	0.0229 (13)	0.0347 (14)	0.0191 (12)	0.0012 (10)	-0.0021 (9)	0.0021 (10)
N3A	0.0307 (17)	0.0313 (16)	0.0155 (14)	0.0007 (13)	0.0039 (12)	0.0062 (12)
N2A	0.0287 (16)	0.0257 (16)	0.0151 (14)	-0.0002 (13)	0.0036 (12)	0.0025 (12)
C10A	0.0265 (19)	0.0247 (18)	0.0209 (18)	-0.0022 (15)	0.0018 (14)	0.0019 (13)
C25	0.0282 (19)	0.0256 (18)	0.0215 (18)	0.0037 (15)	-0.0007 (14)	0.0008 (14)
C8A	0.0254 (19)	0.0301 (19)	0.0204 (17)	0.0020 (15)	0.0040 (14)	0.0052 (14)
C14A	0.0204 (18)	0.0308 (19)	0.0205 (18)	0.0019 (15)	0.0058 (14)	0.0021 (14)
C13A	0.0234 (18)	0.0294 (19)	0.0191 (17)	-0.0025 (15)	-0.0017 (14)	0.0039 (14)
N1A	0.0236 (18)	0.0335 (19)	0.0379 (19)	0.0033 (15)	0.0006 (14)	-0.0054 (15)
C11A	0.0248 (18)	0.0297 (19)	0.0138 (16)	0.0010 (15)	0.0028 (13)	0.0044 (13)
C9A	0.0209 (18)	0.0284 (19)	0.0257 (18)	-0.0017 (15)	0.0031 (14)	0.0037 (14)
C16A	0.035 (2)	0.034 (2)	0.0198 (18)	0.0003 (16)	0.0036 (15)	0.0041 (15)
C18A	0.044 (2)	0.030 (2)	0.0200 (18)	-0.0044 (17)	0.0072 (16)	0.0028 (15)
C17A	0.049 (2)	0.031 (2)	0.0231 (19)	-0.0045 (18)	0.0022 (17)	0.0070 (15)
C15A	0.048 (2)	0.038 (2)	0.0199 (19)	-0.0092 (18)	-0.0009 (17)	0.0096 (15)
C19A	0.077 (3)	0.036 (2)	0.022 (2)	-0.012 (2)	0.001 (2)	0.0062 (16)
S2	0.0262 (5)	0.0316 (5)	0.0162 (4)	0.0064 (4)	0.0020 (3)	0.0017 (3)
O3B	0.0300 (14)	0.0355 (14)	0.0198 (12)	0.0104 (11)	-0.0008 (10)	0.0031 (10)
N3B	0.0222 (15)	0.0250 (15)	0.0173 (14)	0.0035 (12)	0.0049 (11)	0.0032 (11)
N34B	0.0212 (15)	0.0226 (15)	0.0231 (15)	0.0045 (12)	0.0036 (11)	0.0043 (11)
O2A	0.0445 (17)	0.0335 (15)	0.0252 (14)	-0.0114 (13)	-0.0041 (12)	0.0073 (11)
O4B	0.0311 (14)	0.0296 (13)	0.0208 (12)	0.0043 (11)	0.0011 (10)	-0.0028 (10)
N2B	0.0294 (16)	0.0283 (17)	0.0166 (14)	0.0113 (13)	0.0027 (12)	0.0011 (12)
O1A	0.0443 (16)	0.0359 (15)	0.0188 (13)	-0.0053 (12)	-0.0011 (11)	0.0037 (10)
O6A	0.0524 (19)	0.0437 (17)	0.0391 (17)	-0.0080 (14)	-0.0153 (14)	0.0012 (13)
O5A	0.066 (2)	0.0397 (17)	0.0359 (16)	-0.0218 (15)	0.0024 (14)	0.0072 (13)
C18B	0.0188 (17)	0.0243 (18)	0.0234 (18)	-0.0001 (14)	0.0011 (14)	0.0033 (14)
N1B	0.037 (2)	0.0265 (18)	0.0388 (19)	0.0061 (16)	0.0073 (15)	0.0045 (14)
C14B	0.0201 (17)	0.0236 (17)	0.0161 (16)	0.0012 (14)	0.0039 (13)	0.0035 (13)
C17B	0.0242 (18)	0.0278 (19)	0.0222 (18)	0.0032 (15)	-0.0016 (14)	0.0054 (14)
C11B	0.0298 (19)	0.0308 (19)	0.0126 (16)	0.0083 (15)	0.0029 (13)	0.0027 (13)
C8B	0.0255 (19)	0.033 (2)	0.0159 (17)	0.0046 (15)	0.0008 (14)	0.0047 (14)
C13B	0.032 (2)	0.032 (2)	0.0220 (18)	0.0111 (16)	0.0062 (15)	0.0016 (15)
C1A	0.029 (2)	0.0295 (19)	0.0227 (19)	0.0016 (15)	0.0064 (15)	0.0041 (14)
C9B	0.033 (2)	0.0258 (19)	0.0228 (18)	0.0064 (15)	-0.0031 (15)	0.0023 (14)
C2A	0.0250 (19)	0.033 (2)	0.0194 (17)	0.0008 (15)	0.0037 (14)	-0.0014 (14)
N5A	0.0295 (17)	0.0355 (18)	0.0292 (17)	-0.0009 (14)	0.0017 (13)	-0.0009 (14)
C12B	0.033 (2)	0.0257 (19)	0.0222 (18)	0.0083 (15)	0.0061 (15)	0.0049 (14)

C7A	0.035 (2)	0.030 (2)	0.0201 (18)	0.0003 (16)	0.0012 (15)	0.0001 (14)
C16B	0.0242 (18)	0.0269 (18)	0.0184 (17)	-0.0011 (14)	0.0068 (13)	0.0025 (13)
C5A	0.0245 (19)	0.0250 (18)	0.0272 (19)	-0.0025 (15)	0.0046 (15)	-0.0014 (14)
C10B	0.0282 (19)	0.032 (2)	0.0182 (17)	0.0106 (16)	0.0014 (14)	0.0011 (14)
C19B	0.0268 (19)	0.032 (2)	0.0272 (19)	0.0074 (16)	0.0023 (15)	0.0037 (15)
C6A	0.037 (2)	0.033 (2)	0.0241 (19)	0.0013 (17)	0.0055 (16)	0.0043 (15)
C15B	0.035 (2)	0.031 (2)	0.0187 (18)	0.0060 (16)	0.0047 (15)	0.0028 (14)
C3A	0.030 (2)	0.031 (2)	0.0262 (19)	-0.0046 (16)	0.0012 (15)	0.0067 (15)
C4A	0.031 (2)	0.035 (2)	0.0232 (19)	0.0005 (17)	-0.0028 (15)	0.0027 (15)
O2B	0.0324 (14)	0.0281 (14)	0.0191 (12)	0.0105 (11)	0.0023 (10)	0.0045 (10)
O1B	0.0370 (14)	0.0325 (14)	0.0198 (13)	0.0124 (11)	0.0086 (10)	0.0052 (10)
O6B	0.0356 (15)	0.0353 (15)	0.0304 (14)	0.0077 (12)	0.0044 (11)	-0.0078 (11)
O5B	0.0462 (16)	0.0357 (15)	0.0321 (15)	0.0158 (13)	0.0048 (12)	0.0109 (11)
C2B	0.0199 (17)	0.0255 (18)	0.0182 (17)	0.0014 (14)	0.0027 (13)	0.0041 (13)
N5B	0.0226 (16)	0.0276 (16)	0.0299 (17)	0.0038 (13)	0.0016 (13)	0.0010 (13)
C3B	0.0283 (19)	0.0281 (19)	0.0173 (17)	0.0038 (15)	0.0043 (14)	0.0043 (14)
C5B	0.0168 (17)	0.0240 (18)	0.0243 (18)	0.0026 (14)	0.0017 (13)	0.0010 (14)
C4B	0.0215 (18)	0.0282 (19)	0.0239 (18)	0.0003 (15)	0.0042 (14)	0.0083 (14)
C6B	0.0260 (19)	0.0280 (19)	0.0189 (17)	-0.0005 (15)	0.0030 (14)	-0.0032 (14)
C1B	0.0199 (18)	0.0264 (18)	0.0237 (19)	0.0023 (14)	0.0022 (14)	0.0052 (14)
C7B	0.0232 (18)	0.0256 (18)	0.0192 (17)	0.0016 (14)	0.0015 (14)	0.0048 (13)

Geometric parameters (Å, °)

S1—O4A	1.434 (2)	N1B—C8B	1.359 (5)
S1—O3A	1.435 (2)	N1B—H30D	0.861 (18)
S1—N2A	1.658 (3)	N1B—H30C	0.849 (19)
S1—C11A	1.738 (3)	C17B—C16B	1.382 (5)
N4A—C14A	1.318 (4)	C17B—H17B	0.9500
N4A—C18A	1.353 (4)	C11B—C10B	1.390 (5)
N3A—C16A	1.351 (4)	C11B—C12B	1.396 (5)
N3A—C14A	1.351 (4)	C8B—C13B	1.396 (5)
N2A—C14A	1.391 (4)	C8B—C9B	1.407 (5)
N2A—H31A	0.873 (19)	C13B—C12B	1.379 (5)
C10A—C9A	1.374 (5)	C13B—H13B	0.9500
C10A—C11A	1.399 (5)	C1A—C2A	1.489 (5)
C10A—H10A	0.9500	C9B—C10B	1.384 (5)
C25—C13A	1.366 (5)	C9B—H9B	0.9500
C25—C8A	1.414 (5)	C2A—C3A	1.380 (5)
C25—H25	0.9500	C2A—C7A	1.388 (5)
C8A—N1A	1.359 (4)	N5A—C5A	1.482 (4)
C8A—C9A	1.413 (5)	C12B—H12B	0.9500
C13A—C11A	1.399 (5)	C7A—C6A	1.383 (5)
C13A—H13A	0.9500	C7A—H7A	0.9500
N1A—H30A	0.845 (19)	C16B—C15B	1.505 (4)
N1A—H30B	0.848 (19)	C5A—C6A	1.373 (5)
C9A—H9A	0.9500	C5A—C4A	1.381 (5)
C16A—C17A	1.380 (5)	C10B—H10B	0.9500
C16A—C15A	1.499 (5)	C19B—H19D	0.9800
C18A—C17A	1.388 (5)	C19B—H19E	0.9800
C18A—C19A	1.487 (5)	C19B—H19F	0.9800
C17A—H17A	0.9500	C6A—H6A	0.9500
C15A—H15A	0.9800	C15B—H15D	0.9800
C15A—H15B	0.9800	C15B—H15E	0.9800
C15A—H15C	0.9800	C15B—H15F	0.9800
C19A—H19A	0.9800	C3A—C4A	1.385 (5)

C19A—H19B	0.9800	C3A—H3A	0.9500
C19A—H19C	0.9800	C4A—H4A	0.9500
S2—O4B	1.419 (2)	O2B—C1B	1.317 (4)
S2—O3B	1.435 (2)	O2B—H32B	0.864 (19)
S2—N2B	1.639 (3)	O1B—C1B	1.225 (4)
S2—C11B	1.747 (4)	O6B—N5B	1.226 (3)
N3B—C16B	1.347 (4)	O5B—N5B	1.226 (4)
N3B—C14B	1.351 (4)	C2B—C3B	1.391 (4)
N34B—C14B	1.325 (4)	C2B—C7B	1.394 (4)
N34B—C18B	1.347 (4)	C2B—C1B	1.491 (4)
O2A—C1A	1.317 (4)	N5B—C5B	1.473 (4)
O2A—H32A	0.865 (19)	C3B—C4B	1.379 (5)
N2B—C14B	1.390 (4)	C3B—H3B	0.9500
N2B—H31B	0.863 (19)	C5B—C4B	1.372 (4)
O1A—C1A	1.217 (4)	C5B—C6B	1.394 (4)
O6A—N5A	1.227 (4)	C4B—H4B	0.9500
O5A—N5A	1.222 (4)	C6B—C7B	1.382 (5)
C18B—C17B	1.388 (5)	C6B—H6B	0.9500
C18B—C19B	1.492 (5)	C7B—H7B	0.9500
O4A—S1—O3A	118.85 (14)	C10B—C11B—S2	118.6 (3)
O4A—S1—N2A	109.89 (14)	C12B—C11B—S2	121.6 (3)
O3A—S1—N2A	101.76 (14)	N1B—C8B—C13B	121.1 (3)
O4A—S1—C11A	109.63 (15)	N1B—C8B—C9B	119.9 (3)
O3A—S1—C11A	109.33 (15)	C13B—C8B—C9B	119.0 (3)
N2A—S1—C11A	106.54 (15)	C12B—C13B—C8B	121.0 (3)
C14A—N4A—C18A	116.4 (3)	C12B—C13B—H13B	119.5
C16A—N3A—C14A	116.8 (3)	C8B—C13B—H13B	119.5
C14A—N2A—S1	123.5 (2)	O1A—C1A—O2A	124.3 (3)
C14A—N2A—H31A	113 (3)	O1A—C1A—C2A	122.5 (3)
S1—N2A—H31A	113 (3)	O2A—C1A—C2A	113.2 (3)
C9A—C10A—C11A	120.3 (3)	C10B—C9B—C8B	119.8 (3)
C9A—C10A—H10A	119.9	C10B—C9B—H9B	120.1
C11A—C10A—H10A	119.9	C8B—C9B—H9B	120.1
C13A—C25—C8A	121.1 (3)	C3A—C2A—C7A	119.5 (3)
C13A—C25—H25	119.4	C3A—C2A—C1A	120.9 (3)
C8A—C25—H25	119.4	C7A—C2A—C1A	119.6 (3)
N1A—C8A—C9A	119.8 (3)	O5A—N5A—O6A	123.4 (3)
N1A—C8A—C25	122.0 (3)	O5A—N5A—C5A	118.3 (3)
C9A—C8A—C25	118.2 (3)	O6A—N5A—C5A	118.3 (3)
N4A—C14A—N3A	126.7 (3)	C13B—C12B—C11B	119.8 (3)
N4A—C14A—N2A	119.5 (3)	C13B—C12B—H12B	120.1
N3A—C14A—N2A	113.7 (3)	C11B—C12B—H12B	120.1
C25—C13A—C11A	120.0 (3)	C6A—C7A—C2A	120.9 (3)
C25—C13A—H13A	120.0	C6A—C7A—H7A	119.6
C11A—C13A—H13A	120.0	C2A—C7A—H7A	119.6
C8A—N1A—H30A	120 (3)	N3B—C16B—C17B	120.4 (3)
C8A—N1A—H30B	122 (3)	N3B—C16B—C15B	117.5 (3)
H30A—N1A—H30B	116 (4)	C17B—C16B—C15B	122.1 (3)
C10A—C11A—C13A	119.8 (3)	C6A—C5A—C4A	123.0 (3)
C10A—C11A—S1	118.6 (3)	C6A—C5A—N5A	119.7 (3)
C13A—C11A—S1	121.6 (3)	C4A—C5A—N5A	117.3 (3)
C10A—C9A—C8A	120.6 (3)	C9B—C10B—C11B	120.6 (3)
C10A—C9A—H9A	119.7	C9B—C10B—H10B	119.7
C8A—C9A—H9A	119.7	C11B—C10B—H10B	119.7
N3A—C16A—C17A	120.1 (3)	C18B—C19B—H19D	109.5



N3A—C16A—C15A	117.1 (3)	C18B—C19B—H19E	109.5
C17A—C16A—C15A	122.8 (3)	H19D—C19B—H19E	109.5
N4A—C18A—C17A	120.9 (3)	C18B—C19B—H19F	109.5
N4A—C18A—C19A	116.4 (3)	H19D—C19B—H19F	109.5
C17A—C18A—C19A	122.7 (3)	H19E—C19B—H19F	109.5
C16A—C17A—C18A	119.0 (3)	C5A—C6A—C7A	117.9 (3)
C16A—C17A—H17A	120.5	C5A—C6A—H6A	121.0
C18A—C17A—H17A	120.5	C7A—C6A—H6A	121.0
C16A—C15A—H15A	109.5	C16B—C15B—H15D	109.5
C16A—C15A—H15B	109.5	C16B—C15B—H15E	109.5
H15A—C15A—H15B	109.5	H15D—C15B—H15E	109.5
C16A—C15A—H15C	109.5	C16B—C15B—H15F	109.5
H15A—C15A—H15C	109.5	H15D—C15B—H15F	109.5
H15B—C15A—H15C	109.5	H15E—C15B—H15F	109.5
C18A—C19A—H19A	109.5	C2A—C3A—C4A	120.8 (3)
C18A—C19A—H19B	109.5	C2A—C3A—H3A	119.6
H19A—C19A—H19B	109.5	C4A—C3A—H3A	119.6
C18A—C19A—H19C	109.5	C5A—C4A—C3A	117.9 (3)
H19A—C19A—H19C	109.5	C5A—C4A—H4A	121.1
H19B—C19A—H19C	109.5	C3A—C4A—H4A	121.1
O4B—S2—O3B	118.98 (14)	C1B—O2B—H32B	109 (3)
O4B—S2—N2B	109.95 (14)	C3B—C2B—C7B	120.4 (3)
O3B—S2—N2B	103.06 (14)	C3B—C2B—C1B	117.4 (3)
O4B—S2—C11B	110.48 (15)	C7B—C2B—C1B	122.1 (3)
O3B—S2—C11B	107.30 (15)	O5B—N5B—O6B	123.9 (3)
N2B—S2—C11B	106.16 (15)	O5B—N5B—C5B	117.4 (3)
C16B—N3B—C14B	116.2 (3)	O6B—N5B—C5B	118.7 (3)
C14B—N34B—C18B	115.6 (3)	C4B—C3B—C2B	120.2 (3)
C1A—O2A—H32A	112 (3)	C4B—C3B—H3B	119.9
C14B—N2B—S2	127.5 (2)	C2B—C3B—H3B	119.9
C14B—N2B—H31B	117 (3)	C4B—C5B—C6B	122.6 (3)
S2—N2B—H31B	114 (3)	C4B—C5B—N5B	118.6 (3)
N34B—C18B—C17B	121.5 (3)	C6B—C5B—N5B	118.8 (3)
N34B—C18B—C19B	117.1 (3)	C5B—C4B—C3B	118.6 (3)
C17B—C18B—C19B	121.5 (3)	C5B—C4B—H4B	120.7
C8B—N1B—H30D	119 (3)	C3B—C4B—H4B	120.7
C8B—N1B—H30C	118 (3)	C7B—C6B—C5B	118.5 (3)
H30D—N1B—H30C	121 (4)	C7B—C6B—H6B	120.8
N34B—C14B—N3B	127.4 (3)	C5B—C6B—H6B	120.8
N34B—C14B—N2B	119.6 (3)	O1B—C1B—O2B	123.7 (3)
N3B—C14B—N2B	112.9 (3)	O1B—C1B—C2B	121.3 (3)
C16B—C17B—C18B	118.7 (3)	O2B—C1B—C2B	115.0 (3)
C16B—C17B—H17B	120.6	C6B—C7B—C2B	119.7 (3)
C18B—C17B—H17B	120.6	C6B—C7B—H7B	120.2
C10B—C11B—C12B	119.8 (3)	C2B—C7B—H7B	120.2
O4A—S1—N2A—C14A	59.9 (3)	N2B—S2—C11B—C12B	-109.5 (3)
O3A—S1—N2A—C14A	-173.2 (3)	N1B—C8B—C13B—C12B	179.4 (3)
C11A—S1—N2A—C14A	-58.8 (3)	C9B—C8B—C13B—C12B	1.1 (5)
C13A—C25—C8A—N1A	177.7 (3)	N1B—C8B—C9B—C10B	-179.6 (3)
C13A—C25—C8A—C9A	-0.8 (5)	C13B—C8B—C9B—C10B	-1.2 (5)
C18A—N4A—C14A—N3A	1.0 (5)	O1A—C1A—C2A—C3A	-173.3 (3)
C18A—N4A—C14A—N2A	-178.0 (3)	O2A—C1A—C2A—C3A	7.6 (5)
C16A—N3A—C14A—N4A	-1.5 (5)	O1A—C1A—C2A—C7A	7.1 (5)
C16A—N3A—C14A—N2A	177.6 (3)	O2A—C1A—C2A—C7A	-172.1 (3)
S1—N2A—C14A—N4A	-34.0 (4)	C8B—C13B—C12B—C11B	-0.4 (5)

S1—N2A—C14A—N3A	146.8 (2)	C10B—C11B—C12B— C13B	-0.1 (5)
C8A—C25—C13A—C11A	1.2 (5)	S2—C11B—C12B—C13B	179.5 (3)
C9A—C10A—C11A—C13A	0.5 (5)	C3A—C2A—C7A—C6A	-1.3 (5)
C9A—C10A—C11A—S1	-177.8 (3)	C1A—C2A—C7A—C6A	178.4 (3)
C25—C13A—C11A—C10A	-1.0 (5)	C14B—N3B—C16B—C17B	0.0 (5)
C25—C13A—C11A—S1	177.3 (3)	C14B—N3B—C16B—C15B	-179.8 (3)
O4A—S1—C11A—C10A	177.6 (2)	C18B—C17B—C16B—N3B	-2.5 (5)
O3A—S1—C11A—C10A	45.7 (3)	C18B—C17B—C16B— C15B	177.3 (3)
N2A—S1—C11A—C10A	-63.6 (3)	O5A—N5A—C5A—C6A	-5.3 (5)
O4A—S1—C11A—C13A	-0.7 (3)	O6A—N5A—C5A—C6A	174.4 (3)
O3A—S1—C11A—C13A	-132.6 (3)	O5A—N5A—C5A—C4A	174.8 (3)
N2A—S1—C11A—C13A	118.1 (3)	O6A—N5A—C5A—C4A	-5.5 (5)
C11A—C10A—C9A—C8A	-0.2 (5)	C8B—C9B—C10B—C11B	0.7 (5)
N1A—C8A—C9A—C10A	-178.3 (3)	C12B—C11B—C10B—C9B	-0.1 (5)
C25—C8A—C9A—C10A	0.3 (5)	S2—C11B—C10B—C9B	-179.6 (2)
C14A—N3A—C16A— C17A	1.1 (5)	C4A—C5A—C6A—C7A	-0.9 (5)
C14A—N3A—C16A— C15A	-179.3 (3)	N5A—C5A—C6A—C7A	179.2 (3)
C14A—N4A—C18A— C17A	-0.1 (5)	C2A—C7A—C6A—C5A	1.7 (5)
C14A—N4A—C18A— C19A	-179.0 (3)	C7A—C2A—C3A—C4A	-0.1 (5)
N3A—C16A—C17A— C18A	-0.4 (6)	C1A—C2A—C3A—C4A	-179.7 (3)
C15A—C16A—C17A— C18A	-179.9 (4)	C6A—C5A—C4A—C3A	-0.3 (5)
N4A—C18A—C17A— C16A	-0.1 (6)	N5A—C5A—C4A—C3A	179.5 (3)
C19A—C18A—C17A— C16A	178.7 (4)	C2A—C3A—C4A—C5A	0.8 (5)
O4B—S2—N2B—C14B	-43.3 (3)	C7B—C2B—C3B—C4B	-1.3 (5)
O3B—S2—N2B—C14B	-171.2 (3)	C1B—C2B—C3B—C4B	178.7 (3)
C11B—S2—N2B—C14B	76.2 (3)	O5B—N5B—C5B—C4B	-3.6 (4)
C14B—N34B—C18B— C17B	1.2 (5)	O6B—N5B—C5B—C4B	177.2 (3)
C14B—N34B—C18B— C19B	-177.6 (3)	O5B—N5B—C5B—C6B	178.0 (3)
C18B—N34B—C14B—N3B	-4.2 (5)	O6B—N5B—C5B—C6B	-1.2 (4)
C18B—N34B—C14B—N2B	174.3 (3)	C6B—C5B—C4B—C3B	0.9 (5)
C16B—N3B—C14B—N34B	3.6 (5)	N5B—C5B—C4B—C3B	-177.4 (3)
C16B—N3B—C14B—N2B	-174.9 (3)	C2B—C3B—C4B—C5B	0.2 (5)
S2—N2B—C14B—N34B	6.0 (5)	C4B—C5B—C6B—C7B	-0.9 (5)
S2—N2B—C14B—N3B	-175.3 (2)	N5B—C5B—C6B—C7B	177.4 (3)
N34B—C18B—C17B— C16B	1.9 (5)	C3B—C2B—C1B—O1B	-2.6 (5)
C19B—C18B—C17B— C16B	-179.4 (3)	C7B—C2B—C1B—O1B	177.3 (3)
O4B—S2—C11B—C10B	-170.8 (2)	C3B—C2B—C1B—O2B	177.2 (3)
O3B—S2—C11B—C10B	-39.7 (3)	C7B—C2B—C1B—O2B	-2.8 (5)
N2B—S2—C11B—C10B	70.0 (3)	C5B—C6B—C7B—C2B	-0.2 (5)
O4B—S2—C11B—C12B	9.7 (3)	C3B—C2B—C7B—C6B	1.2 (5)
O3B—S2—C11B—C12B	140.8 (3)	C1B—C2B—C7B—C6B	-178.7 (3)

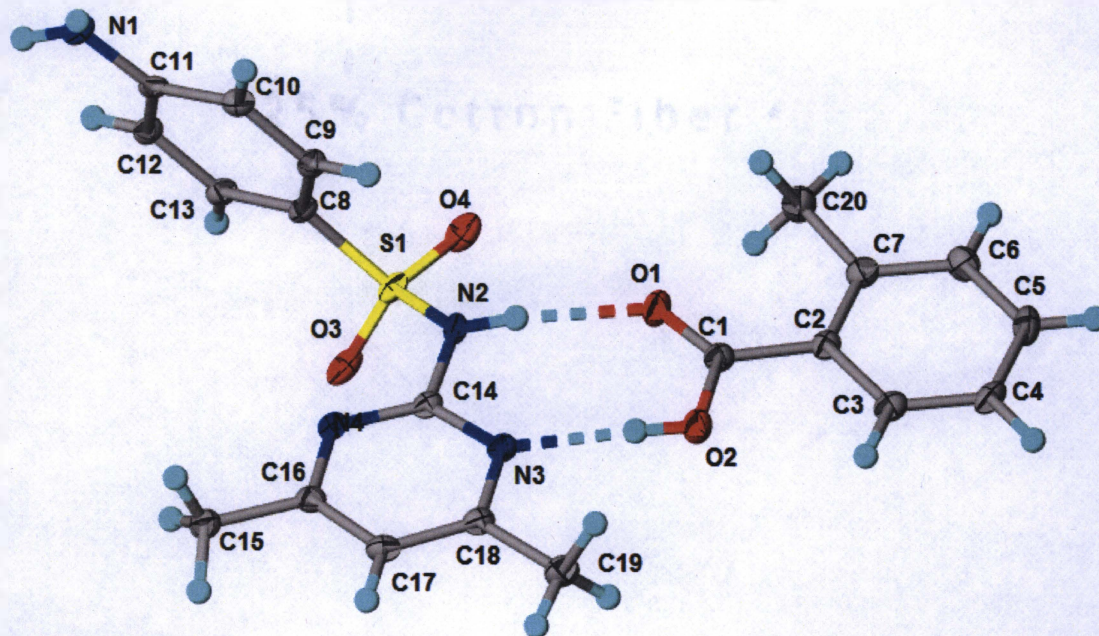


Figure S.5: Crystal Structure of the Cocrystal of Sulfamethazine and *o*-Methylbenzoic Acid Showing Thermal Parameters (50% Thermal Ellipsoids) and Hydrogen Bonding.

### Crystal data

$C_{12}H_{14}N_4O_2S \cdot C_8H_8O_2$

$M_r = 414.47$

Triclinic, *P*

$a = 8.1595$  (7) Å

$b = 9.9424$  (8) Å

$c = 13.2334$  (12) Å

$\alpha = 107.191$  (4)°

$\beta = 90.459$  (5)°

$\gamma = 107.881$  (4)°

$V = 970.28$  (15) Å<sup>3</sup>

$Z = 2$

$F(000) = 436$

$D_x = 1.419$  Mg m<sup>-3</sup>

Melting point: 431–435 K

Cu  $K\alpha$  radiation,  $\lambda = 1.54178$  Å

Cell parameters from 9834 reflections

$\theta = 4.9$ – $68.4$ °

$\mu = 1.79$  mm<sup>-1</sup>

$T = 100$  K

Plates, colourless

$0.40 \times 0.25 \times 0.14$  mm

### Data collection

Bruker APEXII CCD

diffractometer

Radiation source: fine-focus sealed tube

Detector resolution: 8.33 pixels mm<sup>-1</sup>

3467 independent reflections

3139 reflections with  $I > 2\sigma(I)$

$R_{int} = ?$

### Crystal data

$C_{12}H_{14}N_4O_2S \cdot C_8H_8O_2$   
 $M_r = 414.47$   
Triclinic,  $P$   
 $a = 8.1595$  (7) Å  
 $b = 9.9424$  (8) Å  
 $c = 13.2334$  (12) Å  
 $\alpha = 107.191$  (4)°  
 $\beta = 90.459$  (5)°  
 $\gamma = 107.881$  (4)°  
 $V = 970.28$  (15) Å<sup>3</sup>  
 $Z = 2$

$F(000) = 436$   
 $D_x = 1.419$  Mg m<sup>-3</sup>  
Melting point: 431–435 K  
Cu  $K\alpha$  radiation,  $\lambda = 1.54178$  Å  
Cell parameters from 9834 reflections  
 $\theta = 4.9$ – $68.4$ °  
 $\mu = 1.79$  mm<sup>-1</sup>  
 $T = 100$  K  
Plates, colourless  
 $0.40 \times 0.25 \times 0.14$  mm

### Data collection

Bruker APEXII CCD  
diffractometer  
Radiation source: fine-focus sealed tube  
Detector resolution: 8.33 pixels mm<sup>-1</sup>  
phi and  $\omega$  scans  
Absorption correction: multi-scan  
SADABS2014/7, Bruker AXS  
 $T_{\min} = 0.417$ ,  $T_{\max} = 0.753$   
3467 measured reflections

3467 independent reflections

3139 reflections with  $I > 2\sigma(I)$   
 $R_{\text{int}} = ?$   
 $\theta_{\max} = 68.2$ °,  $\theta_{\min} = 3.5$ °  
 $h = -9$  9  
 $k = -10$  11  
 $l = -15$  15

### Refinement

Refinement on  $F^2$   
Least-squares matrix: full  
 $R[F^2 > 2\sigma(F^2)] = 0.044$   
 $wR(F^2) = 0.110$   
 $S = 1.15$   
3467 reflections  
281 parameters  
4 restraints  
0 constraints

Hydrogen site location: mixed  
H atoms treated by a mixture of independent and constrained refinement  
 $w = 1/[\sigma^2(F_o^2) + (0.0416P)^2 + 0.9699P]$   
where  $P = (F_o^2 + 2F_c^2)/3$   
 $(\Delta/\sigma)_{\max} = 0.002$   
 $\Delta\rho_{\max} = 0.31$  e Å<sup>-3</sup>  
 $\Delta\rho_{\min} = -0.35$  e Å<sup>-3</sup>  
Extinction correction: none

### Fractional atomic coordinates and isotropic or equivalent isotropic displacement parameters (Å<sup>2</sup>)

	x	y	z	$U_{\text{iso}}^*/U_{\text{eq}}$
S1	0.04963 (7)	0.89273 (6)	0.29535 (4)	0.01845 (15)
O2	-0.2855 (2)	0.44565 (17)	-0.02890 (13)	0.0246 (4)
O1	-0.1954 (2)	0.69368 (18)	0.02373 (13)	0.0277 (4)
H32	-0.222 (4)	0.463 (4)	0.028 (2)	0.056 (11)*
O3	-0.0306 (2)	0.87615 (18)	0.38900 (13)	0.0270 (4)
O4	-0.0070 (2)	0.97832 (17)	0.24073 (15)	0.0283 (4)
N1	0.8023 (2)	1.1567 (2)	0.43164 (17)	0.0218 (4)

H30A	0.830 (3)	1.194 (3)	0.4976 (14)	0.015 (6)*
H30B	0.863 (4)	1.105 (3)	0.399 (2)	0.042 (9)*
N2	0.0150 (2)	0.7309 (2)	0.20407 (15)	0.0181 (4)
H31	-0.042 (3)	0.724 (3)	0.1478 (17)	0.028 (8)*
N3	-0.0811 (2)	0.4757 (2)	0.14419 (15)	0.0187 (4)
N4	0.0914 (2)	0.60646 (19)	0.31252 (15)	0.0179 (4)
C1	-0.2833 (3)	0.5747 (2)	-0.03895 (18)	0.0198 (5)
C2	-0.3958 (3)	0.5607 (2)	-0.13317 (17)	0.0192 (5)
C3	-0.4939 (3)	0.4190 (3)	-0.19812 (19)	0.0220 (5)
H3	-0.4890	0.3346	-0.1801	0.026*
C4	-0.5975 (3)	0.3982 (3)	-0.28739 (19)	0.0237 (5)
H4	-0.6628	0.3007	-0.3308	0.028*
C5	-0.6053 (3)	0.5215 (3)	-0.31314 (19)	0.0273 (5)
H5	-0.6763	0.5088	-0.3747	0.033*
C6	-0.5093 (3)	0.6636 (3)	-0.24911 (19)	0.0263 (5)
H6	-0.5153	0.7471	-0.2681	0.032*
C7	-0.4048 (3)	0.6869 (3)	-0.15794 (19)	0.0229 (5)
C8	0.2743 (3)	0.9680 (2)	0.33077 (18)	0.0177 (4)
C9	0.3922 (3)	0.9249 (2)	0.26382 (18)	0.0187 (4)
H9	0.3523	0.8518	0.1961	0.022*
C10	0.5677 (3)	0.9889 (2)	0.29645 (18)	0.0196 (5)
H10	0.6482	0.9603	0.2504	0.023*
C11	0.6283 (3)	1.0958 (2)	0.39689 (18)	0.0179 (4)
C12	0.5071 (3)	1.1419 (2)	0.46137 (18)	0.0188 (5)
H12	0.5464	1.2180	0.5279	0.023*
C13	0.3317 (3)	1.0779 (2)	0.42911 (18)	0.0191 (5)
H13	0.2506	1.1086	0.4737	0.023*
C14	0.0092 (3)	0.5986 (2)	0.22277 (17)	0.0174 (4)
C15	0.1790 (3)	0.4769 (3)	0.42217 (19)	0.0231 (5)
H15A	0.3016	0.4931	0.4120	0.035*
H15B	0.1294	0.3817	0.4359	0.035*
H15C	0.1685	0.5577	0.4829	0.035*
C16	0.0840 (3)	0.4741 (2)	0.32422 (18)	0.0189 (5)
C17	-0.0061 (3)	0.3403 (2)	0.24707 (19)	0.0219 (5)
H17	-0.0110	0.2480	0.2562	0.026*
C18	-0.0877 (3)	0.3446 (2)	0.15767 (18)	0.0202 (5)
C19	-0.1895 (3)	0.2056 (3)	0.07106 (19)	0.0262 (5)
H19A	-0.3083	0.2060	0.0599	0.039*
H19B	-0.1918	0.1183	0.0918	0.039*
H19C	-0.1350	0.2020	0.0050	0.039*
C20	-0.3092 (4)	0.8453 (3)	-0.0913 (2)	0.0302 (6)
H20A	-0.3407	0.8614	-0.0184	0.045*
H20B	-0.3407	0.9138	-0.1217	0.045*
H20C	-0.1841	0.8634	-0.0906	0.045*

### Atomic displacement parameters ( $\text{\AA}^2$ )

	$U^{11}$	$U^{22}$	$U^{33}$	$U^{12}$	$U^{13}$	$U^{23}$
S1	0.0143 (3)	0.0131 (3)	0.0235 (3)	0.00386 (19)	-0.0014 (2)	0.0001 (2)
O2	0.0293 (9)	0.0173 (8)	0.0237 (9)	0.0053 (7)	-0.0052 (7)	0.0041 (7)
O1	0.0310 (9)	0.0187 (8)	0.0258 (9)	0.0016 (7)	-0.0096 (7)	0.0031 (7)
O3	0.0156 (8)	0.0257 (9)	0.0283 (9)	0.0024 (6)	0.0022 (7)	-0.0039 (7)
O4	0.0230 (8)	0.0168 (8)	0.0425 (10)	0.0079 (7)	-0.0060 (7)	0.0039 (7)
N1	0.0164 (9)	0.0200 (10)	0.0263 (11)	0.0045 (8)	0.0012 (8)	0.0047 (8)

N2	0.0190 (9)	0.0155 (9)	0.0171 (10)	0.0044 (7)	-0.0042 (8)	0.0027 (7)
N3	0.0199 (9)	0.0148 (9)	0.0194 (9)	0.0045 (7)	0.0019 (7)	0.0036 (7)
N4	0.0156 (9)	0.0155 (9)	0.0211 (10)	0.0040 (7)	0.0016 (7)	0.0045 (7)
C1	0.0190 (10)	0.0194 (11)	0.0204 (11)	0.0058 (9)	0.0036 (9)	0.0057 (9)
C2	0.0165 (10)	0.0209 (11)	0.0189 (11)	0.0060 (9)	0.0036 (9)	0.0044 (9)
C3	0.0180 (11)	0.0213 (11)	0.0253 (12)	0.0062 (9)	0.0045 (9)	0.0056 (9)
C4	0.0174 (11)	0.0220 (11)	0.0227 (12)	0.0017 (9)	0.0015 (9)	-0.0012 (9)
C5	0.0215 (11)	0.0381 (14)	0.0206 (12)	0.0104 (10)	-0.0020 (10)	0.0059 (10)
C6	0.0280 (12)	0.0270 (12)	0.0274 (13)	0.0119 (10)	0.0022 (10)	0.0108 (10)
C7	0.0207 (11)	0.0220 (12)	0.0253 (12)	0.0066 (9)	0.0031 (10)	0.0068 (9)
C8	0.0130 (10)	0.0145 (10)	0.0248 (12)	0.0033 (8)	-0.0006 (9)	0.0062 (9)
C9	0.0205 (11)	0.0132 (10)	0.0204 (11)	0.0047 (8)	-0.0004 (9)	0.0034 (8)
C10	0.0195 (11)	0.0176 (10)	0.0243 (12)	0.0083 (9)	0.0051 (9)	0.0078 (9)
C11	0.0163 (10)	0.0136 (10)	0.0253 (12)	0.0029 (8)	0.0011 (9)	0.0105 (9)
C12	0.0200 (11)	0.0134 (10)	0.0205 (11)	0.0038 (8)	0.0001 (9)	0.0036 (8)
C13	0.0184 (11)	0.0146 (10)	0.0240 (12)	0.0051 (8)	0.0023 (9)	0.0059 (9)
C14	0.0147 (10)	0.0160 (10)	0.0200 (11)	0.0050 (8)	0.0040 (9)	0.0036 (8)
C15	0.0210 (11)	0.0209 (11)	0.0273 (12)	0.0047 (9)	-0.0003 (10)	0.0097 (9)
C16	0.0164 (10)	0.0204 (11)	0.0209 (11)	0.0054 (8)	0.0046 (9)	0.0086 (9)
C17	0.0229 (11)	0.0162 (11)	0.0265 (12)	0.0047 (9)	0.0046 (10)	0.0080 (9)
C18	0.0196 (11)	0.0175 (11)	0.0217 (11)	0.0043 (9)	0.0039 (9)	0.0052 (9)
C19	0.0309 (13)	0.0165 (11)	0.0257 (12)	0.0026 (9)	0.0003 (10)	0.0038 (9)
C20	0.0367 (14)	0.0192 (12)	0.0329 (14)	0.0069 (10)	-0.0051 (11)	0.0080 (10)

### Geometric parameters (Å, °)

S1—O3	1.4348 (18)	C6—H6	0.9500
S1—O4	1.4352 (18)	C7—C20	1.510 (3)
S1—N2	1.6418 (18)	C8—C9	1.392 (3)
S1—C8	1.754 (2)	C8—C13	1.393 (3)
O2—C1	1.323 (3)	C9—C10	1.382 (3)
O2—H32	0.852 (18)	C9—H9	0.9500
O1—C1	1.221 (3)	C10—C11	1.404 (3)
N1—C11	1.375 (3)	C10—H10	0.9500
N1—H30A	0.840 (17)	C11—C12	1.406 (3)
N1—H30B	0.853 (18)	C12—C13	1.381 (3)
N2—C14	1.395 (3)	C12—H12	0.9500
N2—H31	0.847 (17)	C13—H13	0.9500
N3—C14	1.342 (3)	C15—C16	1.494 (3)
N3—C18	1.352 (3)	C15—H15A	0.9800
N4—C14	1.329 (3)	C15—H15B	0.9800
N4—C16	1.353 (3)	C15—H15C	0.9800
C1—C2	1.489 (3)	C16—C17	1.392 (3)
C2—C3	1.395 (3)	C17—C18	1.371 (3)
C2—C7	1.409 (3)	C17—H17	0.9500
C3—C4	1.373 (3)	C18—C19	1.502 (3)
C3—H3	0.9500	C19—H19A	0.9800
C4—C5	1.385 (4)	C19—H19B	0.9800
C4—H4	0.9500	C19—H19C	0.9800
C5—C6	1.389 (4)	C20—H20A	0.9800
C5—H5	0.9500	C20—H20B	0.9800
C6—C7	1.391 (4)	C20—H20C	0.9800
O3—S1—O4	116.92 (11)	C9—C10—C11	120.7 (2)
O3—S1—N2	111.34 (10)	C9—C10—H10	119.6

O4—S1—N2	103.91 (10)	C11—C10—H10	119.6
O3—S1—C8	107.72 (10)	N1—C11—C10	121.3 (2)
O4—S1—C8	110.15 (10)	N1—C11—C12	120.1 (2)
N2—S1—C8	106.32 (10)	C10—C11—C12	118.6 (2)
C1—O2—H32	108 (2)	C13—C12—C11	120.7 (2)
C11—N1—H30A	117.3 (17)	C13—C12—H12	119.6
C11—N1—H30B	114 (2)	C11—C12—H12	119.6
H30A—N1—H30B	114 (3)	C12—C13—C8	119.6 (2)
C14—N2—S1	125.85 (16)	C12—C13—H13	120.2
C14—N2—H31	117.2 (19)	C8—C13—H13	120.2
S1—N2—H31	112.2 (19)	N4—C14—N3	127.7 (2)
C14—N3—C18	116.0 (2)	N4—C14—N2	118.55 (19)
C14—N4—C16	115.37 (19)	N3—C14—N2	113.8 (2)
O1—C1—O2	122.3 (2)	C16—C15—H15A	109.5
O1—C1—C2	123.7 (2)	C16—C15—H15B	109.5
O2—C1—C2	113.95 (19)	H15A—C15—H15B	109.5
C3—C2—C7	119.6 (2)	C16—C15—H15C	109.5
C3—C2—C1	118.9 (2)	H15A—C15—H15C	109.5
C7—C2—C1	121.5 (2)	H15B—C15—H15C	109.5
C4—C3—C2	121.8 (2)	N4—C16—C17	121.3 (2)
C4—C3—H3	119.1	N4—C16—C15	117.5 (2)
C2—C3—H3	119.1	C17—C16—C15	121.2 (2)
C3—C4—C5	119.0 (2)	C18—C17—C16	118.6 (2)
C3—C4—H4	120.5	C18—C17—H17	120.7
C5—C4—H4	120.5	C16—C17—H17	120.7
C4—C5—C6	120.1 (2)	N3—C18—C17	121.0 (2)
C4—C5—H5	119.9	N3—C18—C19	116.9 (2)
C6—C5—H5	119.9	C17—C18—C19	122.2 (2)
C5—C6—C7	121.7 (2)	C18—C19—H19A	109.5
C5—C6—H6	119.1	C18—C19—H19B	109.5
C7—C6—H6	119.1	H19A—C19—H19B	109.5
C6—C7—C2	117.8 (2)	C18—C19—H19C	109.5
C6—C7—C20	118.1 (2)	H19A—C19—H19C	109.5
C2—C7—C20	124.1 (2)	H19B—C19—H19C	109.5
C9—C8—C13	120.6 (2)	C7—C20—H20A	109.5
C9—C8—S1	122.52 (17)	C7—C20—H20B	109.5
C13—C8—S1	116.84 (16)	H20A—C20—H20B	109.5
C10—C9—C8	119.6 (2)	C7—C20—H20C	109.5
C10—C9—H9	120.2	H20A—C20—H20C	109.5
C8—C9—H9	120.2	H20B—C20—H20C	109.5
O3—S1—N2—C14	-36.8 (2)	C13—C8—C9—C10	1.7 (3)
O4—S1—N2—C14	-163.51 (18)	S1—C8—C9—C10	179.83 (17)
C8—S1—N2—C14	80.2 (2)	C8—C9—C10—C11	0.7 (3)
O1—C1—C2—C3	-178.5 (2)	C9—C10—C11—N1	177.9 (2)
O2—C1—C2—C3	1.9 (3)	C9—C10—C11—C12	-3.2 (3)
O1—C1—C2—C7	1.6 (3)	N1—C11—C12—C13	-177.7 (2)
O2—C1—C2—C7	-178.0 (2)	C10—C11—C12—C13	3.4 (3)
C7—C2—C3—C4	1.3 (3)	C11—C12—C13—C8	-1.0 (3)
C1—C2—C3—C4	-178.6 (2)	C9—C8—C13—C12	-1.5 (3)
C2—C3—C4—C5	-0.4 (3)	S1—C8—C13—C12	-179.77 (17)
C3—C4—C5—C6	0.0 (3)	C16—N4—C14—N3	0.9 (3)
C4—C5—C6—C7	-0.5 (4)	C16—N4—C14—N2	-178.43 (18)
C5—C6—C7—C2	1.3 (3)	C18—N3—C14—N4	-0.6 (3)
C5—C6—C7—C20	-178.2 (2)	C18—N3—C14—N2	178.78 (18)
C3—C2—C7—C6	-1.7 (3)	S1—N2—C14—N4	-23.9 (3)



Symmetry codes: (i)  $-x+1, -y+2, -z+1$ ; (ii)  $x+1, y, z$ .

All esds (except the esd in the dihedral angle between two l.s. planes) are estimated using the full covariance matrix. The cell esds are taken into account individually in the estimation of esds in distances, angles and torsion angles; correlations between esds in cell parameters are only used when they are defined by crystal symmetry. An approximate (isotropic) treatment of cell esds is used for estimating esds involving l.s. planes.

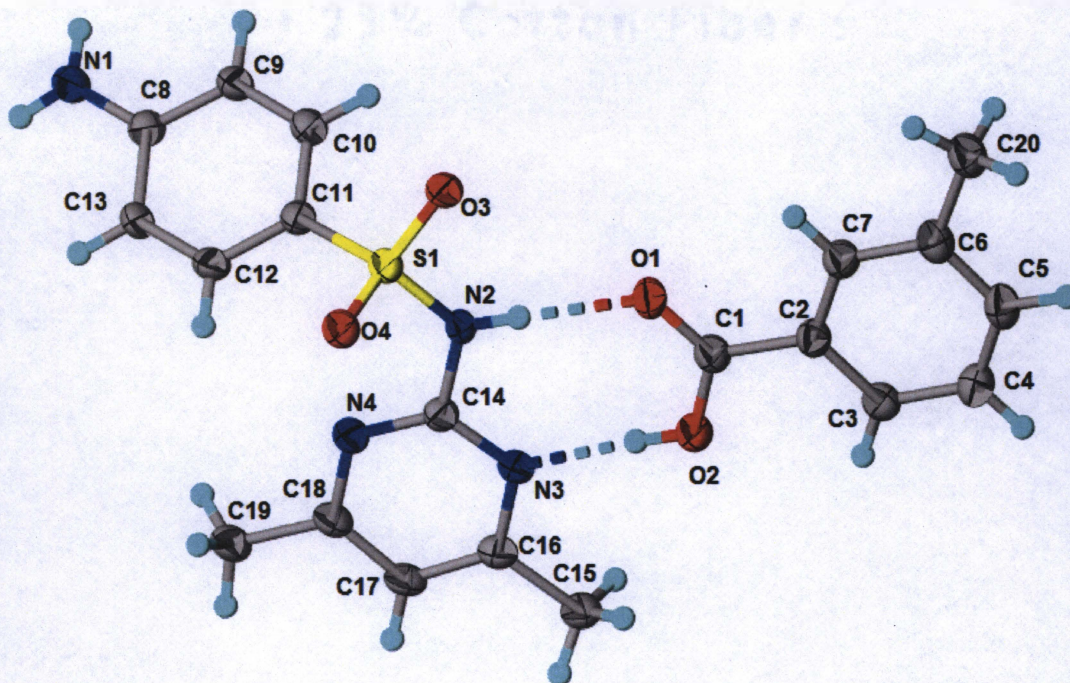


Figure S.6: Crystal Structure of the Cocrystal of Sulfamethazine and *m*-Methylbenzoic Acid Showing Thermal Parameters (50% Thermal Ellipsoids) and Hydrogen Bonding.

#### Crystal data

$C_{12}H_{14}N_4O_2S \cdot C_8H_8O_2$

$M_r = 414.47$

Monoclinic,  $P2_1/c$

$a = 8.2898$  (3) Å

$b = 14.3256$  (5) Å

$c = 17.6458$  (7) Å

$\beta = 102.930$  (2)°

$V = 2042.42$  (13) Å<sup>3</sup>

$Z = 4$

$F(000) = 872$

$D_x = 1.348$  Mg m<sup>-3</sup>

Melting point: 436–438K

Cu  $K\alpha$  radiation,  $\lambda = 1.54178$  Å

Cell parameters from 9865 reflections

$\theta = 4.0$ – $68.1$ °

$\mu = 1.70$  mm<sup>-1</sup>

$T = 100$  K

Plate, colourless

$0.28 \times 0.19 \times 0.12$  mm

#### Data collection

Radiation source: fine-focus sealed tube

Detector resolution: 8.33 pixels mm<sup>-1</sup>

2365 reflections with  $I > 2\sigma(I)$

$R_{int} = ?$

### Crystal data

$C_{12}H_{14}N_4O_2S \cdot C_8H_8O_2$   
 $M_r = 414.47$   
Monoclinic,  $P2_1/c$   
 $a = 8.2898$  (3) Å  
 $b = 14.3256$  (5) Å  
 $c = 17.6458$  (7) Å  
 $\beta = 102.930$  (2)°  
 $V = 2042.42$  (13) Å<sup>3</sup>  
 $Z = 4$   
 $F(000) = 872$

$D_x = 1.348$  Mg m<sup>-3</sup>  
Melting point: 436-438K  
Cu  $K\alpha$  radiation,  $\lambda = 1.54178$  Å  
Cell parameters from 9865 reflections  
 $\theta = 4.0$ – $68.1$ °  
 $\mu = 1.70$  mm<sup>-1</sup>  
 $T = 100$  K  
Plate, colourless  
 $0.28 \times 0.19 \times 0.12$  mm

### Data collection

Radiation source: fine-focus sealed tube  
Detector resolution: 8.33 pixels mm<sup>-1</sup>  
phi and  $\omega$  scans  
Absorption correction: multi-scan  
SADABS2014/7, Bruker AXS  
 $T_{\min} = 0.533$ ,  $T_{\max} = 0.753$   
3669 measured reflections

2365 reflections with  $I > 2\sigma(I)$   
 $R_{\text{int}} = ?$   
 $\theta_{\max} = 68.2$ °,  $\theta_{\min} = 4.0$ °  
 $h = -9$  9  
 $k = -11$  11  
 $l = -21$  21

### Refinement

Refinement on  $F^2$   
Least-squares matrix: full  
 $R[F^2 > 2\sigma(F^2)] = 0.069$   
 $wR(F^2) = 0.193$   
 $S = 1.01$   
3669 reflections  
281 parameters  
4 restraints  
0 constraints

Hydrogen site location: mixed  
H atoms treated by a mixture of independent and constrained refinement  
 $w = 1/[\sigma^2(F_o^2) + (0.1106P)^2]$   
where  $P = (F_o^2 + 2F_c^2)/3$   
 $(\Delta/\sigma)_{\max} < 0.001$   
 $\Delta\rho_{\max} = 0.35$  e Å<sup>-3</sup>  
 $\Delta\rho_{\min} = -0.64$  e Å<sup>-3</sup>  
Extinction correction: none

### Fractional atomic coordinates and isotropic or equivalent isotropic displacement parameters (Å<sup>2</sup>)

	<i>x</i>	<i>y</i>	<i>z</i>	$U_{\text{iso}}^*/U_{\text{eq}}$
S1	0.21823 (12)	0.48129 (6)	0.23342 (6)	0.0320 (3)
O4	0.1365 (3)	0.51845 (18)	0.29060 (16)	0.0350 (7)
O2	-0.2535 (4)	0.4168 (2)	0.00036 (18)	0.0395 (7)
H32	-0.205 (8)	0.465 (3)	0.023 (4)	0.11 (3)*
O1	-0.0652 (4)	0.33378 (18)	0.08376 (17)	0.0395 (7)
O3	0.2499 (3)	0.38283 (18)	0.23260 (17)	0.0361 (7)
N4	0.0795 (4)	0.6580 (2)	0.1598 (2)	0.0331 (8)
N3	-0.1101 (4)	0.5745 (2)	0.06140 (19)	0.0321 (8)
N2	0.1000 (4)	0.4981 (2)	0.1464 (2)	0.0325 (8)
H31	0.053 (5)	0.449 (2)	0.125 (2)	0.042 (13)*
C14	0.0190 (5)	0.5813 (3)	0.1223 (2)	0.0310 (9)
C3	-0.4009 (5)	0.2625 (3)	-0.0755 (2)	0.0359 (9)
H3	-0.4391	0.3226	-0.0940	0.043*

N1	0.8695 (5)	0.6668 (3)	0.2970 (2)	0.0402 (9)
H30A	0.878 (5)	0.7234 (16)	0.314 (2)	0.031 (11)*
H30B	0.950 (5)	0.639 (3)	0.284 (3)	0.068 (18)*
C16	-0.1882 (5)	0.6553 (3)	0.0359 (2)	0.0337 (9)
C2	-0.2688 (5)	0.2534 (3)	-0.0109 (2)	0.0337 (9)
C10	0.5412 (5)	0.4974 (3)	0.2225 (2)	0.0345 (9)
H10	0.5278	0.4385	0.1971	0.041*
C11	0.4039 (5)	0.5409 (3)	0.2422 (2)	0.0320 (9)
C17	-0.1327 (5)	0.7388 (3)	0.0719 (2)	0.0355 (10)
H17	-0.1865	0.7958	0.0540	0.043*
C18	0.0022 (5)	0.7380 (3)	0.1342 (2)	0.0348 (9)
C8	0.7170 (5)	0.6263 (3)	0.2766 (2)	0.0331 (9)
C9	0.6940 (5)	0.5391 (3)	0.2393 (2)	0.0345 (9)
H9	0.7853	0.5087	0.2257	0.041*
C4	-0.4758 (5)	0.1827 (3)	-0.1122 (3)	0.0409 (10)
H4	-0.5647	0.1881	-0.1565	0.049*
C7	-0.2137 (5)	0.1654 (3)	0.0160 (2)	0.0363 (10)
H7	-0.1239	0.1601	0.0600	0.044*
C6	-0.2870 (6)	0.0848 (3)	-0.0200 (3)	0.0378 (10)
C1	-0.1864 (5)	0.3374 (3)	0.0287 (2)	0.0357 (10)
C13	0.5781 (5)	0.6713 (3)	0.2938 (2)	0.0350 (9)
H13	0.5901	0.7315	0.3168	0.042*
C19	0.0719 (5)	0.8247 (3)	0.1767 (3)	0.0393 (10)
H19A	0.0672	0.8194	0.2315	0.059*
H19B	0.0070	0.8789	0.1535	0.059*
H19C	0.1872	0.8325	0.1728	0.059*
C15	-0.3318 (5)	0.6488 (3)	-0.0326 (3)	0.0409 (10)
H15A	-0.2919	0.6311	-0.0789	0.061*
H15B	-0.3875	0.7095	-0.0414	0.061*
H15C	-0.4099	0.6016	-0.0225	0.061*
C12	0.4247 (5)	0.6287 (3)	0.2774 (2)	0.0337 (9)
H12	0.3326	0.6594	0.2901	0.040*
C20	-0.2265 (6)	-0.0114 (3)	0.0066 (3)	0.0463 (11)
H20A	-0.1623	-0.0369	-0.0289	0.069*
H20B	-0.3215	-0.0520	0.0068	0.069*
H20C	-0.1565	-0.0079	0.0592	0.069*
C5	-0.4203 (6)	0.0952 (3)	-0.0840 (3)	0.0404 (10)
H5	-0.4741	0.0411	-0.1087	0.049*

Atomic displacement parameters ( $\text{\AA}^2$ )

	$U^{11}$	$U^{22}$	$U^{33}$	$U^{12}$	$U^{13}$	$U^{23}$
S1	0.0320 (5)	0.0236 (5)	0.0383 (6)	-0.0004 (4)	0.0035 (4)	0.0001 (4)
O4	0.0363 (16)	0.0318 (14)	0.0367 (16)	-0.0009 (12)	0.0079 (12)	0.0001 (12)
O2	0.0384 (18)	0.0289 (16)	0.0469 (19)	-0.0003 (13)	0.0005 (14)	-0.0005 (13)
O1	0.0433 (18)	0.0289 (15)	0.0410 (18)	-0.0029 (12)	-0.0022 (14)	-0.0032 (12)
O3	0.0341 (16)	0.0227 (14)	0.0483 (18)	0.0010 (11)	0.0022 (13)	0.0029 (12)
N4	0.0333 (19)	0.0270 (17)	0.039 (2)	0.0001 (14)	0.0074 (15)	-0.0008 (14)
N3	0.0324 (19)	0.0265 (17)	0.037 (2)	0.0037 (14)	0.0063 (15)	0.0000 (13)
N2	0.0321 (19)	0.0222 (17)	0.038 (2)	0.0005 (14)	-0.0023 (15)	-0.0045 (14)
C14	0.030 (2)	0.027 (2)	0.035 (2)	-0.0001 (16)	0.0056 (17)	0.0018 (16)
C3	0.038 (2)	0.035 (2)	0.036 (2)	0.0009 (18)	0.0105 (18)	-0.0003 (17)
N1	0.030 (2)	0.032 (2)	0.060 (3)	-0.0030 (16)	0.0128 (17)	-0.0081 (17)
C16	0.036 (2)	0.032 (2)	0.034 (2)	0.0063 (17)	0.0096 (17)	0.0035 (17)

C2	0.033 (2)	0.032 (2)	0.037 (2)	-0.0044 (17)	0.0082 (17)	-0.0026 (16)
C10	0.037 (2)	0.027 (2)	0.039 (2)	0.0000 (17)	0.0073 (18)	0.0013 (16)
C11	0.032 (2)	0.0262 (19)	0.036 (2)	0.0013 (16)	0.0027 (17)	0.0019 (16)
C17	0.037 (2)	0.027 (2)	0.045 (3)	0.0067 (17)	0.0122 (19)	0.0067 (17)
C18	0.039 (2)	0.026 (2)	0.041 (3)	0.0039 (17)	0.0119 (18)	0.0023 (16)
C8	0.031 (2)	0.028 (2)	0.040 (2)	-0.0019 (17)	0.0083 (18)	0.0026 (16)
C9	0.033 (2)	0.027 (2)	0.043 (3)	0.0023 (17)	0.0083 (18)	-0.0020 (17)
C4	0.039 (3)	0.042 (2)	0.039 (3)	-0.006 (2)	0.0045 (19)	-0.0022 (19)
C7	0.038 (2)	0.033 (2)	0.037 (3)	-0.0008 (18)	0.0050 (18)	0.0001 (17)
C6	0.044 (3)	0.033 (2)	0.039 (3)	-0.0067 (19)	0.0154 (19)	-0.0018 (17)
C1	0.038 (2)	0.030 (2)	0.038 (3)	-0.0006 (17)	0.0063 (19)	-0.0007 (17)
C13	0.036 (2)	0.0236 (19)	0.044 (3)	-0.0012 (17)	0.0062 (18)	-0.0040 (17)
C19	0.039 (3)	0.028 (2)	0.053 (3)	0.0012 (18)	0.014 (2)	-0.0005 (18)
C15	0.040 (3)	0.039 (2)	0.041 (3)	0.008 (2)	0.0012 (19)	0.0007 (19)
C12	0.032 (2)	0.027 (2)	0.042 (2)	0.0039 (17)	0.0083 (18)	0.0006 (17)
C20	0.052 (3)	0.033 (2)	0.053 (3)	-0.005 (2)	0.008 (2)	-0.003 (2)
C5	0.043 (3)	0.038 (2)	0.042 (3)	-0.010 (2)	0.012 (2)	-0.0074 (18)

### Geometric parameters (Å, °)

S1—O3	1.435 (3)	C11—C12	1.395 (5)
S1—O4	1.438 (3)	C17—C18	1.382 (6)
S1—N2	1.644 (3)	C17—H17	0.9500
S1—C11	1.737 (4)	C18—C19	1.498 (5)
O2—C1	1.315 (5)	C8—C9	1.406 (5)
O2—H32	0.86 (2)	C8—C13	1.410 (6)
O1—C1	1.232 (5)	C9—H9	0.9500
N4—C14	1.322 (5)	C4—C5	1.390 (6)
N4—C18	1.342 (5)	C4—H4	0.9500
N3—C14	1.339 (5)	C7—C6	1.389 (6)
N3—C16	1.354 (5)	C7—H7	0.9500
N2—C14	1.388 (5)	C6—C5	1.400 (6)
N2—H31	0.849 (19)	C6—C20	1.505 (6)
C3—C4	1.390 (6)	C13—C12	1.382 (6)
C3—C2	1.398 (6)	C13—H13	0.9500
C3—H3	0.9500	C19—H19A	0.9800
N1—C8	1.364 (5)	C19—H19B	0.9800
N1—H30A	0.860 (19)	C19—H19C	0.9800
N1—H30B	0.85 (2)	C15—H15A	0.9800
C16—C17	1.383 (6)	C15—H15B	0.9800
C16—C15	1.498 (6)	C15—H15C	0.9800
C2—C7	1.388 (5)	C12—H12	0.9500
C2—C1	1.481 (5)	C20—H20A	0.9800
C10—C9	1.372 (6)	C20—H20B	0.9800
C10—C11	1.408 (6)	C20—H20C	0.9800
C10—H10	0.9500	C5—H5	0.9500
O3—S1—O4	119.14 (17)	C10—C9—C8	120.7 (4)
O3—S1—N2	101.93 (16)	C10—C9—H9	119.6
O4—S1—N2	108.96 (17)	C8—C9—H9	119.6
O3—S1—C11	108.88 (17)	C3—C4—C5	119.8 (4)
O4—S1—C11	107.60 (18)	C3—C4—H4	120.1
N2—S1—C11	110.07 (19)	C5—C4—H4	120.1
C1—O2—H32	114 (5)	C2—C7—C6	121.4 (4)
C14—N4—C18	116.2 (3)	C2—C7—H7	119.3

C14—N3—C16	116.1 (3)	C6—C7—H7	119.3
C14—N2—S1	124.0 (3)	C7—C6—C5	117.8 (4)
C14—N2—H31	115 (3)	C7—C6—C20	122.5 (4)
S1—N2—H31	115 (3)	C5—C6—C20	119.7 (4)
N4—C14—N3	127.5 (3)	O1—C1—O2	122.5 (4)
N4—C14—N2	117.1 (3)	O1—C1—C2	123.2 (4)
N3—C14—N2	115.3 (3)	O2—C1—C2	114.3 (4)
C4—C3—C2	119.3 (4)	C12—C13—C8	120.8 (4)
C4—C3—H3	120.3	C12—C13—H13	119.6
C2—C3—H3	120.3	C8—C13—H13	119.6
C8—N1—H30A	119 (3)	C18—C19—H19A	109.5
C8—N1—H30B	118 (4)	C18—C19—H19B	109.5
H30A—N1—H30B	122 (5)	H19A—C19—H19B	109.5
N3—C16—C17	120.2 (4)	C18—C19—H19C	109.5
N3—C16—C15	116.7 (4)	H19A—C19—H19C	109.5
C17—C16—C15	123.1 (4)	H19B—C19—H19C	109.5
C7—C2—C3	120.1 (4)	C16—C15—H15A	109.5
C7—C2—C1	119.7 (4)	C16—C15—H15B	109.5
C3—C2—C1	120.3 (4)	H15A—C15—H15B	109.5
C9—C10—C11	120.8 (4)	C16—C15—H15C	109.5
C9—C10—H10	119.6	H15A—C15—H15C	109.5
C11—C10—H10	119.6	H15B—C15—H15C	109.5
C12—C11—C10	118.9 (4)	C13—C12—C11	120.4 (4)
C12—C11—S1	120.1 (3)	C13—C12—H12	119.8
C10—C11—S1	120.6 (3)	C11—C12—H12	119.8
C18—C17—C16	119.0 (4)	C6—C20—H20A	109.5
C18—C17—H17	120.5	C6—C20—H20B	109.5
C16—C17—H17	120.5	H20A—C20—H20B	109.5
N4—C18—C17	121.0 (4)	C6—C20—H20C	109.5
N4—C18—C19	116.0 (4)	H20A—C20—H20C	109.5
C17—C18—C19	123.0 (4)	H20B—C20—H20C	109.5
N1—C8—C9	121.5 (4)	C4—C5—C6	121.5 (4)
N1—C8—C13	120.2 (4)	C4—C5—H5	119.2
C9—C8—C13	118.3 (4)	C6—C5—H5	119.2
O3—S1—N2—C14	171.6 (3)	C14—N4—C18—C19	-179.7 (4)
O4—S1—N2—C14	44.9 (4)	C16—C17—C18—N4	0.2 (6)
C11—S1—N2—C14	-72.9 (4)	C16—C17—C18—C19	179.7 (4)
C18—N4—C14—N3	0.4 (6)	C11—C10—C9—C8	-0.1 (6)
C18—N4—C14—N2	178.2 (4)	N1—C8—C9—C10	177.0 (4)
C16—N3—C14—N4	-0.6 (6)	C13—C8—C9—C10	-2.2 (6)
C16—N3—C14—N2	-178.5 (3)	C2—C3—C4—C5	0.8 (7)
S1—N2—C14—N4	22.5 (5)	C3—C2—C7—C6	0.1 (7)
S1—N2—C14—N3	-159.4 (3)	C1—C2—C7—C6	-179.5 (4)
C14—N3—C16—C17	0.6 (6)	C2—C7—C6—C5	-0.8 (6)
C14—N3—C16—C15	179.4 (4)	C2—C7—C6—C20	178.2 (4)
C4—C3—C2—C7	-0.1 (6)	C7—C2—C1—O1	2.7 (7)
C4—C3—C2—C1	179.5 (4)	C3—C2—C1—O1	-176.9 (4)
C9—C10—C11—C12	1.9 (6)	C7—C2—C1—O2	-177.2 (4)
C9—C10—C11—S1	-170.9 (3)	C3—C2—C1—O2	3.2 (6)
O3—S1—C11—C12	-152.0 (3)	N1—C8—C13—C12	-176.4 (4)
O4—S1—C11—C12	-21.6 (4)	C9—C8—C13—C12	2.8 (6)
N2—S1—C11—C12	97.0 (4)	C8—C13—C12—C11	-1.1 (6)
O3—S1—C11—C10	20.6 (4)	C10—C11—C12—C13	-1.2 (6)
O4—S1—C11—C10	151.1 (3)	S1—C11—C12—C13	171.6 (3)
N2—S1—C11—C10	-90.3 (3)	C3—C4—C5—C6	-1.6 (7)
N3—C16—C17—C18	-0.5 (6)	C7—C6—C5—C4	1.5 (7)



defined by crystal symmetry. An approximate (isotropic) treatment of cell esds is used for estimating esds involving l.s. planes.

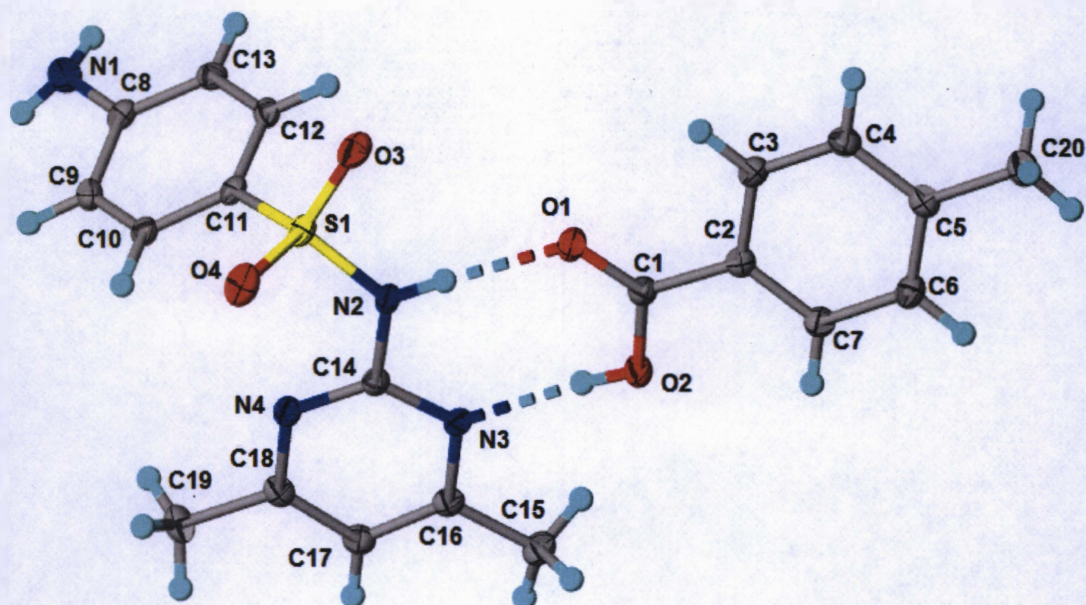


Figure S.7: Crystal Structure of the Cocrystal of Sulfamethazine and *p*-Methylbenzoic Acid Showing Thermal Parameters (50% Thermal Ellipsoids) and Hydrogen Bonding.

#### Crystal data

$C_{12}H_{14}N_4O_2S \cdot C_8H_8O_2$   
 $M_r = 414.47$   
 Monoclinic,  $P2_1$   
 $a = 7.3207$  (2) Å  
 $b = 13.1812$  (4) Å  
 $c = 11.2377$  (3) Å  
 $\beta = 107.343$  (1)°  
 $V = 1035.09$  (5) Å<sup>3</sup>  
 $Z = 2$   
 $F(000) = 436$

$D_x = 1.330$  Mg m<sup>-3</sup>  
 Melting point: 481–483 K  
 Cu  $K\alpha$  radiation,  $\lambda = 1.54178$  Å  
 Cell parameters from 9942 reflections  
 $\theta = 3.4$ – $68.2$ °  
 $\mu = 1.68$  mm<sup>-1</sup>  
 $T = 100$  K  
 Plates, colourless  
 × × mm

#### Data collection

Bruker APEXII CCD  
 diffractometer

3706 independent reflections

$a = 7.3207 (2) \text{ \AA}$   
 $b = 13.1812 (4) \text{ \AA}$   
 $c = 11.2377 (3) \text{ \AA}$   
 $\beta = 107.343 (1)^\circ$   
 $V = 1035.09 (5) \text{ \AA}^3$   
 $Z = 2$   
 $F(000) = 436$

Cell parameters from 9942 reflections

$\theta = 3.4\text{--}68.2^\circ$   
 $\mu = 1.68 \text{ mm}^{-1}$   
 $T = 100 \text{ K}$   
 Plates, colourless  
 $\times \times \text{ mm}$

### Data collection

Bruker APEXII CCD  
 diffractometer  
 Radiation source: fine-focus sealed tube  
 Detector resolution:  $8.33 \text{ pixels mm}^{-1}$   
 phi and  $\omega$  scans  
 Absorption correction: multi-scan  
 SADABS2014/7, Bruker AXS  
 $T_{\min} = 0.542$ ,  $T_{\max} = 0.753$   
 15644 measured reflections

3706 independent reflections  
 3675 reflections with  $I > 2\sigma(I)$   
 $R_{\text{int}} = 0.023$   
 $\theta_{\max} = 68.2^\circ$ ,  $\theta_{\min} = 4.1^\circ$   
 $h = -8 \quad 8$   
 $k = -15 \quad 15$   
 $l = -13 \quad 13$

### Refinement

Refinement on  $F^2$   
 Least-squares matrix: full  
 $R[F^2 > 2\sigma(F^2)] = 0.024$   
 $wR(F^2) = 0.062$   
 $S = 1.07$   
 3706 reflections  
 281 parameters  
 5 restraints  
  
 0 constraints

Hydrogen site location: mixed  
 H atoms treated by a mixture of independent and  
 constrained refinement  
 $w = 1/[\sigma^2(F_o^2) + (0.0397P)^2 + 0.0901P]$   
 where  $P = (F_o^2 + 2F_c^2)/3$   
 $(\Delta/\sigma)_{\max} < 0.001$   
 $\Delta\rho_{\max} = 0.15 \text{ e \AA}^{-3}$   
 $\Delta\rho_{\min} = -0.23 \text{ e \AA}^{-3}$   
 Extinction correction: none

Absolute structure: Flack x determined using 1683  
 quotients  $[(I^+)-(I^-)]/[(I^+)+(I^-)]$  (Parsons, Flack and  
 Wagner, Acta Cryst. B69 (2013) 249-259).  
 Absolute structure parameter: 0.039 (4)

### Fractional atomic coordinates and isotropic or equivalent isotropic displacement parameters ( $\text{\AA}^2$ )

	x	y	z	$U_{\text{iso}}^*/U_{\text{eq}}$
S1	0.28941 (6)	-0.00515 (4)	0.15997 (4)	0.02031 (12)
O1	0.0876 (2)	-0.01505 (13)	0.43249 (12)	0.0274 (3)
O4	0.4404 (2)	-0.07014 (11)	0.15000 (14)	0.0313 (4)
O3	0.1021 (2)	-0.04813 (12)	0.14132 (13)	0.0280 (3)
N3	0.4975 (2)	0.12997 (12)	0.47709 (14)	0.0185 (3)
O2	0.2555 (2)	0.06475 (12)	0.60630 (13)	0.0262 (3)
C1	0.1111 (3)	0.00847 (15)	0.54138 (18)	0.0198 (4)
N4	0.6224 (2)	0.11865 (13)	0.30333 (15)	0.0204 (3)
C14	0.4950 (3)	0.09864 (15)	0.36254 (17)	0.0180 (4)
C18	0.7704 (3)	0.17799 (15)	0.36430 (19)	0.0213 (4)
C12	0.0996 (3)	0.15156 (15)	0.02372 (17)	0.0199 (4)
H12	-0.0002	0.1352	0.0584	0.024*
N2	0.3387 (2)	0.03992 (14)	0.30266 (15)	0.0218 (4)



C11	0.2696 (3)	0.09684 (15)	0.05841 (17)	0.0187 (4)
C2	-0.0219 (3)	-0.02465 (14)	0.61074 (18)	0.0198 (4)
N1	0.1934 (3)	0.32726 (15)	-0.20427 (17)	0.0284 (4)
C3	-0.1939 (3)	-0.07142 (15)	0.54454 (18)	0.0211 (4)
H3	-0.2217	-0.0831	0.4575	0.025*
C5	-0.2840 (3)	-0.08711 (15)	0.73448 (19)	0.0217 (4)
C16	0.6468 (3)	0.18835 (15)	0.53730 (19)	0.0207 (4)
C7	0.0185 (3)	-0.00971 (18)	0.73899 (17)	0.0225 (4)
H7	0.1342	0.0225	0.7846	0.027*
C13	0.0763 (3)	0.22960 (16)	-0.06127 (18)	0.0213 (4)
H13	-0.0396	0.2673	-0.0840	0.026*
C10	0.4178 (3)	0.12085 (15)	0.00898 (17)	0.0196 (4)
H10	0.5345	0.0840	0.0339	0.023*
C9	0.3935 (3)	0.19853 (16)	-0.07638 (18)	0.0225 (4)
H9	0.4943	0.2150	-0.1101	0.027*
C6	-0.1108 (3)	-0.04206 (16)	0.79982 (18)	0.0240 (4)
H6	-0.0807	-0.0333	0.8875	0.029*
C17	0.7878 (3)	0.21435 (15)	0.48327 (19)	0.0226 (4)
H17	0.8930	0.2557	0.5263	0.027*
C20	-0.4249 (3)	-0.12048 (17)	0.8008 (2)	0.0283 (5)
H20A	-0.4186	-0.1944	0.8110	0.042*
H20B	-0.5544	-0.1008	0.7516	0.042*
H20C	-0.3932	-0.0880	0.8829	0.042*
C15	0.6522 (3)	0.22316 (18)	0.6652 (2)	0.0283 (5)
H15A	0.5271	0.2511	0.6630	0.042*
H15B	0.7504	0.2756	0.6934	0.042*
H15C	0.6824	0.1655	0.7229	0.042*
C4	-0.3235 (3)	-0.10071 (15)	0.60608 (19)	0.0220 (4)
H4	-0.4414	-0.1306	0.5600	0.026*
C19	0.9120 (3)	0.20192 (18)	0.2962 (2)	0.0287 (5)
H19A	0.9495	0.1392	0.2629	0.043*
H19B	1.0253	0.2337	0.3536	0.043*
H19C	0.8540	0.2486	0.2274	0.043*
C8	0.2206 (3)	0.25405 (15)	-0.11438 (17)	0.0210 (4)
H31	0.259 (3)	0.0240 (18)	0.341 (2)	0.021 (6)*
H32	0.323 (4)	0.085 (2)	0.562 (3)	0.040 (8)*
H30B	0.296 (3)	0.352 (2)	-0.213 (2)	0.026 (6)*
H30A	0.101 (3)	0.3669 (19)	-0.212 (2)	0.024 (6)*

### Atomic displacement parameters ( $\text{\AA}^2$ )

	$U^{11}$	$U^{22}$	$U^{33}$	$U^{12}$	$U^{13}$	$U^{23}$
S1	0.0277 (2)	0.0170 (2)	0.0165 (2)	-0.00184 (19)	0.00702 (16)	-0.00112 (18)
O1	0.0290 (7)	0.0352 (8)	0.0198 (7)	-0.0088 (7)	0.0099 (5)	-0.0033 (7)
O4	0.0456 (9)	0.0221 (8)	0.0283 (8)	0.0072 (7)	0.0141 (7)	0.0023 (6)
O3	0.0364 (8)	0.0258 (7)	0.0204 (7)	-0.0107 (6)	0.0063 (6)	-0.0019 (6)
N3	0.0205 (8)	0.0184 (8)	0.0158 (8)	0.0022 (6)	0.0043 (6)	0.0006 (6)
O2	0.0246 (7)	0.0337 (8)	0.0222 (7)	-0.0099 (6)	0.0099 (6)	-0.0045 (6)
C1	0.0209 (9)	0.0188 (10)	0.0196 (9)	0.0012 (7)	0.0060 (7)	0.0010 (7)
N4	0.0221 (8)	0.0213 (8)	0.0186 (8)	0.0020 (7)	0.0074 (6)	0.0021 (6)
C14	0.0197 (9)	0.0169 (9)	0.0172 (9)	0.0023 (7)	0.0050 (7)	0.0027 (7)
C18	0.0208 (9)	0.0173 (10)	0.0260 (10)	0.0028 (8)	0.0075 (8)	0.0033 (8)
C12	0.0210 (9)	0.0217 (10)	0.0182 (9)	-0.0045 (8)	0.0080 (7)	-0.0051 (7)
N2	0.0225 (8)	0.0290 (9)	0.0151 (7)	-0.0058 (7)	0.0073 (7)	-0.0004 (7)

C11	0.0243 (9)	0.0183 (9)	0.0131 (8)	-0.0016 (8)	0.0049 (7)	-0.0034 (7)
C2	0.0219 (9)	0.0159 (10)	0.0218 (9)	0.0014 (7)	0.0069 (7)	0.0015 (7)
N1	0.0267 (10)	0.0291 (10)	0.0302 (10)	0.0055 (8)	0.0100 (8)	0.0090 (8)
C3	0.0242 (9)	0.0200 (10)	0.0186 (9)	-0.0006 (8)	0.0054 (8)	-0.0004 (7)
C5	0.0228 (9)	0.0162 (9)	0.0274 (10)	0.0016 (7)	0.0094 (8)	0.0012 (8)
C16	0.0217 (9)	0.0182 (9)	0.0205 (9)	0.0036 (8)	0.0035 (8)	-0.0001 (7)
C7	0.0225 (9)	0.0225 (9)	0.0221 (9)	-0.0037 (9)	0.0058 (7)	-0.0019 (9)
C13	0.0196 (9)	0.0223 (10)	0.0205 (9)	0.0011 (7)	0.0036 (8)	-0.0038 (8)
C10	0.0216 (9)	0.0211 (9)	0.0165 (9)	0.0027 (8)	0.0065 (7)	-0.0015 (7)
C9	0.0227 (10)	0.0268 (10)	0.0200 (9)	0.0006 (8)	0.0096 (8)	-0.0015 (8)
C6	0.0287 (10)	0.0235 (10)	0.0201 (9)	-0.0014 (8)	0.0081 (8)	-0.0026 (8)
C17	0.0210 (9)	0.0203 (10)	0.0251 (10)	-0.0008 (8)	0.0048 (8)	-0.0002 (8)
C20	0.0277 (10)	0.0303 (12)	0.0294 (11)	-0.0036 (9)	0.0122 (9)	0.0021 (9)
C15	0.0315 (11)	0.0311 (11)	0.0218 (10)	-0.0028 (9)	0.0070 (9)	-0.0062 (8)
C4	0.0198 (9)	0.0196 (10)	0.0254 (10)	-0.0020 (8)	0.0048 (8)	0.0004 (8)
C19	0.0283 (11)	0.0287 (11)	0.0338 (11)	-0.0029 (9)	0.0165 (10)	-0.0007 (9)
C8	0.0269 (10)	0.0203 (10)	0.0149 (9)	-0.0008 (8)	0.0050 (8)	-0.0021 (7)

Geometric parameters (Å, °)

S1—O4	1.4290 (16)	C3—H3	0.9500
S1—O3	1.4401 (16)	C5—C6	1.395 (3)
S1—N2	1.6460 (17)	C5—C4	1.396 (3)
S1—C11	1.741 (2)	C5—C20	1.507 (3)
O1—C1	1.224 (2)	C16—C17	1.387 (3)
N3—C16	1.343 (3)	C16—C15	1.498 (3)
N3—C14	1.347 (2)	C7—C6	1.389 (3)
O2—C1	1.319 (2)	C7—H7	0.9500
O2—H32	0.84 (2)	C13—C8	1.397 (3)
C1—C2	1.483 (3)	C13—H13	0.9500
N4—C14	1.324 (3)	C10—C9	1.378 (3)
N4—C18	1.346 (3)	C10—H10	0.9500
C14—N2	1.379 (3)	C9—C8	1.413 (3)
C18—C17	1.390 (3)	C9—H9	0.9500
C18—C19	1.495 (3)	C6—H6	0.9500
C12—C13	1.379 (3)	C17—H17	0.9500
C12—C11	1.390 (3)	C20—H20A	0.9800
C12—H12	0.9500	C20—H20B	0.9800
N2—H31	0.85 (2)	C20—H20C	0.9800
C11—C10	1.394 (3)	C15—H15A	0.9800
C2—C7	1.396 (3)	C15—H15B	0.9800
C2—C3	1.400 (3)	C15—H15C	0.9800
N1—C8	1.368 (3)	C4—H4	0.9500
N1—H30B	0.85 (2)	C19—H19A	0.9800
N1—H30A	0.84 (2)	C19—H19B	0.9800
C3—C4	1.385 (3)	C19—H19C	0.9800
O4—S1—O3	118.56 (10)	C6—C7—C2	119.93 (17)
O4—S1—N2	110.05 (9)	C6—C7—H7	120.0
O3—S1—N2	101.90 (9)	C2—C7—H7	120.0
O4—S1—C11	109.06 (9)	C12—C13—C8	120.97 (19)
O3—S1—C11	108.59 (9)	C12—C13—H13	119.5
N2—S1—C11	108.13 (9)	C8—C13—H13	119.5
C16—N3—C14	115.73 (17)	C9—C10—C11	119.46 (18)
C1—O2—H32	112 (2)	C9—C10—H10	120.3

O1—C1—O2	123.10 (18)	C11—C10—H10	120.3
O1—C1—C2	122.16 (18)	C10—C9—C8	120.89 (18)
O2—C1—C2	114.73 (17)	C10—C9—H9	119.6
C14—N4—C18	116.14 (17)	C8—C9—H9	119.6
N4—C14—N3	127.48 (18)	C7—C6—C5	121.16 (18)
N4—C14—N2	118.23 (17)	C7—C6—H6	119.4
N3—C14—N2	114.28 (17)	C5—C6—H6	119.4
N4—C18—C17	121.27 (18)	C16—C17—C18	117.97 (18)
N4—C18—C19	115.96 (18)	C16—C17—H17	121.0
C17—C18—C19	122.77 (19)	C18—C17—H17	121.0
C13—C12—C11	119.80 (18)	C5—C20—H20A	109.5
C13—C12—H12	120.1	C5—C20—H20B	109.5
C11—C12—H12	120.1	H20A—C20—H20B	109.5
C14—N2—S1	125.93 (14)	C5—C20—H20C	109.5
C14—N2—H31	119.3 (16)	H20A—C20—H20C	109.5
S1—N2—H31	114.8 (16)	H20B—C20—H20C	109.5
C12—C11—C10	120.55 (18)	C16—C15—H15A	109.5
C12—C11—S1	118.49 (15)	C16—C15—H15B	109.5
C10—C11—S1	120.92 (15)	H15A—C15—H15B	109.5
C7—C2—C3	119.38 (18)	C16—C15—H15C	109.5
C7—C2—C1	122.07 (17)	H15A—C15—H15C	109.5
C3—C2—C1	118.55 (17)	H15B—C15—H15C	109.5
C8—N1—H30B	114.6 (18)	C3—C4—C5	121.27 (18)
C8—N1—H30A	116.4 (18)	C3—C4—H4	119.4
H30B—N1—H30A	118 (3)	C5—C4—H4	119.4
C4—C3—C2	119.91 (18)	C18—C19—H19A	109.5
C4—C3—H3	120.0	C18—C19—H19B	109.5
C2—C3—H3	120.0	H19A—C19—H19B	109.5
C6—C5—C4	118.31 (18)	C18—C19—H19C	109.5
C6—C5—C20	120.86 (18)	H19A—C19—H19C	109.5
C4—C5—C20	120.84 (18)	H19B—C19—H19C	109.5
N3—C16—C17	121.40 (18)	N1—C8—C13	121.08 (19)
N3—C16—C15	116.31 (18)	N1—C8—C9	120.55 (19)
C17—C16—C15	122.29 (19)	C13—C8—C9	118.33 (18)
C18—N4—C14—N3	-0.7 (3)	C1—C2—C3—C4	-178.24 (18)
C18—N4—C14—N2	178.64 (17)	C14—N3—C16—C17	0.3 (3)
C16—N3—C14—N4	0.1 (3)	C14—N3—C16—C15	-179.59 (17)
C16—N3—C14—N2	-179.25 (16)	C3—C2—C7—C6	0.6 (3)
C14—N4—C18—C17	0.9 (3)	C1—C2—C7—C6	179.97 (19)
C14—N4—C18—C19	-178.93 (17)	C11—C12—C13—C8	0.7 (3)
N4—C14—N2—S1	-2.5 (3)	C12—C11—C10—C9	-1.0 (3)
N3—C14—N2—S1	176.93 (14)	S1—C11—C10—C9	176.47 (15)
O4—S1—N2—C14	60.45 (19)	C11—C10—C9—C8	0.0 (3)
O3—S1—N2—C14	-172.89 (17)	C2—C7—C6—C5	-1.8 (3)
C11—S1—N2—C14	-58.57 (19)	C4—C5—C6—C7	1.1 (3)
C13—C12—C11—C10	0.7 (3)	C20—C5—C6—C7	-179.0 (2)
C13—C12—C11—S1	-176.86 (14)	N3—C16—C17—C18	-0.1 (3)
O4—S1—C11—C12	160.32 (14)	C15—C16—C17—C18	179.78 (19)
O3—S1—C11—C12	29.80 (17)	N4—C18—C17—C16	-0.5 (3)
N2—S1—C11—C12	-80.03 (16)	C19—C18—C17—C16	179.29 (19)
O4—S1—C11—C10	-17.20 (18)	C2—C3—C4—C5	-1.8 (3)
O3—S1—C11—C10	-147.73 (15)	C6—C5—C4—C3	0.7 (3)
N2—S1—C11—C10	102.45 (16)	C20—C5—C4—C3	-179.20 (19)
O1—C1—C2—C7	171.1 (2)	C12—C13—C8—N1	175.98 (19)
O2—C1—C2—C7	-8.9 (3)	C12—C13—C8—C9	-1.7 (3)

N2—H31···O1	0.85 (2)	1.91 (2)	2.762 (2)	177 (2)
O2—H32···N3	0.84 (2)	1.90 (2)	2.742 (2)	174 (3)

Symmetry codes: (i)  $-x+1, y+1/2, -z$ ; (ii)  $-x, y+1/2, -z$ .

All esds (except the esd in the dihedral angle between two l.s. planes) are estimated using the full covariance matrix. The cell esds are taken into account individually in the estimation of esds in distances, angles and torsion angles; correlations between esds in cell parameters are only used when they are defined by crystal symmetry. An approximate (isotropic) treatment of cell esds is used for estimating esds involving l.s. planes.

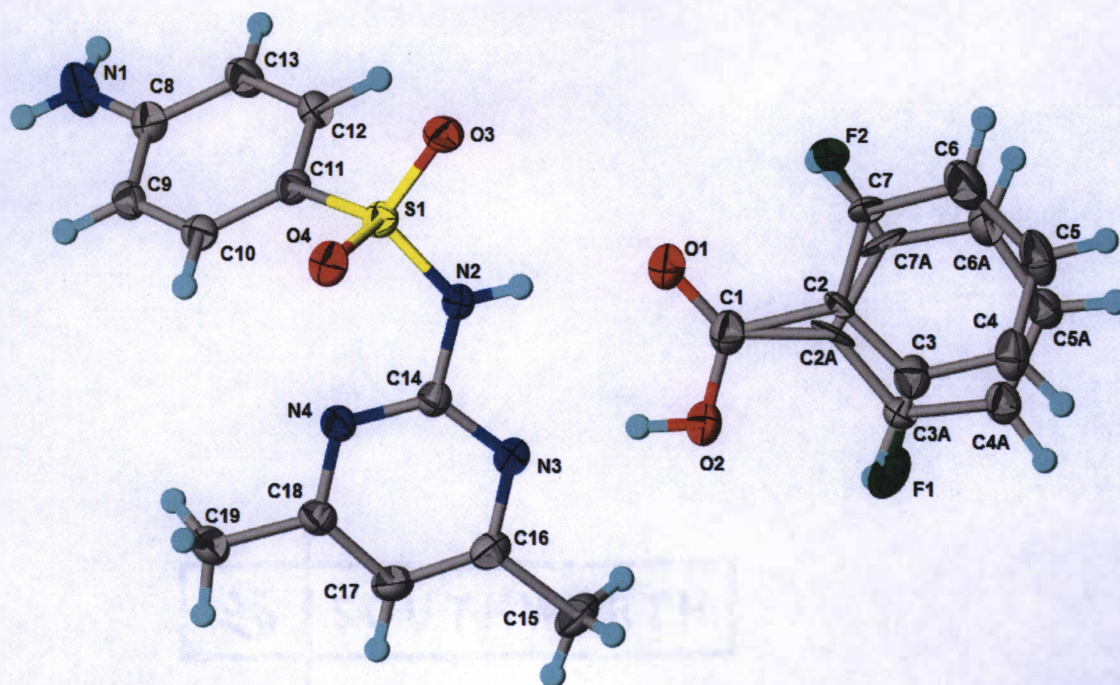


Figure S.8: Crystal Structure of the Cocrystal of Sulfamethazine and *o*-Fluorobenzoic Acid Showing Thermal Parameters (50% Thermal Ellipsoids) and Hydrogen Bonding.

#### Crystal data

$C_{12}H_{14}N_4O_2S \cdot C_7H_5FO_2$

$M_r = 418.44$

Orthorhombic, *Pbca*

$a = 9.5883$  (3) Å

$b = 15.4399$  (4) Å

$c = 26.7427$  (7) Å

$V = 3959.05$  (19) Å<sup>3</sup>

$Z = 8$

$F(000) = 1744$

$D_x = 1.404$  Mg m<sup>-3</sup>

Melting point: 460–469 K

Cu  $K\alpha$  radiation,  $\lambda = 1.54178$  Å

Cell parameters from 4988 reflections

$\theta = 3.3$ – $67.7^\circ$

$\mu = 1.84$  mm<sup>-1</sup>

$T = 100$  K

Plate, colourless

$\times \times$  mm

$M_r = 418.44$   
 Orthorhombic, *Pbca*  
 $a = 9.5883$  (3) Å  
 $b = 15.4399$  (4) Å  
 $c = 26.7427$  (7) Å  
 $V = 3959.05$  (19) Å<sup>3</sup>  
 $Z = 8$   
 $F(000) = 1744$

Melting point: 460-469 K  
 Cu  $K\alpha$  radiation,  $\lambda = 1.54178$  Å  
 Cell parameters from 4988 reflections  
 $\theta = 3.3$ – $67.7^\circ$   
 $\mu = 1.84$  mm<sup>-1</sup>  
 $T = 100$  K  
 Plate, colourless  
 × × mm

### Data collection

Bruker APEXII CCD  
 diffractometer  
 Radiation source: fine-focus sealed tube  
 Detector resolution: 8.33 pixels mm<sup>-1</sup>  
 phi and  $\omega$  scans  
 Absorption correction: multi-scan  
 SADABS2014/7, Bruker AXS  
 $T_{\min} = 0.598$ ,  $T_{\max} = 0.753$   
 54427 measured reflections

3627 independent reflections  
 3068 reflections with  $I > 2\sigma(I)$   
 $R_{\text{int}} = 0.073$   
 $\theta_{\max} = 68.2^\circ$ ,  $\theta_{\min} = 3.3^\circ$   
 $h = -10$  11  
 $k = -18$  18  
 $l = -31$  32

### Refinement

Refinement on  $F^2$   
 Least-squares matrix: full  
 $R[F^2 > 2\sigma(F^2)] = 0.036$   
 $wR(F^2) = 0.094$   
 $S = 1.03$   
 3627 reflections  
 344 parameters  
 34 restraints  
 0 constraints

Hydrogen site location: mixed  
 H atoms treated by a mixture of independent and  
 constrained refinement  
 $w = 1/[\sigma^2(F_o^2) + (0.038P)^2 + 1.6491P]$   
 where  $P = (F_o^2 + 2F_c^2)/3$   
 $(\Delta/\sigma)_{\max} < 0.001$   
 $\Delta\rho_{\max} = 0.19$  e Å<sup>-3</sup>  
 $\Delta\rho_{\min} = -0.42$  e Å<sup>-3</sup>  
 Extinction correction: none

### Fractional atomic coordinates and isotropic or equivalent isotropic displacement parameters (Å<sup>2</sup>)

	<i>x</i>	<i>y</i>	<i>z</i>	$U_{\text{iso}}^*/U_{\text{eq}}$	Occ. (<1)
S1	0.12467 (4)	0.22413 (3)	0.15595 (2)	0.02806 (13)	
O1	0.16377 (14)	0.12737 (9)	0.02122 (5)	0.0442 (3)	
O2	-0.03970 (14)	0.10783 (9)	-0.01786 (5)	0.0405 (3)	
O3	0.26555 (12)	0.20765 (8)	0.14002 (5)	0.0342 (3)	
O4	0.06934 (13)	0.17119 (8)	0.19537 (4)	0.0350 (3)	
N1	0.1038 (2)	0.58674 (11)	0.22392 (7)	0.0489 (5)	

H30A	0.153 (2)	0.6243 (14)	0.2079 (8)	0.058 (7)*	
H30B	0.046 (2)	0.6017 (14)	0.2463 (7)	0.049 (6)*	
N2	0.03437 (15)	0.20962 (10)	0.10427 (5)	0.0295 (3)	
N3	-0.16266 (15)	0.19042 (9)	0.05649 (5)	0.0297 (3)	
N4	-0.17851 (15)	0.24589 (9)	0.13976 (5)	0.0281 (3)	
C1	0.0960 (2)	0.10026 (11)	-0.01418 (7)	0.0353 (4)	
C8	0.10501 (19)	0.50346 (11)	0.20768 (7)	0.0324 (4)	
C9	0.01237 (18)	0.44170 (11)	0.22693 (6)	0.0303 (4)	
H9	-0.0528	0.4583	0.2519	0.036*	
C10	0.01429 (18)	0.35756 (11)	0.21027 (6)	0.0283 (4)	
H10	-0.0496	0.3166	0.2235	0.034*	
C11	0.11023 (17)	0.33236 (11)	0.17384 (6)	0.0274 (4)	
C12	0.20288 (18)	0.39266 (11)	0.15396 (6)	0.0312 (4)	
H12	0.2677	0.3755	0.1290	0.037*	
C13	0.20049 (19)	0.47721 (12)	0.17051 (7)	0.0355 (4)	
H13	0.2637	0.5182	0.1568	0.043*	
C14	-0.10949 (17)	0.21539 (10)	0.10061 (6)	0.0263 (3)	
C15	-0.3625 (2)	0.16640 (14)	0.00283 (8)	0.0475 (5)	
H15B	-0.3580	0.1031	0.0008	0.071*	
H15A	-0.3088	0.1917	-0.0247	0.071*	
H15C	-0.4599	0.1852	0.0004	0.071*	
C16	-0.30253 (19)	0.19581 (11)	0.05169 (7)	0.0338 (4)	
C17	-0.38375 (19)	0.22639 (11)	0.09066 (7)	0.0354 (4)	
H17	-0.4822	0.2303	0.0874	0.043*	
C18	-0.31791 (18)	0.25118 (11)	0.13460 (6)	0.0294 (4)	
C19	-0.39555 (19)	0.28420 (12)	0.17898 (7)	0.0359 (4)	
H19B	-0.3802	0.2453	0.2074	0.054*	
H19C	-0.4954	0.2866	0.1713	0.054*	
H19A	-0.3621	0.3424	0.1874	0.054*	
C2	0.1769 (7)	0.0559 (8)	-0.0574 (4)	0.0245 (16)	0.620 (5)
C3	0.1082 (6)	0.0194 (5)	-0.0971 (3)	0.0340 (15)	0.620 (5)
C4	0.1778 (8)	-0.0198 (3)	-0.1360 (2)	0.0401 (16)	0.620 (5)
H4	0.1288	-0.0424	-0.1640	0.048*	0.620 (5)
C5	0.3216 (7)	-0.0252 (3)	-0.1329 (2)	0.0464 (12)	0.620 (5)
H5A	0.3722	-0.0529	-0.1589	0.056*	0.620 (5)
C7	0.3193 (6)	0.0499 (4)	-0.0555 (2)	0.0357 (13)	0.620 (5)
H7A	0.3678	0.0745	-0.0279	0.043*	0.620 (5)
C6	0.3930 (6)	0.0092 (4)	-0.0925 (2)	0.0526 (13)	0.620 (5)
H6A	0.4917	0.0046	-0.0905	0.063*	0.620 (5)
C2A	0.1356 (12)	0.0568 (13)	-0.0586 (7)	0.029 (3)	0.380 (5)
C3A	0.0532 (9)	0.0230 (7)	-0.0973 (4)	0.026 (2)	0.380 (5)
H3A	-0.0452	0.0277	-0.0943	0.031*	0.380 (5)
C4A	0.1066 (8)	-0.0169 (6)	-0.1396 (3)	0.0339 (19)	0.380 (5)
H4A	0.0456	-0.0421	-0.1635	0.041*	0.380 (5)
C5A	0.2503 (10)	-0.0198 (5)	-0.1468 (3)	0.0315 (17)	0.380 (5)
H5A1	0.2864	-0.0465	-0.1761	0.038*	0.380 (5)
C6A	0.3414 (9)	0.0153 (6)	-0.1124 (3)	0.0424 (18)	0.380 (5)
H6A1	0.4395	0.0156	-0.1172	0.051*	0.380 (5)
C7A	0.2786 (11)	0.0505 (8)	-0.0698 (4)	0.042 (3)	0.380 (5)

F1	-0.0326 (3)	0.02161 (17)	-0.10023 (8)	0.0625 (9)	0.620 (5)
F2	0.3742 (4)	0.0837 (3)	-0.03673 (14)	0.0656 (15)	0.380 (5)
H31	0.079 (2)	0.1864 (13)	0.0800 (7)	0.043 (6)*	
H32	-0.071 (3)	0.1375 (17)	0.0085 (8)	0.084 (9)*	

### Atomic displacement parameters (Å<sup>2</sup>)

	$U^{11}$	$U^{22}$	$U^{33}$	$U^{12}$	$U^{13}$	$U^{23}$
S1	0.0278 (2)	0.0288 (2)	0.0275 (2)	0.00147 (16)	-0.00212 (16)	-0.00086 (16)
O1	0.0426 (8)	0.0509 (8)	0.0392 (7)	0.0023 (6)	0.0022 (6)	-0.0149 (6)
O2	0.0433 (8)	0.0454 (8)	0.0328 (7)	-0.0029 (6)	0.0043 (6)	-0.0100 (6)
O3	0.0262 (6)	0.0345 (6)	0.0419 (7)	0.0043 (5)	-0.0025 (5)	-0.0052 (5)
O4	0.0444 (7)	0.0315 (6)	0.0291 (6)	0.0008 (5)	-0.0005 (5)	0.0035 (5)
N1	0.0613 (12)	0.0327 (9)	0.0529 (11)	-0.0050 (8)	0.0280 (9)	-0.0070 (8)
N2	0.0272 (8)	0.0367 (8)	0.0247 (7)	-0.0005 (6)	0.0007 (6)	-0.0053 (6)
N3	0.0319 (8)	0.0288 (7)	0.0283 (7)	-0.0007 (6)	-0.0021 (6)	-0.0023 (6)
N4	0.0280 (7)	0.0279 (7)	0.0285 (7)	-0.0007 (6)	0.0019 (6)	-0.0005 (6)
C1	0.0445 (11)	0.0293 (9)	0.0320 (10)	-0.0027 (8)	0.0057 (8)	-0.0031 (8)
C8	0.0352 (10)	0.0303 (9)	0.0318 (9)	0.0025 (7)	0.0028 (7)	-0.0015 (7)
C9	0.0302 (9)	0.0362 (9)	0.0245 (8)	0.0039 (7)	0.0017 (7)	0.0002 (7)
C10	0.0283 (9)	0.0333 (9)	0.0233 (8)	-0.0004 (7)	-0.0026 (6)	0.0035 (7)
C11	0.0278 (9)	0.0283 (9)	0.0260 (8)	0.0014 (7)	-0.0035 (6)	-0.0014 (7)
C12	0.0281 (9)	0.0336 (9)	0.0320 (9)	0.0012 (7)	0.0025 (7)	-0.0036 (7)
C13	0.0328 (10)	0.0339 (10)	0.0398 (10)	-0.0032 (7)	0.0086 (8)	-0.0018 (8)
C14	0.0293 (9)	0.0238 (8)	0.0258 (8)	-0.0026 (6)	0.0002 (6)	0.0005 (6)
C15	0.0465 (12)	0.0484 (12)	0.0475 (11)	0.0053 (9)	-0.0180 (9)	-0.0165 (10)
C16	0.0336 (10)	0.0298 (9)	0.0381 (10)	-0.0003 (7)	-0.0076 (7)	-0.0042 (7)
C17	0.0281 (9)	0.0332 (9)	0.0450 (11)	-0.0009 (7)	-0.0036 (8)	-0.0052 (8)
C18	0.0282 (9)	0.0243 (8)	0.0356 (9)	-0.0018 (7)	0.0033 (7)	0.0009 (7)
C19	0.0307 (10)	0.0368 (10)	0.0401 (10)	0.0005 (8)	0.0067 (8)	-0.0035 (8)
C2	0.015 (5)	0.0262 (19)	0.032 (2)	-0.003 (3)	0.012 (3)	-0.0054 (14)
C3	0.038 (4)	0.034 (2)	0.031 (2)	0.009 (3)	-0.001 (3)	-0.0014 (15)
C4	0.060 (5)	0.0308 (19)	0.030 (2)	-0.002 (4)	0.011 (3)	-0.0010 (15)
C5	0.065 (4)	0.030 (2)	0.045 (3)	-0.005 (3)	0.030 (3)	-0.001 (2)
C7	0.024 (3)	0.039 (2)	0.045 (3)	-0.017 (2)	0.004 (2)	-0.017 (2)
C6	0.052 (3)	0.046 (2)	0.060 (3)	-0.010 (2)	0.026 (2)	-0.010 (3)
C2A	0.010 (6)	0.029 (3)	0.049 (5)	-0.002 (5)	0.014 (4)	0.008 (3)
C3A	0.022 (6)	0.028 (3)	0.028 (3)	0.000 (5)	0.001 (4)	-0.002 (2)
C4A	0.039 (5)	0.031 (3)	0.032 (3)	-0.005 (4)	0.009 (3)	-0.001 (2)
C5A	0.034 (6)	0.025 (3)	0.036 (4)	0.000 (4)	0.008 (3)	-0.001 (3)
C6A	0.041 (5)	0.047 (4)	0.040 (5)	-0.004 (4)	0.012 (3)	-0.012 (4)
C7A	0.031 (6)	0.046 (4)	0.049 (5)	-0.016 (4)	-0.021 (4)	-0.016 (4)
F1	0.0510 (19)	0.0820 (17)	0.0544 (14)	0.0240 (15)	-0.0238 (13)	-0.0329 (11)
F2	0.030 (2)	0.104 (3)	0.063 (2)	-0.015 (2)	0.0048 (17)	-0.043 (2)

### Geometric parameters (Å, °)

S1—O4	1.4356 (12)	C15—H15C	0.9800
S1—O3	1.4391 (12)	C16—C17	1.384 (3)



S1—N2	1.6462 (14)	C17—C18	1.388 (2)
S1—C11	1.7437 (17)	C17—H17	0.9500
O1—C1	1.222 (2)	C18—C19	1.491 (2)
O2—C1	1.310 (2)	C19—H19B	0.9800
O2—H32	0.891 (17)	C19—H19C	0.9800
N1—C8	1.357 (2)	C19—H19A	0.9800
N1—H30A	0.859 (16)	C2—C3	1.369 (9)
N1—H30B	0.847 (16)	C2—C7	1.370 (7)
N2—C14	1.386 (2)	C3—F1	1.353 (5)
N2—H31	0.856 (15)	C3—C4	1.377 (8)
N3—C14	1.342 (2)	C4—C5	1.384 (7)
N3—C16	1.350 (2)	C4—H4	0.9500
N4—C14	1.325 (2)	C5—C6	1.384 (7)
N4—C18	1.346 (2)	C5—H5A	0.9500
C1—C2A	1.415 (18)	C7—C6	1.369 (7)
C1—C2	1.553 (9)	C7—H7A	0.9500
C8—C9	1.401 (2)	C6—H6A	0.9500
C8—C13	1.411 (2)	C2A—C3A	1.404 (13)
C9—C10	1.374 (2)	C2A—C7A	1.407 (11)
C9—H9	0.9500	C3A—C4A	1.386 (11)
C10—C11	1.395 (2)	C3A—H3A	0.9500
C10—H10	0.9500	C4A—C5A	1.391 (8)
C11—C12	1.392 (2)	C4A—H4A	0.9500
C12—C13	1.379 (3)	C5A—C6A	1.381 (9)
C12—H12	0.9500	C5A—H5A1	0.9500
C13—H13	0.9500	C6A—C7A	1.399 (11)
C15—C16	1.498 (2)	C6A—H6A1	0.9500
C15—H15B	0.9800	C7A—F2	1.372 (8)
C15—H15A	0.9800		
O4—S1—O3	117.61 (7)	C17—C16—C15	122.99 (17)
O4—S1—N2	110.15 (7)	C16—C17—C18	118.41 (17)
O3—S1—N2	102.78 (7)	C16—C17—H17	120.8
O4—S1—C11	108.35 (8)	C18—C17—H17	120.8
O3—S1—C11	108.98 (8)	N4—C18—C17	121.45 (16)
N2—S1—C11	108.61 (8)	N4—C18—C19	115.78 (15)
C1—O2—H32	108.4 (19)	C17—C18—C19	122.77 (16)
C8—N1—H30A	118.4 (16)	C18—C19—H19B	109.5
C8—N1—H30B	119.3 (15)	C18—C19—H19C	109.5
H30A—N1—H30B	122 (2)	H19B—C19—H19C	109.5
C14—N2—S1	125.04 (12)	C18—C19—H19A	109.5
C14—N2—H31	118.1 (14)	H19B—C19—H19A	109.5
S1—N2—H31	115.5 (14)	H19C—C19—H19A	109.5
C14—N3—C16	116.33 (15)	C3—C2—C7	118.8 (6)
C14—N4—C18	115.87 (14)	C3—C2—C1	121.2 (5)
O1—C1—O2	123.78 (17)	C7—C2—C1	120.0 (6)
O1—C1—C2A	132.0 (5)	F1—C3—C2	121.2 (5)
O2—C1—C2A	104.2 (5)	F1—C3—C4	116.5 (6)
O1—C1—C2	117.5 (3)	C2—C3—C4	122.2 (6)
O2—C1—C2	118.7 (3)	C3—C4—C5	117.5 (5)

N1—C8—C9	121.44 (16)	C3—C4—H4	121.2
N1—C8—C13	120.21 (17)	C5—C4—H4	121.2
C9—C8—C13	118.34 (16)	C4—C5—C6	121.2 (4)
C10—C9—C8	121.07 (16)	C4—C5—H5A	119.4
C10—C9—H9	119.5	C6—C5—H5A	119.4
C8—C9—H9	119.5	C6—C7—C2	121.2 (6)
C9—C10—C11	119.94 (16)	C6—C7—H7A	119.4
C9—C10—H10	120.0	C2—C7—H7A	119.4
C11—C10—H10	120.0	C7—C6—C5	119.0 (5)
C12—C11—C10	120.05 (16)	C7—C6—H6A	120.5
C12—C11—S1	119.04 (13)	C5—C6—H6A	120.5
C10—C11—S1	120.74 (13)	C3A—C2A—C7A	111.4 (13)
C13—C12—C11	120.00 (16)	C3A—C2A—C1	130.1 (10)
C13—C12—H12	120.0	C7A—C2A—C1	118.2 (10)
C11—C12—H12	120.0	C4A—C3A—C2A	124.1 (10)
C12—C13—C8	120.59 (17)	C4A—C3A—H3A	118.0
C12—C13—H13	119.7	C2A—C3A—H3A	118.0
C8—C13—H13	119.7	C3A—C4A—C5A	119.6 (8)
N4—C14—N3	127.38 (16)	C3A—C4A—H4A	120.2
N4—C14—N2	117.65 (15)	C5A—C4A—H4A	120.2
N3—C14—N2	114.95 (15)	C6A—C5A—C4A	121.4 (7)
C16—C15—H15B	109.5	C6A—C5A—H5A1	119.3
C16—C15—H15A	109.5	C4A—C5A—H5A1	119.3
H15B—C15—H15A	109.5	C5A—C6A—C7A	115.1 (7)
C16—C15—H15C	109.5	C5A—C6A—H6A1	122.5
H15B—C15—H15C	109.5	C7A—C6A—H6A1	122.5
H15A—C15—H15C	109.5	F2—C7A—C6A	112.4 (9)
N3—C16—C17	120.55 (16)	F2—C7A—C2A	119.2 (10)
N3—C16—C15	116.46 (17)	C6A—C7A—C2A	128.3 (11)
O4—S1—N2—C14	51.62 (16)	C16—C17—C18—C19	-179.42 (16)
O3—S1—N2—C14	177.74 (14)	O1—C1—C2—C3	176.3 (8)
C11—S1—N2—C14	-66.90 (16)	O2—C1—C2—C3	-4.8 (12)
N1—C8—C9—C10	179.99 (18)	O1—C1—C2—C7	-1.3 (12)
C13—C8—C9—C10	0.2 (3)	O2—C1—C2—C7	177.6 (7)
C8—C9—C10—C11	0.4 (3)	C7—C2—C3—F1	178.4 (9)
C9—C10—C11—C12	-0.7 (2)	C1—C2—C3—F1	0.8 (15)
C9—C10—C11—S1	174.52 (13)	C7—C2—C3—C4	-2.8 (15)
O4—S1—C11—C12	153.73 (13)	C1—C2—C3—C4	179.6 (7)
O3—S1—C11—C12	24.63 (16)	F1—C3—C4—C5	-178.1 (5)
N2—S1—C11—C12	-86.62 (15)	C2—C3—C4—C5	3.0 (12)
O4—S1—C11—C10	-21.58 (16)	C3—C4—C5—C6	-1.2 (8)
O3—S1—C11—C10	-150.68 (13)	C3—C2—C7—C6	0.7 (15)
N2—S1—C11—C10	98.07 (14)	C1—C2—C7—C6	178.3 (7)
C10—C11—C12—C13	0.4 (3)	C2—C7—C6—C5	1.0 (11)
S1—C11—C12—C13	-174.92 (14)	C4—C5—C6—C7	-0.7 (7)
C11—C12—C13—C8	0.2 (3)	O1—C1—C2A—C3A	176.5 (13)
N1—C8—C13—C12	179.69 (19)	O2—C1—C2A—C3A	-4 (2)
C9—C8—C13—C12	-0.5 (3)	O1—C1—C2A—C7A	-9 (2)
C18—N4—C14—N3	0.9 (2)	O2—C1—C2A—C7A	170.3 (15)

C18—N4—C14—N2	179.46 (14)	C7A—C2A—C3A—C4A	4 (2)
C16—N3—C14—N4	-1.0 (3)	C1—C2A—C3A—C4A	178.6 (15)
C16—N3—C14—N2	-179.61 (15)	C2A—C3A—C4A—C5A	-4.3 (19)
S1—N2—C14—N4	9.4 (2)	C3A—C4A—C5A—C6A	0.9 (15)
S1—N2—C14—N3	-171.89 (12)	C4A—C5A—C6A—C7A	2.1 (14)
C14—N3—C16—C17	0.5 (2)	C5A—C6A—C7A—F2	179.5 (8)
C14—N3—C16—C15	-178.87 (16)	C5A—C6A—C7A—C2A	-2 (2)
N3—C16—C17—C18	0.0 (3)	C3A—C2A—C7A—F2	177.5 (11)
C15—C16—C17—C18	179.32 (17)	C1—C2A—C7A—F2	2 (2)
C14—N4—C18—C17	-0.3 (2)	C3A—C2A—C7A—C6A	-1 (3)
C14—N4—C18—C19	179.07 (15)	C1—C2A—C7A—C6A	-176.1 (11)
C16—C17—C18—N4	-0.1 (3)		

#### Hydrogen-bond geometry (Å, °)

<i>D</i> —H··· <i>A</i>	<i>D</i> —H	H··· <i>A</i>	<i>D</i> ··· <i>A</i>	<i>D</i> —H··· <i>A</i>
N1—H30 <i>A</i> ···O3 <sup>i</sup>	0.86 (2)	2.36 (2)	3.176 (2)	159 (2)
N1—H30 <i>B</i> ···O4 <sup>ii</sup>	0.85 (2)	2.19 (2)	3.019 (2)	165 (2)
N2—H31···O1	0.86 (2)	1.99 (2)	2.8435 (19)	174 (2)
O2—H32···N3	0.89 (2)	1.76 (2)	2.6401 (19)	169 (3)

Symmetry codes: (i)  $-x+1/2, y+1/2, z$ ; (ii)  $-x, y+1/2, -z+1/2$ .

All esds (except the esd in the dihedral angle between two l.s. planes) are estimated using the full covariance matrix. The cell esds are taken into account individually in the estimation of esds in distances, angles and torsion angles; correlations between esds in cell parameters are only used when they are defined by crystal symmetry. An approximate (isotropic) treatment of cell esds is used for estimating esds involving l.s. planes.

S1—N2—C14—N3	-171.89 (12)	C4A—C5A—C6A—C7A	2.1 (14)
C14—N3—C16—C17	0.5 (2)	C5A—C6A—C7A—F2	179.5 (8)
C14—N3—C16—C15	-178.87 (16)	C5A—C6A—C7A—C2A	-2 (2)
N3—C16—C17—C18	0.0 (3)	C3A—C2A—C7A—F2	177.5 (11)
C15—C16—C17—C18	179.32 (17)	C1—C2A—C7A—F2	2 (2)
C14—N4—C18—C17	-0.3 (2)	C3A—C2A—C7A—C6A	-1 (3)
C14—N4—C18—C19	179.07 (15)	C1—C2A—C7A—C6A	-176.1 (11)
C16—C17—C18—N4	-0.1 (3)		

#### Hydrogen-bond geometry (Å, °)

<i>D</i> —H··· <i>A</i>	<i>D</i> —H	H··· <i>A</i>	<i>D</i> ··· <i>A</i>	<i>D</i> —H··· <i>A</i>
N1—H30 <i>A</i> ···O3 <sup>i</sup>	0.86 (2)	2.36 (2)	3.176 (2)	159 (2)
N1—H30 <i>B</i> ···O4 <sup>ii</sup>	0.85 (2)	2.19 (2)	3.019 (2)	165 (2)
N2—H31···O1	0.86 (2)	1.99 (2)	2.8435 (19)	174 (2)
O2—H32···N3	0.89 (2)	1.76 (2)	2.6401 (19)	169 (3)

Symmetry codes: (i)  $-x+1/2, y+1/2, z$ ; (ii)  $-x, y+1/2, -z+1/2$ .

All esds (except the esd in the dihedral angle between two l.s. planes) are estimated using the full covariance matrix. The cell esds are taken into account individually in the estimation of esds in distances, angles and torsion angles; correlations between esds in cell parameters are only used when they are defined by crystal symmetry. An approximate (isotropic) treatment of cell esds is used for estimating esds involving l.s. planes.

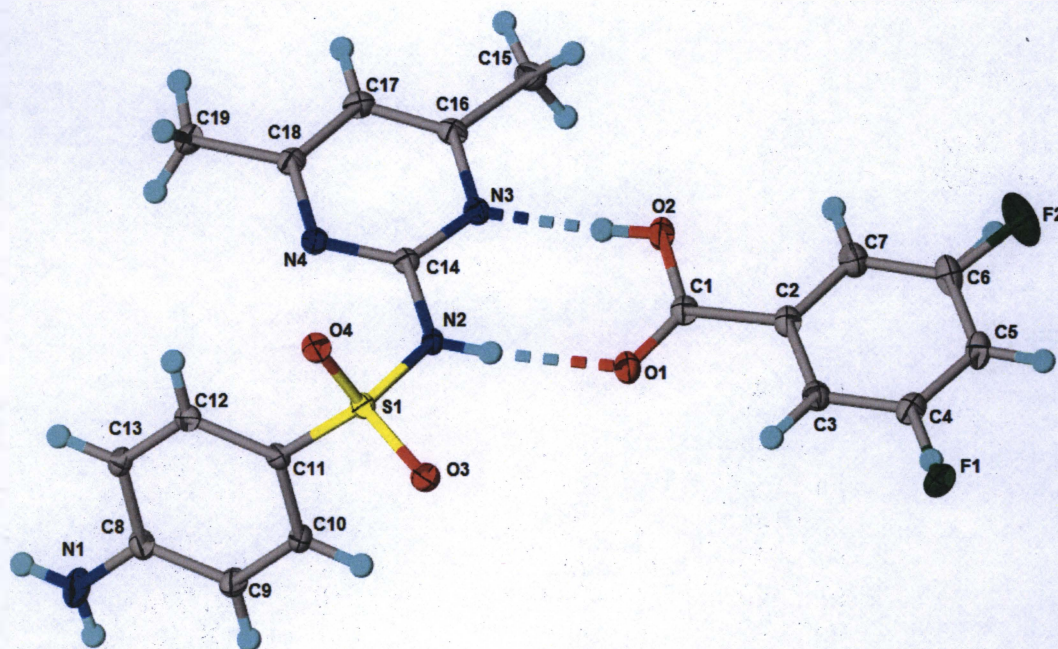


Figure S.9: Crystal Structure of the Cocrystal of Sulfamethazine and *m*-Fluorobenzoic Acid Showing Thermal Parameters (50% Thermal Ellipsoids) and Hydrogen Bonding.

Bruker APEXII CCD  
 diffractometer  
 Radiation source: fine-focus sealed tube  
 Detector resolution: 8.33 pixels mm<sup>-1</sup>  
 phi and  $\omega$  scans  
 Absorption correction: multi-scan  
 SADABS2014/7, Bruker AXS  
 $T_{\min} = 0.627$ ,  $T_{\max} = 0.753$   
 56279 measured reflections

3588 independent reflections  
 3343 reflections with  $I > 2\sigma(I)$   
 $R_{\text{int}} = 0.037$   
 $\theta_{\max} = 68.2^\circ$ ,  $\theta_{\min} = 3.5^\circ$   
 $h = -11 \ 11$   
 $k = -16 \ 18$   
 $l = -30 \ 30$

### Refinement

Refinement on  $F^2$   
 Least-squares matrix: full  
 $R[F^2 > 2\sigma(F^2)] = 0.034$   
 $wR(F^2) = 0.089$   
 $S = 1.05$   
 3588 reflections  
 289 parameters  
 5 restraints  
 0 constraints

Hydrogen site location: mixed  
 H atoms treated by a mixture of independent and  
 constrained refinement  
 $w = 1/[\sigma^2(F_o^2) + (0.0443P)^2 + 2.9748P]$   
 where  $P = (F_o^2 + 2F_c^2)/3$   
 $(\Delta/\sigma)_{\max} = 7.552$   
 $\Delta\rho_{\max} = 0.85 \text{ e } \text{\AA}^{-3}$   
 $\Delta\rho_{\min} = -0.42 \text{ e } \text{\AA}^{-3}$   
 Extinction correction: none

### Fractional atomic coordinates and isotropic or equivalent isotropic displacement parameters ( $\text{\AA}^2$ )

	x	y	z	$U_{\text{iso}}^*/U_{\text{eq}}$	Occ. (<1)
S1	0.14616 (4)	0.01757 (2)	0.15740 (2)	0.01547 (11)	
F1	0.57252 (10)	0.25347 (7)	-0.08383 (4)	0.0297 (4)	0.926 (4)
F2	0.202 (4)	0.270 (8)	-0.138 (3)	0.9 (2)	0.074 (4)
O1	0.20702 (11)	0.11037 (8)	0.01893 (4)	0.0240 (3)	
O2	0.01712 (11)	0.14171 (8)	-0.02580 (4)	0.0231 (3)	
H32	-0.0215 (19)	0.1152 (12)	-0.0010 (7)	0.028*	
O3	0.28587 (11)	0.02930 (7)	0.14244 (4)	0.0201 (2)	
O4	0.09250 (11)	0.07202 (7)	0.19781 (4)	0.0211 (2)	
N1	0.07660 (18)	-0.34230 (10)	0.22079 (7)	0.0343 (4)	
H30B	0.120 (2)	-0.3817 (13)	0.2040 (8)	0.041*	
H30A	0.018 (2)	-0.3577 (14)	0.2430 (8)	0.041*	
N2	0.06451 (13)	0.03454 (8)	0.10205 (5)	0.0172 (3)	
H31	0.1101 (17)	0.0546 (12)	0.0775 (6)	0.021*	
N4	-0.14842 (13)	0.00399 (8)	0.13611 (5)	0.0177 (3)	
N3	-0.12128 (13)	0.06089 (8)	0.04965 (5)	0.0174 (3)	
C1	0.14891 (16)	0.14416 (10)	-0.01824 (6)	0.0192 (3)	
C2	0.22613 (17)	0.19117 (10)	-0.05970 (6)	0.0197 (3)	
C3	0.36497 (17)	0.20142 (10)	-0.05247 (6)	0.0212 (3)	
H3	0.4084	0.1806	-0.0217	0.025*	
C4	0.43770 (17)	0.24242 (10)	-0.09090 (7)	0.0227 (3)	
H4	0.5328	0.2490	-0.0862	0.027*	0.074 (4)
C5	0.37935 (18)	0.27445 (10)	-0.13598 (6)	0.0243 (4)	

H5	0.4329	0.3023	-0.1619	0.029*	
C6	0.2415 (2)	0.26503 (11)	-0.14245 (7)	0.0269 (4)	
H6	0.1992	0.2873	-0.1730	0.032*	0.926 (4)
C7	0.16225 (19)	0.22302 (11)	-0.10461 (6)	0.0235 (4)	
H7	0.065 (2)	0.2136 (13)	-0.1098 (7)	0.028*	
C8	0.09121 (17)	-0.25911 (10)	0.20657 (6)	0.0210 (3)	
C9	0.18848 (17)	-0.23588 (10)	0.16866 (6)	0.0227 (3)	
H9	0.2442	-0.2787	0.1533	0.027*	
C13	0.00964 (16)	-0.19449 (10)	0.22875 (6)	0.0187 (3)	
H13	-0.0555	-0.2089	0.2548	0.022*	
C10	0.20360 (16)	-0.15169 (10)	0.15362 (6)	0.0191 (3)	
H10	0.2702	-0.1366	0.1283	0.023*	
C12	0.02349 (15)	-0.11039 (10)	0.21306 (6)	0.0170 (3)	
H12	-0.0331	-0.0674	0.2277	0.020*	
C11	0.12090 (15)	-0.08876 (10)	0.17562 (6)	0.0161 (3)	
C14	-0.07524 (15)	0.03302 (9)	0.09611 (6)	0.0160 (3)	
C15	-0.31002 (17)	0.09080 (12)	-0.00869 (6)	0.0249 (4)	
H15B	-0.2855	0.1511	-0.0135	0.037*	
H15C	-0.4090	0.0849	-0.0095	0.037*	
H15A	-0.2700	0.0566	-0.0370	0.037*	
C16	-0.25749 (16)	0.06006 (10)	0.04304 (6)	0.0191 (3)	
C17	-0.34209 (16)	0.03168 (10)	0.08284 (6)	0.0208 (3)	
H17	-0.4378	0.0317	0.0785	0.025*	
C18	-0.28367 (16)	0.00327 (10)	0.12912 (6)	0.0187 (3)	
C19	-0.36607 (17)	-0.03019 (11)	0.17394 (7)	0.0243 (4)	
H19C	-0.3392	-0.0893	0.1815	0.036*	
H19A	-0.4625	-0.0286	0.1646	0.036*	
H19B	-0.3505	0.0054	0.2050	0.036*	

### Atomic displacement parameters ( $\text{\AA}^2$ )

	$U^{11}$	$U^{22}$	$U^{33}$	$U^{12}$	$U^{13}$	$U^{23}$
S1	0.0168 (2)	0.0143 (2)	0.01531 (19)	-0.00038 (13)	-0.00067 (13)	0.00002 (13)
F1	0.0206 (6)	0.0344 (7)	0.0339 (7)	-0.0018 (4)	0.0073 (4)	0.0045 (5)
F2	0.003 (17)	0.7 (2)	2.0 (7)	-0.03 (5)	-0.05 (8)	-0.4 (3)
O1	0.0234 (6)	0.0284 (6)	0.0202 (6)	-0.0010 (5)	0.0011 (5)	0.0065 (5)
O2	0.0219 (6)	0.0267 (6)	0.0207 (6)	-0.0028 (5)	0.0021 (5)	0.0056 (5)
O3	0.0176 (6)	0.0198 (6)	0.0230 (6)	-0.0022 (4)	-0.0010 (4)	0.0012 (4)
O4	0.0262 (6)	0.0188 (6)	0.0183 (5)	0.0007 (5)	0.0006 (4)	-0.0024 (4)
N1	0.0457 (10)	0.0183 (8)	0.0388 (9)	0.0031 (7)	0.0239 (8)	0.0058 (7)
N2	0.0164 (6)	0.0204 (7)	0.0148 (6)	-0.0009 (5)	0.0014 (5)	0.0040 (5)
N4	0.0187 (7)	0.0162 (6)	0.0182 (7)	0.0007 (5)	0.0011 (5)	-0.0001 (5)
N3	0.0196 (6)	0.0162 (6)	0.0166 (6)	0.0007 (5)	-0.0001 (5)	0.0000 (5)
C1	0.0233 (8)	0.0159 (8)	0.0185 (8)	-0.0001 (6)	0.0023 (6)	-0.0026 (6)
C2	0.0270 (9)	0.0146 (8)	0.0175 (7)	0.0000 (6)	0.0027 (6)	-0.0023 (6)
C3	0.0258 (8)	0.0181 (8)	0.0198 (8)	0.0018 (6)	0.0024 (6)	-0.0001 (6)

C4	0.0244 (8)	0.0173 (8)	0.0263 (8)	-0.0017 (6)	0.0060 (7)	-0.0037 (6)
C5	0.0359 (9)	0.0175 (8)	0.0193 (8)	-0.0066 (7)	0.0076 (7)	-0.0023 (6)
C6	0.0376 (11)	0.0245 (9)	0.0186 (8)	-0.0060 (7)	-0.0008 (7)	0.0030 (7)
C7	0.0264 (10)	0.0226 (9)	0.0215 (8)	-0.0049 (7)	-0.0013 (7)	0.0008 (7)
C8	0.0251 (8)	0.0185 (8)	0.0194 (8)	-0.0003 (6)	0.0021 (6)	0.0027 (6)
C9	0.0257 (8)	0.0181 (8)	0.0243 (8)	0.0041 (6)	0.0068 (7)	0.0007 (6)
C13	0.0195 (8)	0.0226 (8)	0.0140 (7)	-0.0018 (6)	0.0023 (6)	-0.0002 (6)
C10	0.0191 (8)	0.0203 (8)	0.0178 (7)	0.0003 (6)	0.0040 (6)	0.0022 (6)
C12	0.0184 (7)	0.0192 (8)	0.0135 (7)	0.0014 (6)	-0.0008 (6)	-0.0020 (6)
C11	0.0181 (7)	0.0156 (7)	0.0145 (7)	-0.0009 (6)	-0.0020 (6)	0.0012 (6)
C14	0.0190 (7)	0.0123 (7)	0.0168 (7)	0.0002 (6)	0.0000 (6)	-0.0016 (6)
C15	0.0229 (8)	0.0297 (9)	0.0222 (8)	0.0045 (7)	-0.0035 (7)	0.0015 (7)
C16	0.0216 (8)	0.0159 (8)	0.0199 (8)	0.0024 (6)	-0.0024 (6)	-0.0025 (6)
C17	0.0176 (8)	0.0204 (8)	0.0245 (8)	0.0008 (6)	-0.0006 (6)	-0.0025 (6)
C18	0.0198 (8)	0.0142 (7)	0.0220 (8)	0.0006 (6)	0.0030 (6)	-0.0030 (6)
C19	0.0216 (8)	0.0261 (9)	0.0252 (8)	0.0000 (7)	0.0051 (7)	0.0026 (7)

### Geometric parameters (Å, °)

S1—O4	1.4367 (11)	C5—C6	1.377 (3)
S1—O3	1.4402 (11)	C5—H5	0.9500
S1—N2	1.6454 (13)	C6—C7	1.404 (3)
S1—C11	1.7429 (15)	C6—H6	0.9500
F1—C4	1.352 (2)	C7—H7	0.98 (2)
F2—C7	1.19 (3)	C8—C9	1.409 (2)
F2—C5	1.75 (4)	C8—C13	1.409 (2)
O1—C1	1.2265 (19)	C9—C10	1.378 (2)
O2—C1	1.314 (2)	C9—H9	0.9500
O2—H32	0.846 (15)	C13—C12	1.380 (2)
N1—C8	1.357 (2)	C13—H13	0.9500
N1—H30B	0.863 (16)	C10—C11	1.395 (2)
N1—H30A	0.845 (16)	C10—H10	0.9500
N2—C14	1.386 (2)	C12—C11	1.395 (2)
N2—H31	0.831 (14)	C12—H12	0.9500
N4—C14	1.329 (2)	C15—C16	1.496 (2)
N4—C18	1.345 (2)	C15—H15B	0.9800
N3—C14	1.3408 (19)	C15—H15C	0.9800
N3—C16	1.353 (2)	C15—H15A	0.9800
C1—C2	1.495 (2)	C16—C17	1.386 (2)
C2—C3	1.390 (2)	C17—C18	1.385 (2)
C2—C7	1.398 (2)	C17—H17	0.9500
C3—C4	1.372 (2)	C18—C19	1.496 (2)
C3—H3	0.9500	C19—H19C	0.9800
C4—C5	1.379 (2)	C19—H19A	0.9800
C4—H4	0.9500	C19—H19B	0.9800
O4—S1—O3	117.79 (7)	C6—C7—H7	121.4 (12)
O4—S1—N2	109.83 (7)	N1—C8—C9	120.14 (15)
O3—S1—N2	102.70 (7)	N1—C8—C13	121.25 (15)
O4—S1—C11	108.72 (7)	C9—C8—C13	118.60 (15)
O3—S1—C11	109.17 (7)	C10—C9—C8	120.68 (15)



N2—S1—C11	108.19 (7)	C10—C9—H9	119.7
C7—F2—C5	109 (3)	C8—C9—H9	119.7
C1—O2—H32	110.4 (14)	C12—C13—C8	120.64 (14)
C8—N1—H30B	120.0 (16)	C12—C13—H13	119.7
C8—N1—H30A	121.6 (16)	C8—C13—H13	119.7
H30B—N1—H30A	118 (2)	C9—C10—C11	119.87 (14)
C14—N2—S1	125.23 (11)	C9—C10—H10	120.1
C14—N2—H31	117.5 (13)	C11—C10—H10	120.1
S1—N2—H31	116.1 (13)	C13—C12—C11	119.79 (14)
C14—N4—C18	116.05 (13)	C13—C12—H12	120.1
C14—N3—C16	116.26 (13)	C11—C12—H12	120.1
O1—C1—O2	124.22 (14)	C10—C11—C12	120.40 (14)
O1—C1—C2	121.33 (14)	C10—C11—S1	118.79 (12)
O2—C1—C2	114.45 (14)	C12—C11—S1	120.76 (12)
C3—C2—C7	120.71 (15)	N4—C14—N3	127.23 (14)
C3—C2—C1	117.65 (14)	N4—C14—N2	117.48 (13)
C7—C2—C1	121.63 (16)	N3—C14—N2	115.29 (13)
C4—C3—C2	118.25 (15)	C16—C15—H15B	109.5
C4—C3—H3	120.9	C16—C15—H15C	109.5
C2—C3—H3	120.9	H15B—C15—H15C	109.5
F1—C4—C3	118.53 (15)	C16—C15—H15A	109.5
F1—C4—C5	118.34 (15)	H15B—C15—H15A	109.5
C3—C4—C5	123.12 (16)	H15C—C15—H15A	109.5
C3—C4—H4	118.4	N3—C16—C17	120.58 (14)
C5—C4—H4	118.4	N3—C16—C15	116.75 (14)
C6—C5—C4	118.20 (15)	C17—C16—C15	122.67 (15)
C6—C5—F2	6 (4)	C18—C17—C16	118.41 (14)
C4—C5—F2	115.3 (12)	C18—C17—H17	120.8
C6—C5—H5	120.9	C16—C17—H17	120.8
C4—C5—H5	120.9	N4—C18—C17	121.46 (14)
F2—C5—H5	123.4	N4—C18—C19	116.08 (14)
C5—C6—C7	121.10 (17)	C17—C18—C19	122.45 (14)
C5—C6—H6	119.4	C18—C19—H19C	109.5
C7—C6—H6	119.4	C18—C19—H19A	109.5
F2—C7—C2	131 (3)	H19C—C19—H19A	109.5
F2—C7—C6	15 (3)	C18—C19—H19B	109.5
C2—C7—C6	118.60 (18)	H19C—C19—H19B	109.5
F2—C7—H7	109 (3)	H19A—C19—H19B	109.5
C2—C7—H7	119.9 (11)		
O4—S1—N2—C14	-52.01 (14)	N1—C8—C13—C12	-178.53 (16)
O3—S1—N2—C14	-178.12 (12)	C9—C8—C13—C12	0.9 (2)
C11—S1—N2—C14	66.52 (14)	C8—C9—C10—C11	-0.7 (3)
O1—C1—C2—C3	-5.2 (2)	C8—C13—C12—C11	-1.2 (2)
O2—C1—C2—C3	175.72 (14)	C9—C10—C11—C12	0.5 (2)
O1—C1—C2—C7	174.00 (15)	C9—C10—C11—S1	177.93 (13)
O2—C1—C2—C7	-5.1 (2)	C13—C12—C11—C10	0.5 (2)
C7—C2—C3—C4	-0.9 (2)	C13—C12—C11—S1	-176.89 (12)
C1—C2—C3—C4	178.26 (14)	O4—S1—C11—C10	-157.36 (12)
C2—C3—C4—F1	179.23 (14)	O3—S1—C11—C10	-27.65 (14)

C2—C3—C4—C5	0.6 (2)	N2—S1—C11—C10	83.41 (13)
F1—C4—C5—C6	-178.36 (15)	O4—S1—C11—C12	20.10 (14)
C3—C4—C5—C6	0.3 (2)	O3—S1—C11—C12	149.82 (12)
C3—C4—C5—F2	7 (5)	N2—S1—C11—C12	-99.12 (13)
C7—F2—C5—C6	104 (26)	C18—N4—C14—N3	-0.6 (2)
C7—F2—C5—C4	-15 (11)	C18—N4—C14—N2	-179.96 (13)
C4—C5—C6—C7	-0.8 (3)	C16—N3—C14—N4	0.7 (2)
F2—C5—C6—C7	-65 (18)	C16—N3—C14—N2	-179.91 (13)
C5—F2—C7—C2	17 (13)	S1—N2—C14—N4	-10.0 (2)
C5—F2—C7—C6	-23 (15)	S1—N2—C14—N3	170.53 (11)
C3—C2—C7—F2	-11 (8)	C14—N3—C16—C17	0.1 (2)
C1—C2—C7—F2	170 (8)	C14—N3—C16—C15	-179.85 (14)
C3—C2—C7—C6	0.5 (2)	N3—C16—C17—C18	-0.8 (2)
C1—C2—C7—C6	-178.72 (15)	C15—C16—C17—C18	179.08 (15)
C5—C6—C7—F2	146 (22)	C14—N4—C18—C17	-0.3 (2)
C5—C6—C7—C2	0.4 (3)	C14—N4—C18—C19	179.44 (14)
N1—C8—C9—C10	179.53 (17)	C16—C17—C18—N4	1.0 (2)
C13—C8—C9—C10	0.1 (2)	C16—C17—C18—C19	-178.76 (15)

#### Hydrogen-bond geometry (Å, °)

<i>D</i> —H··· <i>A</i>	<i>D</i> —H	H··· <i>A</i>	<i>D</i> ··· <i>A</i>	<i>D</i> —H··· <i>A</i>
N1—H30 <i>A</i> ···O4 <sup>ii</sup>	0.85 (2)	2.16 (2)	2.9788 (19)	163 (2)
N1—H30 <i>B</i> ···O3 <sup>i</sup>	0.86 (2)	2.29 (2)	3.1383 (19)	166 (2)
N2—H31···O1	0.83 (1)	1.98 (2)	2.8042 (17)	175 (2)
O2—H32···N3	0.85 (2)	1.83 (2)	2.6744 (17)	174 (2)

Symmetry codes: (i)  $-x+1/2, y-1/2, z$ ; (ii)  $-x, y-1/2, -z+1/2$ .

All esds (except the esd in the dihedral angle between two l.s. planes) are estimated using the full covariance matrix. The cell esds are taken into account individually in the estimation of esds in distances, angles and torsion angles; correlations between esds in cell parameters are only used when they are defined by crystal symmetry. An approximate (isotropic) treatment of cell esds is used for estimating esds involving l.s. planes.

$D-H\cdots A$	$D-H$	$H\cdots A$	$D\cdots A$	$D-H\cdots A$
$N1-H30A\cdots O4^{ii}$	0.85 (2)	2.16 (2)	2.9788 (19)	163 (2)
$N1-H30B\cdots O3^i$	0.86 (2)	2.29 (2)	3.1383 (19)	166 (2)
$N2-H31\cdots O1$	0.83 (1)	1.98 (2)	2.8042 (17)	175 (2)
$O2-H32\cdots N3$	0.85 (2)	1.83 (2)	2.6744 (17)	174 (2)

Symmetry codes: (i)  $-x+1/2, y-1/2, z$ ; (ii)  $-x, y-1/2, -z+1/2$ .

All esds (except the esd in the dihedral angle between two l.s. planes) are estimated using the full covariance matrix. The cell esds are taken into account individually in the estimation of esds in distances, angles and torsion angles; correlations between esds in cell parameters are only used when they are defined by crystal symmetry. An approximate (isotropic) treatment of cell esds is used for estimating esds involving l.s. planes.

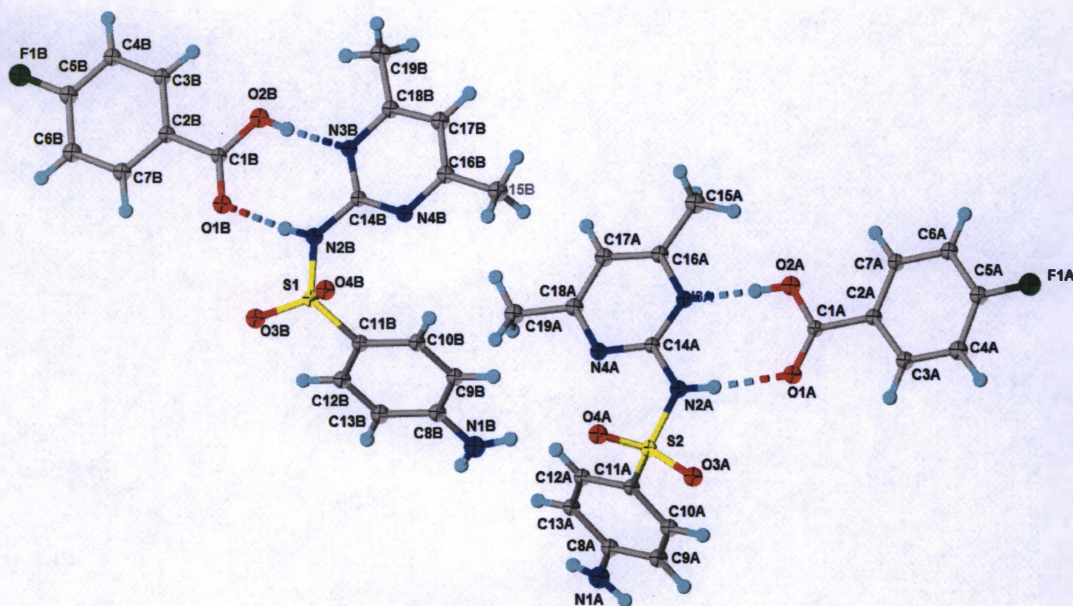


Figure S.10: Crystal Structure of the Cocrystal of Sulfamethazine and *p*-Fluorobenzoic Acid Showing Thermal Parameters (50% Thermal Ellipsoids) and Hydrogen Bonding.

## Data collection

Bruker APEXII CCD diffractometer	7088 independent reflections
Radiation source: fine-focus sealed tube	6362 reflections with $I > 2\sigma(I)$
Detector resolution: 8.33 pixels $\text{mm}^{-1}$	$R_{\text{int}} = 0.038$
phi and $\omega$ scans	$\theta_{\text{max}} = 68.3^\circ$ , $\theta_{\text{min}} = 2.8^\circ$
Absorption correction: multi-scan SADABS2014/7, Bruker AXS	$h = -17 \ 18$
$T_{\text{min}} = 0.594$ , $T_{\text{max}} = 0.753$	$k = -16 \ 16$
57694 measured reflections	$l = -21 \ 21$

## Refinement

Refinement on $F^2$	Hydrogen site location: mixed
Least-squares matrix: full	H atoms treated by a mixture of independent and constrained refinement
$R[F^2 > 2\sigma(F^2)] = 0.058$	$w = 1/[\sigma^2(F_o^2) + (0.0698P)^2 + 7.8397P]$ where $P = (F_o^2 + 2F_c^2)/3$
$wR(F^2) = 0.151$	$(\Delta/\sigma)_{\text{max}} = 0.001$
$S = 1.05$	$\Delta\rho_{\text{max}} = 0.74 \text{ e } \text{\AA}^{-3}$
7088 reflections	$\Delta\rho_{\text{min}} = -1.05 \text{ e } \text{\AA}^{-3}$
269 parameters	Extinction correction: none
8 restraints	
0 constraints	

## Fractional atomic coordinates and isotropic or equivalent isotropic displacement parameters ( $\text{\AA}^2$ )

	x	y	z	$U_{\text{iso}}^*/U_{\text{eq}}$
S1	0.04732 (4)	0.11025 (4)	0.23081 (3)	0.01803 (16)*
S2	0.45268 (4)	-0.38975 (4)	0.23080 (3)	0.01805 (16)*
F1A	1.01267 (11)	-0.36075 (13)	-0.04296 (10)	0.0317 (4)*
F1B	-0.51272 (11)	0.13919 (13)	-0.04296 (10)	0.0319 (4)*
O1A	0.64633 (12)	-0.40921 (14)	0.09953 (10)	0.0222 (4)*
O2A	0.61424 (12)	-0.38731 (14)	-0.02072 (11)	0.0237 (4)*
H32A	0.5615 (16)	-0.380 (4)	-0.006 (3)	0.081 (17)*
O3A	0.53567 (12)	-0.39352 (14)	0.26456 (10)	0.0236 (4)*
O4A	0.39860 (12)	-0.30775 (14)	0.24519 (10)	0.0240 (4)*
O1B	-0.14634 (12)	0.09072 (14)	0.09946 (10)	0.0226 (4)*
O2B	-0.11424 (13)	0.11267 (14)	-0.02068 (11)	0.0238 (4)*
H32B	-0.0616 (16)	0.119 (4)	-0.006 (3)	0.088 (18)*
O3B	-0.03559 (12)	0.10651 (14)	0.26451 (10)	0.0239 (4)*
O4B	0.10143 (12)	0.19230 (14)	0.24513 (11)	0.0243 (4)*
N1B	0.22428 (17)	-0.25725 (19)	0.29612 (14)	0.0297 (5)*
H30D	0.191 (2)	-0.304 (2)	0.308 (2)	0.056 (12)*
H30C	0.2760 (14)	-0.264 (3)	0.278 (2)	0.042 (10)*
N2B	0.02525 (14)	0.10854 (16)	0.14094 (12)	0.0195 (5)*
H31B	-0.0287 (13)	0.102 (3)	0.131 (2)	0.035 (9)*
N1A	0.27581 (17)	-0.75726 (19)	0.29606 (14)	0.0298 (5)*

H30B	0.2240 (14)	-0.765 (3)	0.278 (2)	0.042 (10)*
H30A	0.308 (2)	-0.804 (2)	0.310 (2)	0.055 (12)*
N2A	0.47475 (14)	-0.39150 (16)	0.14090 (12)	0.0193 (5)*
H31A	0.5288 (13)	-0.399 (2)	0.1308 (19)	0.032 (9)*
N3A	0.45096 (14)	-0.37791 (15)	0.01532 (12)	0.0182 (4)*
N4A	0.33355 (14)	-0.37975 (16)	0.10053 (12)	0.0193 (5)*
N3B	0.04901 (14)	0.12213 (15)	0.01528 (12)	0.0180 (4)*
N4B	0.16646 (14)	0.12034 (16)	0.10052 (12)	0.0190 (4)*
C1A	0.66832 (16)	-0.39763 (18)	0.03436 (14)	0.0177 (5)*
C2A	0.75985 (16)	-0.39266 (18)	0.01212 (14)	0.0190 (5)*
C3A	0.82315 (17)	-0.4090 (2)	0.06551 (15)	0.0219 (5)*
H3A	0.8074	-0.4266	0.1147	0.026*
C4A	0.90907 (18)	-0.3996 (2)	0.04720 (16)	0.0247 (6)*
H4A	0.9526	-0.4111	0.0831	0.030*
C5A	0.92951 (17)	-0.3730 (2)	-0.02499 (15)	0.0226 (6)*
C6A	0.86855 (17)	-0.35766 (19)	-0.07954 (15)	0.0215 (5)*
H6A	0.8848	-0.3402	-0.1287	0.026*
C7A	0.78299 (16)	-0.36841 (19)	-0.06066 (14)	0.0192 (5)*
H7A	0.7399	-0.3592	-0.0974	0.023*
C8A	0.31563 (17)	-0.67192 (19)	0.28131 (15)	0.0211 (5)*
C9A	0.40371 (17)	-0.6609 (2)	0.29408 (15)	0.0231 (6)*
H9A	0.4358	-0.7137	0.3134	0.028*
C10A	0.44420 (17)	-0.57469 (19)	0.27898 (14)	0.0212 (5)*
H10A	0.5041	-0.5687	0.2872	0.025*
C11A	0.39768 (16)	-0.49607 (18)	0.25169 (14)	0.0181 (5)*
C12A	0.30928 (16)	-0.50424 (19)	0.24055 (14)	0.0187 (5)*
H12A	0.2772	-0.4504	0.2230	0.022*
C13A	0.26902 (17)	-0.59121 (19)	0.25527 (14)	0.0199 (5)*
H13A	0.2090	-0.5968	0.2477	0.024*
C14A	0.41617 (16)	-0.38287 (18)	0.08370 (14)	0.0172 (5)*
C15A	0.43404 (19)	-0.3602 (2)	-0.11826 (16)	0.0280 (6)*
H15A	0.4961	-0.3698	-0.1151	0.042*
H15B	0.4220	-0.2963	-0.1396	0.042*
H15C	0.4089	-0.4105	-0.1501	0.042*
C16A	0.39601 (17)	-0.36649 (19)	-0.04214 (15)	0.0203 (5)*
C17A	0.30858 (17)	-0.3615 (2)	-0.02927 (15)	0.0227 (6)*
H17A	0.2696	-0.3533	-0.0695	0.027*
C18A	0.27889 (17)	-0.3688 (2)	0.04337 (15)	0.0215 (5)*
C19A	0.18561 (18)	-0.3653 (2)	0.06223 (16)	0.0267 (6)*
H19D	0.1624	-0.4313	0.0630	0.040*
H19E	0.1551	-0.3269	0.0247	0.040*
H19F	0.1782	-0.3355	0.1113	0.040*
C1B	-0.16827 (16)	0.10240 (18)	0.03438 (14)	0.0175 (5)*
C2B	-0.25997 (16)	0.10734 (18)	0.01214 (14)	0.0190 (5)*
C3B	-0.28294 (17)	0.13168 (19)	-0.06069 (14)	0.0195 (5)*
H3B	-0.2399	0.1410	-0.0973	0.023*
C4B	-0.36857 (17)	0.14222 (19)	-0.07947 (15)	0.0213 (5)*
H4B	-0.3850	0.1595	-0.1287	0.026*
C5B	-0.42947 (17)	0.1270 (2)	-0.02504 (15)	0.0229 (6)*

C6B	-0.40910 (18)	0.1004 (2)	0.04721 (16)	0.0244 (6)*
H6B	-0.4526	0.0890	0.0831	0.029*
C7B	-0.32314 (17)	0.0911 (2)	0.06558 (15)	0.0218 (5)*
H7B	-0.3072	0.0735	0.1148	0.026*
C8B	0.18433 (17)	-0.1720 (2)	0.28126 (15)	0.0212 (5)*
C9B	0.23099 (17)	-0.09117 (19)	0.25532 (14)	0.0197 (5)*
H9B	0.2910	-0.0967	0.2479	0.024*
C10B	0.19063 (16)	-0.00437 (19)	0.24054 (14)	0.0190 (5)*
H10B	0.2226	0.0495	0.2229	0.023*
C11B	0.10229 (16)	0.00386 (18)	0.25166 (14)	0.0180 (5)*
C12B	0.05579 (17)	-0.07480 (19)	0.27892 (14)	0.0210 (5)*
H12B	-0.0041	-0.0688	0.2870	0.025*
C13B	0.09626 (17)	-0.1609 (2)	0.29417 (15)	0.0231 (6)*
H13B	0.0642	-0.2136	0.3137	0.028*
C14B	0.08388 (16)	0.11715 (18)	0.08366 (14)	0.0173 (5)*
C15B	0.31435 (18)	0.1347 (2)	0.06223 (16)	0.0266 (6)*
H15D	0.3221	0.1669	0.1104	0.040*
H15E	0.3451	0.1708	0.0236	0.040*
H15F	0.3370	0.0685	0.0650	0.040*
C16B	0.22101 (17)	0.1313 (2)	0.04336 (15)	0.0213 (5)*
C17B	0.19142 (17)	0.1385 (2)	-0.02925 (15)	0.0226 (5)*
H17B	0.2303	0.1466	-0.0694	0.027*
C18B	0.10395 (17)	0.13345 (19)	-0.04215 (15)	0.0203 (5)*
C19B	0.06584 (19)	0.1399 (2)	-0.11820 (16)	0.0277 (6)*
H19A	0.0044	0.1258	-0.1156	0.042*
H19B	0.0938	0.0928	-0.1510	0.042*
H19C	0.0743	0.2053	-0.1380	0.042*

Geometric parameters (Å, °)

S1—O3B	1.431 (2)	C10A—C11A	1.394 (4)
S1—O4B	1.436 (2)	C10A—H10A	0.9500
S1—N2B	1.650 (2)	C11A—C12A	1.399 (3)
S1—C11B	1.742 (3)	C12A—C13A	1.381 (4)
S2—O3A	1.431 (2)	C12A—H12A	0.9500
S2—O4A	1.436 (2)	C13A—H13A	0.9500
S2—N2A	1.652 (2)	C15A—C16A	1.494 (4)
S2—C11A	1.742 (3)	C15A—H15A	0.9800
F1A—C5A	1.349 (3)	C15A—H15B	0.9800
F1B—C5B	1.349 (3)	C15A—H15C	0.9800
O1A—C1A	1.231 (3)	C16A—C17A	1.386 (4)
O2A—C1A	1.307 (3)	C17A—C18A	1.389 (4)
O2A—H32A	0.870 (19)	C17A—H17A	0.9500
O1B—C1B	1.228 (3)	C18A—C19A	1.496 (4)
O2B—C1B	1.308 (3)	C19A—H19D	0.9800
O2B—H32B	0.867 (19)	C19A—H19E	0.9800
N1B—C8B	1.359 (4)	C19A—H19F	0.9800
N1B—H30D	0.861 (19)	C1B—C2B	1.487 (3)
N1B—H30C	0.877 (18)	C2B—C7B	1.395 (4)
N2B—C14B	1.383 (3)	C2B—C3B	1.397 (4)

N2B—H31B	0.868 (18)	C3B—C4B	1.386 (4)
N1A—C8A	1.358 (4)	C3B—H3B	0.9500
N1A—H30B	0.876 (18)	C4B—C5B	1.381 (4)
N1A—H30A	0.859 (19)	C4B—H4B	0.9500
N2A—C14A	1.380 (3)	C5B—C6B	1.385 (4)
N2A—H31A	0.869 (18)	C6B—C7B	1.388 (4)
N3A—C14A	1.345 (3)	C6B—H6B	0.9500
N3A—C16A	1.350 (3)	C7B—H7B	0.9500
N4A—C14A	1.326 (3)	C8B—C13B	1.403 (4)
N4A—C18A	1.342 (3)	C8B—C9B	1.412 (4)
N3B—C14B	1.344 (3)	C9B—C10B	1.379 (4)
N3B—C18B	1.352 (3)	C9B—H9B	0.9500
N4B—C14B	1.325 (3)	C10B—C11B	1.398 (3)
N4B—C16B	1.343 (3)	C10B—H10B	0.9500
C1A—C2A	1.486 (3)	C11B—C12B	1.395 (4)
C2A—C3A	1.394 (4)	C12B—C13B	1.374 (4)
C2A—C7A	1.397 (4)	C12B—H12B	0.9500
C3A—C4A	1.388 (4)	C13B—H13B	0.9500
C3A—H3A	0.9500	C15B—C16B	1.496 (4)
C4A—C5A	1.385 (4)	C15B—H15D	0.9800
C4A—H4A	0.9500	C15B—H15E	0.9800
C5A—C6A	1.381 (4)	C15B—H15F	0.9800
C6A—C7A	1.387 (4)	C16B—C17B	1.386 (4)
C6A—H6A	0.9500	C17B—C18B	1.386 (4)
C7A—H7A	0.9500	C17B—H17B	0.9500
C8A—C9A	1.402 (4)	C18B—C19B	1.492 (4)
C8A—C13A	1.410 (4)	C19B—H19A	0.9800
C9A—C10A	1.375 (4)	C19B—H19B	0.9800
C9A—H9A	0.9500	C19B—H19C	0.9800
O3B—S1—O4B	119.01 (11)	N3A—C16A—C17A	120.2 (2)
O3B—S1—N2B	103.04 (11)	N3A—C16A—C15A	116.9 (2)
O4B—S1—N2B	107.96 (11)	C17A—C16A—C15A	122.9 (2)
O3B—S1—C11B	108.93 (12)	C16A—C17A—C18A	118.9 (2)
O4B—S1—C11B	109.71 (12)	C16A—C17A—H17A	120.6
N2B—S1—C11B	107.48 (12)	C18A—C17A—H17A	120.6
O3A—S2—O4A	119.00 (11)	N4A—C18A—C17A	120.9 (2)
O3A—S2—N2A	102.92 (11)	N4A—C18A—C19A	116.6 (2)
O4A—S2—N2A	108.12 (11)	C17A—C18A—C19A	122.5 (2)
O3A—S2—C11A	108.94 (12)	C18A—C19A—H19D	109.5
O4A—S2—C11A	109.60 (12)	C18A—C19A—H19E	109.5
N2A—S2—C11A	107.58 (12)	H19D—C19A—H19E	109.5
C1A—O2A—H32A	113 (3)	C18A—C19A—H19F	109.5
C1B—O2B—H32B	113 (4)	H19D—C19A—H19F	109.5
C8B—N1B—H30D	115 (3)	H19E—C19A—H19F	109.5
C8B—N1B—H30C	116 (3)	O1B—C1B—O2B	123.7 (2)
H30D—N1B—H30C	125 (4)	O1B—C1B—C2B	121.9 (2)
C14B—N2B—S1	126.08 (19)	O2B—C1B—C2B	114.4 (2)
C14B—N2B—H31B	120 (2)	C7B—C2B—C3B	120.1 (2)
S1—N2B—H31B	114 (2)	C7B—C2B—C1B	119.3 (2)



C8A—N1A—H30B	118 (3)	C3B—C2B—C1B	120.5 (2)
C8A—N1A—H30A	116 (3)	C4B—C3B—C2B	120.0 (2)
H30B—N1A—H30A	124 (4)	C4B—C3B—H3B	120.0
C14A—N2A—S2	125.99 (19)	C2B—C3B—H3B	120.0
C14A—N2A—H31A	120 (2)	C5B—C4B—C3B	118.5 (3)
S2—N2A—H31A	114 (2)	C5B—C4B—H4B	120.8
C14A—N3A—C16A	116.5 (2)	C3B—C4B—H4B	120.8
C14A—N4A—C18A	116.5 (2)	F1B—C5B—C4B	118.5 (2)
C14B—N3B—C18B	116.5 (2)	F1B—C5B—C6B	118.4 (2)
C14B—N4B—C16B	116.5 (2)	C4B—C5B—C6B	123.1 (3)
O1A—C1A—O2A	123.6 (2)	C5B—C6B—C7B	117.9 (3)
O1A—C1A—C2A	122.1 (2)	C5B—C6B—H6B	121.0
O2A—C1A—C2A	114.3 (2)	C7B—C6B—H6B	121.0
C3A—C2A—C7A	119.9 (2)	C6B—C7B—C2B	120.4 (3)
C3A—C2A—C1A	119.3 (2)	C6B—C7B—H7B	119.8
C7A—C2A—C1A	120.8 (2)	C2B—C7B—H7B	119.8
C4A—C3A—C2A	120.4 (3)	N1B—C8B—C13B	120.8 (2)
C4A—C3A—H3A	119.8	N1B—C8B—C9B	120.8 (2)
C2A—C3A—H3A	119.8	C13B—C8B—C9B	118.4 (2)
C5A—C4A—C3A	118.1 (3)	C10B—C9B—C8B	120.9 (2)
C5A—C4A—H4A	121.0	C10B—C9B—H9B	119.5
C3A—C4A—H4A	121.0	C8B—C9B—H9B	119.5
F1A—C5A—C6A	118.3 (2)	C9B—C10B—C11B	119.6 (2)
F1A—C5A—C4A	118.7 (2)	C9B—C10B—H10B	120.2
C6A—C5A—C4A	123.0 (3)	C11B—C10B—H10B	120.2
C5A—C6A—C7A	118.2 (3)	C12B—C11B—C10B	120.0 (2)
C5A—C6A—H6A	120.9	C12B—C11B—S1	118.38 (19)
C7A—C6A—H6A	120.9	C10B—C11B—S1	121.57 (19)
C6A—C7A—C2A	120.3 (2)	C13B—C12B—C11B	120.3 (2)
C6A—C7A—H7A	119.8	C13B—C12B—H12B	119.9
C2A—C7A—H7A	119.8	C11B—C12B—H12B	119.9
N1A—C8A—C9A	120.8 (2)	C12B—C13B—C8B	120.8 (3)
N1A—C8A—C13A	120.9 (2)	C12B—C13B—H13B	119.6
C9A—C8A—C13A	118.3 (2)	C8B—C13B—H13B	119.6
C10A—C9A—C8A	120.9 (3)	N4B—C14B—N3B	126.9 (2)
C10A—C9A—H9A	119.6	N4B—C14B—N2B	118.5 (2)
C8A—C9A—H9A	119.6	N3B—C14B—N2B	114.6 (2)
C9A—C10A—C11A	120.2 (2)	C16B—C15B—H15D	109.5
C9A—C10A—H10A	119.9	C16B—C15B—H15E	109.5
C11A—C10A—H10A	119.9	H15D—C15B—H15E	109.5
C10A—C11A—C12A	120.1 (2)	C16B—C15B—H15F	109.5
C10A—C11A—S2	118.36 (19)	H15D—C15B—H15F	109.5
C12A—C11A—S2	121.58 (19)	H15E—C15B—H15F	109.5
C13A—C12A—C11A	119.5 (2)	N4B—C16B—C17B	121.1 (2)
C13A—C12A—H12A	120.3	N4B—C16B—C15B	116.7 (2)
C11A—C12A—H12A	120.3	C17B—C16B—C15B	122.3 (2)
C12A—C13A—C8A	121.0 (2)	C16B—C17B—C18B	118.7 (2)
C12A—C13A—H13A	119.5	C16B—C17B—H17B	120.6
C8A—C13A—H13A	119.5	C18B—C17B—H17B	120.6

N4A—C14A—N3A	126.9 (2)	N3B—C18B—C17B	120.3 (2)
N4A—C14A—N2A	118.5 (2)	N3B—C18B—C19B	116.9 (2)
N3A—C14A—N2A	114.6 (2)	C17B—C18B—C19B	122.8 (2)
C16A—C15A—H15A	109.5	C18B—C19B—H19A	109.5
C16A—C15A—H15B	109.5	C18B—C19B—H19B	109.5
H15A—C15A—H15B	109.5	H19A—C19B—H19B	109.5
C16A—C15A—H15C	109.5	C18B—C19B—H19C	109.5
H15A—C15A—H15C	109.5	H19A—C19B—H19C	109.5
H15B—C15A—H15C	109.5	H19B—C19B—H19C	109.5
O3B—S1—N2B—C14B	175.6 (2)	C14A—N4A—C18A— C19A	180.0 (2)
O4B—S1—N2B—C14B	48.9 (2)	C16A—C17A—C18A— N4A	0.5 (4)
C11B—S1—N2B—C14B	-69.4 (2)	C16A—C17A—C18A— C19A	-179.3 (3)
O3A—S2—N2A—C14A	-175.6 (2)	O1B—C1B—C2B—C7B	-4.9 (4)
O4A—S2—N2A—C14A	-48.8 (2)	O2B—C1B—C2B—C7B	175.9 (2)
C11A—S2—N2A—C14A	69.4 (2)	O1B—C1B—C2B—C3B	172.6 (2)
O1A—C1A—C2A—C3A	5.0 (4)	O2B—C1B—C2B—C3B	-6.6 (3)
O2A—C1A—C2A—C3A	-175.9 (2)	C7B—C2B—C3B—C4B	1.7 (4)
O1A—C1A—C2A—C7A	-172.6 (2)	C1B—C2B—C3B—C4B	-175.8 (2)
O2A—C1A—C2A—C7A	6.5 (3)	C2B—C3B—C4B—C5B	-0.7 (4)
C7A—C2A—C3A—C4A	1.1 (4)	C3B—C4B—C5B—F1B	178.7 (2)
C1A—C2A—C3A—C4A	-176.5 (2)	C3B—C4B—C5B—C6B	-0.9 (4)
C2A—C3A—C4A—C5A	0.5 (4)	F1B—C5B—C6B—C7B	-178.1 (2)
C3A—C4A—C5A—F1A	178.0 (2)	C4B—C5B—C6B—C7B	1.6 (4)
C3A—C4A—C5A—C6A	-1.5 (4)	C5B—C6B—C7B—C2B	-0.6 (4)
F1A—C5A—C6A—C7A	-178.7 (2)	C3B—C2B—C7B—C6B	-1.1 (4)
C4A—C5A—C6A—C7A	0.8 (4)	C1B—C2B—C7B—C6B	176.5 (2)
C5A—C6A—C7A—C2A	1.0 (4)	N1B—C8B—C9B—C10B	-179.7 (2)
C3A—C2A—C7A—C6A	-1.9 (4)	C13B—C8B—C9B—C10B	-2.2 (4)
C1A—C2A—C7A—C6A	175.7 (2)	C8B—C9B—C10B—C11B	0.2 (4)
N1A—C8A—C9A—C10A	179.8 (3)	C9B—C10B—C11B—C12B	1.3 (4)
C13A—C8A—C9A—C10A	-2.4 (4)	C9B—C10B—C11B—S1	-177.7 (2)
C8A—C9A—C10A—C11A	1.0 (4)	O3B—S1—C11B—C12B	15.4 (2)
C9A—C10A—C11A— C12A	0.9 (4)	O4B—S1—C11B—C12B	147.3 (2)
C9A—C10A—C11A—S2	-178.1 (2)	N2B—S1—C11B—C12B	-95.6 (2)
O3A—S2—C11A—C10A	-15.5 (2)	O3B—S1—C11B—C10B	-165.6 (2)
O4A—S2—C11A—C10A	-147.2 (2)	O4B—S1—C11B—C10B	-33.8 (2)
N2A—S2—C11A—C10A	95.4 (2)	N2B—S1—C11B—C10B	83.4 (2)
O3A—S2—C11A—C12A	165.6 (2)	C10B—C11B—C12B— C13B	-0.7 (4)
O4A—S2—C11A—C12A	33.8 (2)	S1—C11B—C12B—C13B	178.2 (2)
N2A—S2—C11A—C12A	-83.5 (2)	C11B—C12B—C13B—C8B	-1.3 (4)
C10A—C11A—C12A— C13A	-1.4 (4)	N1B—C8B—C13B—C12B	-179.8 (3)
S2—C11A—C12A—C13A	177.5 (2)	C9B—C8B—C13B—C12B	2.7 (4)
C11A—C12A—C13A— C8A	0.0 (4)	C16B—N4B—C14B—N3B	1.2 (4)

N1A—C8A—C13A—C12A	179.7 (2)	C16B—N4B—C14B—N2B	-178.3 (2)
C9A—C8A—C13A—C12A	1.9 (4)	C18B—N3B—C14B—N4B	-1.4 (4)
C18A—N4A—C14A—N3A	-1.2 (4)	C18B—N3B—C14B—N2B	178.1 (2)
C18A—N4A—C14A—N2A	178.3 (2)	S1—N2B—C14B—N4B	5.1 (3)
C16A—N3A—C14A—N4A	1.5 (4)	S1—N2B—C14B—N3B	-174.41 (18)
C16A—N3A—C14A—N2A	-178.1 (2)	C14B—N4B—C16B— C17B	-0.2 (4)
S2—N2A—C14A—N4A	-5.2 (3)	C14B—N4B—C16B— C15B	-179.8 (2)
S2—N2A—C14A—N3A	174.40 (18)	N4B—C16B—C17B— C18B	-0.4 (4)
C14A—N3A—C16A— C17A	-0.7 (4)	C15B—C16B—C17B— C18B	179.2 (3)
C14A—N3A—C16A— C15A	179.6 (2)	C14B—N3B—C18B— C17B	0.6 (4)
N3A—C16A—C17A— C18A	-0.2 (4)	C14B—N3B—C18B— C19B	-179.5 (2)
C15A—C16A—C17A— C18A	179.5 (3)	C16B—C17B—C18B— N3B	0.2 (4)
C14A—N4A—C18A— C17A	0.2 (4)	C16B—C17B—C18B— C19B	-179.7 (3)

#### Hydrogen-bond geometry (Å, °)

<i>D</i> —H··· <i>A</i>	<i>D</i> —H	H··· <i>A</i>	<i>D</i> ··· <i>A</i>	<i>D</i> —H··· <i>A</i>
N1A—H30A···O1A <sup>iii</sup>	0.86 (2)	2.29 (3)	3.064 (3)	149 (4)
N1A—H30B···O4B <sup>ii</sup>	0.88 (2)	2.09 (2)	2.954 (3)	170 (4)
N1B—H30C···O4A	0.88 (2)	2.09 (2)	2.956 (3)	168 (4)
N1B—H30D···O1B <sup>i</sup>	0.86 (2)	2.32 (3)	3.068 (3)	146 (4)
N2A—H31A···O1A	0.87 (2)	1.93 (2)	2.792 (3)	175 (3)
N2B—H31B···O1B	0.87 (2)	1.93 (2)	2.790 (3)	175 (4)
O2A—H32A···N3A	0.87 (2)	1.77 (2)	2.634 (3)	172 (5)
O2B—H32B···N3B	0.87 (2)	1.77 (2)	2.631 (3)	173 (5)

Symmetry codes: (i)  $-x, y-1/2, -z+1/2$ ; (ii)  $x, y-1, z$ ; (iii)  $-x+1, y-1/2, -z+1/2$ .

All esds (except the esd in the dihedral angle between two l.s. planes) are estimated using the full covariance matrix. The cell esds are taken into account individually in the estimation of esds in distances, angles and torsion angles; correlations between esds in cell parameters are only used when they are defined by crystal symmetry. An approximate (isotropic) treatment of cell esds is used for estimating esds involving l.s. planes.

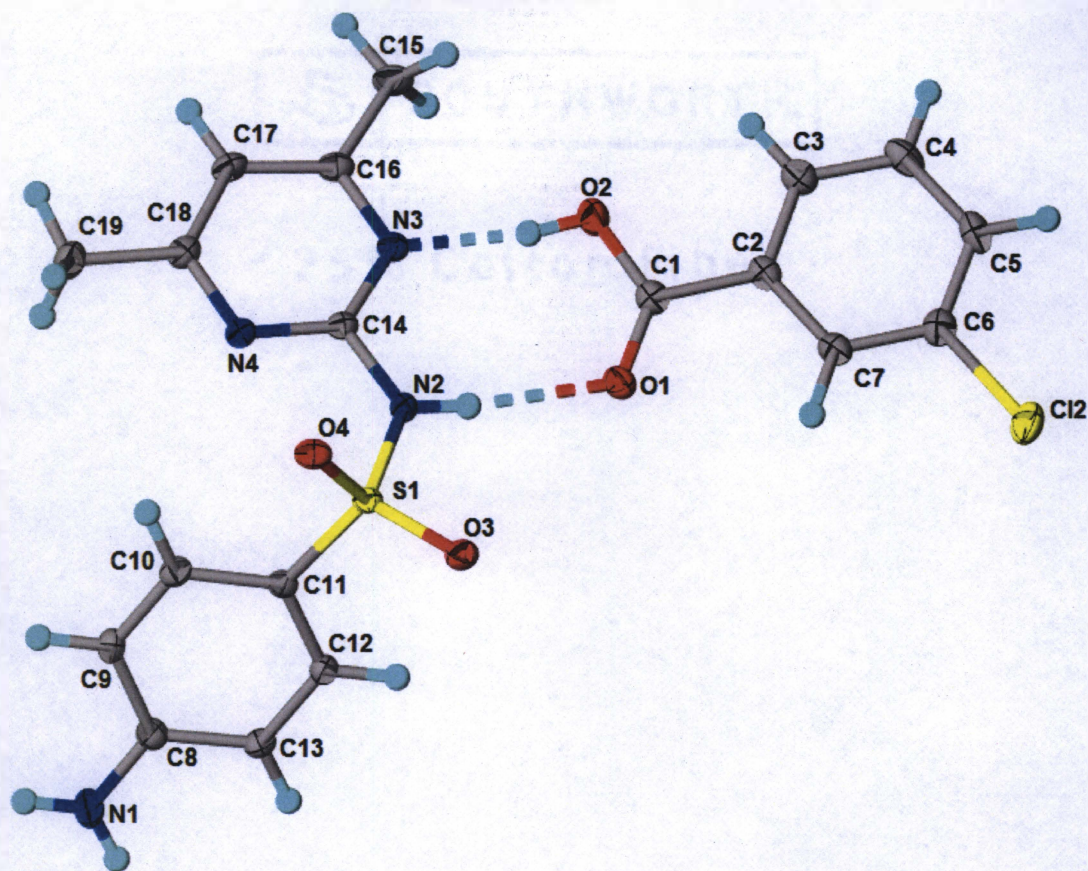


Figure S.11: Crystal Structure of the Cocrystal of Sulfamethazine and *m*-Chlorobenzoic Acid Showing Thermal Parameters (50% Thermal Ellipsoids) and Hydrogen Bonding.

*Crystal data*

$C_{12}H_{14}N_4O_2S \cdot C_7H_5ClO_2$

$M_r = 434.89$

Monoclinic,  $P2_1/c$

$a = 8.2042(4) \text{ \AA}$

$b = 28.2960(11) \text{ \AA}$

$c = 9.6571(4) \text{ \AA}$

$\beta = 114.825(2)^\circ$

$V = 2034.70(16) \text{ \AA}^3$

$Z = 4$

$F(000) = 904$

$D_x = 1.420 \text{ Mg m}^{-3}$

Melting point: 446–448 K

Cu  $K\alpha$  radiation,  $\lambda = 1.54178 \text{ \AA}$

Cell parameters from 9365 reflections

$\theta = 3.1\text{--}68.2^\circ$

$\mu = 2.92 \text{ mm}^{-1}$

$T = 100 \text{ K}$

Plates, colourless

$0.40 \times 0.30 \times 0.18 \text{ mm}$

### Data collection

Bruker APEXII CCD diffractometer	3707 independent reflections
Radiation source: fine-focus sealed tube	3614 reflections with $I > 2\sigma(I)$
Detector resolution: 8.33 pixels $\text{mm}^{-1}$	$R_{\text{int}} = 0.029$
phi and $\omega$ scans	$\theta_{\text{max}} = 68.2^\circ$ , $\theta_{\text{min}} = 3.1^\circ$
Absorption correction: multi-scan SADABS2014/7, Bruker AXS	$h = -9 \quad 9$
$T_{\text{min}} = 0.571$ , $T_{\text{max}} = 0.753$	$k = -34 \quad 33$
30572 measured reflections	$l = -11 \quad 11$

### Refinement

Refinement on $F^2$	Hydrogen site location: mixed
Least-squares matrix: full	H atoms treated by a mixture of independent and constrained refinement
$R[F^2 > 2\sigma(F^2)] = 0.031$	$w = 1/[\sigma^2(F_o^2) + (0.0335P)^2 + 1.4222P]$
$wR(F^2) = 0.079$	where $P = (F_o^2 + 2F_c^2)/3$
$S = 1.09$	$(\Delta/\sigma)_{\text{max}} = 0.001$
3707 reflections	$\Delta\rho_{\text{max}} = 0.35 \text{ e } \text{\AA}^{-3}$
280 parameters	$\Delta\rho_{\text{min}} = -0.40 \text{ e } \text{\AA}^{-3}$
4 restraints	Extinction correction: none
0 constraints	

### Fractional atomic coordinates and isotropic or equivalent isotropic displacement parameters ( $\text{\AA}^2$ )

	<i>x</i>	<i>y</i>	<i>z</i>	$U_{\text{iso}}^*/U_{\text{eq}}$
S1	0.53092 (5)	0.66026 (2)	0.62097 (4)	0.01646 (10)
Cl2	0.95600 (6)	0.41356 (2)	1.20135 (5)	0.03151 (12)
O3	0.56883 (14)	0.64535 (4)	0.77332 (12)	0.0225 (2)
O4	0.64270 (14)	0.69622 (4)	0.59967 (12)	0.0213 (2)
O1	0.66804 (15)	0.52484 (4)	0.71434 (13)	0.0247 (3)
O2	0.75909 (18)	0.49458 (4)	0.54405 (13)	0.0301 (3)
H32	0.706 (3)	0.5195 (7)	0.491 (3)	0.055 (7)*
N2	0.55233 (18)	0.61118 (5)	0.53860 (15)	0.0188 (3)
H31	0.583 (3)	0.5869 (6)	0.596 (2)	0.030 (5)*
N4	0.48834 (17)	0.64515 (5)	0.30188 (14)	0.0189 (3)
N3	0.61073 (17)	0.56739 (4)	0.36413 (14)	0.0186 (3)
N1	-0.2082 (2)	0.73395 (6)	0.37111 (19)	0.0312 (3)
H30A	-0.278 (3)	0.7234 (7)	0.409 (2)	0.030 (5)*
H30B	-0.242 (3)	0.7542 (7)	0.300 (2)	0.032 (5)*
C14	0.5504 (2)	0.60823 (5)	0.39441 (17)	0.0171 (3)
C18	0.4864 (2)	0.64040 (6)	0.16257 (18)	0.0210 (3)
C13	0.0175 (2)	0.68102 (6)	0.53736 (17)	0.0203 (3)
H13	-0.0630	0.6697	0.5774	0.024*

C12	0.1900 (2)	0.66354 (5)	0.59296 (17)	0.0186 (3)
H12	0.2283	0.6405	0.6719	0.022*
C7	0.8551 (2)	0.45280 (5)	0.92326 (19)	0.0217 (3)
H7	0.8016	0.4769	0.9589	0.026*
C10	0.2520 (2)	0.71267 (5)	0.41607 (17)	0.0189 (3)
H10	0.3319	0.7230	0.3740	0.023*
C6	0.9449 (2)	0.41564 (6)	1.01727 (19)	0.0238 (3)
C16	0.6085 (2)	0.56308 (6)	0.22427 (18)	0.0211 (3)
C17	0.5463 (2)	0.59944 (6)	0.11988 (18)	0.0224 (3)
H17	0.5446	0.5965	0.0213	0.027*
C11	0.3087 (2)	0.67945 (5)	0.53381 (17)	0.0167 (3)
C9	0.0801 (2)	0.73048 (5)	0.36105 (18)	0.0205 (3)
H9	0.0422	0.7531	0.2811	0.025*
C5	1.0241 (2)	0.38004 (6)	0.9683 (2)	0.0266 (4)
H5	1.0854	0.3548	1.0344	0.032*
C3	0.9229 (2)	0.41876 (6)	0.72417 (19)	0.0238 (3)
H3	0.9152	0.4197	0.6233	0.029*
C19	0.4142 (2)	0.68135 (6)	0.05641 (19)	0.0277 (4)
H19A	0.2850	0.6845	0.0278	0.042*
H19B	0.4346	0.6761	-0.0354	0.042*
H19C	0.4755	0.7104	0.1072	0.042*
C8	-0.0403 (2)	0.71549 (5)	0.42191 (18)	0.0202 (3)
C2	0.8443 (2)	0.45432 (5)	0.77564 (18)	0.0204 (3)
C1	0.7477 (2)	0.49478 (5)	0.67579 (18)	0.0211 (3)
C15	0.6756 (3)	0.51723 (6)	0.1910 (2)	0.0285 (4)
H15A	0.7982	0.5116	0.2676	0.043*
H15B	0.6752	0.5186	0.0895	0.043*
H15C	0.5973	0.4915	0.1941	0.043*
C4	1.0121 (2)	0.38200 (6)	0.8209 (2)	0.0276 (4)
H4	1.0658	0.3578	0.7859	0.033*

#### Atomic displacement parameters ( $\text{\AA}^2$ )

	$U^{11}$	$U^{22}$	$U^{33}$	$U^{12}$	$U^{13}$	$U^{23}$
S1	0.01585 (19)	0.01887 (19)	0.01512 (18)	0.00059 (13)	0.00694 (14)	-0.00223 (13)
C12	0.0335 (2)	0.0332 (2)	0.0287 (2)	-0.00094 (17)	0.01395 (18)	0.00958 (16)
O3	0.0204 (6)	0.0308 (6)	0.0156 (5)	0.0038 (5)	0.0068 (4)	-0.0010 (4)
O4	0.0186 (5)	0.0231 (6)	0.0234 (6)	-0.0026 (4)	0.0100 (5)	-0.0051 (4)
O1	0.0271 (6)	0.0202 (6)	0.0302 (6)	0.0044 (5)	0.0153 (5)	0.0036 (5)
O2	0.0413 (7)	0.0251 (6)	0.0237 (6)	0.0119 (5)	0.0135 (6)	0.0031 (5)
N2	0.0238 (7)	0.0167 (6)	0.0170 (6)	0.0043 (5)	0.0098 (5)	0.0018 (5)
N4	0.0200 (7)	0.0199 (6)	0.0176 (6)	0.0003 (5)	0.0087 (5)	-0.0002 (5)
N3	0.0187 (6)	0.0187 (6)	0.0186 (6)	0.0001 (5)	0.0081 (5)	-0.0018 (5)
N1	0.0215 (8)	0.0363 (8)	0.0379 (9)	0.0079 (6)	0.0145 (7)	0.0192 (7)
C14	0.0152 (7)	0.0192 (7)	0.0172 (7)	-0.0019 (6)	0.0072 (6)	-0.0026 (6)
C18	0.0199 (8)	0.0242 (8)	0.0183 (7)	-0.0036 (6)	0.0076 (6)	-0.0008 (6)
C13	0.0202 (8)	0.0223 (8)	0.0214 (8)	-0.0005 (6)	0.0117 (6)	0.0016 (6)
C12	0.0209 (8)	0.0184 (7)	0.0172 (7)	0.0011 (6)	0.0087 (6)	0.0014 (6)
C7	0.0195 (8)	-0.0184 (8)	0.0281 (8)	-0.0014 (6)	0.0108 (7)	-0.0007 (6)

C10	0.0210 (8)	0.0183 (7)	0.0196 (7)	-0.0033 (6)	0.0106 (6)	-0.0011 (6)
C6	0.0198 (8)	0.0239 (8)	0.0259 (8)	-0.0054 (6)	0.0078 (7)	0.0016 (6)
C16	0.0188 (8)	0.0237 (8)	0.0220 (8)	-0.0031 (6)	0.0099 (6)	-0.0059 (6)
C17	0.0238 (8)	0.0275 (8)	0.0183 (7)	-0.0025 (6)	0.0112 (6)	-0.0039 (6)
C11	0.0168 (7)	0.0162 (7)	0.0172 (7)	0.0000 (6)	0.0072 (6)	-0.0025 (6)
C9	0.0225 (8)	0.0179 (7)	0.0200 (7)	-0.0002 (6)	0.0080 (6)	0.0037 (6)
C5	0.0194 (8)	0.0194 (8)	0.0340 (9)	0.0005 (6)	0.0044 (7)	0.0040 (7)
C3	0.0221 (8)	0.0209 (8)	0.0256 (8)	-0.0023 (6)	0.0072 (7)	-0.0052 (6)
C19	0.0355 (10)	0.0274 (9)	0.0202 (8)	0.0020 (7)	0.0116 (7)	0.0033 (7)
C8	0.0188 (8)	0.0200 (7)	0.0210 (7)	-0.0001 (6)	0.0076 (6)	-0.0006 (6)
C2	0.0165 (7)	0.0171 (7)	0.0254 (8)	-0.0030 (6)	0.0068 (6)	-0.0013 (6)
C1	0.0195 (8)	0.0187 (8)	0.0237 (8)	-0.0026 (6)	0.0075 (7)	-0.0018 (6)
C15	0.0357 (10)	0.0264 (9)	0.0282 (9)	0.0022 (7)	0.0179 (8)	-0.0067 (7)
C4	0.0218 (8)	0.0198 (8)	0.0369 (10)	0.0016 (6)	0.0082 (7)	-0.0054 (7)

### Geometric parameters (Å, °)

S1—O3	1.4336 (11)	C7—C2	1.392 (2)
S1—O4	1.4413 (11)	C7—H7	0.9500
S1—N2	1.6460 (13)	C10—C9	1.377 (2)
S1—C11	1.7434 (15)	C10—C11	1.396 (2)
C12—C6	1.7424 (17)	C10—H10	0.9500
O1—C1	1.222 (2)	C6—C5	1.385 (2)
O2—C1	1.314 (2)	C16—C17	1.380 (2)
O2—H32	0.872 (16)	C16—C15	1.496 (2)
N2—C14	1.3882 (19)	C17—H17	0.9500
N2—H31	0.852 (15)	C9—C8	1.410 (2)
N4—C14	1.329 (2)	C9—H9	0.9500
N4—C18	1.345 (2)	C5—C4	1.386 (3)
N3—C14	1.337 (2)	C5—H5	0.9500
N3—C16	1.349 (2)	C3—C4	1.384 (2)
N1—C8	1.358 (2)	C3—C2	1.394 (2)
N1—H30A	0.851 (15)	C3—H3	0.9500
N1—H30B	0.844 (15)	C19—H19A	0.9800
C18—C17	1.388 (2)	C19—H19B	0.9800
C18—C19	1.495 (2)	C19—H19C	0.9800
C13—C12	1.377 (2)	C2—C1	1.492 (2)
C13—C8	1.405 (2)	C15—H15A	0.9800
C13—H13	0.9500	C15—H15B	0.9800
C12—C11	1.394 (2)	C15—H15C	0.9800
C12—H12	0.9500	C4—H4	0.9500
C7—C6	1.382 (2)		
O3—S1—O4	118.51 (7)	C16—C17—C18	118.32 (14)
O3—S1—N2	103.10 (7)	C16—C17—H17	120.8
O4—S1—N2	108.86 (7)	C18—C17—H17	120.8
O3—S1—C11	108.63 (7)	C12—C11—C10	120.01 (14)
O4—S1—C11	108.08 (7)	C12—C11—S1	118.06 (12)
N2—S1—C11	109.37 (7)	C10—C11—S1	121.74 (12)
C1—O2—H32	110.3 (17)	C10—C9—C8	120.82 (14)
C14—N2—S1	125.22 (11)	C10—C9—H9	119.6



C14—N2—H31	118.6 (14)	C8—C9—H9	119.6
S1—N2—H31	115.4 (14)	C6—C5—C4	118.71 (15)
C14—N4—C18	115.74 (13)	C6—C5—H5	120.6
C14—N3—C16	116.53 (13)	C4—C5—H5	120.6
C8—N1—H30A	118.0 (14)	C4—C3—C2	119.62 (16)
C8—N1—H30B	119.5 (15)	C4—C3—H3	120.2
H30A—N1—H30B	122 (2)	C2—C3—H3	120.2
N4—C14—N3	127.20 (14)	C18—C19—H19A	109.5
N4—C14—N2	117.84 (13)	C18—C19—H19B	109.5
N3—C14—N2	114.95 (13)	H19A—C19—H19B	109.5
N4—C18—C17	121.57 (14)	C18—C19—H19C	109.5
N4—C18—C19	116.30 (14)	H19A—C19—H19C	109.5
C17—C18—C19	122.12 (14)	H19B—C19—H19C	109.5
C12—C13—C8	120.53 (14)	N1—C8—C13	120.45 (15)
C12—C13—H13	119.7	N1—C8—C9	121.05 (15)
C8—C13—H13	119.7	C13—C8—C9	118.49 (14)
C13—C12—C11	120.27 (14)	C7—C2—C3	120.19 (15)
C13—C12—H12	119.9	C7—C2—C1	118.28 (14)
C11—C12—H12	119.9	C3—C2—C1	121.53 (15)
C6—C7—C2	118.91 (15)	O1—C1—O2	124.21 (15)
C6—C7—H7	120.5	O1—C1—C2	122.96 (15)
C2—C7—H7	120.5	O2—C1—C2	112.83 (14)
C9—C10—C11	119.84 (14)	C16—C15—H15A	109.5
C9—C10—H10	120.1	C16—C15—H15B	109.5
C11—C10—H10	120.1	H15A—C15—H15B	109.5
C7—C6—C5	121.73 (16)	C16—C15—H15C	109.5
C7—C6—C12	118.74 (13)	H15A—C15—H15C	109.5
C5—C6—C12	119.53 (13)	H15B—C15—H15C	109.5
N3—C16—C17	120.64 (14)	C3—C4—C5	120.83 (16)
N3—C16—C15	116.24 (14)	C3—C4—H4	119.6
C17—C16—C15	123.12 (14)	C5—C4—H4	119.6
O3—S1—N2—C14	-171.63 (12)	O3—S1—C11—C12	-21.55 (14)
O4—S1—N2—C14	-44.95 (14)	O4—S1—C11—C12	-151.34 (12)
C11—S1—N2—C14	72.94 (14)	N2—S1—C11—C12	90.29 (13)
C18—N4—C14—N3	0.1 (2)	O3—S1—C11—C10	153.39 (12)
C18—N4—C14—N2	-179.00 (13)	O4—S1—C11—C10	23.61 (14)
C16—N3—C14—N4	0.0 (2)	N2—S1—C11—C10	-94.77 (13)
C16—N3—C14—N2	179.16 (13)	C11—C10—C9—C8	-0.2 (2)
S1—N2—C14—N4	-15.6 (2)	C7—C6—C5—C4	-0.1 (2)
S1—N2—C14—N3	165.18 (11)	C12—C6—C5—C4	179.27 (13)
C14—N4—C18—C17	-0.2 (2)	C12—C13—C8—N1	-177.59 (16)
C14—N4—C18—C19	179.04 (14)	C12—C13—C8—C9	2.1 (2)
C8—C13—C12—C11	-0.8 (2)	C10—C9—C8—N1	178.08 (16)
C2—C7—C6—C5	0.0 (2)	C10—C9—C8—C13	-1.6 (2)
C2—C7—C6—C12	-179.34 (12)	C6—C7—C2—C3	0.1 (2)
C14—N3—C16—C17	-0.1 (2)	C6—C7—C2—C1	-179.70 (14)
C14—N3—C16—C15	-179.78 (14)	C4—C3—C2—C7	-0.2 (2)
N3—C16—C17—C18	0.0 (2)	C4—C3—C2—C1	179.62 (15)
C15—C16—C17—C18	179.70 (15)	C7—C2—C1—O1	-4.9 (2)



C15—C16—C17—C18	179.70 (15)	C7—C2—C1—O1	-4.9 (2)
N4—C18—C17—C16	0.1 (2)	C3—C2—C1—O1	175.27 (15)
C19—C18—C17—C16	-179.06 (15)	C7—C2—C1—O2	174.66 (14)
C13—C12—C11—C10	-1.0 (2)	C3—C2—C1—O2	-5.2 (2)
C13—C12—C11—S1	174.01 (12)	C2—C3—C4—C5	0.1 (2)
C9—C10—C11—C12	1.5 (2)	C6—C5—C4—C3	0.0 (2)
C9—C10—C11—S1	-173.33 (12)		

#### Hydrogen-bond geometry (Å, °)

$D-H\cdots A$	$D-H$	$H\cdots A$	$D\cdots A$	$D-H\cdots A$
N1—H30A $\cdots$ O4 <sup>ii</sup>	0.85 (2)	2.33 (2)	3.1262 (19)	157 (2)
N1—H30B $\cdots$ O4 <sup>i</sup>	0.84 (2)	2.25 (2)	3.0951 (18)	174 (2)
N2—H31 $\cdots$ O1	0.85 (2)	2.05 (2)	2.8978 (17)	173 (2)
O2—H32 $\cdots$ N3	0.87 (2)	1.77 (2)	2.6399 (17)	172 (2)

Symmetry codes: (i)  $x-1, -y+3/2, z-1/2$ ; (ii)  $x-1, y, z$ .

All esds (except the esd in the dihedral angle between two l.s. planes) are estimated using the full covariance matrix. The cell esds are taken into account individually in the estimation of esds in distances, angles and torsion angles; correlations between esds in cell parameters are only used when they are defined by crystal symmetry. An approximate (isotropic) treatment of cell esds is used for estimating esds involving l.s. planes.

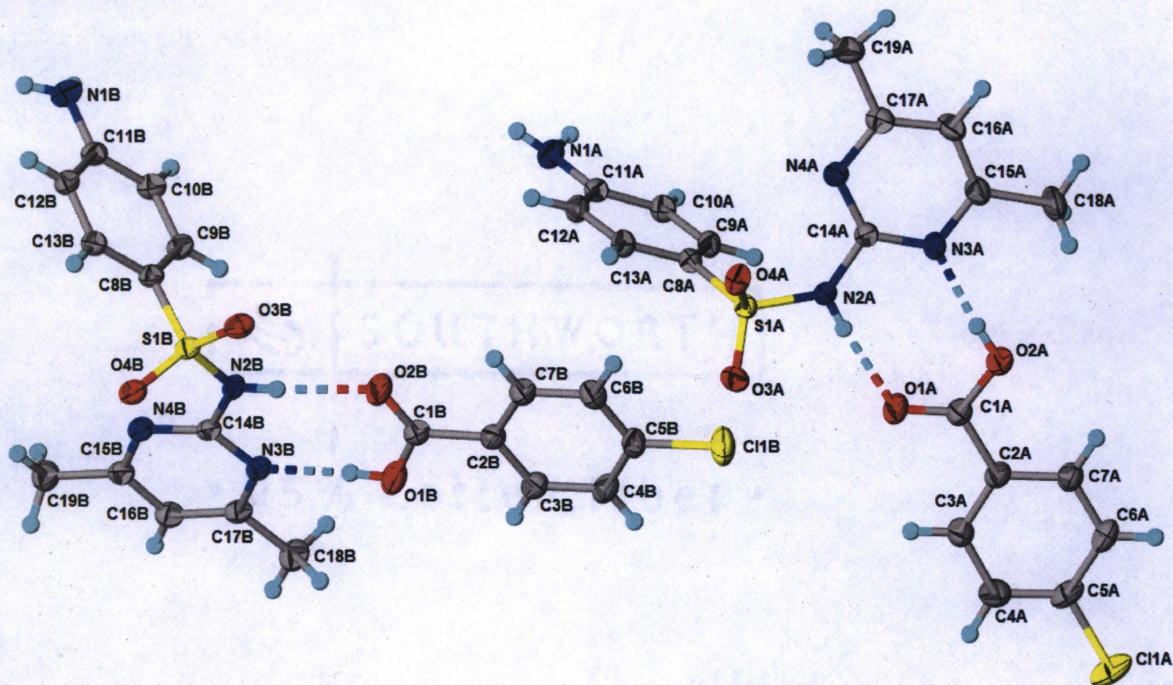


Figure S.12: Crystal Structure of the Cocrystal of Sulfamethazine and *p*-Chlorobenzoic Acid Showing Thermal Parameters (50% Thermal Ellipsoids) and Hydrogen Bonding.



### Crystal data

$C_{12}H_{14}N_4O_2S \cdot C_7H_5ClO_2$

$M_r = 434.89$

Triclinic,  $P$

$a = 7.8082$  (3) Å

$b = 14.9985$  (5) Å

$c = 17.8133$  (6) Å

$\alpha = 88.142$  (2)°

$\beta = 80.879$  (2)°

$\gamma = 77.939$  (2)°

$V = 2014.29$  (12) Å<sup>3</sup>

$Z = 4$

$F(000) = 904$

$F(000) = 904$

$D_x = 1.434$  Mg m<sup>-3</sup>

Melting point: 478-481 K

Cu  $K\alpha$  radiation,  $\lambda = 1.54178$  Å

Cell parameters from 9803 reflections

$\theta = 2.5 - 68.3^\circ$

$\mu = 2.95$  mm<sup>-1</sup>

$T = 100$  K

Block

0.21 × 0.21 × 0.17 mm

### Data collection

Bruker APEXII CCD  
diffractometer

Radiation source: fine-focus sealed tube  
? monochromator

Detector resolution: 8.33 pixels mm<sup>-1</sup>  
phi and  $\omega$  scans

Absorption correction: multi-scan  
SADABS2014/7, Bruker AXS

$T_{\min} = 0.627$ ,  $T_{\max} = 0.753$

12669 measured reflections

12669 independent reflections

10592 reflections with  $I > 2\sigma(I)$

$R_{\text{int}} = ?$

$\theta_{\max} = 68.2^\circ$ ,  $\theta_{\min} = 2.5^\circ$

$h = -9 \quad 9$

$k = -18 \quad 18$

$l = 0 \quad 21$

### Refinement

Refinement on  $F^2$

Least-squares matrix: full

$R[F^2 > 2\sigma(F^2)] = 0.046$

$wR(F^2) = 0.114$

$S = 1.02$

12669 reflections

552 parameters

8 restraints

0 constraints

Refined as a 2-component twin.

Hydrogen site location: mixed

H atoms treated by a mixture of independent and  
constrained refinement

$w = 1/[\sigma^2(F_o^2) + (0.0495P)^2 + 1.0678P]$

where  $P = (F_o^2 + 2F_c^2)/3$

$(\Delta/\sigma)_{\max} < 0.001$

$\Delta\rho_{\max} = 0.31$  e Å<sup>-3</sup>

$\Delta\rho_{\min} = -0.38$  e Å<sup>-3</sup>

Extinction correction: none

Fractional atomic coordinates and isotropic or equivalent isotropic displacement parameters ( $\text{\AA}^2$ )

	<i>x</i>	<i>y</i>	<i>z</i>	$U_{\text{iso}}^*/U_{\text{eq}}$
C11A	0.15845 (14)	-0.32624 (6)	0.27195 (6)	0.0614 (3)
C11B	0.46422 (13)	0.19139 (6)	0.24259 (6)	0.0537 (2)
S1A	0.18743 (10)	0.32329 (5)	0.45642 (4)	0.02717 (17)
S1B	0.65238 (10)	0.82792 (4)	0.03927 (4)	0.02676 (17)
O3A	0.1372 (3)	0.30071 (15)	0.38661 (12)	0.0372 (5)
O1A	0.2473 (4)	0.06841 (14)	0.41219 (12)	0.0516 (7)
O2A	0.2282 (4)	-0.01670 (15)	0.51652 (12)	0.0491 (7)
H32A	0.239 (5)	0.030 (2)	0.539 (2)	0.059*
O4A	0.0562 (3)	0.38218 (13)	0.50796 (12)	0.0341 (5)
O1B	0.7411 (4)	0.48399 (15)	-0.01167 (12)	0.0470 (6)
H32B	0.771 (5)	0.531 (2)	-0.034 (2)	0.056*
O2B	0.6658 (4)	0.57673 (14)	0.08828 (12)	0.0497 (7)
O3B	0.5500 (3)	0.80777 (14)	0.10945 (11)	0.0343 (5)
O4B	0.5605 (3)	0.88520 (13)	-0.01368 (11)	0.0333 (5)
N1A	0.8098 (4)	0.49438 (18)	0.38447 (16)	0.0352 (6)
H30B	0.906 (4)	0.462 (2)	0.394 (2)	0.042*
H30A	0.797 (5)	0.5518 (16)	0.3944 (19)	0.042*
N2A	0.2517 (3)	0.22429 (15)	0.49594 (13)	0.0275 (5)
H31A	0.250 (4)	0.1803 (18)	0.4685 (16)	0.033*
N3A	0.2743 (3)	0.12246 (15)	0.59373 (13)	0.0297 (5)
N4A	0.2987 (3)	0.27625 (15)	0.61232 (13)	0.0279 (5)
N1B	1.2206 (4)	0.99394 (19)	0.12028 (17)	0.0381 (6)
H30C	1.211 (5)	1.0500 (16)	0.110 (2)	0.046*
H30D	1.328 (3)	0.965 (2)	0.109 (2)	0.046*
N2B	0.7437 (3)	0.72754 (15)	0.00228 (13)	0.0280 (5)
H31B	0.712 (4)	0.6842 (18)	0.0281 (16)	0.034*
N3B	0.8479 (3)	0.62108 (15)	-0.09130 (13)	0.0276 (5)
N4B	0.8779 (3)	0.77538 (16)	-0.11542 (13)	0.0291 (5)
C1A	0.2310 (5)	-0.0033 (2)	0.44372 (17)	0.0357 (7)
C2A	0.2128 (4)	-0.08418 (19)	0.40168 (17)	0.0324 (7)
C3A	0.2150 (6)	-0.0787 (2)	0.32380 (19)	0.0463 (9)
H3A	0.2278	-0.0236	0.2978	0.056*
C4A	0.1985 (6)	-0.1532 (2)	0.2835 (2)	0.0504 (9)
H4A	0.1998	-0.1496	0.2301	0.060*
C5A	0.1802 (5)	-0.2326 (2)	0.3224 (2)	0.0405 (8)
C6A	0.1792 (5)	-0.2400 (2)	0.39935 (19)	0.0390 (8)
H6A	0.1679	-0.2956	0.4249	0.047*
C7A	0.1947 (4)	-0.1651 (2)	0.43920 (18)	0.0359 (7)
H7A	0.1930	-0.1691	0.4926	0.043*
C8A	0.3747 (4)	0.37143 (19)	0.43699 (15)	0.0268 (6)
C9A	0.5440 (4)	0.31850 (19)	0.42723 (16)	0.0289 (6)
H9A	0.5609	0.2542	0.4328	0.035*
C10A	0.6890 (4)	0.35901 (19)	0.40942 (16)	0.0302 (6)
H10A	0.8053	0.3224	0.4031	0.036*
C11A	0.6653 (4)	0.4537 (2)	0.40061 (15)	0.0284 (6)

C12A	0.4925 (4)	0.5060 (2)	0.40841 (16)	0.0307 (7)
H12A	0.4746	0.5701	0.4010	0.037*
C13A	0.3483 (4)	0.46592 (19)	0.42661 (16)	0.0290 (6)
H13A	0.2316	0.5021	0.4321	0.035*
C14A	0.2755 (4)	0.20853 (18)	0.57101 (15)	0.0255 (6)
C15A	0.2944 (5)	0.1028 (2)	0.66646 (17)	0.0354 (7)
C16A	0.3160 (5)	0.1688 (2)	0.71377 (17)	0.0390 (8)
H16A	0.3285	0.1552	0.7653	0.047*
C17A	0.3193 (4)	0.2552 (2)	0.68502 (16)	0.0323 (7)
C18A	0.2917 (6)	0.0065 (2)	0.6918 (2)	0.0550 (11)
H18A	0.1844	-0.0105	0.6799	0.083*
H18B	0.2923	0.0019	0.7468	0.083*
H18C	0.3965	-0.0347	0.6653	0.083*
C19A	0.3486 (5)	0.3287 (2)	0.73377 (18)	0.0409 (8)
H19A	0.4662	0.3418	0.7164	0.061*
H19B	0.3408	0.3082	0.7868	0.061*
H19C	0.2578	0.3839	0.7300	0.061*
C1B	0.6793 (4)	0.5021 (2)	0.05951 (17)	0.0335 (7)
C2B	0.6247 (4)	0.42437 (19)	0.10438 (16)	0.0316 (7)
C3B	0.6451 (4)	0.3394 (2)	0.07049 (18)	0.0358 (7)
H3B	0.6930	0.3310	0.0181	0.043*
C4B	0.5957 (5)	0.2674 (2)	0.11304 (19)	0.0388 (8)
H4B	0.6095	0.2094	0.0903	0.047*
C5B	0.5262 (4)	0.2812 (2)	0.18876 (19)	0.0359 (7)
C6B	0.5025 (5)	0.3656 (2)	0.22332 (18)	0.0404 (8)
H6B	0.4522	0.3742	0.2754	0.048*
C7B	0.5535 (5)	0.4363 (2)	0.18055 (17)	0.0383 (7)
H7B	0.5397	0.4941	0.2036	0.046*
C8B	0.8265 (4)	0.87524 (19)	0.05939 (15)	0.0274 (6)
C9B	0.9882 (4)	0.82114 (19)	0.06875 (16)	0.0303 (7)
H9B	1.0089	0.7570	0.0619	0.036*
C10B	1.1193 (4)	0.8609 (2)	0.08808 (17)	0.0322 (7)
H10B	1.2313	0.8239	0.0935	0.039*
C11B	1.0898 (4)	0.9551 (2)	0.09985 (15)	0.0299 (7)
C12B	0.9235 (4)	1.0081 (2)	0.09215 (16)	0.0314 (7)
H12B	0.9004	1.0718	0.1015	0.038*
C13B	0.7927 (4)	0.96966 (19)	0.07129 (16)	0.0293 (6)
H13B	0.6812	1.0066	0.0650	0.035*
C14B	0.8270 (4)	0.70886 (18)	-0.07178 (15)	0.0255 (6)
C15B	0.9550 (4)	0.75129 (19)	-0.18683 (16)	0.0300 (6)
C16B	0.9824 (4)	0.6619 (2)	-0.21207 (16)	0.0329 (7)
H16B	1.0385	0.6457	-0.2625	0.040*
C17B	0.9272 (4)	0.59761 (19)	-0.16296 (16)	0.0297 (6)
C18B	0.9490 (5)	0.4998 (2)	-0.18439 (18)	0.0422 (8)
H18D	1.0336	0.4616	-0.1555	0.063*
H18E	0.9934	0.4921	-0.2389	0.063*
H18F	0.8343	0.4815	-0.1728	0.063*
C19B	1.0107 (5)	0.8237 (2)	-0.23913 (18)	0.0420 (8)
H19D	0.9541	0.8839	-0.2175	0.063*

H19E	0.9748	0.8180	-0.2887	0.063*
H19F	1.1398	0.8166	-0.2454	0.063*

Atomic displacement parameters ( $\text{\AA}^2$ )

	$U^{11}$	$U^{22}$	$U^{33}$	$U^{12}$	$U^{13}$	$U^{23}$
C11A	0.0633 (6)	0.0438 (5)	0.0821 (7)	-0.0141 (4)	-0.0158 (5)	-0.0292 (4)
C11B	0.0550 (6)	0.0395 (4)	0.0683 (6)	-0.0132 (4)	-0.0148 (5)	0.0238 (4)
S1A	0.0272 (4)	0.0256 (3)	0.0302 (3)	-0.0067 (3)	-0.0082 (3)	0.0050 (3)
S1B	0.0281 (4)	0.0239 (3)	0.0285 (3)	-0.0047 (3)	-0.0050 (3)	-0.0050 (3)
O3A	0.0377 (13)	0.0444 (12)	0.0350 (11)	-0.0146 (10)	-0.0156 (10)	0.0080 (9)
O1A	0.095 (2)	0.0290 (11)	0.0357 (12)	-0.0241 (13)	-0.0104 (13)	0.0001 (9)
O2A	0.088 (2)	0.0320 (12)	0.0338 (12)	-0.0217 (13)	-0.0149 (13)	-0.0009 (9)
O4A	0.0282 (12)	0.0275 (10)	0.0455 (12)	-0.0066 (9)	-0.0021 (9)	0.0028 (9)
O1B	0.0741 (19)	0.0321 (12)	0.0349 (12)	-0.0216 (12)	0.0056 (12)	-0.0033 (9)
O2B	0.086 (2)	0.0308 (12)	0.0347 (12)	-0.0228 (13)	-0.0021 (12)	-0.0035 (9)
O3B	0.0335 (12)	0.0370 (11)	0.0327 (11)	-0.0092 (10)	-0.0016 (9)	-0.0082 (9)
O4B	0.0350 (12)	0.0278 (10)	0.0392 (11)	-0.0052 (9)	-0.0128 (10)	-0.0029 (8)
N1A	0.0308 (15)	0.0323 (14)	0.0446 (15)	-0.0104 (12)	-0.0076 (12)	0.0026 (12)
N2A	0.0364 (15)	0.0214 (11)	0.0266 (12)	-0.0075 (11)	-0.0083 (11)	-0.0009 (9)
N3A	0.0356 (15)	0.0220 (11)	0.0307 (12)	-0.0042 (10)	-0.0057 (11)	0.0025 (9)
N4A	0.0306 (14)	0.0243 (11)	0.0287 (12)	-0.0038 (10)	-0.0065 (10)	-0.0023 (9)
N1B	0.0348 (16)	0.0368 (15)	0.0459 (16)	-0.0114 (13)	-0.0095 (13)	-0.0059 (12)
N2B	0.0363 (15)	0.0210 (11)	0.0273 (12)	-0.0091 (11)	-0.0027 (11)	-0.0014 (9)
N3B	0.0295 (14)	0.0230 (11)	0.0302 (12)	-0.0048 (10)	-0.0048 (10)	-0.0033 (9)
N4B	0.0310 (14)	0.0275 (12)	0.0296 (12)	-0.0077 (11)	-0.0048 (11)	-0.0026 (9)
C1A	0.045 (2)	0.0274 (15)	0.0353 (16)	-0.0081 (14)	-0.0079 (15)	-0.0011 (12)
C2A	0.0348 (18)	0.0256 (14)	0.0372 (16)	-0.0062 (13)	-0.0065 (14)	-0.0029 (12)
C3A	0.073 (3)	0.0314 (17)	0.0380 (17)	-0.0135 (17)	-0.0166 (18)	0.0027 (13)
C4A	0.074 (3)	0.0421 (19)	0.0392 (18)	-0.0132 (18)	-0.0180 (18)	-0.0051 (15)
C5A	0.0359 (19)	0.0303 (16)	0.057 (2)	-0.0055 (14)	-0.0103 (16)	-0.0149 (14)
C6A	0.0388 (19)	0.0262 (15)	0.0514 (19)	-0.0105 (14)	0.0000 (15)	-0.0035 (13)
C7A	0.0410 (19)	0.0303 (15)	0.0366 (16)	-0.0096 (14)	-0.0041 (14)	0.0004 (12)
C8A	0.0289 (16)	0.0266 (14)	0.0259 (14)	-0.0063 (12)	-0.0068 (12)	0.0032 (11)
C9A	0.0296 (17)	0.0236 (14)	0.0332 (15)	-0.0033 (12)	-0.0076 (13)	0.0035 (11)
C10A	0.0263 (16)	0.0292 (15)	0.0335 (15)	-0.0025 (12)	-0.0049 (13)	0.0014 (12)
C11A	0.0318 (17)	0.0311 (15)	0.0239 (13)	-0.0099 (13)	-0.0046 (12)	0.0013 (11)
C12A	0.0357 (18)	0.0246 (14)	0.0314 (15)	-0.0061 (13)	-0.0045 (13)	0.0013 (11)
C13A	0.0272 (16)	0.0266 (14)	0.0317 (15)	-0.0027 (12)	-0.0043 (12)	0.0021 (11)
C14A	0.0245 (15)	0.0240 (13)	0.0276 (13)	-0.0033 (12)	-0.0053 (12)	-0.0003 (11)
C15A	0.043 (2)	0.0297 (15)	0.0311 (15)	-0.0021 (14)	-0.0073 (14)	0.0027 (12)
C16A	0.054 (2)	0.0339 (16)	0.0274 (15)	-0.0004 (15)	-0.0117 (15)	-0.0007 (12)
C17A	0.0319 (17)	0.0313 (15)	0.0313 (15)	0.0009 (13)	-0.0065 (13)	-0.0044 (12)
C18A	0.094 (3)	0.0313 (17)	0.0393 (18)	-0.0088 (19)	-0.016 (2)	0.0092 (14)

C19A	0.048 (2)	0.0372 (17)	0.0377 (17)	-0.0034 (15)	-0.0141 (15)	-0.0063 (13)
C1B	0.0391 (19)	0.0312 (15)	0.0320 (15)	-0.0099 (14)	-0.0070 (14)	-0.0014 (12)
C2B	0.0351 (18)	0.0273 (14)	0.0334 (15)	-0.0064 (13)	-0.0090 (13)	-0.0001 (12)
C3B	0.0413 (19)	0.0287 (15)	0.0379 (16)	-0.0070 (14)	-0.0073 (15)	-0.0032 (12)
C4B	0.041 (2)	0.0243 (15)	0.0531 (19)	-0.0063 (14)	-0.0140 (16)	0.0011 (13)
C5B	0.0307 (18)	0.0313 (16)	0.0482 (18)	-0.0080 (13)	-0.0143 (14)	0.0125 (13)
C6B	0.049 (2)	0.0401 (17)	0.0323 (16)	-0.0106 (16)	-0.0073 (15)	0.0049 (13)
C7B	0.052 (2)	0.0307 (16)	0.0341 (16)	-0.0108 (15)	-0.0092 (15)	-0.0009 (12)
C8B	0.0314 (17)	0.0280 (14)	0.0239 (13)	-0.0080 (12)	-0.0041 (12)	-0.0034 (11)
C9B	0.0316 (17)	0.0245 (14)	0.0342 (15)	-0.0035 (12)	-0.0054 (13)	-0.0054 (11)
C10B	0.0277 (17)	0.0327 (16)	0.0351 (16)	-0.0018 (13)	-0.0069 (13)	-0.0048 (12)
C11B	0.0342 (18)	0.0343 (15)	0.0229 (14)	-0.0122 (14)	-0.0021 (12)	-0.0029 (11)
C12B	0.0427 (19)	0.0252 (14)	0.0279 (15)	-0.0098 (13)	-0.0061 (13)	-0.0029 (11)
C13B	0.0323 (17)	0.0257 (14)	0.0294 (14)	-0.0021 (12)	-0.0083 (13)	-0.0017 (11)
C14B	0.0255 (16)	0.0248 (13)	0.0274 (14)	-0.0051 (12)	-0.0076 (12)	-0.0031 (11)
C15B	0.0306 (17)	0.0334 (15)	0.0280 (14)	-0.0096 (13)	-0.0067 (12)	-0.0002 (12)
C16B	0.0349 (18)	0.0338 (16)	0.0286 (14)	-0.0046 (13)	-0.0023 (13)	-0.0057 (12)
C17B	0.0290 (16)	0.0292 (15)	0.0305 (15)	-0.0034 (12)	-0.0052 (12)	-0.0068 (11)
C18B	0.054 (2)	0.0302 (16)	0.0394 (17)	-0.0068 (15)	0.0010 (16)	-0.0101 (13)
C19B	0.054 (2)	0.0385 (17)	0.0342 (16)	-0.0162 (16)	0.0000 (16)	0.0004 (13)

Geometric parameters (Å, °)

C11A—C5A	1.743 (3)	C10A—C11A	1.401 (4)
C11B—C5B	1.735 (3)	C10A—H10A	0.9500
S1A—O4A	1.431 (2)	C11A—C12A	1.401 (4)
S1A—O3A	1.433 (2)	C12A—C13A	1.374 (4)
S1A—N2A	1.639 (2)	C12A—H12A	0.9500
S1A—C8A	1.744 (3)	C13A—H13A	0.9500
S1B—O4B	1.431 (2)	C15A—C16A	1.374 (4)
S1B—O3B	1.433 (2)	C15A—C18A	1.502 (4)
S1B—N2B	1.636 (2)	C16A—C17A	1.383 (4)
S1B—C8B	1.748 (3)	C16A—H16A	0.9500
O1A—C1A	1.218 (4)	C17A—C19A	1.500 (4)
O2A—C1A	1.303 (4)	C18A—H18A	0.9800
O2A—H32A	0.85 (2)	C18A—H18B	0.9800
O1B—C1B	1.299 (4)	C18A—H18C	0.9800
O1B—H32B	0.86 (2)	C19A—H19A	0.9800
O2B—C1B	1.223 (3)	C19A—H19B	0.9800
N1A—C11A	1.379 (4)	C19A—H19C	0.9800
N1A—H30B	0.85 (2)	C1B—C2B	1.490 (4)
N1A—H30A	0.87 (2)	C2B—C7B	1.385 (4)
N2A—C14A	1.385 (3)	C2B—C3B	1.395 (4)
N2A—H31A	0.84 (2)	C3B—C4B	1.385 (4)
N3A—C14A	1.342 (3)	C3B—H3B	0.9500
N3A—C15A	1.346 (4)	C4B—C5B	1.377 (5)
N4A—C14A	1.332 (3)	C4B—H4B	0.9500
N4A—C17A	1.349 (4)	C5B—C6B	1.390 (4)
N1B—C11B	1.377 (4)	C6B—C7B	1.375 (4)
N1B—H30C	0.84 (2)	C6B—H6B	0.9500



N1B—H30D	0.85 (2)	C7B—H7B	0.9500
N2B—C14B	1.385 (3)	C8B—C9B	1.382 (4)
N2B—H31B	0.84 (2)	C8B—C13B	1.402 (4)
N3B—C14B	1.343 (3)	C9B—C10B	1.380 (4)
N3B—C17B	1.351 (4)	C9B—H9B	0.9500
N4B—C14B	1.332 (4)	C10B—C11B	1.399 (4)
N4B—C15B	1.344 (4)	C10B—H10B	0.9500
C1A—C2A	1.489 (4)	C11B—C12B	1.398 (4)
C2A—C3A	1.385 (4)	C12B—C13B	1.376 (4)
C2A—C7A	1.389 (4)	C12B—H12B	0.9500
C3A—C4A	1.386 (5)	C13B—H13B	0.9500
C3A—H3A	0.9500	C15B—C16B	1.390 (4)
C4A—C5A	1.381 (5)	C15B—C19B	1.496 (4)
C4A—H4A	0.9500	C16B—C17B	1.372 (4)
C5A—C6A	1.371 (5)	C16B—H16B	0.9500
C6A—C7A	1.384 (4)	C17B—C18B	1.496 (4)
C6A—H6A	0.9500	C18B—H18D	0.9800
C7A—H7A	0.9500	C18B—H18E	0.9800
C8A—C9A	1.381 (4)	C18B—H18F	0.9800
C8A—C13A	1.399 (4)	C19B—H19D	0.9800
C9A—C10A	1.383 (4)	C19B—H19E	0.9800
C9A—H9A	0.9500	C19B—H19F	0.9800
O4A—S1A—O3A	117.27 (13)	N4A—C17A—C16A	121.5 (3)
O4A—S1A—N2A	110.83 (12)	N4A—C17A—C19A	117.8 (3)
O3A—S1A—N2A	104.14 (12)	C16A—C17A—C19A	120.8 (3)
O4A—S1A—C8A	108.26 (13)	C15A—C18A—H18A	109.5
O3A—S1A—C8A	109.69 (13)	C15A—C18A—H18B	109.5
N2A—S1A—C8A	106.08 (13)	H18A—C18A—H18B	109.5
O4B—S1B—O3B	117.36 (13)	C15A—C18A—H18C	109.5
O4B—S1B—N2B	110.87 (12)	H18A—C18A—H18C	109.5
O3B—S1B—N2B	103.88 (12)	H18B—C18A—H18C	109.5
O4B—S1B—C8B	109.19 (13)	C17A—C19A—H19A	109.5
O3B—S1B—C8B	108.84 (13)	C17A—C19A—H19B	109.5
N2B—S1B—C8B	106.06 (14)	H19A—C19A—H19B	109.5
C1A—O2A—H32A	112 (3)	C17A—C19A—H19C	109.5
C1B—O1B—H32B	110 (3)	H19A—C19A—H19C	109.5
C11A—N1A—H30B	115 (3)	H19B—C19A—H19C	109.5
C11A—N1A—H30A	119 (2)	O2B—C1B—O1B	123.5 (3)
H30B—N1A—H30A	115 (3)	O2B—C1B—C2B	121.9 (3)
C14A—N2A—S1A	126.82 (19)	O1B—C1B—C2B	114.7 (3)
C14A—N2A—H31A	119 (2)	C7B—C2B—C3B	119.6 (3)
S1A—N2A—H31A	113 (2)	C7B—C2B—C1B	119.8 (3)
C14A—N3A—C15A	116.8 (2)	C3B—C2B—C1B	120.7 (3)
C14A—N4A—C17A	115.6 (2)	C4B—C3B—C2B	120.1 (3)
C11B—N1B—H30C	115 (3)	C4B—C3B—H3B	120.0
C11B—N1B—H30D	118 (3)	C2B—C3B—H3B	120.0
H30C—N1B—H30D	111 (4)	C5B—C4B—C3B	119.0 (3)
C14B—N2B—S1B	126.95 (19)	C5B—C4B—H4B	120.5
C14B—N2B—H31B	117 (2)	C3B—C4B—H4B	120.5

S1B—N2B—H31B	114 (2)	C4B—C5B—C6B	121.8 (3)
C14B—N3B—C17B	116.8 (2)	C4B—C5B—C11B	119.4 (2)
C14B—N4B—C15B	115.7 (2)	C6B—C5B—C11B	118.9 (3)
O1A—C1A—O2A	123.7 (3)	C7B—C6B—C5B	118.6 (3)
O1A—C1A—C2A	122.4 (3)	C7B—C6B—H6B	120.7
O2A—C1A—C2A	113.9 (3)	C5B—C6B—H6B	120.7
C3A—C2A—C7A	119.5 (3)	C6B—C7B—C2B	120.9 (3)
C3A—C2A—C1A	119.4 (3)	C6B—C7B—H7B	119.5
C7A—C2A—C1A	121.1 (3)	C2B—C7B—H7B	119.5
C2A—C3A—C4A	120.4 (3)	C9B—C8B—C13B	120.8 (3)
C2A—C3A—H3A	119.8	C9B—C8B—S1B	121.4 (2)
C4A—C3A—H3A	119.8	C13B—C8B—S1B	117.7 (2)
C5A—C4A—C3A	118.8 (3)	C10B—C9B—C8B	119.5 (3)
C5A—C4A—H4A	120.6	C10B—C9B—H9B	120.2
C3A—C4A—H4A	120.6	C8B—C9B—H9B	120.2
C6A—C5A—C4A	122.0 (3)	C9B—C10B—C11B	121.0 (3)
C6A—C5A—C11A	119.1 (3)	C9B—C10B—H10B	119.5
C4A—C5A—C11A	118.9 (3)	C11B—C10B—H10B	119.5
C5A—C6A—C7A	118.8 (3)	N1B—C11B—C12B	121.0 (3)
C5A—C6A—H6A	120.6	N1B—C11B—C10B	120.5 (3)
C7A—C6A—H6A	120.6	C12B—C11B—C10B	118.5 (3)
C6A—C7A—C2A	120.5 (3)	C13B—C12B—C11B	121.2 (3)
C6A—C7A—H7A	119.7	C13B—C12B—H12B	119.4
C2A—C7A—H7A	119.7	C11B—C12B—H12B	119.4
C9A—C8A—C13A	120.3 (3)	C12B—C13B—C8B	119.0 (3)
C9A—C8A—S1A	121.8 (2)	C12B—C13B—H13B	120.5
C13A—C8A—S1A	117.7 (2)	C8B—C13B—H13B	120.5
C8A—C9A—C10A	120.1 (3)	N4B—C14B—N3B	126.9 (3)
C8A—C9A—H9A	120.0	N4B—C14B—N2B	119.8 (2)
C10A—C9A—H9A	120.0	N3B—C14B—N2B	113.3 (2)
C9A—C10A—C11A	120.4 (3)	N4B—C15B—C16B	121.4 (3)
C9A—C10A—H10A	119.8	N4B—C15B—C19B	118.1 (3)
C11A—C10A—H10A	119.8	C16B—C15B—C19B	120.4 (3)
N1A—C11A—C12A	120.8 (3)	C17B—C16B—C15B	118.9 (3)
N1A—C11A—C10A	120.4 (3)	C17B—C16B—H16B	120.6
C12A—C11A—C10A	118.7 (3)	C15B—C16B—H16B	120.6
C13A—C12A—C11A	120.9 (3)	N3B—C17B—C16B	120.3 (3)
C13A—C12A—H12A	119.5	N3B—C17B—C18B	116.4 (3)
C11A—C12A—H12A	119.5	C16B—C17B—C18B	123.3 (3)
C12A—C13A—C8A	119.5 (3)	C17B—C18B—H18D	109.5
C12A—C13A—H13A	120.2	C17B—C18B—H18E	109.5
C8A—C13A—H13A	120.2	H18D—C18B—H18E	109.5
N4A—C14A—N3A	126.9 (2)	C17B—C18B—H18F	109.5
N4A—C14A—N2A	119.4 (2)	H18D—C18B—H18F	109.5
N3A—C14A—N2A	113.7 (2)	H18E—C18B—H18F	109.5
N3A—C15A—C16A	120.4 (3)	C15B—C19B—H19D	109.5
N3A—C15A—C18A	116.6 (3)	C15B—C19B—H19E	109.5
C16A—C15A—C18A	123.0 (3)	H19D—C19B—H19E	109.5
C15A—C16A—C17A	118.8 (3)	C15B—C19B—H19F	109.5

C15A—C16A—H16A	120.6	H19D—C19B—H19F	109.5
C17A—C16A—H16A	120.6	H19E—C19B—H19F	109.5
O4A—S1A—N2A—C14A	-37.5 (3)	C14A—N4A—C17A— C19A	179.2 (3)
O3A—S1A—N2A—C14A	-164.4 (3)	C15A—C16A—C17A— N4A	1.2 (5)
C8A—S1A—N2A—C14A	79.8 (3)	C15A—C16A—C17A— C19A	-178.0 (3)
O4B—S1B—N2B—C14B	39.3 (3)	O2B—C1B—C2B—C7B	1.1 (5)
O3B—S1B—N2B—C14B	166.2 (3)	O1B—C1B—C2B—C7B	-178.7 (3)
C8B—S1B—N2B—C14B	-79.1 (3)	O2B—C1B—C2B—C3B	-178.6 (3)
O1A—C1A—C2A—C3A	0.3 (5)	O1B—C1B—C2B—C3B	1.5 (5)
O2A—C1A—C2A—C3A	-179.6 (3)	C7B—C2B—C3B—C4B	-0.5 (5)
O1A—C1A—C2A—C7A	179.9 (3)	C1B—C2B—C3B—C4B	179.3 (3)
O2A—C1A—C2A—C7A	0.0 (5)	C2B—C3B—C4B—C5B	0.1 (5)
C7A—C2A—C3A—C4A	0.3 (6)	C3B—C4B—C5B—C6B	0.7 (5)
C1A—C2A—C3A—C4A	179.9 (4)	C3B—C4B—C5B—C11B	-179.9 (3)
C2A—C3A—C4A—C5A	-0.1 (6)	C4B—C5B—C6B—C7B	-1.3 (5)
C3A—C4A—C5A—C6A	-0.5 (6)	C11B—C5B—C6B—C7B	179.4 (3)
C3A—C4A—C5A—C11A	179.7 (3)	C5B—C6B—C7B—C2B	0.9 (5)
C4A—C5A—C6A—C7A	0.8 (6)	C3B—C2B—C7B—C6B	0.0 (5)
C11A—C5A—C6A—C7A	-179.4 (3)	C1B—C2B—C7B—C6B	-179.8 (3)
C5A—C6A—C7A—C2A	-0.6 (5)	O4B—S1B—C8B—C9B	-141.8 (2)
C3A—C2A—C7A—C6A	0.1 (5)	O3B—S1B—C8B—C9B	89.0 (3)
C1A—C2A—C7A—C6A	-179.5 (3)	N2B—S1B—C8B—C9B	-22.2 (3)
O4A—S1A—C8A—C9A	143.6 (2)	O4B—S1B—C8B—C13B	42.8 (3)
O3A—S1A—C8A—C9A	-87.4 (3)	O3B—S1B—C8B—C13B	-86.4 (2)
N2A—S1A—C8A—C9A	24.6 (3)	N2B—S1B—C8B—C13B	162.4 (2)
O4A—S1A—C8A—C13A	-40.5 (3)	C13B—C8B—C9B—C10B	-1.7 (4)
O3A—S1A—C8A—C13A	88.6 (2)	S1B—C8B—C9B—C10B	-177.0 (2)
N2A—S1A—C8A—C13A	-159.5 (2)	C8B—C9B—C10B—C11B	1.3 (4)
C13A—C8A—C9A—C10A	2.0 (4)	C9B—C10B—C11B—N1B	179.0 (3)
S1A—C8A—C9A—C10A	177.9 (2)	C9B—C10B—C11B—C12B	0.5 (4)
C8A—C9A—C10A—C11A	-0.5 (4)	N1B—C11B—C12B— C13B	179.6 (3)
C9A—C10A—C11A—N1A	178.6 (3)	C10B—C11B—C12B— C13B	-1.9 (4)
C9A—C10A—C11A— C12A	-1.5 (4)	C11B—C12B—C13B—C8B	1.5 (4)
N1A—C11A—C12A— C13A	-178.2 (3)	C9B—C8B—C13B—C12B	0.3 (4)
C10A—C11A—C12A— C13A	1.9 (4)	S1B—C8B—C13B—C12B	175.8 (2)
C11A—C12A—C13A— C8A	-0.4 (4)	C15B—N4B—C14B—N3B	1.4 (4)
C9A—C8A—C13A—C12A	-1.6 (4)	C15B—N4B—C14B—N2B	-178.9 (3)
S1A—C8A—C13A—C12A	-177.6 (2)	C17B—N3B—C14B—N4B	-0.7 (4)
C17A—N4A—C14A—N3A	-1.5 (5)	C17B—N3B—C14B—N2B	179.6 (2)
C17A—N4A—C14A—N2A	179.4 (3)	S1B—N2B—C14B—N4B	16.7 (4)
C15A—N3A—C14A—N4A	1.8 (5)	S1B—N2B—C14B—N3B	-163.6 (2)

C15A—N3A—C14A—N2A	-179.1 (3)	C14B—N4B—C15B—C16B	-1.4 (4)
S1A—N2A—C14A—N4A	-20.5 (4)	C14B—N4B—C15B—C19B	178.5 (3)
S1A—N2A—C14A—N3A	160.4 (2)	N4B—C15B—C16B—C17B	0.9 (5)
C14A—N3A—C15A—C16A	-0.4 (5)	C19B—C15B—C16B—C17B	-179.0 (3)
C14A—N3A—C15A—C18A	179.6 (3)	C14B—N3B—C17B—C16B	0.1 (4)
N3A—C15A—C16A—C17A	-0.9 (5)	C14B—N3B—C17B—C18B	-179.7 (3)
C18A—C15A—C16A—C17A	179.1 (3)	C15B—C16B—C17B—N3B	-0.2 (5)
C14A—N4A—C17A—C16A	0.0 (4)	C15B—C16B—C17B—C18B	179.6 (3)

#### Hydrogen-bond geometry (Å, °)

<i>D</i> —H··· <i>A</i>	<i>D</i> —H	H··· <i>A</i>	<i>D</i> ··· <i>A</i>	<i>D</i> —H··· <i>A</i>
N1A—H30A···O4A <sup>ii</sup>	0.87 (2)	2.56 (3)	3.141 (3)	125 (3)
N1A—H30B···O4A <sup>i</sup>	0.85 (2)	2.63 (3)	3.335 (3)	141 (3)
N1B—H30C···O4B <sup>iii</sup>	0.84 (2)	2.60 (3)	3.140 (4)	123 (3)
N1B—H30D···O3B <sup>i</sup>	0.85 (2)	2.62 (3)	3.365 (4)	146 (3)
N2A—H31A···O1A	0.84 (2)	1.99 (2)	2.823 (3)	175 (3)
N2B—H31B···O2B	0.84 (2)	1.97 (2)	2.809 (3)	174 (3)
O1B—H32B···N3B	0.86 (2)	1.81 (2)	2.662 (3)	173 (4)
O2A—H32A···N3A	0.85 (2)	1.80 (2)	2.652 (3)	175 (4)

Symmetry codes: (i)  $x+1, y, z$ ; (ii)  $-x+1, -y+1, -z+1$ ; (iii)  $-x+2, -y+2, -z$ .

All esds (except the esd in the dihedral angle between two l.s. planes) are estimated using the full covariance matrix. The cell esds are taken into account individually in the estimation of esds in distances, angles and torsion angles; correlations between esds in cell parameters are only used when they are defined by crystal symmetry. An approximate (isotropic) treatment of cell esds is used for estimating esds involving l.s. planes.

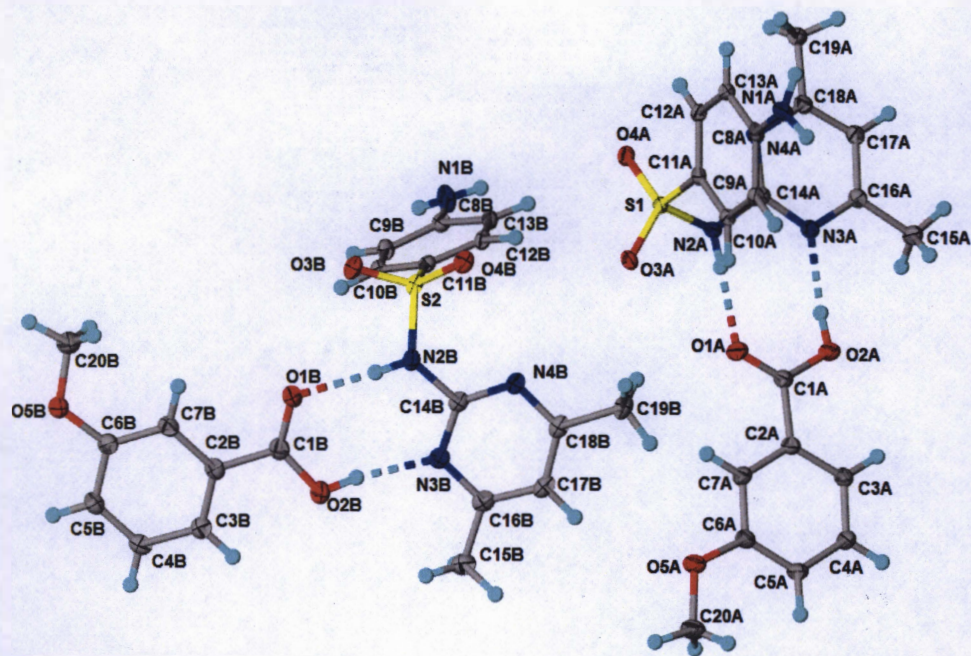


Figure S.13: Crystal Structure of the Cocrystal of Sulfamethazine and *m*-Methoxybenzoic Acid Showing Thermal Parameters (50% Thermal Ellipsoids) and Hydrogen Bonding.

#### Crystal data

$C_{12}H_{14}N_4O_2S \cdot C_8H_8O_3$

$M_r = 430.47$

Monoclinic,  $P2_1/n$

$a = 7.9803 (2) \text{ \AA}$

$b = 24.0097 (6) \text{ \AA}$

$c = 21.7459 (5) \text{ \AA}$

$\beta = 92.269 (1)^\circ$

$V = 4163.35 (18) \text{ \AA}^3$

$Z = 8$

$F(000) = 1808$

$D_x = 1.374 \text{ Mg m}^{-3}$

Melting point: 466–469 K

Cu  $K\alpha$  radiation,  $\lambda = 1.54178 \text{ \AA}$

Cell parameters from 9881 reflections

$\theta = 4.1\text{--}68.3^\circ$

$\mu = 1.73 \text{ mm}^{-1}$

$T = 100 \text{ K}$

Plates, colourless

$0.38 \times 0.27 \times 0.24 \text{ mm}$

#### Data collection

Bruker APEXII CCD  
diffractometer

Radiation source: fine-focus sealed tube

Detector resolution:  $8.33 \text{ pixels mm}^{-1}$

$\phi$  and  $\omega$  scans

Absorption correction: multi-scan

SADABS2014/7, Bruker AXS

7594 independent reflections

7113 reflections with  $I > 2\sigma(I)$

$R_{\text{int}} = 0.031$

$\theta_{\text{max}} = 68.2^\circ$ ,  $\theta_{\text{min}} = 2.7^\circ$

$h = -9 \text{--} 9$

$T_{\min} = 0.693$ ,  $T_{\max} = 0.753$   
62640 measured reflections

$k = -28 \quad 28$   
 $l = -26 \quad 26$

### Refinement

Refinement on  $F^2$   
Least-squares matrix: full

$R[F^2 > 2\sigma(F^2)] = 0.032$

$wR(F^2) = 0.084$

$S = 1.03$

7594 reflections

579 parameters

8 restraints

0 constraints

Hydrogen site location: mixed

H atoms treated by a mixture of independent and constrained refinement

$w = 1/[\sigma^2(F_o^2) + (0.0461P)^2 + 1.9388P]$

where  $P = (F_o^2 + 2F_c^2)/3$

$(\Delta/\sigma)_{\max} = 0.001$

$\Delta\rho_{\max} = 0.37 \text{ e } \text{\AA}^{-3}$

$\Delta\rho_{\min} = -0.43 \text{ e } \text{\AA}^{-3}$

Extinction correction: none

### Fractional atomic coordinates and isotropic or equivalent isotropic displacement parameters ( $\text{\AA}^2$ )

	x	y	z	$U_{\text{iso}}^*/U_{\text{eq}}$
S1	0.23997 (4)	0.13432 (2)	0.13533 (2)	0.01622 (8)
S2	0.25392 (4)	0.15845 (2)	0.40901 (2)	0.01810 (9)
O1A	0.32833 (17)	-0.01429 (5)	0.11601 (5)	0.0366 (3)
O2A	0.31480 (15)	-0.05108 (4)	0.02184 (5)	0.0313 (3)
H32A	0.276 (3)	-0.0177 (7)	0.0136 (10)	0.061 (7)*
O3A	0.28144 (12)	0.10178 (4)	0.18922 (4)	0.0210 (2)
O4A	0.11097 (12)	0.17557 (4)	0.13807 (4)	0.0203 (2)
O5A	0.54999 (17)	-0.16037 (4)	0.25428 (5)	0.0349 (3)
O1B	0.14120 (16)	0.09321 (5)	0.55306 (5)	0.0370 (3)
O2B	0.16208 (14)	0.00046 (4)	0.55851 (5)	0.0298 (2)
H32B	0.206 (3)	0.0048 (11)	0.5230 (9)	0.072 (8)*
O3B	0.22341 (12)	0.19296 (4)	0.46139 (5)	0.0237 (2)
O4B	0.38179 (12)	0.17417 (4)	0.36829 (5)	0.0237 (2)
O5B	-0.10284 (16)	0.14446 (4)	0.76031 (5)	0.0329 (3)
N1A	0.86671 (15)	0.24095 (5)	0.06146 (6)	0.0228 (3)
H30A	0.955 (2)	0.2197 (8)	0.0569 (9)	0.047 (6)*
H30B	0.861 (2)	0.2683 (7)	0.0363 (8)	0.031 (5)*
N2A	0.18555 (15)	0.08633 (5)	0.08389 (5)	0.0187 (2)
H31A	0.2282 (19)	0.0556 (6)	0.0931 (7)	0.018 (4)*
N3A	0.18752 (14)	0.05017 (5)	-0.01384 (5)	0.0190 (2)
N4A	0.11142 (14)	0.14556 (5)	0.00165 (5)	0.0194 (2)
N1B	-0.39092 (17)	0.14947 (6)	0.26960 (6)	0.0288 (3)
H30D	-0.395 (2)	0.1460 (7)	0.2313 (7)	0.029 (5)*
H30C	-0.478 (2)	0.1424 (8)	0.2893 (9)	0.041 (5)*
N2B	0.30035 (15)	0.09830 (5)	0.44192 (6)	0.0218 (3)
H31B	0.252 (2)	0.0957 (8)	0.4760 (8)	0.039 (5)*
N3B	0.31766 (15)	0.00308 (5)	0.44737 (5)	0.0225 (3)
N4B	0.41705 (14)	0.05161 (5)	0.35962 (5)	0.0212 (2)
C1A	0.35116 (18)	-0.05337 (6)	0.08139 (6)	0.0229 (3)
C2A	0.42278 (18)	-0.10707 (6)	0.10409 (6)	0.0210 (3)
C3A	0.45353 (19)	-0.15163 (6)	0.06505 (7)	0.0226 (3)
H3A	0.4311	-0.1485	0.0220	0.027*

C4A	0.51737 (19)	-0.20053 (6)	0.09029 (7)	0.0249 (3)
H4A	0.5383	-0.2312	0.0640	0.030*
C5A	0.55162 (19)	-0.20580 (6)	0.15333 (7)	0.0245 (3)
H5A	0.5952	-0.2397	0.1699	0.029*
C6A	0.52128 (19)	-0.16091 (6)	0.19179 (7)	0.0240 (3)
C7A	0.45675 (19)	-0.11159 (6)	0.16681 (7)	0.0244 (3)
H7A	0.4359	-0.0809	0.1930	0.029*
C8A	0.72018 (17)	0.21607 (6)	0.07690 (6)	0.0181 (3)
C9A	0.71868 (17)	0.16015 (6)	0.09701 (6)	0.0192 (3)
H9A	0.8202	0.1395	0.0993	0.023*
C10A	0.57155 (17)	0.13540 (6)	0.11333 (6)	0.0183 (3)
H10A	0.5714	0.0977	0.1265	0.022*
C11A	0.42181 (16)	0.16599 (6)	0.11042 (6)	0.0167 (3)
C12A	0.42027 (17)	0.22098 (6)	0.09020 (6)	0.0189 (3)
H12A	0.3180	0.2413	0.0876	0.023*
C13A	0.56810 (17)	0.24595 (6)	0.07387 (6)	0.0195 (3)
H13A	0.5672	0.2836	0.0605	0.023*
C14A	0.16033 (16)	0.09535 (6)	0.02077 (6)	0.0175 (3)
C15A	0.1931 (2)	0.00650 (6)	-0.11444 (7)	0.0272 (3)
H15A	0.3118	-0.0037	-0.1098	0.041*
H15B	0.1656	0.0154	-0.1576	0.041*
H15C	0.1238	-0.0248	-0.1016	0.041*
C16A	0.15972 (17)	0.05639 (6)	-0.07514 (6)	0.0205 (3)
C17A	0.10608 (18)	0.10677 (6)	-0.09947 (6)	0.0226 (3)
H17A	0.0847	0.1110	-0.1425	0.027*
C18A	0.08404 (18)	0.15111 (6)	-0.05966 (6)	0.0212 (3)
C19A	0.0261 (2)	0.20705 (6)	-0.08257 (7)	0.0289 (3)
H19A	-0.0918	0.2124	-0.0730	0.043*
H19B	0.0378	0.2091	-0.1272	0.043*
H19C	0.0944	0.2362	-0.0625	0.043*
C20A	0.5998 (3)	-0.21169 (8)	0.28297 (8)	0.0442 (5)
H20A	0.5109	-0.2394	0.2762	0.066*
H20B	0.6193	-0.2057	0.3273	0.066*
H20C	0.7032	-0.2251	0.2651	0.066*
C1B	0.12032 (19)	0.04958 (6)	0.58045 (7)	0.0254 (3)
C2B	0.04407 (18)	0.04766 (6)	0.64186 (6)	0.0231 (3)
C3B	0.01110 (18)	-0.00267 (6)	0.67031 (7)	0.0243 (3)
H3B	0.0375	-0.0369	0.6510	0.029*
C4B	-0.06123 (18)	-0.00237 (6)	0.72755 (7)	0.0257 (3)
H4B	-0.0855	-0.0366	0.7472	0.031*
C5B	-0.09771 (19)	0.04721 (6)	0.75583 (7)	0.0255 (3)
H5B	-0.1465	0.0469	0.7950	0.031*
C6B	-0.06362 (19)	0.09790 (6)	0.72743 (7)	0.0249 (3)
C7B	0.00687 (19)	0.09842 (6)	0.67004 (7)	0.0247 (3)
H7B	0.0295	0.1327	0.6502	0.030*
C8B	-0.24063 (17)	0.14730 (6)	0.30117 (6)	0.0202 (3)
C9B	-0.23388 (17)	0.14531 (6)	0.36612 (6)	0.0205 (3)
H9B	-0.3348	0.1427	0.3877	0.025*
C10B	-0.08261 (17)	0.14718 (6)	0.39841 (6)	0.0185 (3)
H10B	-0.0790	0.1462	0.4421	0.022*
C11B	0.06606 (16)	0.15058 (5)	0.36674 (6)	0.0172 (3)
C12B	0.06281 (17)	0.15062 (6)	0.30280 (6)	0.0197 (3)
H12B	0.1646	0.1519	0.2816	0.024*
C13B	-0.08921 (18)	0.14872 (6)	0.27026 (6)	0.0203 (3)
H13B	-0.0915	0.1484	0.2265	0.024*



C14B	0.34628 (17)	0.04883 (6)	0.41380 (6)	0.0201 (3)
C15B	0.3325 (2)	-0.09738 (7)	0.45917 (8)	0.0323 (4)
H15D	0.3561	-0.0904	0.5031	0.048*
H15E	0.4039	-0.1277	0.4454	0.048*
H15F	0.2144	-0.1078	0.4526	0.048*
C16B	0.36762 (18)	-0.04567 (6)	0.42323 (7)	0.0247 (3)
C17B	0.44477 (18)	-0.04708 (6)	0.36738 (7)	0.0258 (3)
H17B	0.4812	-0.0814	0.3507	0.031*
C18B	0.46776 (17)	0.00262 (6)	0.33628 (7)	0.0233 (3)
C19B	0.5509 (2)	0.00518 (7)	0.27588 (7)	0.0288 (3)
H19D	0.4677	0.0150	0.2433	0.043*
H19E	0.5998	-0.0312	0.2669	0.043*
H19F	0.6395	0.0334	0.2779	0.043*
C20B	-0.1110 (3)	0.19639 (7)	0.72858 (8)	0.0422 (4)
H20D	0.0006	0.2061	0.7146	0.063*
H20E	-0.1497	0.2254	0.7563	0.063*
H20F	-0.1895	0.1933	0.6929	0.063*

### Atomic displacement parameters ( $\text{\AA}^2$ )

	$U^{11}$	$U^{22}$	$U^{33}$	$U^{12}$	$U^{13}$	$U^{23}$
S1	0.01647 (16)	0.01908 (16)	0.01319 (15)	0.00140 (12)	0.00138 (12)	0.00057 (12)
S2	0.01453 (16)	0.01959 (17)	0.02021 (17)	-0.00098 (12)	0.00102 (12)	-0.00501 (12)
O1A	0.0665 (8)	0.0228 (6)	0.0200 (5)	0.0149 (5)	-0.0047 (5)	-0.0009 (4)
O2A	0.0525 (7)	0.0226 (5)	0.0183 (5)	0.0105 (5)	-0.0060 (5)	0.0002 (4)
O3A	0.0235 (5)	0.0251 (5)	0.0146 (5)	0.0015 (4)	0.0017 (4)	0.0025 (4)
O4A	0.0184 (5)	0.0234 (5)	0.0192 (5)	0.0030 (4)	0.0033 (4)	-0.0009 (4)
O5A	0.0606 (8)	0.0248 (6)	0.0184 (5)	0.0106 (5)	-0.0080 (5)	0.0013 (4)
O1B	0.0558 (8)	0.0293 (6)	0.0270 (6)	0.0063 (5)	0.0147 (5)	0.0035 (5)
O2B	0.0376 (6)	0.0274 (6)	0.0248 (6)	0.0004 (5)	0.0057 (5)	-0.0024 (4)
O3B	0.0214 (5)	0.0254 (5)	0.0242 (5)	-0.0006 (4)	-0.0003 (4)	-0.0094 (4)
O4B	0.0171 (5)	0.0245 (5)	0.0298 (5)	-0.0037 (4)	0.0041 (4)	-0.0044 (4)
O5B	0.0503 (7)	0.0258 (5)	0.0228 (5)	0.0037 (5)	0.0056 (5)	-0.0003 (4)
N1A	0.0190 (6)	0.0274 (7)	0.0222 (6)	0.0016 (5)	0.0016 (5)	0.0076 (5)
N2A	0.0231 (6)	0.0164 (6)	0.0164 (6)	0.0010 (5)	-0.0008 (5)	0.0024 (4)
N3A	0.0198 (6)	0.0195 (6)	0.0176 (6)	-0.0004 (4)	-0.0017 (4)	0.0006 (4)
N4A	0.0203 (6)	0.0200 (6)	0.0181 (6)	0.0012 (4)	0.0013 (5)	0.0018 (4)
N1B	0.0198 (7)	0.0484 (8)	0.0182 (6)	-0.0004 (6)	-0.0007 (5)	-0.0028 (6)
N2B	0.0214 (6)	0.0260 (6)	0.0181 (6)	0.0032 (5)	0.0008 (5)	-0.0029 (5)
N3B	0.0190 (6)	0.0256 (6)	0.0226 (6)	0.0021 (5)	-0.0036 (5)	-0.0014 (5)
N4B	0.0182 (6)	0.0238 (6)	0.0213 (6)	0.0010 (5)	-0.0021 (5)	-0.0050 (5)
C1A	0.0280 (8)	0.0205 (7)	0.0199 (7)	0.0012 (6)	-0.0003 (6)	0.0016 (6)
C2A	0.0240 (7)	0.0184 (7)	0.0205 (7)	-0.0004 (5)	-0.0002 (5)	0.0012 (5)
C3A	0.0285 (8)	0.0212 (7)	0.0180 (7)	-0.0015 (6)	-0.0011 (6)	-0.0001 (5)
C4A	0.0328 (8)	0.0185 (7)	0.0235 (7)	0.0004 (6)	0.0014 (6)	-0.0029 (6)
C5A	0.0301 (8)	0.0180 (7)	0.0253 (7)	0.0025 (6)	-0.0005 (6)	0.0036 (6)
C6A	0.0307 (8)	0.0225 (7)	0.0184 (7)	0.0010 (6)	-0.0029 (6)	0.0013 (5)
C7A	0.0332 (8)	0.0191 (7)	0.0206 (7)	0.0032 (6)	-0.0007 (6)	-0.0025 (5)
C8A	0.0191 (7)	0.0242 (7)	0.0111 (6)	0.0003 (5)	0.0002 (5)	-0.0015 (5)
C9A	0.0183 (7)	0.0233 (7)	0.0158 (6)	0.0047 (5)	-0.0011 (5)	-0.0006 (5)
C10A	0.0207 (7)	0.0191 (7)	0.0148 (6)	0.0027 (5)	-0.0003 (5)	0.0002 (5)
C11A	0.0171 (6)	0.0201 (6)	0.0128 (6)	-0.0002 (5)	0.0007 (5)	-0.0018 (5)
C12A	0.0190 (7)	0.0213 (7)	0.0164 (6)	0.0051 (5)	0.0007 (5)	-0.0013 (5)
C13A	0.0237 (7)	0.0188 (6)	0.0163 (6)	0.0019 (5)	0.0020 (5)	0.0008 (5)

C14A	0.0147 (6)	0.0201 (6)	0.0178 (6)	-0.0015 (5)	0.0000 (5)	0.0007 (5)
C15A	0.0373 (9)	0.0232 (7)	0.0206 (7)	0.0047 (6)	-0.0037 (6)	-0.0021 (6)
C16A	0.0201 (7)	0.0227 (7)	0.0185 (7)	-0.0009 (5)	-0.0010 (5)	0.0001 (5)
C17A	0.0253 (7)	0.0253 (7)	0.0171 (7)	0.0026 (6)	-0.0014 (5)	0.0010 (6)
C18A	0.0208 (7)	0.0231 (7)	0.0195 (7)	0.0021 (5)	0.0007 (5)	0.0029 (5)
C19A	0.0405 (9)	0.0256 (8)	0.0206 (7)	0.0107 (7)	0.0020 (6)	0.0039 (6)
C20A	0.0746 (14)	0.0337 (9)	0.0235 (8)	0.0185 (9)	-0.0078 (8)	0.0056 (7)
C1B	0.0250 (8)	0.0294 (8)	0.0215 (7)	0.0003 (6)	-0.0025 (6)	-0.0012 (6)
C2B	0.0212 (7)	0.0282 (8)	0.0195 (7)	-0.0021 (6)	-0.0032 (6)	-0.0002 (6)
C3B	0.0233 (7)	0.0257 (7)	0.0237 (7)	-0.0020 (6)	-0.0032 (6)	-0.0023 (6)
C4B	0.0253 (7)	0.0261 (7)	0.0255 (7)	-0.0041 (6)	-0.0028 (6)	0.0043 (6)
C5B	0.0251 (7)	0.0315 (8)	0.0198 (7)	-0.0015 (6)	0.0001 (6)	0.0019 (6)
C6B	0.0277 (8)	0.0260 (7)	0.0209 (7)	0.0004 (6)	-0.0032 (6)	-0.0016 (6)
C7B	0.0277 (8)	0.0250 (7)	0.0212 (7)	-0.0019 (6)	-0.0011 (6)	0.0023 (6)
C8B	0.0200 (7)	0.0203 (7)	0.0203 (7)	-0.0009 (5)	-0.0003 (5)	-0.0020 (5)
C9B	0.0163 (7)	0.0254 (7)	0.0201 (7)	-0.0017 (5)	0.0043 (5)	-0.0007 (5)
C10B	0.0193 (7)	0.0207 (7)	0.0157 (6)	-0.0008 (5)	0.0016 (5)	-0.0008 (5)
C11B	0.0157 (6)	0.0157 (6)	0.0203 (7)	-0.0003 (5)	0.0000 (5)	-0.0022 (5)
C12B	0.0192 (7)	0.0196 (7)	0.0206 (7)	-0.0012 (5)	0.0058 (5)	-0.0035 (5)
C13B	0.0235 (7)	0.0216 (7)	0.0160 (6)	-0.0011 (5)	0.0029 (5)	-0.0022 (5)
C14B	0.0141 (6)	0.0239 (7)	0.0217 (7)	0.0015 (5)	-0.0049 (5)	-0.0033 (5)
C15B	0.0344 (9)	0.0269 (8)	0.0355 (9)	0.0023 (6)	-0.0021 (7)	0.0023 (7)
C16B	0.0192 (7)	0.0264 (7)	0.0281 (8)	0.0021 (6)	-0.0063 (6)	-0.0016 (6)
C17B	0.0219 (7)	0.0231 (7)	0.0321 (8)	0.0028 (6)	-0.0027 (6)	-0.0068 (6)
C18B	0.0163 (7)	0.0272 (7)	0.0261 (7)	0.0009 (5)	-0.0043 (6)	-0.0076 (6)
C19B	0.0284 (8)	0.0289 (8)	0.0295 (8)	0.0009 (6)	0.0045 (6)	-0.0090 (6)
C20B	0.0648 (12)	0.0262 (8)	0.0363 (9)	0.0041 (8)	0.0114 (9)	0.0022 (7)

### Geometric parameters (Å, °)

S1—O4A	1.4314 (10)	C11A—C12A	1.3916 (19)
S1—O3A	1.4361 (10)	C12A—C13A	1.382 (2)
S1—N2A	1.6520 (12)	C12A—H12A	0.9500
S1—C11A	1.7434 (13)	C13A—H13A	0.9500
S2—O4B	1.4281 (10)	C15A—C16A	1.5013 (19)
S2—O3B	1.4371 (10)	C15A—H15A	0.9800
S2—N2B	1.6474 (12)	C15A—H15B	0.9800
S2—C11B	1.7376 (14)	C15A—H15C	0.9800
O1A—C1A	1.2211 (18)	C16A—C17A	1.382 (2)
O2A—C1A	1.3169 (17)	C17A—C18A	1.388 (2)
O2A—H32A	0.876 (16)	C17A—H17A	0.9500
O5A—C6A	1.3693 (17)	C18A—C19A	1.4990 (19)
O5A—C20A	1.4301 (19)	C19A—H19A	0.9800
O1B—C1B	1.2198 (19)	C19A—H19B	0.9800
O2B—C1B	1.3199 (19)	C19A—H19C	0.9800
O2B—H32B	0.867 (17)	C20A—H20A	0.9800
O5B—C6B	1.3699 (18)	C20A—H20B	0.9800
O5B—C20B	1.425 (2)	C20A—H20C	0.9800
N1A—C8A	1.3668 (18)	C1B—C2B	1.490 (2)
N1A—H30A	0.876 (15)	C2B—C3B	1.388 (2)
N1A—H30B	0.855 (14)	C2B—C7B	1.401 (2)
N2A—C14A	1.3964 (17)	C3B—C4B	1.393 (2)
N2A—H31A	0.834 (13)	C3B—H3B	0.9500
N3A—C14A	1.3427 (17)	C4B—C5B	1.376 (2)
N3A—C16A	1.3510 (18)	C4B—H4B	0.9500
N4A—C14A	1.3288 (18)	C5B—C6B	1.396 (2)

N4A—C18A	1.3492 (18)	C5B—H5B	0.9500
N1B—C8B	1.3592 (19)	C6B—C7B	1.389 (2)
N1B—H30D	0.837 (14)	C7B—H7B	0.9500
N1B—H30C	0.848 (15)	C8B—C13B	1.406 (2)
N2B—C14B	1.3918 (18)	C8B—C9B	1.4121 (19)
N2B—H31B	0.853 (15)	C9B—C10B	1.373 (2)
N3B—C14B	1.3435 (19)	C9B—H9B	0.9500
N3B—C16B	1.3495 (19)	C10B—C11B	1.3976 (19)
N4B—C14B	1.3281 (19)	C10B—H10B	0.9500
N4B—C18B	1.3494 (18)	C11B—C12B	1.3896 (19)
C1A—C2A	1.4867 (19)	C12B—C13B	1.381 (2)
C2A—C7A	1.384 (2)	C12B—H12B	0.9500
C2A—C3A	1.393 (2)	C13B—H13B	0.9500
C3A—C4A	1.385 (2)	C15B—C16B	1.499 (2)
C3A—H3A	0.9500	C15B—H15D	0.9800
C4A—C5A	1.393 (2)	C15B—H15E	0.9800
C4A—H4A	0.9500	C15B—H15F	0.9800
C5A—C6A	1.391 (2)	C16B—C17B	1.384 (2)
C5A—H5A	0.9500	C17B—C18B	1.387 (2)
C6A—C7A	1.393 (2)	C17B—H17B	0.9500
C7A—H7A	0.9500	C18B—C19B	1.496 (2)
C8A—C13A	1.4092 (19)	C19B—H19D	0.9800
C8A—C9A	1.4122 (19)	C19B—H19E	0.9800
C9A—C10A	1.375 (2)	C19B—H19F	0.9800
C9A—H9A	0.9500	C20B—H20D	0.9800
C10A—C11A	1.4020 (19)	C20B—H20E	0.9800
C10A—H10A	0.9500	C20B—H20F	0.9800
O4A—S1—O3A	119.04 (6)	C18A—C17A—H17A	120.7
O4A—S1—N2A	109.91 (6)	N4A—C18A—C17A	121.41 (13)
O3A—S1—N2A	102.64 (6)	N4A—C18A—C19A	116.91 (12)
O4A—S1—C11A	108.66 (6)	C17A—C18A—C19A	121.67 (13)
O3A—S1—C11A	108.84 (6)	C18A—C19A—H19A	109.5
N2A—S1—C11A	107.07 (6)	C18A—C19A—H19B	109.5
O4B—S2—O3B	119.12 (6)	H19A—C19A—H19B	109.5
O4B—S2—N2B	110.31 (6)	C18A—C19A—H19C	109.5
O3B—S2—N2B	101.73 (6)	H19A—C19A—H19C	109.5
O4B—S2—C11B	108.87 (6)	H19B—C19A—H19C	109.5
O3B—S2—C11B	108.20 (6)	O5A—C20A—H20A	109.5
N2B—S2—C11B	108.01 (6)	O5A—C20A—H20B	109.5
C1A—O2A—H32A	107.6 (15)	H20A—C20A—H20B	109.5
C6A—O5A—C20A	117.21 (12)	O5A—C20A—H20C	109.5
C1B—O2B—H32B	109.3 (17)	H20A—C20A—H20C	109.5
C6B—O5B—C20B	117.91 (12)	H20B—C20A—H20C	109.5
C8A—N1A—H30A	117.9 (14)	O1B—C1B—O2B	123.34 (13)
C8A—N1A—H30B	117.9 (12)	O1B—C1B—C2B	122.19 (14)
H30A—N1A—H30B	113.6 (18)	O2B—C1B—C2B	114.48 (13)
C14A—N2A—S1	125.53 (10)	C3B—C2B—C7B	121.01 (13)
C14A—N2A—H31A	114.6 (11)	C3B—C2B—C1B	121.20 (13)
S1—N2A—H31A	111.1 (11)	C7B—C2B—C1B	117.79 (13)
C14A—N3A—C16A	116.10 (12)	C2B—C3B—C4B	119.13 (14)
C14A—N4A—C18A	115.64 (12)	C2B—C3B—H3B	120.4
C8B—N1B—H30D	119.7 (13)	C4B—C3B—H3B	120.4
C8B—N1B—H30C	117.5 (14)	C5B—C4B—C3B	120.41 (14)
H30D—N1B—H30C	118.9 (19)	C5B—C4B—H4B	119.8
C14B—N2B—S2	128.01 (10)	C3B—C4B—H4B	119.8

C14B—N2B—H31B	117.2 (13)	C4B—C5B—C6B	120.53 (14)
S2—N2B—H31B	109.8 (13)	C4B—C5B—H5B	119.7
C14B—N3B—C16B	116.01 (12)	C6B—C5B—H5B	119.7
C14B—N4B—C18B	115.74 (13)	O5B—C6B—C7B	124.80 (13)
O1A—C1A—O2A	122.81 (13)	O5B—C6B—C5B	115.33 (13)
O1A—C1A—C2A	121.76 (13)	C7B—C6B—C5B	119.86 (14)
O2A—C1A—C2A	115.43 (12)	C6B—C7B—C2B	119.05 (14)
C7A—C2A—C3A	120.50 (13)	C6B—C7B—H7B	120.5
C7A—C2A—C1A	116.93 (13)	C2B—C7B—H7B	120.5
C3A—C2A—C1A	122.57 (13)	N1B—C8B—C13B	121.02 (13)
C4A—C3A—C2A	118.72 (13)	N1B—C8B—C9B	120.30 (13)
C4A—C3A—H3A	120.6	C13B—C8B—C9B	118.65 (13)
C2A—C3A—H3A	120.6	C10B—C9B—C8B	120.55 (12)
C3A—C4A—C5A	121.46 (13)	C10B—C9B—H9B	119.7
C3A—C4A—H4A	119.3	C8B—C9B—H9B	119.7
C5A—C4A—H4A	119.3	C9B—C10B—C11B	119.76 (13)
C6A—C5A—C4A	119.29 (13)	C9B—C10B—H10B	120.1
C6A—C5A—H5A	120.4	C11B—C10B—H10B	120.1
C4A—C5A—H5A	120.4	C12B—C11B—C10B	120.70 (13)
O5A—C6A—C5A	125.29 (13)	C12B—C11B—S2	120.72 (10)
O5A—C6A—C7A	115.07 (13)	C10B—C11B—S2	118.50 (10)
C5A—C6A—C7A	119.64 (13)	C13B—C12B—C11B	119.60 (12)
C2A—C7A—C6A	120.39 (13)	C13B—C12B—H12B	120.2
C2A—C7A—H7A	119.8	C11B—C12B—H12B	120.2
C6A—C7A—H7A	119.8	C12B—C13B—C8B	120.66 (13)
N1A—C8A—C13A	120.63 (13)	C12B—C13B—H13B	119.7
N1A—C8A—C9A	120.63 (12)	C8B—C13B—H13B	119.7
C13A—C8A—C9A	118.73 (12)	N4B—C14B—N3B	127.63 (13)
C10A—C9A—C8A	120.58 (12)	N4B—C14B—N2B	118.40 (13)
C10A—C9A—H9A	119.7	N3B—C14B—N2B	113.92 (12)
C8A—C9A—H9A	119.7	C16B—C15B—H15D	109.5
C9A—C10A—C11A	119.80 (12)	C16B—C15B—H15E	109.5
C9A—C10A—H10A	120.1	H15D—C15B—H15E	109.5
C11A—C10A—H10A	120.1	C16B—C15B—H15F	109.5
C12A—C11A—C10A	120.54 (12)	H15D—C15B—H15F	109.5
C12A—C11A—S1	120.99 (10)	H15E—C15B—H15F	109.5
C10A—C11A—S1	118.43 (10)	N3B—C16B—C17B	120.75 (14)
C13A—C12A—C11A	119.73 (12)	N3B—C16B—C15B	116.81 (13)
C13A—C12A—H12A	120.1	C17B—C16B—C15B	122.43 (14)
C11A—C12A—H12A	120.1	C16B—C17B—C18B	118.61 (13)
C12A—C13A—C8A	120.62 (12)	C16B—C17B—H17B	120.7
C12A—C13A—H13A	119.7	C18B—C17B—H17B	120.7
C8A—C13A—H13A	119.7	N4B—C18B—C17B	121.26 (13)
N4A—C14A—N3A	127.56 (12)	N4B—C18B—C19B	116.39 (13)
N4A—C14A—N2A	118.52 (12)	C17B—C18B—C19B	122.35 (13)
N3A—C14A—N2A	113.91 (12)	C18B—C19B—H19D	109.5
C16A—C15A—H15A	109.5	C18B—C19B—H19E	109.5
C16A—C15A—H15B	109.5	H19D—C19B—H19E	109.5
H15A—C15A—H15B	109.5	C18B—C19B—H19F	109.5
C16A—C15A—H15C	109.5	H19D—C19B—H19F	109.5
H15A—C15A—H15C	109.5	H19E—C19B—H19F	109.5
H15B—C15A—H15C	109.5	O5B—C20B—H20D	109.5
N3A—C16A—C17A	120.73 (13)	O5B—C20B—H20E	109.5
N3A—C16A—C15A	116.60 (12)	H20D—C20B—H20E	109.5
C17A—C16A—C15A	122.67 (12)	O5B—C20B—H20F	109.5

C16A—C17A—C18A	118.54 (13)	H20D—C20B—H20F	109.5
C16A—C17A—H17A	120.7	H20E—C20B—H20F	109.5
O4A—S1—N2A—C14A	63.59 (12)	C14A—N4A—C18A— C19A	179.07 (13)
O3A—S1—N2A—C14A	-168.80 (11)	C16A—C17A—C18A— N4A	-1.0 (2)
C11A—S1—N2A—C14A	-54.27 (13)	C16A—C17A—C18A— C19A	-179.98 (14)
O4B—S2—N2B—C14B	-50.73 (14)	O1B—C1B—C2B—C3B	175.59 (15)
O3B—S2—N2B—C14B	-178.09 (12)	O2B—C1B—C2B—C3B	-4.1 (2)
C11B—S2—N2B—C14B	68.15 (13)	O1B—C1B—C2B—C7B	-4.5 (2)
O1A—C1A—C2A—C7A	2.4 (2)	O2B—C1B—C2B—C7B	175.77 (13)
O2A—C1A—C2A—C7A	-177.71 (13)	C7B—C2B—C3B—C4B	0.5 (2)
O1A—C1A—C2A—C3A	-178.39 (15)	C1B—C2B—C3B—C4B	-179.61 (13)
O2A—C1A—C2A—C3A	1.5 (2)	C2B—C3B—C4B—C5B	-0.7 (2)
C7A—C2A—C3A—C4A	0.5 (2)	C3B—C4B—C5B—C6B	0.3 (2)
C1A—C2A—C3A—C4A	-178.73 (14)	C20B—O5B—C6B—C7B	16.0 (2)
C2A—C3A—C4A—C5A	-0.3 (2)	C20B—O5B—C6B—C5B	-164.68 (15)
C3A—C4A—C5A—C6A	-0.1 (2)	C4B—C5B—C6B—O5B	-179.04 (14)
C20A—O5A—C6A—C5A	-6.4 (2)	C4B—C5B—C6B—C7B	0.3 (2)
C20A—O5A—C6A—C7A	173.73 (16)	O5B—C6B—C7B—C2B	178.71 (14)
C4A—C5A—C6A—O5A	-179.65 (15)	C5B—C6B—C7B—C2B	-0.6 (2)
C4A—C5A—C6A—C7A	0.2 (2)	C3B—C2B—C7B—C6B	0.2 (2)
C3A—C2A—C7A—C6A	-0.4 (2)	C1B—C2B—C7B—C6B	-179.72 (13)
C1A—C2A—C7A—C6A	178.89 (14)	N1B—C8B—C9B—C10B	-175.26 (14)
O5A—C6A—C7A—C2A	179.90 (14)	C13B—C8B—C9B—C10B	2.8 (2)
C5A—C6A—C7A—C2A	0.0 (2)	C8B—C9B—C10B—C11B	-0.6 (2)
N1A—C8A—C9A—C10A	179.12 (12)	C9B—C10B—C11B—C12B	-1.7 (2)
C13A—C8A—C9A—C10A	-0.01 (19)	C9B—C10B—C11B—S2	174.97 (11)
C8A—C9A—C10A—C11A	-0.47 (19)	O4B—S2—C11B—C12B	10.34 (13)
C9A—C10A—C11A—C12A	1.05 (19)	O3B—S2—C11B—C12B	141.16 (11)
C9A—C10A—C11A—S1	-176.66 (10)	N2B—S2—C11B—C12B	-109.45 (12)
O4A—S1—C11A—C12A	-7.36 (13)	O4B—S2—C11B—C10B	-166.33 (10)
O3A—S1—C11A—C12A	-138.39 (11)	O3B—S2—C11B—C10B	-35.50 (12)
N2A—S1—C11A—C12A	111.32 (11)	N2B—S2—C11B—C10B	73.88 (12)
O4A—S1—C11A—C10A	170.35 (10)	C10B—C11B—C12B— C13B	1.7 (2)
O3A—S1—C11A—C10A	39.31 (12)	S2—C11B—C12B—C13B	-174.91 (10)
N2A—S1—C11A—C10A	-70.98 (12)	C11B—C12B—C13B—C8B	0.6 (2)
C10A—C11A—C12A— C13A	-1.15 (19)	N1B—C8B—C13B—C12B	175.22 (14)
S1—C11A—C12A—C13A	176.51 (10)	C9B—C8B—C13B—C12B	-2.8 (2)
C11A—C12A—C13A—C8A	0.7 (2)	C18B—N4B—C14B—N3B	-0.9 (2)
N1A—C8A—C13A—C12A	-179.22 (12)	C18B—N4B—C14B—N2B	176.28 (12)
C9A—C8A—C13A—C12A	-0.09 (19)	C16B—N3B—C14B—N4B	0.4 (2)
C18A—N4A—C14A—N3A	1.0 (2)	C16B—N3B—C14B—N2B	-176.96 (12)
C18A—N4A—C14A—N2A	-177.95 (12)	S2—N2B—C14B—N4B	25.42 (18)
C16A—N3A—C14A—N4A	-0.9 (2)	S2—N2B—C14B—N3B	-156.99 (10)
C16A—N3A—C14A—N2A	178.04 (11)	C14B—N3B—C16B—C17B	0.56 (19)
S1—N2A—C14A—N4A	-27.82 (18)	C14B—N3B—C16B—C15B	-178.35 (13)
S1—N2A—C14A—N3A	153.09 (10)	N3B—C16B—C17B—C18B	-0.8 (2)
C14A—N3A—C16A— C17A	-0.15 (19)	C15B—C16B—C17B— C18B	178.00 (14)
C14A—N3A—C16A— C15A	178.77 (12)	C14B—N4B—C18B—C17B	0.58 (19)

C14A—N3A—C16A— C15A	178.77 (12)	C14B—N4B—C18B—C17B	0.58 (19)
N3A—C16A—C17A— C18A	1.1 (2)	C14B—N4B—C18B—C19B	-178.81 (12)
C15A—C16A—C17A— C18A	-177.80 (13)	C16B—C17B—C18B—N4B	0.2 (2)
C14A—N4A—C18A— C17A	0.0 (2)	C16B—C17B—C18B— C19B	179.60 (13)

#### Hydrogen-bond geometry (Å, °)

<i>D</i> —H··· <i>A</i>	<i>D</i> —H	H··· <i>A</i>	<i>D</i> ··· <i>A</i>	<i>D</i> —H··· <i>A</i>
N1A—H30A···O4 <i>A</i> i	0.88 (2)	2.37 (2)	2.9635 (16)	125 (2)
N1A—H30B···O3Bii	0.86 (1)	2.14 (2)	2.8920 (16)	147 (2)
N1B—H30C···O4Biii	0.85 (2)	2.22 (2)	2.9250 (17)	140 (2)
N2A—H31A···O1A	0.83 (1)	1.92 (1)	2.7495 (16)	179 (2)
N2B—H31B···O1B	0.85 (2)	1.93 (2)	2.7770 (16)	178 (2)
O2A—H32A···N3A	0.88 (2)	1.86 (2)	2.7353 (15)	173 (2)
O2B—H32B···N3B	0.87 (2)	1.90 (2)	2.7612 (16)	171 (3)

Symmetry codes: (i)  $x+1, y, z$ ; (ii)  $x+1/2, -y+1/2, z-1/2$ ; (iii)  $x-1, y, z$ .

All esds (except the esd in the dihedral angle between two l.s. planes) are estimated using the full covariance matrix. The cell esds are taken into account individually in the estimation of esds in distances, angles and torsion angles; correlations between esds in cell parameters are only used when they are defined by crystal symmetry. An approximate (isotropic) treatment of cell esds is used for estimating esds involving l.s. planes.

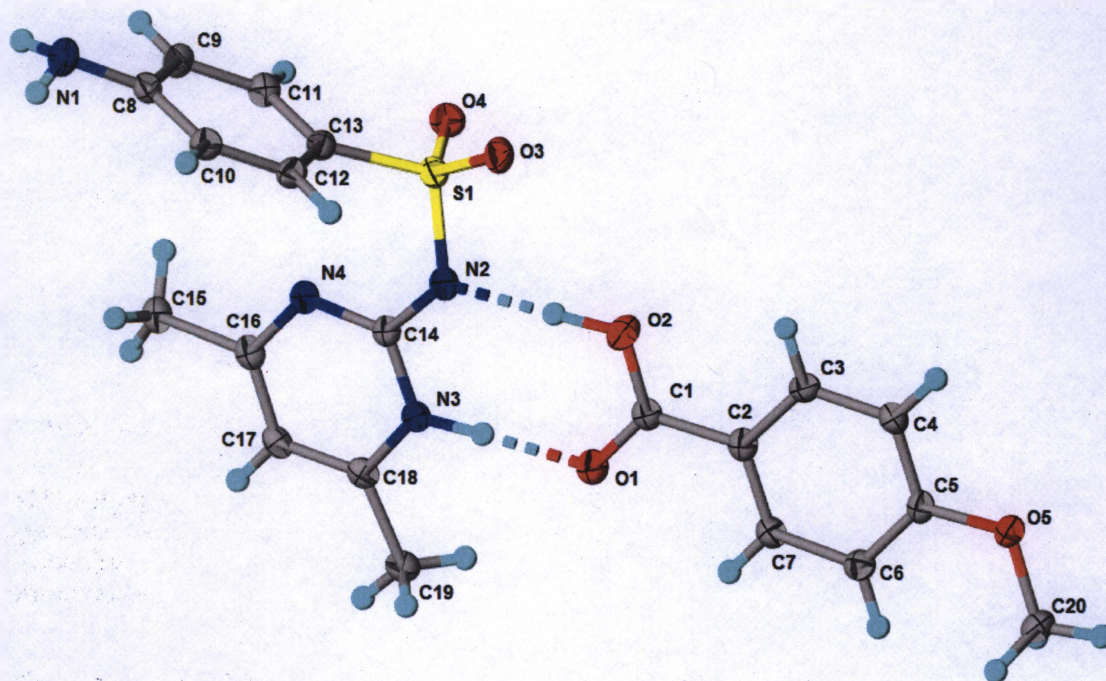


Figure S.14: Crystal Structure of the Cocrystal of Sulfamethazine and *p*-Methoxybenzoic Acid Showing Thermal Parameters (50% Thermal Ellipsoids) and Hydrogen Bonding.

### Crystal data

$C_{12}H_{14}N_4O_2S \cdot C_8H_8O_3$

$M_r = 430.47$

Monoclinic,  $P2_1/c$

$a = 8.1902$  (3) Å

$b = 21.2180$  (9) Å

$c = 12.3529$  (5) Å

$\beta = 108.135$  (2)°

$V = 2040.05$  (14) Å<sup>3</sup>

$Z = 4$

$F(000) = 904$

$D_x = 1.402$  Mg m<sup>-3</sup>

Melting point: 447-451 K

Cu  $K\alpha$  radiation,  $\lambda = 1.54178$  Å

Cell parameters from 6506 reflections

$\theta = 4.2$ – $68.1$ °

$\mu = 1.76$  mm<sup>-1</sup>

$T = 100$  K

Plate, colourless

$0.39 \times 0.18 \times 0.12$  mm

### Data collection

Bruker APEXII CCD

diffractometer

Radiation source: fine-focus sealed tube

Detector resolution: 8.33 pixels mm<sup>-1</sup>

phi and  $\omega$  scans

Absorption correction: multi-scan

SADABS2014/7, Bruker AXS

$T_{\min} = 0.567$ ,  $T_{\max} = 0.753$

30180 measured reflections

3711 independent reflections

3174 reflections with  $I > 2\sigma(I)$

$R_{\text{int}} = 0.057$

$\theta_{\max} = 68.2$ °,  $\theta_{\min} = 4.2$ °

$h = -9$  9

$k = -25$  25

$l = -14$  13

### Refinement

Refinement on  $F^2$

Least-squares matrix: full

$R[F^2 > 2\sigma(F^2)] = 0.059$

$wR(F^2) = 0.180$

$S = 1.14$

3711 reflections

290 parameters

3 restraints

0 constraints

Hydrogen site location: mixed

H atoms treated by a mixture of independent and constrained refinement

$w = 1/[\sigma^2(F_o^2) + (0.0947P)^2 + 2.847P]$

where  $P = (F_o^2 + 2F_c^2)/3$

$(\Delta/\sigma)_{\max} < 0.001$

$\Delta\rho_{\max} = 0.73$  e Å<sup>-3</sup>

$\Delta\rho_{\min} = -0.49$  e Å<sup>-3</sup>

Extinction correction: none

### Fractional atomic coordinates and isotropic or equivalent isotropic displacement parameters (Å<sup>2</sup>)

	<i>x</i>	<i>y</i>	<i>z</i>	$U_{\text{iso}}^*/U_{\text{eq}}$
S1	0.06326 (9)	0.68737 (3)	0.43157 (6)	0.0242 (2)



O1	0.2859 (3)	0.47278 (10)	0.51964 (19)	0.0310 (5)
O2	0.3423 (3)	0.56881 (10)	0.5985 (2)	0.0314 (5)
H32	0.233 (8)	0.585 (3)	0.534 (5)	0.085 (18)*
O4	0.1451 (3)	0.71128 (10)	0.3519 (2)	0.0314 (5)
O3	0.1443 (3)	0.70235 (10)	0.5506 (2)	0.0323 (6)
O5	0.9327 (3)	0.41452 (10)	0.95129 (18)	0.0260 (5)
N1	-0.6249 (4)	0.80618 (14)	0.2994 (3)	0.0305 (6)
H30A	-0.673 (7)	0.816 (2)	0.228 (5)	0.059 (15)*
H30B	-0.699 (6)	0.789 (2)	0.321 (4)	0.043 (12)*
N2	0.0604 (3)	0.61074 (12)	0.4308 (2)	0.0239 (6)
H31	0.114 (7)	0.500 (2)	0.415 (4)	0.071 (15)*
N4	-0.1457 (3)	0.60230 (12)	0.2494 (2)	0.0224 (5)
N3	0.0138 (3)	0.51417 (12)	0.3441 (2)	0.0223 (5)
C1	0.3748 (4)	0.50916 (14)	0.5954 (3)	0.0229 (6)
C2	0.5235 (4)	0.48422 (14)	0.6878 (3)	0.0227 (6)
C3	0.6232 (4)	0.52340 (14)	0.7746 (3)	0.0227 (6)
H3	0.5968	0.5670	0.7745	0.027*
C4	0.7599 (4)	0.49880 (14)	0.8605 (3)	0.0235 (6)
H4	0.8286	0.5256	0.9186	0.028*
C5	0.7966 (4)	0.43441 (14)	0.8616 (3)	0.0216 (6)
C6	0.6982 (4)	0.39494 (14)	0.7758 (3)	0.0241 (6)
H6	0.7234	0.3512	0.7764	0.029*
C7	0.5626 (4)	0.42046 (14)	0.6892 (3)	0.0247 (6)
H7	0.4956	0.3939	0.6301	0.030*
C8	-0.4695 (4)	0.77609 (14)	0.3273 (3)	0.0249 (6)
C9	-0.3630 (4)	0.78171 (15)	0.2581 (3)	0.0252 (7)
H9	-0.4005	0.8057	0.1899	0.030*
C10	-0.4100 (4)	0.74081 (14)	0.4282 (3)	0.0250 (7)
H10	-0.4793	0.7368	0.4768	0.030*
C11	-0.2035 (4)	0.75253 (14)	0.2882 (3)	0.0253 (6)
H11	-0.1332	0.7560	0.2401	0.030*
C12	-0.2504 (4)	0.71170 (14)	0.4571 (3)	0.0247 (6)
H12	-0.2124	0.6871	0.5246	0.030*
C13	-0.1466 (4)	0.71810 (13)	0.3890 (3)	0.0225 (6)
C14	-0.0260 (4)	0.57652 (14)	0.3379 (2)	0.0212 (6)
C15	-0.3712 (4)	0.59215 (16)	0.0690 (3)	0.0288 (7)
H15A	-0.4728	0.5994	0.0933	0.043*
H15B	-0.4012	0.5638	0.0031	0.043*
H15C	-0.3307	0.6324	0.0481	0.043*
C16	-0.2321 (4)	0.56281 (15)	0.1647 (3)	0.0237 (6)
C17	-0.1962 (4)	0.49817 (14)	0.1677 (3)	0.0239 (6)
H17	-0.2588	0.4713	0.1075	0.029*
C18	-0.0690 (4)	0.47427 (14)	0.2588 (3)	0.0228 (6)
C19	-0.0128 (4)	0.40671 (14)	0.2722 (3)	0.0262 (7)
H19A	0.1123	0.4045	0.2897	0.039*
H19B	-0.0679	0.3839	0.2012	0.039*
H19C	-0.0459	0.3875	0.3344	0.039*
C20	0.9666 (4)	0.34812 (15)	0.9608 (3)	0.0304 (7)
H20A	0.8642	0.3258	0.9654	0.046*
H20B	1.0628	0.3397	1.0298	0.046*
H20C	0.9959	0.3335	0.8939	0.046*

Atomic displacement parameters ( $\text{\AA}^2$ )

	$U^{11}$	$U^{22}$	$U^{33}$	$U^{12}$	$U^{13}$	$U^{23}$
S1	0.0208 (4)	0.0244 (4)	0.0260 (4)	0.0000 (3)	0.0052 (3)	-0.0041 (3)
O1	0.0291 (12)	0.0307 (12)	0.0289 (12)	-0.0001 (9)	0.0029 (10)	-0.0003 (9)
O2	0.0340 (13)	0.0294 (12)	0.0269 (12)	0.0085 (9)	0.0039 (10)	0.0001 (9)
O4	0.0269 (12)	0.0289 (12)	0.0417 (14)	-0.0005 (9)	0.0154 (10)	0.0004 (10)
O3	0.0280 (12)	0.0288 (12)	0.0311 (13)	0.0031 (9)	-0.0038 (10)	-0.0086 (9)
O5	0.0250 (11)	0.0249 (11)	0.0257 (11)	0.0028 (8)	0.0044 (9)	0.0021 (8)
N1	0.0234 (14)	0.0375 (16)	0.0306 (17)	0.0042 (12)	0.0082 (13)	0.0062 (12)
N2	0.0228 (13)	0.0282 (14)	0.0191 (13)	-0.0004 (10)	0.0044 (10)	-0.0025 (10)
N4	0.0203 (12)	0.0269 (13)	0.0208 (13)	0.0010 (10)	0.0075 (10)	-0.0011 (10)
N3	0.0203 (13)	0.0245 (13)	0.0224 (13)	-0.0007 (10)	0.0072 (10)	-0.0007 (10)
C1	0.0217 (15)	0.0272 (15)	0.0216 (15)	-0.0007 (12)	0.0093 (12)	-0.0005 (12)
C2	0.0205 (15)	0.0292 (16)	0.0209 (15)	0.0002 (12)	0.0100 (12)	0.0009 (12)
C3	0.0228 (15)	0.0219 (14)	0.0259 (16)	0.0010 (11)	0.0111 (12)	0.0013 (11)
C4	0.0215 (15)	0.0262 (15)	0.0226 (15)	-0.0025 (12)	0.0068 (12)	-0.0020 (12)
C5	0.0177 (14)	0.0288 (16)	0.0200 (15)	0.0016 (11)	0.0084 (12)	0.0028 (11)
C6	0.0241 (15)	0.0224 (14)	0.0279 (16)	0.0011 (12)	0.0110 (13)	-0.0007 (12)
C7	0.0231 (15)	0.0260 (15)	0.0248 (16)	-0.0020 (12)	0.0070 (12)	-0.0022 (12)
C8	0.0217 (15)	0.0238 (15)	0.0263 (16)	-0.0017 (12)	0.0034 (12)	-0.0030 (12)
C9	0.0288 (16)	0.0286 (16)	0.0163 (14)	0.0020 (12)	0.0042 (12)	0.0016 (11)
C10	0.0250 (15)	0.0261 (15)	0.0258 (16)	-0.0004 (12)	0.0107 (13)	0.0002 (12)
C11	0.0264 (15)	0.0283 (15)	0.0224 (15)	0.0005 (12)	0.0091 (13)	-0.0020 (12)
C12	0.0260 (16)	0.0241 (15)	0.0224 (15)	0.0005 (12)	0.0053 (13)	0.0017 (12)
C13	0.0227 (15)	0.0212 (14)	0.0220 (15)	0.0009 (11)	0.0045 (12)	-0.0037 (11)
C14	0.0192 (14)	0.0266 (15)	0.0195 (15)	0.0004 (11)	0.0082 (12)	-0.0006 (11)
C15	0.0237 (16)	0.0358 (17)	0.0253 (16)	0.0012 (13)	0.0055 (13)	-0.0023 (13)
C16	0.0204 (15)	0.0320 (16)	0.0216 (15)	-0.0019 (12)	0.0107 (12)	-0.0015 (12)
C17	0.0214 (15)	0.0289 (16)	0.0228 (15)	-0.0049 (12)	0.0088 (12)	-0.0046 (12)
C18	0.0228 (15)	0.0260 (15)	0.0235 (15)	-0.0029 (12)	0.0127 (12)	-0.0010 (11)
C19	0.0297 (16)	0.0237 (15)	0.0267 (16)	-0.0026 (12)	0.0108 (13)	-0.0020 (12)
C20	0.0321 (17)	0.0254 (16)	0.0322 (18)	0.0049 (13)	0.0080 (14)	0.0054 (13)

Geometric parameters (Å, °)

S1—O4	1.444 (2)	C6—H6	0.9500
S1—O3	1.448 (2)	C7—H7	0.9500
S1—N2	1.626 (3)	C8—C10	1.404 (4)
S1—C13	1.759 (3)	C8—C9	1.404 (4)
O1—C1	1.256 (4)	C9—C11	1.388 (4)
O2—C1	1.296 (4)	C9—H9	0.9500
O2—H32	1.06 (6)	C10—C12	1.388 (4)
O5—C5	1.371 (4)	C10—H10	0.9500
O5—C20	1.434 (4)	C11—C13	1.393 (4)
N1—C8	1.368 (4)	C11—H11	0.9500
N1—H30A	0.87 (5)	C12—C13	1.376 (4)
N1—H30B	0.82 (5)	C12—H12	0.9500
N2—C14	1.356 (4)	C15—C16	1.498 (4)
N4—C14	1.338 (4)	C15—H15A	0.9800
N4—C16	1.355 (4)	C15—H15B	0.9800
N3—C18	1.357 (4)	C15—H15C	0.9800
N3—C14	1.359 (4)	C16—C17	1.401 (4)
N3—H31	1.04 (5)	C17—C18	1.371 (4)
C1—C2	1.484 (4)	C17—H17	0.9500
C2—C7	1.389 (4)	C18—C19	1.499 (4)
C2—C3	1.401 (4)	C19—H19A	0.9800
C3—C4	1.383 (4)	C19—H19B	0.9800

C3—H3	0.9500	C19—H19C	0.9800
C4—C5	1.398 (4)	C20—H20A	0.9800
C4—H4	0.9500	C20—H20B	0.9800
C5—C6	1.394 (4)	C20—H20C	0.9800
C6—C7	1.389 (4)		
O4—S1—O3	116.87 (15)	C12—C10—C8	120.3 (3)
O4—S1—N2	110.87 (13)	C12—C10—H10	119.9
O3—S1—N2	103.09 (13)	C8—C10—H10	119.9
O4—S1—C13	106.48 (14)	C9—C11—C13	119.9 (3)
O3—S1—C13	108.57 (14)	C9—C11—H11	120.0
N2—S1—C13	110.96 (13)	C13—C11—H11	120.0
C1—O2—H32	115 (3)	C13—C12—C10	120.7 (3)
C5—O5—C20	117.2 (2)	C13—C12—H12	119.7
C8—N1—H30A	117 (3)	C10—C12—H12	119.7
C8—N1—H30B	116 (3)	C12—C13—C11	120.0 (3)
H30A—N1—H30B	107 (5)	C12—C13—S1	120.9 (2)
C14—N2—S1	122.9 (2)	C11—C13—S1	119.0 (2)
C14—N4—C16	116.9 (3)	N4—C14—N2	122.0 (3)
C18—N3—C14	120.7 (3)	N4—C14—N3	123.1 (3)
C18—N3—H31	123 (3)	N2—C14—N3	114.9 (3)
C14—N3—H31	116 (3)	C16—C15—H15A	109.5
O1—C1—O2	123.0 (3)	C16—C15—H15B	109.5
O1—C1—C2	120.0 (3)	H15A—C15—H15B	109.5
O2—C1—C2	116.9 (3)	C16—C15—H15C	109.5
C7—C2—C3	119.4 (3)	H15A—C15—H15C	109.5
C7—C2—C1	119.2 (3)	H15B—C15—H15C	109.5
C3—C2—C1	121.4 (3)	N4—C16—C17	122.0 (3)
C4—C3—C2	120.2 (3)	N4—C16—C15	116.0 (3)
C4—C3—H3	119.9	C17—C16—C15	122.0 (3)
C2—C3—H3	119.9	C18—C17—C16	118.9 (3)
C3—C4—C5	119.8 (3)	C18—C17—H17	120.5
C3—C4—H4	120.1	C16—C17—H17	120.5
C5—C4—H4	120.1	N3—C18—C17	118.4 (3)
O5—C5—C6	124.2 (3)	N3—C18—C19	116.7 (3)
O5—C5—C4	115.3 (3)	C17—C18—C19	125.0 (3)
C6—C5—C4	120.5 (3)	C18—C19—H19A	109.5
C7—C6—C5	119.0 (3)	C18—C19—H19B	109.5
C7—C6—H6	120.5	H19A—C19—H19B	109.5
C5—C6—H6	120.5	C18—C19—H19C	109.5
C6—C7—C2	121.0 (3)	H19A—C19—H19C	109.5
C6—C7—H7	119.5	H19B—C19—H19C	109.5
C2—C7—H7	119.5	O5—C20—H20A	109.5
N1—C8—C10	120.7 (3)	O5—C20—H20B	109.5
N1—C8—C9	120.8 (3)	H20A—C20—H20B	109.5
C10—C8—C9	118.4 (3)	O5—C20—H20C	109.5
C11—C9—C8	120.7 (3)	H20A—C20—H20C	109.5
C11—C9—H9	119.7	H20B—C20—H20C	109.5
C8—C9—H9	119.7		
O4—S1—N2—C14	-63.4 (3)	C10—C12—C13—C11	-1.9 (5)
O3—S1—N2—C14	170.8 (2)	C10—C12—C13—S1	174.2 (2)
C13—S1—N2—C14	54.8 (3)	C9—C11—C13—C12	1.7 (4)
O1—C1—C2—C7	0.0 (4)	C9—C11—C13—S1	-174.5 (2)
O2—C1—C2—C7	179.2 (3)	O4—S1—C13—C12	-170.4 (2)
O1—C1—C2—C3	-178.8 (3)	O3—S1—C13—C12	-43.8 (3)
O2—C1—C2—C3	0.4 (4)	N2—S1—C13—C12	68.8 (3)

C7—C2—C3—C4	0.4 (4)	O4—S1—C13—C11	5.7 (3)
C1—C2—C3—C4	179.2 (3)	O3—S1—C13—C11	132.4 (2)
C2—C3—C4—C5	-1.1 (4)	N2—S1—C13—C11	-115.0 (2)
C20—O5—C5—C6	-4.7 (4)	C16—N4—C14—N2	-175.5 (3)
C20—O5—C5—C4	175.2 (3)	C16—N4—C14—N3	1.8 (4)
C3—C4—C5—O5	-178.9 (3)	S1—N2—C14—N4	-15.6 (4)
C3—C4—C5—C6	1.0 (4)	S1—N2—C14—N3	166.9 (2)
O5—C5—C6—C7	179.7 (3)	C18—N3—C14—N4	-0.4 (4)
C4—C5—C6—C7	-0.1 (4)	C18—N3—C14—N2	177.1 (3)
C5—C6—C7—C2	-0.6 (5)	C14—N4—C16—C17	-1.5 (4)
C3—C2—C7—C6	0.4 (4)	C14—N4—C16—C15	177.2 (3)
C1—C2—C7—C6	-178.4 (3)	N4—C16—C17—C18	-0.3 (4)
N1—C8—C9—C11	178.2 (3)	C15—C16—C17—C18	-178.9 (3)
C10—C8—C9—C11	0.6 (4)	C14—N3—C18—C17	-1.5 (4)
N1—C8—C10—C12	-178.4 (3)	C14—N3—C18—C19	178.4 (3)
C9—C8—C10—C12	-0.8 (4)	C16—C17—C18—N3	1.7 (4)
C8—C9—C11—C13	-1.1 (5)	C16—C17—C18—C19	-178.1 (3)
C8—C10—C12—C13	1.5 (5)		

### Hydrogen-bond geometry (Å, °)

<i>D</i> —H··· <i>A</i>	<i>D</i> —H	H··· <i>A</i>	<i>D</i> ··· <i>A</i>	<i>D</i> —H··· <i>A</i>
N1—H30 <i>A</i> ···O3 <i>i</i>	0.87 (5)	2.27 (5)	3.072 (4)	153 (4)
N1—H30 <i>B</i> ···O4 <i>ii</i>	0.82 (5)	2.19 (5)	2.964 (4)	157 (4)
N3—H31···O1	1.04 (5)	1.69 (5)	2.726 (3)	173 (5)
O2—H32···N2	1.06 (6)	1.67 (6)	2.727 (3)	180 (6)

Symmetry codes: (i)  $x-1, -y+3/2, z-1/2$ ; (ii)  $x-1, y, z$ .

All esds (except the esd in the dihedral angle between two l.s. planes) are estimated using the full covariance matrix. The cell esds are taken into account individually in the estimation of esds in distances, angles and torsion angles; correlations between esds in cell parameters are only used when they are defined by crystal symmetry. An approximate (isotropic) treatment of cell esds is used for estimating esds involving l.s. planes.

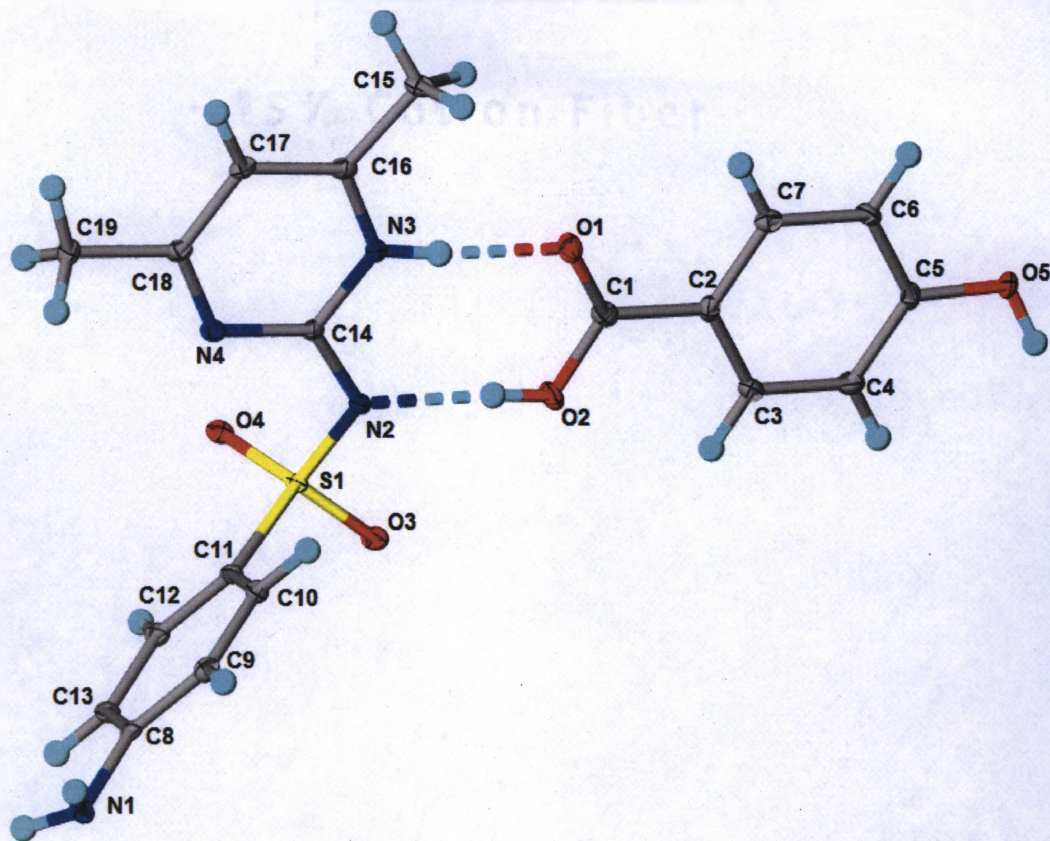


Figure S.15: Crystal Structure of the Cocrystal of Sulfamethazine and *p*-Hydroxybenzoic Acid Showing Thermal Parameters (50% Thermal Ellipsoids) and Hydrogen Bonding.

*Crystal data*

$C_{12}H_{14}N_4O_2S \cdot C_7H_6O_3$

$M_r = 416.45$

Triclinic, *P*

$a = 7.9730$  (5) Å

$b = 9.3867$  (6) Å

$c = 13.2673$  (9) Å

$\alpha = 74.041$  (3)°

$\beta = 75.846$  (2)°

$\gamma = 85.704$  (2)°

$V = 925.65$  (11) Å<sup>3</sup>

$Z = 2$

$F(000) = 436$

$D_x = 1.494$  Mg m<sup>-3</sup>

Melting point: 492-494 K

Cu  $K\alpha$  radiation,  $\lambda = 1.54178$  Å

Cell parameters from 9940 reflections

$\theta = 3.6$ – $68.2$ °

$\mu = 1.92$  mm<sup>-1</sup>

$T = 100$  K

Blocks, colourless

$0.41 \times 0.39 \times 0.23$  mm

Bruker APEXII CCD diffractometer	3305 independent reflections
Radiation source: fine-focus sealed tube	3226 reflections with $I > 2\sigma(I)$
Detector resolution: 8.33 pixels $\text{mm}^{-1}$	$R_{\text{int}} = 0.044$
phi and $\omega$ scans	$\theta_{\text{max}} = 68.2^\circ$ , $\theta_{\text{min}} = 3.6^\circ$
Absorption correction: multi-scan SADABS2014/7, Bruker AXS	$h = -9 \quad 9$
$T_{\text{min}} = 0.604$ , $T_{\text{max}} = 0.753$	$k = -11 \quad 11$
20327 measured reflections	$l = -15 \quad 15$

### Refinement

Refinement on  $F^2$

Least-squares matrix: full

$$R[F^2 > 2\sigma(F^2)] = 0.037$$

$$wR(F^2) = 0.110$$

$$S = 1.06$$

3305 reflections

284 parameters

5 restraints

0 constraints

Hydrogen site location: mixed

H atoms treated by a mixture of independent and constrained refinement

$$w = 1/[\sigma^2(F_o^2) + (0.0668P)^2 + 0.7096P]$$

$$\text{where } P = (F_o^2 + 2F_c^2)/3$$

$$(\Delta/\sigma)_{\text{max}} = 0.005$$

$$\Delta\rho_{\text{max}} = 0.37 \text{ e } \text{\AA}^{-3}$$

$$\Delta\rho_{\text{min}} = -0.60 \text{ e } \text{\AA}^{-3}$$

Extinction correction: none

### Fractional atomic coordinates and isotropic or equivalent isotropic displacement parameters ( $\text{\AA}^2$ )

	<i>x</i>	<i>y</i>	<i>z</i>	$U_{\text{iso}}^*/U_{\text{eq}}$
S1	0.47674 (5)	0.60053 (4)	0.28248 (3)	0.00969 (14)
O1	0.81394 (16)	0.51973 (14)	-0.04807 (10)	0.0163 (3)
O2	0.77103 (17)	0.70903 (15)	0.02895 (11)	0.0188 (3)
H32	0.695 (3)	0.651 (3)	0.0751 (19)	0.041 (8)*
O3	0.55062 (15)	0.74759 (13)	0.23814 (10)	0.0146 (3)
O4	0.54280 (15)	0.50671 (13)	0.37161 (10)	0.0135 (3)
O5	1.34986 (16)	0.98763 (14)	-0.38809 (10)	0.0160 (3)
H33	1.336 (3)	1.0799 (19)	-0.399 (2)	0.031 (7)*
N1	-0.27172 (18)	0.70978 (17)	0.45471 (12)	0.0129 (3)
H30A	-0.298 (3)	0.695 (2)	0.5244 (13)	0.014 (5)*
H30B	-0.335 (3)	0.658 (2)	0.4340 (18)	0.019 (5)*
N2	0.51175 (18)	0.53113 (16)	0.18059 (11)	0.0112 (3)
N3	0.56260 (18)	0.33590 (16)	0.10565 (12)	0.0110 (3)
H31	0.634 (3)	0.397 (2)	0.0543 (15)	0.017 (5)*
N4	0.37057 (18)	0.29949 (16)	0.27730 (12)	0.0115 (3)
C1	0.8498 (2)	0.6454 (2)	-0.04791 (14)	0.0134 (4)
C2	0.9830 (2)	0.73810 (19)	-0.13410 (14)	0.0124 (4)
C3	1.0090 (2)	0.8864 (2)	-0.13867 (14)	0.0145 (4)
H3	0.9422	0.9286	-0.0841	0.017*
C4	1.1315 (2)	0.9717 (2)	-0.22234 (15)	0.0155 (4)
H4	1.1493	1.0715	-0.2244	0.019*

C5	1.2291 (2)	0.9105 (2)	-0.30387 (14)	0.0129 (4)
C6	1.2054 (2)	0.7617 (2)	-0.29867 (14)	0.0131 (4)
H6	1.2730	0.7192	-0.3528	0.016*
C7	1.0833 (2)	0.67679 (19)	-0.21437 (14)	0.0137 (4)
H7	1.0677	0.5762	-0.2112	0.016*
C8	-0.0957 (2)	0.67966 (18)	0.41440 (14)	0.0117 (3)
C9	-0.0418 (2)	0.65015 (19)	0.31313 (14)	0.0131 (4)
H9	-0.1245	0.6495	0.2725	0.016*
C10	0.1316 (2)	0.62187 (19)	0.27174 (14)	0.0123 (3)
H10	0.1675	0.6020	0.2032	0.015*
C11	0.2523 (2)	0.62301 (18)	0.33210 (14)	0.0112 (3)
C12	0.2005 (2)	0.65271 (18)	0.43294 (14)	0.0123 (4)
H12	0.2835	0.6536	0.4733	0.015*
C13	0.0273 (2)	0.68082 (18)	0.47380 (14)	0.0129 (4)
H13	-0.0080	0.7009	0.5423	0.015*
C14	0.4779 (2)	0.38750 (19)	0.19190 (13)	0.0100 (3)
C15	0.6494 (2)	0.1498 (2)	0.00466 (15)	0.0164 (4)
H15A	0.5902	0.1843	-0.0544	0.025*
H15B	0.6610	0.0417	0.0221	0.025*
H15C	0.7645	0.1943	-0.0173	0.025*
C16	0.5464 (2)	0.19462 (19)	0.10202 (14)	0.0123 (4)
C17	0.4368 (2)	0.10319 (19)	0.18733 (14)	0.0132 (4)
H17	0.4197	0.0039	0.1877	0.016*
C18	0.3498 (2)	0.15942 (19)	0.27448 (14)	0.0121 (4)
C19	0.2285 (2)	0.06184 (19)	0.36823 (14)	0.0152 (4)
H19A	0.2637	0.0575	0.4348	0.023*
H19B	0.2317	-0.0381	0.3584	0.023*
H19C	0.1107	0.1022	0.3729	0.023*

### Atomic displacement parameters ( $\text{\AA}^2$ )

	$U^{11}$	$U^{22}$	$U^{33}$	$U^{12}$	$U^{13}$	$U^{23}$
S1	0.0081 (2)	0.0090 (2)	0.0117 (2)	0.00008 (15)	-0.00031 (16)	-0.00415 (17)
O1	0.0157 (6)	0.0162 (6)	0.0152 (7)	-0.0047 (5)	0.0012 (5)	-0.0042 (5)
O2	0.0186 (7)	0.0169 (7)	0.0161 (7)	-0.0036 (5)	0.0067 (5)	-0.0053 (6)
O3	0.0131 (6)	0.0109 (6)	0.0189 (7)	-0.0019 (5)	0.0002 (5)	-0.0054 (5)
O4	0.0111 (6)	0.0152 (6)	0.0151 (7)	0.0021 (5)	-0.0030 (5)	-0.0060 (5)
O5	0.0155 (6)	0.0126 (6)	0.0136 (7)	-0.0006 (5)	0.0024 (5)	0.0020 (5)
N1	0.0104 (7)	0.0148 (7)	0.0129 (8)	-0.0006 (6)	-0.0005 (6)	-0.0045 (6)
N2	0.0114 (7)	0.0093 (7)	0.0116 (7)	-0.0002 (5)	0.0004 (5)	-0.0033 (6)
N3	0.0106 (7)	0.0101 (7)	0.0108 (7)	-0.0005 (5)	-0.0004 (5)	-0.0020 (6)
N4	0.0093 (7)	0.0113 (7)	0.0141 (7)	0.0004 (5)	-0.0023 (5)	-0.0044 (6)
C1	0.0104 (8)	0.0162 (9)	0.0145 (9)	0.0015 (7)	-0.0042 (7)	-0.0047 (7)
C2	0.0107 (8)	0.0136 (8)	0.0109 (8)	-0.0003 (6)	-0.0022 (6)	-0.0004 (7)
C3	0.0135 (8)	0.0146 (9)	0.0143 (9)	0.0025 (7)	-0.0008 (7)	-0.0048 (7)
C4	0.0152 (8)	0.0122 (8)	0.0188 (9)	0.0015 (7)	-0.0028 (7)	-0.0051 (7)



C5	0.0095 (8)	0.0157 (9)	0.0103 (8)	0.0012 (6)	-0.0024 (6)	0.0017 (7)
C6	0.0113 (8)	0.0155 (9)	0.0128 (9)	0.0029 (6)	-0.0018 (6)	-0.0056 (7)
C7	0.0130 (8)	0.0127 (8)	0.0166 (9)	0.0015 (6)	-0.0049 (7)	-0.0047 (7)
C8	0.0118 (8)	0.0062 (7)	0.0148 (9)	-0.0003 (6)	-0.0011 (7)	-0.0005 (7)
C9	0.0130 (8)	0.0121 (8)	0.0142 (9)	-0.0003 (6)	-0.0045 (7)	-0.0025 (7)
C10	0.0134 (8)	0.0115 (8)	0.0114 (8)	0.0001 (6)	-0.0013 (6)	-0.0037 (7)
C11	0.0086 (8)	0.0089 (8)	0.0143 (9)	0.0004 (6)	0.0002 (6)	-0.0029 (7)
C12	0.0122 (8)	0.0108 (8)	0.0138 (9)	-0.0007 (6)	-0.0025 (6)	-0.0035 (7)
C13	0.0139 (8)	0.0107 (8)	0.0141 (9)	0.0010 (6)	-0.0014 (7)	-0.0053 (7)
C14	0.0084 (7)	0.0106 (8)	0.0109 (8)	0.0017 (6)	-0.0034 (6)	-0.0019 (7)
C15	0.0173 (9)	0.0156 (9)	0.0177 (9)	0.0026 (7)	-0.0024 (7)	-0.0092 (8)
C16	0.0113 (8)	0.0130 (8)	0.0145 (9)	0.0032 (6)	-0.0055 (7)	-0.0055 (7)
C17	0.0148 (8)	0.0088 (8)	0.0163 (9)	0.0006 (6)	-0.0043 (7)	-0.0032 (7)
C18	0.0100 (8)	0.0116 (8)	0.0152 (9)	0.0021 (6)	-0.0051 (7)	-0.0029 (7)
C19	0.0165 (9)	0.0114 (8)	0.0152 (9)	-0.0027 (7)	-0.0001 (7)	-0.0017 (7)

### Geometric parameters (Å, °)

S1—O3	1.4506 (12)	C5—C6	1.404 (2)
S1—O4	1.4539 (13)	C6—C7	1.389 (3)
S1—N2	1.6132 (14)	C6—H6	0.9500
S1—C11	1.7677 (16)	C7—H7	0.9500
O1—C1	1.235 (2)	C8—C13	1.403 (2)
O2—C1	1.325 (2)	C8—C9	1.404 (2)
O2—H32	0.850 (17)	C9—C10	1.392 (2)
O5—C5	1.354 (2)	C9—H9	0.9500
O5—H33	0.842 (17)	C10—C11	1.396 (2)
N1—C8	1.412 (2)	C10—H10	0.9500
N1—H30A	0.870 (16)	C11—C12	1.398 (2)
N1—H30B	0.862 (16)	C12—C13	1.388 (2)
N2—C14	1.355 (2)	C12—H12	0.9500
N3—C16	1.357 (2)	C13—H13	0.9500
N3—C14	1.370 (2)	C15—C16	1.499 (2)
N3—H31	0.874 (16)	C15—H15A	0.9800
N4—C14	1.347 (2)	C15—H15B	0.9800
N4—C18	1.349 (2)	C15—H15C	0.9800
C1—C2	1.480 (2)	C16—C17	1.370 (3)
C2—C7	1.399 (2)	C17—C18	1.409 (2)
C2—C3	1.405 (2)	C17—H17	0.9500
C3—C4	1.388 (3)	C18—C19	1.496 (2)
C3—H3	0.9500	C19—H19A	0.9800
C4—C5	1.403 (2)	C19—H19B	0.9800
C4—H4	0.9500	C19—H19C	0.9800
O3—S1—O4	115.25 (7)	C10—C9—C8	120.65 (16)
O3—S1—N2	104.40 (7)	C10—C9—H9	119.7
O4—S1—N2	112.56 (7)	C8—C9—H9	119.7
O3—S1—C11	107.19 (7)	C9—C10—C11	119.28 (16)
O4—S1—C11	106.91 (8)	C9—C10—H10	120.4
N2—S1—C11	110.42 (8)	C11—C10—H10	120.4
C1—O2—H32	109.6 (19)	C10—C11—C12	120.69 (15)

C5—O5—H33	112.4 (18)	C10—C11—S1	122.48 (13)
C8—N1—H30A	112.3 (14)	C12—C11—S1	116.69 (13)
C8—N1—H30B	109.1 (15)	C13—C12—C11	119.76 (16)
H30A—N1—H30B	112 (2)	C13—C12—H12	120.1
C14—N2—S1	122.01 (12)	C11—C12—H12	120.1
C16—N3—C14	122.51 (15)	C12—C13—C8	120.31 (16)
C16—N3—H31	121.0 (15)	C12—C13—H13	119.8
C14—N3—H31	116.3 (15)	C8—C13—H13	119.8
C14—N4—C18	117.56 (15)	N4—C14—N2	125.40 (15)
O1—C1—O2	122.80 (16)	N4—C14—N3	120.95 (15)
O1—C1—C2	122.80 (16)	N2—C14—N3	113.64 (15)
O2—C1—C2	114.40 (15)	C16—C15—H15A	109.5
C7—C2—C3	119.25 (16)	C16—C15—H15B	109.5
C7—C2—C1	118.84 (16)	H15A—C15—H15B	109.5
C3—C2—C1	121.89 (16)	C16—C15—H15C	109.5
C4—C3—C2	120.49 (16)	H15A—C15—H15C	109.5
C4—C3—H3	119.8	H15B—C15—H15C	109.5
C2—C3—H3	119.8	N3—C16—C17	117.74 (15)
C3—C4—C5	120.00 (16)	N3—C16—C15	117.62 (16)
C3—C4—H4	120.0	C17—C16—C15	124.64 (16)
C5—C4—H4	120.0	C16—C17—C18	118.62 (16)
O5—C5—C4	123.07 (16)	C16—C17—H17	120.7
O5—C5—C6	117.25 (15)	C18—C17—H17	120.7
C4—C5—C6	119.66 (16)	N4—C18—C17	122.61 (16)
C7—C6—C5	120.02 (16)	N4—C18—C19	117.84 (15)
C7—C6—H6	120.0	C17—C18—C19	119.55 (15)
C5—C6—H6	120.0	C18—C19—H19A	109.5
C6—C7—C2	120.56 (16)	C18—C19—H19B	109.5
C6—C7—H7	119.7	H19A—C19—H19B	109.5
C2—C7—H7	119.7	C18—C19—H19C	109.5
C13—C8—C9	119.31 (15)	H19A—C19—H19C	109.5
C13—C8—N1	120.73 (15)	H19B—C19—H19C	109.5
C9—C8—N1	119.95 (15)		
O3—S1—N2—C14	172.60 (13)	N2—S1—C11—C10	-17.24 (17)
O4—S1—N2—C14	46.90 (15)	O3—S1—C11—C12	-79.75 (14)
C11—S1—N2—C14	-72.49 (15)	O4—S1—C11—C12	44.36 (15)
O1—C1—C2—C7	-5.6 (3)	N2—S1—C11—C12	167.12 (12)
O2—C1—C2—C7	174.92 (15)	C10—C11—C12—C13	0.2 (3)
O1—C1—C2—C3	173.02 (16)	S1—C11—C12—C13	175.98 (13)
O2—C1—C2—C3	-6.4 (2)	C11—C12—C13—C8	0.0 (3)
C7—C2—C3—C4	0.6 (3)	C9—C8—C13—C12	-0.2 (3)
C1—C2—C3—C4	-178.07 (16)	N1—C8—C13—C12	-179.27 (15)
C2—C3—C4—C5	0.8 (3)	C18—N4—C14—N2	178.98 (15)
C3—C4—C5—O5	179.59 (15)	C18—N4—C14—N3	-0.1 (2)
C3—C4—C5—C6	-1.8 (3)	S1—N2—C14—N4	20.1 (2)
O5—C5—C6—C7	-179.88 (15)	S1—N2—C14—N3	-160.77 (12)
C4—C5—C6—C7	1.4 (3)	C16—N3—C14—N4	-1.3 (2)
C5—C6—C7—C2	0.0 (3)	C16—N3—C14—N2	179.55 (14)
C3—C2—C7—C6	-1.0 (3)	C14—N3—C16—C17	1.9 (2)

C1—C2—C7—C6	177.74 (15)	C14—N3—C16—C15	-178.32 (15)
C13—C8—C9—C10	0.2 (3)	N3—C16—C17—C18	-1.1 (2)
N1—C8—C9—C10	179.28 (15)	C15—C16—C17—C18	179.07 (15)
C8—C9—C10—C11	0.0 (3)	C14—N4—C18—C17	0.8 (2)
C9—C10—C11—C12	-0.2 (3)	C14—N4—C18—C19	-178.99 (14)
C9—C10—C11—S1	-175.71 (13)	C16—C17—C18—N4	-0.2 (3)
O3—S1—C11—C10	95.90 (15)	C16—C17—C18—C19	179.61 (15)
O4—S1—C11—C10	-139.99 (14)		

#### Hydrogen-bond geometry (Å, °)

<i>D</i> —H··· <i>A</i>	<i>D</i> —H	H··· <i>A</i>	<i>D</i> ··· <i>A</i>	<i>D</i> —H··· <i>A</i>
N1—H30 <i>A</i> ···O4ii	0.87 (2)	2.66 (2)	3.1238 (19)	114 (2)
N1—H30 <i>A</i> ···N4ii	0.87 (2)	2.57 (2)	3.426 (2)	170 (2)
N1—H30 <i>B</i> ···S1iii	0.86 (2)	2.96 (2)	3.7593 (16)	154 (2)
N1—H30 <i>B</i> ···O4iii	0.86 (2)	2.21 (2)	3.0677 (19)	171 (2)
N3—H31···O1	0.87 (2)	1.91 (2)	2.7815 (19)	172 (2)
O2—H32···S1	0.85 (2)	2.81 (2)	3.5315 (13)	144 (2)
O2—H32···O3	0.85 (2)	2.56 (3)	2.9989 (18)	113 (2)
O2—H32···N2	0.85 (2)	1.93 (2)	2.7830 (19)	176 (3)
O5—H33···N1i	0.84 (2)	1.98 (2)	2.804 (2)	164 (2)

Symmetry codes: (i)  $-x+1, -y+2, -z$ ; (ii)  $-x, -y+1, -z+1$ ; (iii)  $x-1, y, z$ .

All esds (except the esd in the dihedral angle between two l.s. planes) are estimated using the full covariance matrix. The cell esds are taken into account individually in the estimation of esds in distances, angles and torsion angles; correlations between esds in cell parameters are only used when they are defined by crystal symmetry. An approximate (isotropic) treatment of cell esds is used for estimating esds involving l.s. planes.

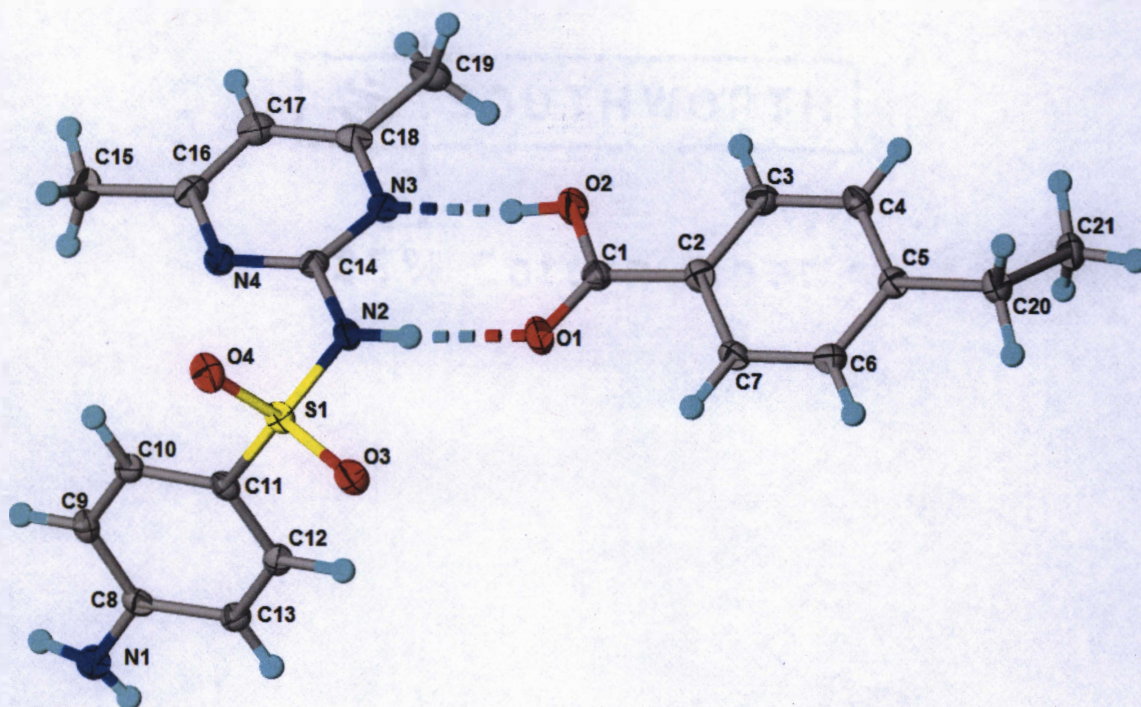


Figure S.16: Crystal Structure of the Cocrystal of Sulfamethazine and *p*-Ethylbenzoic Acid Showing Thermal Parameters (50% Thermal Ellipsoids) and Hydrogen Bonding.

#### Crystal data

$C_{12}H_{14}N_4O_2S \cdot C_9H_{10}O_2$

$M_r = 428.50$

Monoclinic,  $P2_1$

$a = 7.5193 (4) \text{ \AA}$

$b = 13.1705 (7) \text{ \AA}$

$c = 11.3736 (6) \text{ \AA}$

$\beta = 108.609 (3)^\circ$

$V = 1067.47 (10) \text{ \AA}^3$

$Z = 2$

$F(000) = 452$

$D_x = 1.333 \text{ Mg m}^{-3}$

Melting point: 468-471 K

Cu  $K\alpha$  radiation,  $\lambda = 1.54178 \text{ \AA}$

Cell parameters from 8427 reflections

$\theta = 4.1\text{--}68.4^\circ$

$\mu = 1.65 \text{ mm}^{-1}$

$T = 100 \text{ K}$

Plates, colourless

$\times \times \text{ mm}$

#### Data collection

Bruker APEXII CCD  
diffractometer

Radiation source: fine-focus sealed tube

Detector resolution: 8.33 pixels  $\text{mm}^{-1}$

$\phi$  and  $\omega$  scans

Absorption correction: multi-scan

SADABS2014/7, Bruker AXS

$T_{\min} = 0.637$ ,  $T_{\max} = 0.753$

3837 independent reflections

3711 reflections with  $I > 2\sigma(I)$

$R_{\text{int}} = 0.034$

$\theta_{\max} = 68.2^\circ$ ,  $\theta_{\min} = 4.1^\circ$

$h = -9 \text{--} 9$

$k = -15 \text{--} 15$

## Refinement

Refinement on  $F^2$

Least-squares matrix: full

$$R[F^2 > 2\sigma(F^2)] = 0.026$$

$$wR(F^2) = 0.071$$

$$S = 1.07$$

3837 reflections

290 parameters

5 restraints

0 constraints

Hydrogen site location: mixed

H atoms treated by a mixture of independent and constrained refinement

$$w = 1/[\sigma^2(F_o^2) + (0.0408P)^2 + 0.095P]$$

$$\text{where } P = (F_o^2 + 2F_c^2)/3$$

$$(\Delta/\sigma)_{\max} < 0.001$$

$$\Delta\rho_{\max} = 0.16 \text{ e } \text{\AA}^{-3}$$

$$\Delta\rho_{\min} = -0.21 \text{ e } \text{\AA}^{-3}$$

Extinction correction: none

Absolute structure: Flack x determined using 1678 quotients [(I+)-(I-)]/[(I+)+(I-)] (Parsons, Flack and Wagner, Acta Cryst. B69 (2013) 249-259).

Absolute structure parameter: 0.040 (6)

## Fractional atomic coordinates and isotropic or equivalent isotropic displacement parameters ( $\text{\AA}^2$ )

	x	y	z	$U_{\text{iso}}^*/U_{\text{eq}}$
S1	0.13521 (8)	0.80275 (5)	0.84177 (5)	0.02082 (14)
O1	-0.3180 (2)	0.79232 (17)	0.57775 (16)	0.0310 (4)
O2	-0.3244 (3)	0.87370 (15)	0.40403 (18)	0.0298 (4)
H32	-0.211 (4)	0.888 (3)	0.448 (3)	0.059 (12)*
O3	-0.0264 (3)	0.75879 (13)	0.86398 (16)	0.0267 (4)
O4	0.2917 (3)	0.73855 (13)	0.85003 (17)	0.0291 (4)
N1	0.3822 (3)	1.14182 (18)	1.1938 (2)	0.0271 (5)
H30B	0.300 (4)	1.180 (2)	1.204 (3)	0.029 (8)*
H30A	0.493 (3)	1.167 (2)	1.204 (3)	0.032 (9)*
N2	0.0462 (3)	0.84658 (17)	0.6997 (2)	0.0231 (5)
H31	-0.072 (3)	0.835 (2)	0.661 (3)	0.029 (8)*
N3	0.0340 (3)	0.93689 (15)	0.52539 (19)	0.0206 (4)
N4	0.3200 (3)	0.92523 (16)	0.69519 (19)	0.0225 (4)
C1	-0.4004 (3)	0.8162 (2)	0.4700 (2)	0.0222 (5)
C2	-0.5948 (3)	0.78270 (18)	0.4049 (2)	0.0225 (5)
C3	-0.6804 (3)	0.7967 (2)	0.2778 (2)	0.0245 (5)
H3	-0.6145	0.8300	0.2302	0.029*
C4	-0.8611 (4)	0.7620 (2)	0.2210 (2)	0.0244 (5)
H4	-0.9166	0.7701	0.1340	0.029*
C5	-0.9640 (3)	0.71519 (18)	0.2895 (2)	0.0209 (5)
C6	-0.8775 (4)	0.70353 (19)	0.4166 (2)	0.0230 (5)
H6	-0.9455	0.6732	0.4650	0.028*
C7	-0.6950 (4)	0.73503 (19)	0.4741 (2)	0.0221 (5)
H7	-0.6376	0.7243	0.5606	0.027*

C8	0.3239 (4)	1.06696 (19)	1.1073 (2)	0.0211 (5)
C9	0.4547 (3)	1.01328 (19)	1.0657 (2)	0.0230 (5)
H9	0.5833	1.0321	1.0949	0.028*
C10	0.3988 (3)	0.93380 (18)	0.9832 (2)	0.0206 (5)
H10	0.4880	0.8983	0.9555	0.025*
C11	0.2097 (3)	0.90589 (18)	0.9407 (2)	0.0197 (5)
C12	0.0780 (3)	0.95892 (19)	0.9792 (2)	0.0218 (5)
H12	-0.0506	0.9399	0.9492	0.026*
C13	0.1335 (3)	1.03866 (19)	1.0605 (2)	0.0222 (5)
H13	0.0426	1.0751	1.0856	0.027*
C14	0.1401 (3)	0.90521 (18)	0.6383 (2)	0.0193 (5)
C15	0.6063 (4)	1.0095 (2)	0.6994 (3)	0.0329 (6)
H15A	0.6137	1.0590	0.7652	0.049*
H15B	0.6636	1.0382	0.6406	0.049*
H15C	0.6734	0.9475	0.7361	0.049*
C16	0.4050 (4)	0.98467 (19)	0.6329 (2)	0.0243 (5)
C17	0.3093 (4)	1.0212 (2)	0.5159 (2)	0.0267 (5)
H17	0.3705	1.0630	0.4725	0.032*
C18	0.1210 (4)	0.99529 (19)	0.4631 (2)	0.0237 (5)
C19	0.0051 (4)	1.0296 (2)	0.3366 (2)	0.0328 (6)
H19A	-0.0052	0.9743	0.2771	0.049*
H19B	0.0649	1.0885	0.3121	0.049*
H19C	-0.1204	1.0486	0.3376	0.049*
C20	-1.1612 (4)	0.6772 (2)	0.2281 (2)	0.0253 (5)
H20A	-1.2207	0.6653	0.2930	0.030*
H20B	-1.1547	0.6110	0.1884	0.030*
C21	-1.2856 (4)	0.7484 (2)	0.1310 (3)	0.0288 (6)
H21A	-1.2891	0.8151	0.1683	0.043*
H21B	-1.4130	0.7205	0.1001	0.043*
H21C	-1.2350	0.7553	0.0619	0.043*

### Atomic displacement parameters ( $\text{\AA}^2$ )

	$U^{11}$	$U^{22}$	$U^{33}$	$U^{12}$	$U^{13}$	$U^{23}$
S1	0.0227 (3)	0.0178 (3)	0.0197 (3)	-0.0011 (2)	0.0035 (2)	0.0012 (2)
O1	0.0224 (8)	0.0423 (11)	0.0232 (9)	-0.0075 (9)	0.0002 (7)	0.0056 (9)
O2	0.0238 (9)	0.0374 (11)	0.0254 (9)	-0.0072 (8)	0.0040 (8)	0.0053 (8)
O3	0.0304 (10)	0.0250 (9)	0.0229 (9)	-0.0058 (8)	0.0061 (8)	0.0026 (7)
O4	0.0302 (10)	0.0230 (10)	0.0292 (10)	0.0030 (8)	0.0027 (8)	-0.0033 (8)
N1	0.0263 (12)	0.0274 (12)	0.0275 (11)	0.0003 (10)	0.0083 (10)	-0.0066 (9)
N2	0.0190 (11)	0.0289 (11)	0.0189 (10)	-0.0040 (9)	0.0024 (9)	0.0007 (9)
N3	0.0234 (11)	0.0190 (10)	0.0194 (10)	0.0003 (8)	0.0067 (8)	-0.0010 (8)
N4	0.0217 (10)	0.0227 (11)	0.0230 (10)	-0.0006 (8)	0.0069 (9)	-0.0027 (9)
C1	0.0223 (12)	0.0234 (14)	0.0208 (12)	0.0019 (10)	0.0065 (10)	-0.0012 (10)
C2	0.0228 (12)	0.0197 (13)	0.0236 (12)	0.0024 (10)	0.0053 (10)	0.0006 (10)
C3	0.0256 (12)	0.0262 (12)	0.0227 (11)	-0.0001 (12)	0.0091 (10)	0.0026 (12)
C4	0.0254 (13)	0.0254 (12)	0.0184 (11)	0.0009 (10)	0.0014 (10)	0.0039 (10)
C5	0.0218 (12)	0.0176 (11)	0.0224 (12)	0.0035 (10)	0.0059 (10)	-0.0005 (10)

C6	0.0258 (13)	0.0230 (12)	0.0218 (12)	-0.0007 (10)	0.0096 (10)	-0.0001 (10)
C7	0.0248 (13)	0.0235 (13)	0.0169 (12)	0.0021 (10)	0.0048 (10)	0.0004 (9)
C8	0.0259 (13)	0.0217 (12)	0.0151 (11)	0.0023 (10)	0.0055 (10)	0.0029 (9)
C9	0.0186 (12)	0.0258 (13)	0.0211 (12)	0.0010 (10)	0.0014 (10)	0.0017 (10)
C10	0.0206 (12)	0.0220 (12)	0.0190 (11)	0.0047 (10)	0.0059 (10)	0.0021 (9)
C11	0.0229 (12)	0.0186 (12)	0.0155 (11)	-0.0006 (10)	0.0034 (9)	0.0026 (9)
C12	0.0200 (12)	0.0233 (13)	0.0216 (12)	-0.0003 (10)	0.0061 (10)	0.0056 (10)
C13	0.0224 (12)	0.0245 (12)	0.0205 (12)	0.0042 (10)	0.0080 (10)	0.0033 (10)
C14	0.0207 (12)	0.0186 (11)	0.0200 (11)	-0.0001 (9)	0.0084 (9)	-0.0030 (9)
C15	0.0234 (13)	0.0330 (15)	0.0405 (16)	-0.0072 (12)	0.0075 (12)	-0.0012 (12)
C16	0.0257 (13)	0.0198 (12)	0.0303 (13)	-0.0030 (10)	0.0130 (11)	-0.0061 (11)
C17	0.0320 (13)	0.0218 (13)	0.0296 (13)	-0.0028 (11)	0.0143 (11)	-0.0018 (11)
C18	0.0321 (14)	0.0197 (12)	0.0218 (12)	0.0019 (11)	0.0118 (11)	-0.0014 (10)
C19	0.0427 (16)	0.0311 (14)	0.0245 (14)	-0.0017 (13)	0.0107 (13)	0.0043 (11)
C20	0.0240 (13)	0.0253 (13)	0.0237 (13)	-0.0017 (10)	0.0036 (11)	-0.0003 (10)
C21	0.0219 (13)	0.0320 (14)	0.0279 (14)	0.0013 (11)	0.0015 (11)	-0.0013 (11)

### Geometric parameters (Å, °)

S1—O4	1.4275 (19)	C8—C9	1.410 (3)
S1—O3	1.4392 (19)	C8—C13	1.409 (4)
S1—N2	1.644 (2)	C9—C10	1.379 (4)
S1—C11	1.738 (2)	C9—H9	0.9500
O1—C1	1.224 (3)	C10—C11	1.397 (3)
O2—C1	1.318 (3)	C10—H10	0.9500
O2—H32	0.86 (2)	C11—C12	1.392 (3)
N1—C8	1.363 (3)	C12—C13	1.374 (4)
N1—H30B	0.83 (2)	C12—H12	0.9500
N1—H30A	0.87 (2)	C13—H13	0.9500
N2—C14	1.377 (3)	C15—C16	1.496 (4)
N2—H31	0.87 (2)	C15—H15A	0.9800
N3—C14	1.344 (3)	C15—H15B	0.9800
N3—C18	1.348 (3)	C15—H15C	0.9800
N4—C14	1.327 (3)	C16—C17	1.382 (4)
N4—C16	1.346 (3)	C17—C18	1.392 (4)
C1—C2	1.480 (3)	C17—H17	0.9500
C2—C3	1.394 (3)	C18—C19	1.495 (4)
C2—C7	1.400 (3)	C19—H19A	0.9800
C3—C4	1.383 (4)	C19—H19B	0.9800
C3—H3	0.9500	C19—H19C	0.9800
C4—C5	1.404 (4)	C20—C21	1.522 (4)
C4—H4	0.9500	C20—H20A	0.9900
C5—C6	1.392 (3)	C20—H20B	0.9900
C5—C20	1.508 (4)	C21—H21A	0.9800
C6—C7	1.382 (4)	C21—H21B	0.9800
C6—H6	0.9500	C21—H21C	0.9800
C7—H7	0.9500		
O4—S1—O3	118.33 (11)	C12—C11—C10	120.4 (2)
O4—S1—N2	109.95 (11)	C12—C11—S1	118.76 (19)
O3—S1—N2	102.24 (11)	C10—C11—S1	120.78 (18)



O4—S1—C11	109.38 (11)	C13—C12—C11	120.1 (2)
O3—S1—C11	108.45 (11)	C13—C12—H12	119.9
N2—S1—C11	107.91 (11)	C11—C12—H12	119.9
C1—O2—H32	109 (3)	C12—C13—C8	120.7 (2)
C8—N1—H30B	117 (2)	C12—C13—H13	119.7
C8—N1—H30A	116 (2)	C8—C13—H13	119.7
H30B—N1—H30A	118 (3)	N4—C14—N3	127.3 (2)
C14—N2—S1	125.55 (18)	N4—C14—N2	118.2 (2)
C14—N2—H31	117 (2)	N3—C14—N2	114.5 (2)
S1—N2—H31	118 (2)	C16—C15—H15A	109.5
C14—N3—C18	116.1 (2)	C16—C15—H15B	109.5
C14—N4—C16	116.1 (2)	H15A—C15—H15B	109.5
O1—C1—O2	123.0 (2)	C16—C15—H15C	109.5
O1—C1—C2	121.9 (2)	H15A—C15—H15C	109.5
O2—C1—C2	115.1 (2)	H15B—C15—H15C	109.5
C3—C2—C7	119.3 (2)	N4—C16—C17	121.4 (2)
C3—C2—C1	122.4 (2)	N4—C16—C15	115.7 (2)
C7—C2—C1	118.3 (2)	C17—C16—C15	122.9 (2)
C4—C3—C2	120.0 (2)	C16—C17—C18	118.3 (2)
C4—C3—H3	120.0	C16—C17—H17	120.8
C2—C3—H3	120.0	C18—C17—H17	120.8
C3—C4—C5	121.3 (2)	N3—C18—C17	120.7 (2)
C3—C4—H4	119.3	N3—C18—C19	116.5 (2)
C5—C4—H4	119.3	C17—C18—C19	122.7 (2)
C6—C5—C4	117.8 (2)	C18—C19—H19A	109.5
C6—C5—C20	120.6 (2)	C18—C19—H19B	109.5
C4—C5—C20	121.6 (2)	H19A—C19—H19B	109.5
C7—C6—C5	121.5 (2)	C18—C19—H19C	109.5
C7—C6—H6	119.2	H19A—C19—H19C	109.5
C5—C6—H6	119.2	H19B—C19—H19C	109.5
C6—C7—C2	120.0 (2)	C5—C20—C21	114.7 (2)
C6—C7—H7	120.0	C5—C20—H20A	108.6
C2—C7—H7	120.0	C21—C20—H20A	108.6
N1—C8—C9	120.5 (2)	C5—C20—H20B	108.6
N1—C8—C13	121.1 (2)	C21—C20—H20B	108.6
C9—C8—C13	118.3 (2)	H20A—C20—H20B	107.6
C10—C9—C8	121.0 (2)	C20—C21—H21A	109.5
C10—C9—H9	119.5	C20—C21—H21B	109.5
C8—C9—H9	119.5	H21A—C21—H21B	109.5
C9—C10—C11	119.4 (2)	C20—C21—H21C	109.5
C9—C10—H10	120.3	H21A—C21—H21C	109.5
C11—C10—H10	120.3	H21B—C21—H21C	109.5
O4—S1—N2—C14	-60.4 (2)	O4—S1—C11—C10	19.7 (2)
O3—S1—N2—C14	173.1 (2)	O3—S1—C11—C10	150.04 (19)
C11—S1—N2—C14	58.9 (2)	N2—S1—C11—C10	-99.9 (2)
O1—C1—C2—C3	-170.5 (3)	C10—C11—C12—C13	-0.7 (3)
O2—C1—C2—C3	10.0 (4)	S1—C11—C12—C13	177.86 (19)
O1—C1—C2—C7	9.3 (4)	C11—C12—C13—C8	-0.9 (4)
O2—C1—C2—C7	-170.2 (2)	N1—C8—C13—C12	-175.9 (2)

C7—C2—C3—C4	-1.1 (4)	C9—C8—C13—C12	1.8 (4)
C1—C2—C3—C4	178.6 (2)	C16—N4—C14—N3	0.6 (4)
C2—C3—C4—C5	1.9 (4)	C16—N4—C14—N2	-178.5 (2)
C3—C4—C5—C6	-0.8 (4)	C18—N3—C14—N4	0.2 (4)
C3—C4—C5—C20	-180.0 (2)	C18—N3—C14—N2	179.4 (2)
C4—C5—C6—C7	-1.2 (4)	S1—N2—C14—N4	3.0 (3)
C20—C5—C6—C7	178.0 (2)	S1—N2—C14—N3	-176.21 (18)
C5—C6—C7—C2	2.0 (4)	C14—N4—C16—C17	-0.8 (3)
C3—C2—C7—C6	-0.8 (4)	C14—N4—C16—C15	178.2 (2)
C1—C2—C7—C6	179.4 (2)	N4—C16—C17—C18	0.2 (4)
N1—C8—C9—C10	176.5 (2)	C15—C16—C17—C18	-178.7 (2)
C13—C8—C9—C10	-1.2 (3)	C14—N3—C18—C17	-0.9 (3)
C8—C9—C10—C11	-0.3 (4)	C14—N3—C18—C19	179.1 (2)
C9—C10—C11—C12	1.2 (3)	C16—C17—C18—N3	0.7 (4)
C9—C10—C11—S1	-177.27 (18)	C16—C17—C18—C19	-179.2 (2)
O4—S1—C11—C12	-158.83 (18)	C6—C5—C20—C21	138.4 (2)
O3—S1—C11—C12	-28.5 (2)	C4—C5—C20—C21	-42.4 (3)
N2—S1—C11—C12	81.6 (2)		

#### Hydrogen-bond geometry (Å, °)

<i>D</i> —H··· <i>A</i>	<i>D</i> —H	H··· <i>A</i>	<i>D</i> ··· <i>A</i>	<i>D</i> —H··· <i>A</i>
N1—H30 <i>A</i> ···O4ii	0.87 (2)	2.13 (2)	2.944 (3)	156 (3)
N1—H30 <i>B</i> ···O3i	0.83 (2)	2.21 (2)	2.973 (3)	152 (3)
N2—H31···O1	0.87 (2)	1.88 (2)	2.741 (3)	172 (3)
O2—H32···N3	0.86 (2)	1.88 (3)	2.736 (3)	170 (4)

Symmetry codes: (i)  $-x, y+1/2, -z+2$ ; (ii)  $-x+1, y+1/2, -z+2$ .

All esds (except the esd in the dihedral angle between two l.s. planes) are estimated using the full covariance matrix. The cell esds are taken into account individually in the estimation of esds in distances, angles and torsion angles; correlations between esds in cell parameters are only used when they are defined by crystal symmetry. An approximate (isotropic) treatment of cell esds is used for estimating esds involving l.s. planes.

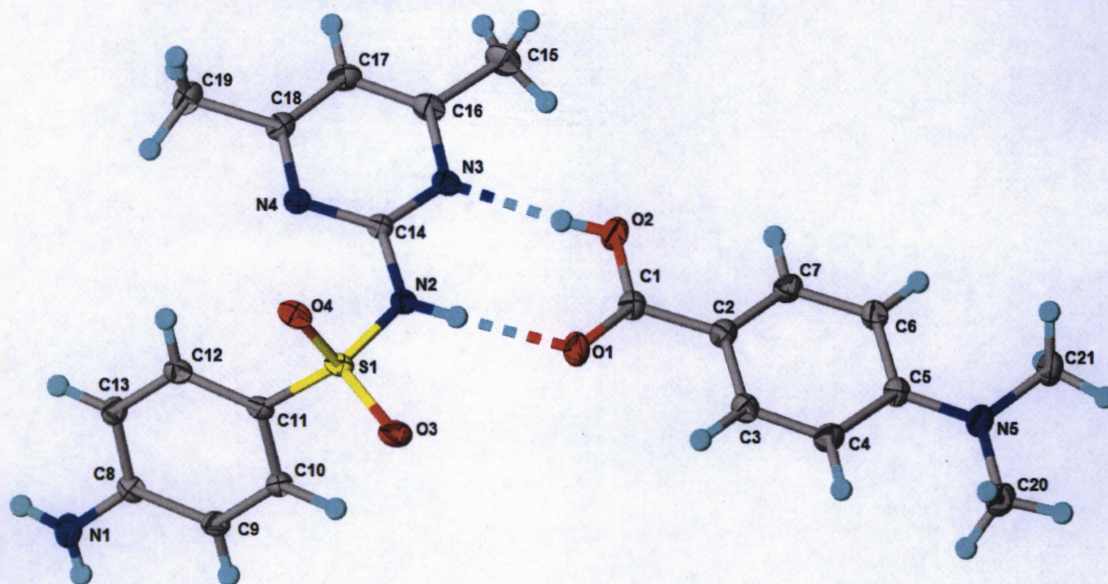


Figure S.17: Crystal Structure of the Cocrystal of Sulfamethazine and *p*-Dimethylaminobenzoic Acid Showing Thermal Parameters (50% Thermal Ellipsoids) and Hydrogen Bonding.

#### Crystal data

$C_{12}H_{14}N_4O_2S \cdot C_9H_{11}NO_2 \cdot O$

$M_r = 459.52$

Monoclinic,  $P2_1/c$

$a = 7.8837$  (3) Å

$b = 31.8034$  (13) Å

$c = 9.6952$  (4) Å

$\beta = 112.284$  (2)°

$V = 2249.31$  (16) Å<sup>3</sup>

$Z = 4$

$F(000) = 968$

$D_x = 1.357$  Mg m<sup>-3</sup>

Melting point: 452-456 K

Cu  $K\alpha$  radiation,  $\lambda = 1.54178$  Å

Cell parameters from 9926 reflections

$\theta = 2.8$ – $72.3$ °

$\mu = 1.65$  mm<sup>-1</sup>

$T = 100$  K

Prism, colourless

$0.28 \times 0.25 \times 0.22$  mm

#### Data collection

Bruker APEXII CCD  
diffractometer

Radiation source: fine-focus sealed tube

Detector resolution: 8.33 pixels mm<sup>-1</sup>

phi and  $\omega$  scans

Absorption correction: multi-scan

SADABS2014/7, Bruker AXS

$T_{\min} = 0.684$ ,  $T_{\max} = 0.753$

4121 independent reflections

3801 reflections with  $I > 2\sigma(I)$

$R_{\text{int}} = 0.043$

$\theta_{\text{max}} = 68.2$ °,  $\theta_{\text{min}} = 2.8$ °

$h = -9$  9

$k = -36$  38

Radiation source: fine-focus sealed tube  
 Detector resolution: 8.33 pixels mm<sup>-1</sup>  
 phi and  $\omega$  scans  
 Absorption correction: multi-scan  
 SADABS2014/7, Bruker AXS  
 $T_{\min} = 0.684$ ,  $T_{\max} = 0.753$   
 34091 measured reflections

3801 reflections with  $I > 2\sigma(I)$   
 $R_{\text{int}} = 0.043$   
 $\theta_{\max} = 68.2^\circ$ ,  $\theta_{\min} = 2.8^\circ$   
 $h = -9 \quad 9$   
 $k = -36 \quad 38$   
 $l = -11 \quad 11$

### Refinement

Refinement on  $F^2$   
 Least-squares matrix: full  
 $R[F^2 > 2\sigma(F^2)] = 0.049$   
 $wR(F^2) = 0.139$   
 $S = 1.10$   
 4121 reflections  
 304 parameters  
 2 restraints  
 0 constraints

Hydrogen site location: mixed  
 H atoms treated by a mixture of independent and constrained refinement  
 $w = 1/[\sigma^2(F_o^2) + (0.0664P)^2 + 2.7068P]$   
 where  $P = (F_o^2 + 2F_c^2)/3$   
 $(\Delta/\sigma)_{\max} < 0.001$   
 $\Delta\rho_{\max} = 0.36 \text{ e } \text{\AA}^{-3}$   
 $\Delta\rho_{\min} = -0.97 \text{ e } \text{\AA}^{-3}$   
 Extinction correction: none

### Fractional atomic coordinates and isotropic or equivalent isotropic displacement parameters ( $\text{\AA}^2$ )

	<i>x</i>	<i>y</i>	<i>z</i>	$U_{\text{iso}}^*/U_{\text{eq}}$
S1	0.07259 (7)	0.16475 (2)	0.59915 (6)	0.01975 (17)
O1	0.1880 (3)	0.04947 (5)	0.67245 (19)	0.0295 (4)
O2	0.2137 (3)	0.01244 (5)	0.48526 (19)	0.0296 (4)
O3	0.0951 (2)	0.14863 (6)	0.74340 (17)	0.0268 (4)
O4	0.1942 (2)	0.19783 (5)	0.59179 (18)	0.0250 (4)
H30A	-0.704 (4)	0.2522 (9)	0.276 (3)	0.023 (7)*
H30B	-0.762 (4)	0.2231 (10)	0.363 (3)	0.035 (8)*
H32	0.199 (6)	0.0374 (8)	0.447 (5)	0.080 (14)*
H31	0.132 (7)	0.1006 (10)	0.562 (5)	0.103 (17)*
N1	-0.6748 (3)	0.23468 (7)	0.3456 (3)	0.0278 (5)
N2	0.1008 (3)	0.12305 (6)	0.5106 (2)	0.0207 (4)
N3	0.1312 (3)	0.08461 (6)	0.3227 (2)	0.0210 (4)
N4	0.0437 (2)	0.15670 (6)	0.2816 (2)	0.0198 (4)
N5	0.4266 (3)	-0.12630 (6)	1.0013 (2)	0.0268 (4)
C1	0.2222 (3)	0.01570 (7)	0.6210 (3)	0.0232 (5)
C2	0.2910 (3)	-0.01914 (8)	0.8636 (3)	0.0263 (5)
H4	0.2670	0.0070	0.9000	0.032*
C3	0.3399 (4)	-0.05305 (8)	0.9582 (3)	0.0274 (5)
H3	0.3480	-0.0501	1.0580	0.033*
C4	0.3783 (3)	-0.09244 (7)	0.9084 (3)	0.0218 (5)
C5	0.3647 (3)	-0.09496 (7)	0.7588 (3)	0.0232 (5)
H5	0.3908	-0.1208	0.7219	0.028*

C6	0.3143 (3)	-0.06053 (7)	0.6658 (3)	0.0236 (5)
H6	0.3057	-0.0631	0.5658	0.028*
C7	0.2754 (3)	-0.02185 (7)	0.7160 (3)	0.0215 (5)
C8	-0.5049 (3)	0.21721 (7)	0.3962 (3)	0.0209 (5)
C9	-0.4632 (3)	0.18279 (7)	0.4949 (3)	0.0221 (5)
H9	-0.5567	0.1708	0.5219	0.027*
C10	-0.2882 (3)	0.16618 (7)	0.5530 (3)	0.0208 (5)
H10	-0.2612	0.1432	0.6203	0.025*
C11	-0.1512 (3)	0.18345 (7)	0.5120 (2)	0.0186 (4)
C12	-0.1913 (3)	0.21651 (7)	0.4109 (3)	0.0210 (5)
H12	-0.0984	0.2276	0.3812	0.025*
C13	-0.3659 (3)	0.23330 (7)	0.3535 (3)	0.0218 (5)
H13	-0.3924	0.2559	0.2845	0.026*
C14	0.0906 (3)	0.12230 (7)	0.3665 (2)	0.0174 (4)
C15	0.1732 (4)	0.03941 (8)	0.1363 (3)	0.0356 (6)
H15A	0.3061	0.0378	0.1634	0.053*
H15B	0.1108	0.0360	0.0282	0.053*
H15C	0.1342	0.0170	0.1873	0.053*
C16	0.1252 (3)	0.08116 (8)	0.1818 (3)	0.0252 (5)
C17	0.0778 (3)	0.11540 (8)	0.0880 (3)	0.0264 (5)
H17	0.0734	0.1134	-0.0111	0.032*
C18	0.0368 (3)	0.15281 (7)	0.1415 (3)	0.0224 (5)
C19	-0.0176 (4)	0.19110 (8)	0.0449 (3)	0.0296 (5)
H19A	-0.0925	0.2095	0.0802	0.044*
H19B	-0.0886	0.1827	-0.0583	0.044*
H19C	0.0926	0.2063	0.0494	0.044*
C20	0.4399 (4)	-0.12262 (8)	1.1540 (3)	0.0298 (5)
H20A	0.5376	-0.1027	1.2078	0.045*
H20B	0.4680	-0.1502	1.2025	0.045*
H20C	0.3231	-0.1124	1.1551	0.045*
C21	0.4867 (4)	-0.16502 (8)	0.9551 (3)	0.0301 (6)
H21A	0.3860	-0.1769	0.8697	0.045*
H21B	0.5236	-0.1852	1.0377	0.045*
H21C	0.5911	-0.1592	0.9267	0.045*
O5	0.1402 (6)	-0.05972 (13)	0.2649 (5)	0.1108 (12)*

### Atomic displacement parameters ( $\text{\AA}^2$ )

	$U^{11}$	$U^{22}$	$U^{33}$	$U^{12}$	$U^{13}$	$U^{23}$
S1	0.0168 (3)	0.0262 (3)	0.0166 (3)	0.0006 (2)	0.0068 (2)	-0.0035 (2)
O1	0.0404 (10)	0.0206 (8)	0.0262 (9)	0.0055 (7)	0.0111 (8)	0.0005 (7)
O2	0.0433 (10)	0.0240 (9)	0.0222 (9)	0.0043 (8)	0.0133 (8)	0.0032 (7)
O3	0.0235 (8)	0.0396 (10)	0.0168 (8)	0.0058 (7)	0.0072 (7)	-0.0008 (7)
O4	0.0191 (8)	0.0277 (9)	0.0293 (9)	-0.0036 (6)	0.0103 (7)	-0.0094 (7)
N1	0.0189 (10)	0.0257 (11)	0.0366 (12)	0.0015 (8)	0.0083 (9)	0.0084 (9)
N2	0.0243 (10)	0.0220 (10)	0.0168 (9)	0.0040 (8)	0.0088 (8)	0.0000 (8)
N3	0.0218 (9)	0.0200 (9)	0.0231 (10)	-0.0009 (7)	0.0108 (8)	-0.0043 (7)
N4	0.0188 (9)	0.0214 (9)	0.0197 (9)	-0.0006 (7)	0.0079 (8)	-0.0003 (7)

N5	0.0344 (11)	0.0240 (10)	0.0201 (10)	0.0032 (8)	0.0083 (8)	0.0027 (8)
C1	0.0210 (11)	0.0229 (12)	0.0244 (12)	-0.0011 (9)	0.0073 (9)	-0.0003 (9)
C2	0.0335 (13)	0.0216 (12)	0.0261 (12)	0.0030 (10)	0.0137 (10)	-0.0017 (9)
C3	0.0379 (14)	0.0272 (13)	0.0184 (11)	0.0019 (11)	0.0122 (10)	-0.0009 (9)
C4	0.0200 (11)	0.0218 (11)	0.0210 (11)	-0.0005 (9)	0.0049 (9)	0.0002 (9)
C5	0.0262 (12)	0.0208 (11)	0.0209 (11)	0.0011 (9)	0.0069 (9)	-0.0029 (9)
C6	0.0271 (12)	0.0251 (12)	0.0167 (11)	-0.0007 (9)	0.0062 (9)	-0.0017 (9)
C7	0.0203 (11)	0.0217 (11)	0.0209 (11)	-0.0007 (9)	0.0060 (9)	0.0004 (9)
C8	0.0191 (11)	0.0205 (11)	0.0218 (11)	-0.0012 (9)	0.0064 (9)	-0.0045 (9)
C9	0.0203 (11)	0.0239 (11)	0.0250 (12)	-0.0013 (9)	0.0118 (9)	-0.0001 (9)
C10	0.0221 (11)	0.0214 (11)	0.0202 (11)	0.0006 (9)	0.0096 (9)	0.0008 (8)
C11	0.0168 (10)	0.0211 (11)	0.0184 (10)	0.0000 (8)	0.0073 (9)	-0.0043 (8)
C12	0.0219 (11)	0.0202 (11)	0.0232 (11)	-0.0028 (9)	0.0112 (9)	-0.0036 (9)
C13	0.0248 (11)	0.0181 (11)	0.0222 (11)	-0.0011 (9)	0.0085 (9)	-0.0001 (9)
C14	0.0148 (10)	0.0191 (11)	0.0179 (10)	-0.0014 (8)	0.0056 (8)	-0.0022 (8)
C15	0.0482 (16)	0.0311 (14)	0.0322 (14)	0.0035 (12)	0.0207 (13)	-0.0091 (11)
C16	0.0250 (12)	0.0259 (12)	0.0260 (12)	-0.0024 (9)	0.0112 (10)	-0.0073 (9)
C17	0.0294 (12)	0.0325 (13)	0.0189 (11)	-0.0027 (10)	0.0109 (10)	-0.0036 (9)
C18	0.0196 (11)	0.0260 (12)	0.0198 (11)	-0.0027 (9)	0.0055 (9)	0.0007 (9)
C19	0.0330 (13)	0.0305 (13)	0.0236 (12)	0.0004 (11)	0.0087 (10)	0.0062 (10)
C20	0.0343 (13)	0.0312 (13)	0.0211 (12)	0.0028 (11)	0.0073 (10)	0.0052 (10)
C21	0.0371 (14)	0.0224 (12)	0.0287 (13)	0.0034 (10)	0.0101 (11)	0.0035 (10)

Geometric parameters (Å, °)

S1—O3	1.4359 (17)	C6—H6	0.9500
S1—O4	1.4433 (17)	C8—C13	1.407 (3)
S1—N2	1.6399 (19)	C8—C9	1.408 (3)
S1—C11	1.747 (2)	C9—C10	1.382 (3)
O1—C1	1.256 (3)	C9—H9	0.9500
O2—C1	1.296 (3)	C10—C11	1.397 (3)
O2—H32	0.865 (19)	C10—H10	0.9500
N1—C8	1.358 (3)	C11—C12	1.390 (3)
N1—H30A	0.83 (3)	C12—C13	1.382 (3)
N1—H30B	0.85 (3)	C12—H12	0.9500
N2—C14	1.369 (3)	C13—H13	0.9500
N2—H31	0.850 (19)	C15—C16	1.493 (3)
N3—C14	1.350 (3)	C15—H15A	0.9800
N3—C16	1.353 (3)	C15—H15B	0.9800
N4—C14	1.334 (3)	C15—H15C	0.9800
N4—C18	1.345 (3)	C16—C17	1.376 (4)
N5—C4	1.362 (3)	C17—C18	1.385 (3)
N5—C20	1.449 (3)	C17—H17	0.9500
N5—C21	1.450 (3)	C18—C19	1.497 (3)
C1—C7	1.469 (3)	C19—H19A	0.9800
C2—C3	1.373 (3)	C19—H19B	0.9800
C2—C7	1.392 (3)	C19—H19C	0.9800
C2—H4	0.9500	C20—H20A	0.9800
C3—C4	1.416 (3)	C20—H20B	0.9800
C3—H3	0.9500	C20—H20C	0.9800

C4—C5	1.416 (3)	C21—H21A	0.9800
C5—C6	1.378 (3)	C21—H21B	0.9800
C5—H5	0.9500	C21—H21C	0.9800
C6—C7	1.399 (3)		
O3—S1—O4	117.99 (10)	C11—C10—H10	120.2
O3—S1—N2	103.29 (10)	C12—C11—C10	120.3 (2)
O4—S1—N2	109.82 (10)	C12—C11—S1	121.12 (17)
O3—S1—C11	108.78 (10)	C10—C11—S1	118.45 (17)
O4—S1—C11	107.21 (10)	C13—C12—C11	120.1 (2)
N2—S1—C11	109.56 (10)	C13—C12—H12	119.9
C1—O2—H32	108 (3)	C11—C12—H12	119.9
C8—N1—H30A	120.0 (19)	C12—C13—C8	120.6 (2)
C8—N1—H30B	121 (2)	C12—C13—H13	119.7
H30A—N1—H30B	117 (3)	C8—C13—H13	119.7
C14—N2—S1	125.52 (16)	N4—C14—N3	125.3 (2)
C14—N2—H31	118 (4)	N4—C14—N2	120.69 (19)
S1—N2—H31	116 (4)	N3—C14—N2	114.04 (19)
C14—N3—C16	117.9 (2)	C16—C15—H15A	109.5
C14—N4—C18	116.31 (19)	C16—C15—H15B	109.5
C4—N5—C20	120.4 (2)	H15A—C15—H15B	109.5
C4—N5—C21	120.6 (2)	C16—C15—H15C	109.5
C20—N5—C21	118.6 (2)	H15A—C15—H15C	109.5
O1—C1—O2	122.4 (2)	H15B—C15—H15C	109.5
O1—C1—C7	119.9 (2)	N3—C16—C17	120.0 (2)
O2—C1—C7	117.7 (2)	N3—C16—C15	117.1 (2)
C3—C2—C7	122.1 (2)	C17—C16—C15	123.0 (2)
C3—C2—H4	119.0	C16—C17—C18	118.4 (2)
C7—C2—H4	119.0	C16—C17—H17	120.8
C2—C3—C4	120.7 (2)	C18—C17—H17	120.8
C2—C3—H3	119.7	N4—C18—C17	122.1 (2)
C4—C3—H3	119.7	N4—C18—C19	116.7 (2)
N5—C4—C3	121.1 (2)	C17—C18—C19	121.1 (2)
N5—C4—C5	121.7 (2)	C18—C19—H19A	109.5
C3—C4—C5	117.1 (2)	C18—C19—H19B	109.5
C6—C5—C4	121.1 (2)	H19A—C19—H19B	109.5
C6—C5—H5	119.5	C18—C19—H19C	109.5
C4—C5—H5	119.5	H19A—C19—H19C	109.5
C5—C6—C7	121.2 (2)	H19B—C19—H19C	109.5
C5—C6—H6	119.4	N5—C20—H20A	109.5
C7—C6—H6	119.4	N5—C20—H20B	109.5
C2—C7—C6	117.8 (2)	H20A—C20—H20B	109.5
C2—C7—C1	119.2 (2)	N5—C20—H20C	109.5
C6—C7—C1	123.0 (2)	H20A—C20—H20C	109.5
N1—C8—C13	121.1 (2)	H20B—C20—H20C	109.5
N1—C8—C9	120.5 (2)	N5—C21—H21A	109.5
C13—C8—C9	118.4 (2)	N5—C21—H21B	109.5
C10—C9—C8	120.9 (2)	H21A—C21—H21B	109.5
C10—C9—H9	119.5	N5—C21—H21C	109.5
C8—C9—H9	119.5	H21A—C21—H21C	109.5



C9—C10—C11	119.6 (2)	H21B—C21—H21C	109.5
C9—C10—H10	120.2		
O3—S1—N2—C14	179.45 (18)	O3—S1—C11—C12	149.96 (18)
O4—S1—N2—C14	-53.8 (2)	O4—S1—C11—C12	21.3 (2)
C11—S1—N2—C14	63.7 (2)	N2—S1—C11—C12	-97.81 (19)
C7—C2—C3—C4	0.6 (4)	O3—S1—C11—C10	-26.1 (2)
C20—N5—C4—C3	-0.1 (3)	O4—S1—C11—C10	-154.73 (17)
C21—N5—C4—C3	-172.6 (2)	N2—S1—C11—C10	86.14 (19)
C20—N5—C4—C5	179.8 (2)	C10—C11—C12—C13	1.8 (3)
C21—N5—C4—C5	7.2 (3)	S1—C11—C12—C13	-174.15 (17)
C2—C3—C4—N5	-179.9 (2)	C11—C12—C13—C8	0.0 (3)
C2—C3—C4—C5	0.3 (4)	N1—C8—C13—C12	177.0 (2)
N5—C4—C5—C6	179.5 (2)	C9—C8—C13—C12	-2.1 (3)
C3—C4—C5—C6	-0.7 (3)	C18—N4—C14—N3	0.1 (3)
C4—C5—C6—C7	0.3 (4)	C18—N4—C14—N2	-179.76 (19)
C3—C2—C7—C6	-1.0 (4)	C16—N3—C14—N4	0.4 (3)
C3—C2—C7—C1	179.9 (2)	C16—N3—C14—N2	-179.74 (19)
C5—C6—C7—C2	0.6 (3)	S1—N2—C14—N4	-4.3 (3)
C5—C6—C7—C1	179.7 (2)	S1—N2—C14—N3	175.78 (16)
O1—C1—C7—C2	-1.4 (3)	C14—N3—C16—C17	-0.3 (3)
O2—C1—C7—C2	178.2 (2)	C14—N3—C16—C15	179.1 (2)
O1—C1—C7—C6	179.6 (2)	N3—C16—C17—C18	-0.2 (3)
O2—C1—C7—C6	-0.9 (3)	C15—C16—C17—C18	-179.6 (2)
N1—C8—C9—C10	-176.7 (2)	C14—N4—C18—C17	-0.7 (3)
C13—C8—C9—C10	2.4 (3)	C14—N4—C18—C19	179.4 (2)
C8—C9—C10—C11	-0.7 (3)	C16—C17—C18—N4	0.7 (4)
C9—C10—C11—C12	-1.4 (3)	C16—C17—C18—C19	-179.4 (2)
C9—C10—C11—S1	174.65 (17)		

#### Hydrogen-bond geometry (Å, °)

<i>D</i> —H··· <i>A</i>	<i>D</i> —H	H··· <i>A</i>	<i>D</i> ··· <i>A</i>	<i>D</i> —H··· <i>A</i>
N1—H30 <i>A</i> ···O4 <i>i</i>	0.83 (3)	2.30 (3)	3.131 (3)	175 (3)
N1—H30 <i>B</i> ···O4 <i>ii</i>	0.85 (3)	2.50 (3)	3.163 (3)	135 (3)
N1—H30 <i>B</i> ···N4 <i>iii</i>	0.85 (3)	2.55 (3)	3.228 (3)	137 (3)
N2—H31···O1	0.85 (2)	1.91 (2)	2.755 (3)	177 (5)
O2—H32···N3	0.87 (2)	1.87 (2)	2.720 (3)	166 (4)

Symmetry codes: (i)  $x-1, -y+1/2, z-1/2$ ; (ii)  $x-1, y, z$ .

All esds (except the esd in the dihedral angle between two l.s. planes) are estimated using the full covariance matrix. The cell esds are taken into account individually in the estimation of esds in distances, angles and torsion angles; correlations between esds in cell parameters are only used when they are defined by crystal symmetry. An approximate (isotropic) treatment of cell esds is used for estimating esds involving l.s. planes.

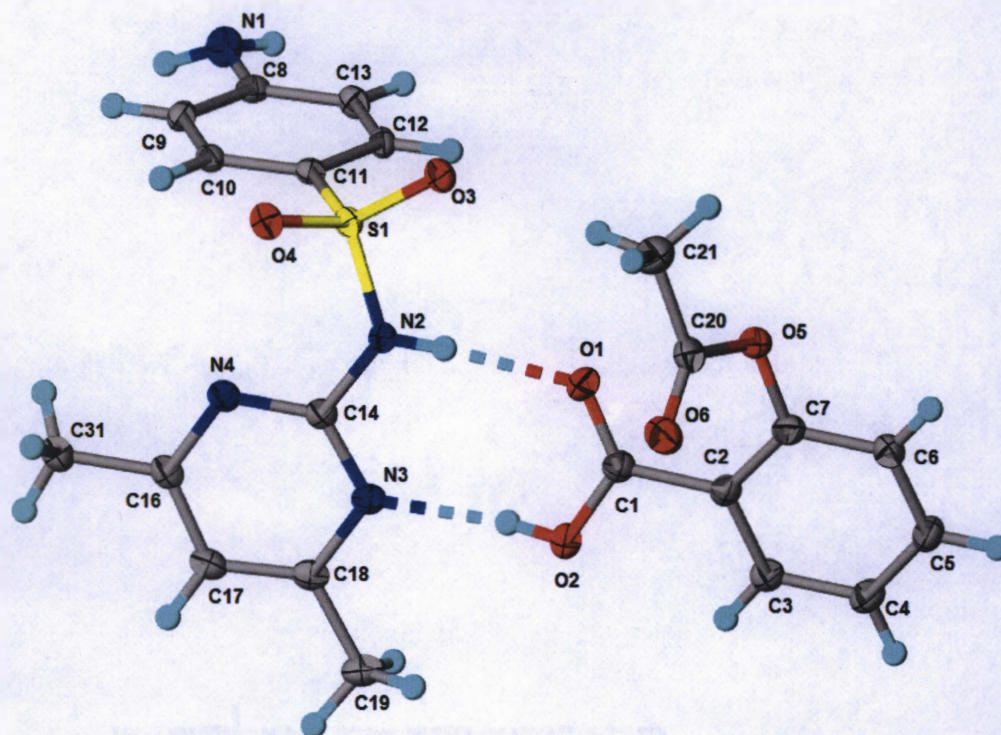


Figure S.18: Crystal Structure of the Cocrystal of Sulfamethazine and *o*-Acetyloxybenzoic Acid Showing Thermal Parameters (50% Thermal Ellipsoids) and Hydrogen Bonding.

*Crystal data*

$C_{12}H_{14}N_4O_2S \cdot C_9H_8O_4$

$M_r = 458.48$

Monoclinic,  $P2_1/c$

$a = 7.6482$  (1) Å

$b = 21.6227$  (4) Å

$c = 13.4404$  (3) Å

$\beta = 102.728$  (1)°

$V = 2168.08$  (7) Å<sup>3</sup>

$Z = 4$

$F(000) = 960$

$D_x = 1.405$  Mg m<sup>-3</sup>

Melting point: 411–415 K

Cu  $K\alpha$  radiation,  $\lambda = 1.54178$  Å

Cell parameters from 855 reflections

$\theta = 2.2$ – $68.7^\circ$

$\mu = 1.73$  mm<sup>-1</sup>

$T = 100$  K

Plates, colourless

$0.24 \times 0.17 \times 0.13$  mm

### Data collection

Bruker APEXII CCD diffractometer	3963 independent reflections
Radiation source: fine-focus sealed tube	3434 reflections with $I > 2\sigma(I)$
Detector resolution: 8.33 pixels $\text{mm}^{-1}$	$R_{\text{int}} = 0.048$
phi and $\omega$ scans	$\theta_{\text{max}} = 68.2^\circ$ , $\theta_{\text{min}} = 3.9^\circ$
Absorption correction: multi-scan <i>SADABS2014/7</i> , Bruker AXS	$h = -9 \quad 9$
$T_{\text{min}} = 0.650$ , $T_{\text{max}} = 0.753$	$k = -25 \quad 26$
32897 measured reflections	$l = -16 \quad 16$

### Refinement

Refinement on $F^2$	Hydrogen site location: mixed
Least-squares matrix: full	H atoms treated by a mixture of independent and constrained refinement
$R[F^2 > 2\sigma(F^2)] = 0.036$	$w = 1/[\sigma^2(F_o^2) + (0.0523P)^2 + 1.1985P]$
$wR(F^2) = 0.100$	where $P = (F_o^2 + 2F_c^2)/3$
$S = 1.05$	$(\Delta/\sigma)_{\text{max}} = 0.001$
3963 reflections	$\Delta\rho_{\text{max}} = 0.41 \text{ e } \text{\AA}^{-3}$
304 parameters	$\Delta\rho_{\text{min}} = -0.32 \text{ e } \text{\AA}^{-3}$
4 restraints	Extinction correction: none
0 constraints	

All nonhydrogen atoms were located in a successive difference Fourier electron density maps and refined using anisotropic displacement parameters. All C-H hydrogen atoms were placed in calculated positions with  $U_{\text{iso}} = 1.2 \times U_{\text{eqiv}}$  ( $1.5 U_{\text{eq}}$  for methyl groups) of the connected C atoms. Those H atoms attached to nitrogen were located in Fourier diff maps and assigned  $U_{\text{iso}} = 1.2 \times U_{\text{eqiv}}$  with N-H bond distances restrained to 0.85 (2) angstroms.

### Fractional atomic coordinates and isotropic or equivalent isotropic displacement parameters ( $\text{\AA}^2$ )

	<i>x</i>	<i>y</i>	<i>z</i>	$U_{\text{iso}}^*/U_{\text{eq}}$
S1	0.25637 (5)	0.30690 (2)	0.56525 (3)	0.01811 (13)
O1	0.1790 (2)	0.45650 (6)	0.70292 (10)	0.0313 (3)
O2	0.19031 (19)	0.54545 (6)	0.62016 (10)	0.0276 (3)
H32	0.199 (3)	0.5220 (10)	0.5719 (15)	0.033*
O3	0.21986 (16)	0.30025 (6)	0.66531 (9)	0.0225 (3)
O4	0.41611 (16)	0.27946 (6)	0.54559 (9)	0.0234 (3)
O5	0.20934 (18)	0.46542 (6)	0.90961 (10)	0.0277 (3)
O6	0.48973 (19)	0.48367 (7)	0.88668 (11)	0.0324 (3)
N1	-0.3732 (2)	0.21628 (8)	0.26287 (13)	0.0290 (4)
H30B	-0.359 (3)	0.2131 (11)	0.2006 (13)	0.035*
H30A	-0.476 (2)	0.2307 (10)	0.2724 (18)	0.035*

N2	0.2625 (2)	0.38244 (7)	0.55124 (11)	0.0213 (3)
N3	0.26773 (19)	0.47512 (7)	0.46729 (12)	0.0214 (3)
H31	0.232 (3)	0.4033 (9)	0.5972 (14)	0.026*
N4	0.33330 (19)	0.37988 (7)	0.39113 (11)	0.0214 (3)
C1	0.1732 (2)	0.51309 (8)	0.70048 (14)	0.0226 (4)
C2	0.1431 (2)	0.55128 (8)	0.78753 (14)	0.0219 (4)
C3	0.0914 (2)	0.61332 (8)	0.77192 (15)	0.0239 (4)
H3	0.0817	0.6313	0.7064	0.029*
C4	0.0543 (3)	0.64881 (9)	0.85051 (16)	0.0281 (4)
H4	0.0182	0.6907	0.8385	0.034*
C5	0.0699 (3)	0.62324 (9)	0.94667 (16)	0.0280 (4)
H5	0.0427	0.6474	1.0003	0.034*
C6	0.1250 (3)	0.56237 (9)	0.96463 (15)	0.0273 (4)
H6	0.1381	0.5451	1.0309	0.033*
C7	0.1607 (3)	0.52688 (8)	0.88601 (15)	0.0249 (4)
C8	-0.2269 (2)	0.23805 (8)	0.33220 (14)	0.0213 (4)
C9	-0.0532 (2)	0.22876 (8)	0.31682 (14)	0.0215 (4)
H9	-0.0369	0.2074	0.2578	0.026*
C10	0.0945 (2)	0.25046 (8)	0.38680 (13)	0.0192 (4)
H10	0.2114	0.2450	0.3748	0.023*
C11	0.0718 (2)	0.28022 (8)	0.47473 (13)	0.0175 (3)
C12	-0.1005 (2)	0.28878 (8)	0.49196 (13)	0.0199 (4)
H12	-0.1156	0.3088	0.5524	0.024*
C13	-0.2485 (2)	0.26828 (8)	0.42160 (14)	0.0219 (4)
H13	-0.3652	0.2745	0.4334	0.026*
C14	0.2888 (2)	0.41334 (8)	0.46503 (13)	0.0197 (4)
C16	0.3616 (2)	0.41167 (9)	0.30979 (14)	0.0226 (4)
C17	0.3433 (2)	0.47580 (9)	0.30470 (15)	0.0252 (4)
H17	0.3630	0.4980	0.2472	0.030*
C18	0.2958 (2)	0.50638 (9)	0.38530 (14)	0.0230 (4)
C19	0.2695 (3)	0.57544 (9)	0.38520 (16)	0.0304 (4)
H19A	0.1410	0.5849	0.3692	0.046*
H19B	0.3258	0.5943	0.3338	0.046*
H19C	0.3246	0.5921	0.4526	0.046*
C20	0.3795 (3)	0.44808 (9)	0.90466 (14)	0.0276 (4)
C21	0.4037 (3)	0.38011 (10)	0.92244 (18)	0.0379 (5)
H21A	0.3614	0.3580	0.8580	0.057*
H21B	0.3347	0.3667	0.9720	0.057*
H21C	0.5310	0.3710	0.9491	0.057*
C31	0.4166 (3)	0.37475 (9)	0.22778 (15)	0.0289 (4)
H31A	0.5369	0.3578	0.2536	0.043*
H31B	0.4175	0.4015	0.1690	0.043*
H31C	0.3315	0.3408	0.2070	0.043*

Atomic displacement parameters ( $\text{\AA}^2$ )

	$U^{11}$	$U^{22}$	$U^{33}$	$U^{12}$	$U^{13}$	$U^{23}$
S1	0.0174 (2)	0.0206 (2)	0.0160 (2)	0.00069 (16)	0.00311 (16)	0.00111 (16)

O1	0.0476 (9)	0.0218 (7)	0.0267 (7)	-0.0040 (6)	0.0126 (6)	-0.0053 (6)
O2	0.0342 (7)	0.0251 (7)	0.0253 (7)	0.0011 (6)	0.0104 (6)	-0.0023 (6)
O3	0.0228 (6)	0.0276 (7)	0.0170 (6)	0.0000 (5)	0.0040 (5)	0.0017 (5)
O4	0.0182 (6)	0.0292 (7)	0.0225 (6)	0.0042 (5)	0.0036 (5)	0.0025 (5)
O5	0.0336 (7)	0.0213 (6)	0.0321 (7)	-0.0001 (6)	0.0154 (6)	0.0006 (6)
O6	0.0318 (8)	0.0337 (8)	0.0333 (8)	-0.0010 (6)	0.0111 (6)	0.0027 (6)
N1	0.0238 (8)	0.0354 (9)	0.0257 (9)	-0.0022 (7)	0.0008 (7)	-0.0043 (7)
N2	0.0266 (8)	0.0200 (8)	0.0183 (7)	-0.0024 (6)	0.0072 (6)	-0.0025 (6)
N3	0.0186 (7)	0.0218 (8)	0.0226 (8)	-0.0033 (6)	0.0017 (6)	-0.0002 (6)
N4	0.0189 (7)	0.0237 (8)	0.0211 (8)	-0.0027 (6)	0.0036 (6)	0.0002 (6)
C1	0.0187 (9)	0.0235 (9)	0.0253 (9)	-0.0037 (7)	0.0041 (7)	-0.0033 (8)
C2	0.0178 (8)	0.0220 (9)	0.0264 (9)	-0.0040 (7)	0.0057 (7)	-0.0044 (7)
C3	0.0206 (9)	0.0240 (9)	0.0265 (10)	-0.0012 (7)	0.0038 (7)	-0.0009 (8)
C4	0.0290 (10)	0.0219 (9)	0.0336 (11)	0.0014 (8)	0.0075 (8)	-0.0024 (8)
C5	0.0286 (10)	0.0256 (10)	0.0317 (10)	-0.0016 (8)	0.0106 (8)	-0.0074 (8)
C6	0.0293 (10)	0.0276 (10)	0.0276 (10)	-0.0032 (8)	0.0116 (8)	-0.0017 (8)
C7	0.0241 (9)	0.0207 (9)	0.0318 (10)	-0.0013 (7)	0.0101 (8)	-0.0002 (8)
C8	0.0231 (9)	0.0183 (9)	0.0212 (9)	-0.0016 (7)	0.0020 (7)	0.0032 (7)
C9	0.0277 (9)	0.0180 (8)	0.0189 (9)	0.0014 (7)	0.0054 (7)	-0.0010 (7)
C10	0.0198 (8)	0.0172 (8)	0.0217 (9)	0.0020 (7)	0.0073 (7)	0.0024 (7)
C11	0.0176 (8)	0.0168 (8)	0.0175 (8)	0.0003 (7)	0.0028 (7)	0.0030 (7)
C12	0.0224 (9)	0.0204 (9)	0.0182 (8)	0.0038 (7)	0.0071 (7)	0.0012 (7)
C13	0.0171 (8)	0.0257 (9)	0.0236 (9)	0.0018 (7)	0.0059 (7)	0.0028 (7)
C14	0.0155 (8)	0.0226 (9)	0.0198 (9)	-0.0040 (7)	0.0012 (7)	-0.0012 (7)
C16	0.0164 (8)	0.0298 (10)	0.0207 (9)	-0.0041 (7)	0.0024 (7)	0.0001 (8)
C17	0.0223 (9)	0.0270 (10)	0.0260 (10)	-0.0030 (7)	0.0046 (8)	0.0057 (8)
C18	0.0172 (8)	0.0240 (9)	0.0263 (9)	-0.0039 (7)	0.0013 (7)	0.0021 (8)
C19	0.0313 (10)	0.0237 (10)	0.0355 (11)	-0.0029 (8)	0.0055 (9)	0.0028 (8)
C20	0.0330 (10)	0.0295 (10)	0.0215 (9)	-0.0013 (8)	0.0086 (8)	-0.0011 (8)
C21	0.0432 (13)	0.0284 (11)	0.0438 (13)	0.0019 (9)	0.0135 (10)	-0.0002 (10)
C31	0.0327 (10)	0.0308 (10)	0.0256 (10)	-0.0009 (8)	0.0115 (8)	0.0013 (8)

Geometric parameters (Å, °)

S1—O4	1.4341 (13)	C6—C7	1.381 (3)
S1—O3	1.4398 (13)	C6—H6	0.9500
S1—N2	1.6459 (15)	C8—C9	1.403 (3)
S1—C11	1.7463 (18)	C8—C13	1.409 (3)
O1—C1	1.225 (2)	C9—C10	1.383 (3)
O2—C1	1.317 (2)	C9—H9	0.9500
O2—H32	0.837 (16)	C10—C11	1.390 (2)
O5—C20	1.370 (2)	C10—H10	0.9500
O5—C7	1.397 (2)	C11—C12	1.400 (2)
O6—C20	1.204 (2)	C12—C13	1.378 (3)
N1—C8	1.372 (2)	C12—H12	0.9500
N1—H30B	0.869 (16)	C13—H13	0.9500
N1—H30A	0.884 (16)	C16—C17	1.394 (3)
N2—C14	1.390 (2)	C16—C31	1.494 (3)
N2—H31	0.839 (15)	C17—C18	1.384 (3)
N3—C14	1.347 (2)	C17—H17	0.9500

N3—C18	1.350 (2)	C18—C19	1.507 (3)
N4—C14	1.332 (2)	C19—H19A	0.9800
N4—C16	1.349 (2)	C19—H19B	0.9800
C1—C2	1.491 (2)	C19—H19C	0.9800
C2—C3	1.401 (3)	C20—C21	1.494 (3)
C2—C7	1.403 (3)	C21—H21A	0.9800
C3—C4	1.385 (3)	C21—H21B	0.9800
C3—H3	0.9500	C21—H21C	0.9800
C4—C5	1.387 (3)	C31—H31A	0.9800
C4—H4	0.9500	C31—H31B	0.9800
C5—C6	1.387 (3)	C31—H31C	0.9800
C5—H5	0.9500		
O4—S1—O3	118.63 (7)	C9—C10—H10	120.0
O4—S1—N2	110.03 (8)	C11—C10—H10	120.0
O3—S1—N2	102.84 (8)	C10—C11—C12	120.05 (16)
O4—S1—C11	109.02 (8)	C10—C11—S1	120.79 (13)
O3—S1—C11	108.92 (8)	C12—C11—S1	119.16 (13)
N2—S1—C11	106.69 (8)	C13—C12—C11	120.30 (16)
C1—O2—H32	110.7 (16)	C13—C12—H12	119.9
C20—O5—C7	117.20 (14)	C11—C12—H12	119.9
C8—N1—H30B	115.3 (16)	C12—C13—C8	120.11 (16)
C8—N1—H30A	113.6 (15)	C12—C13—H13	119.9
H30B—N1—H30A	118 (2)	C8—C13—H13	119.9
C14—N2—S1	125.83 (13)	N4—C14—N3	127.38 (16)
C14—N2—H31	118.1 (15)	N4—C14—N2	117.91 (16)
S1—N2—H31	115.4 (15)	N3—C14—N2	114.71 (15)
C14—N3—C18	115.90 (16)	N4—C16—C17	120.97 (17)
C14—N4—C16	116.14 (16)	N4—C16—C31	116.57 (17)
O1—C1—O2	122.91 (17)	C17—C16—C31	122.45 (16)
O1—C1—C2	122.91 (17)	C18—C17—C16	118.53 (17)
O2—C1—C2	114.18 (16)	C18—C17—H17	120.7
C3—C2—C7	117.81 (17)	C16—C17—H17	120.7
C3—C2—C1	120.00 (17)	N3—C18—C17	121.08 (17)
C7—C2—C1	122.18 (16)	N3—C18—C19	116.85 (16)
C4—C3—C2	120.99 (18)	C17—C18—C19	122.06 (17)
C4—C3—H3	119.5	C18—C19—H19A	109.5
C2—C3—H3	119.5	C18—C19—H19B	109.5
C3—C4—C5	120.00 (18)	H19A—C19—H19B	109.5
C3—C4—H4	120.0	C18—C19—H19C	109.5
C5—C4—H4	120.0	H19A—C19—H19C	109.5
C4—C5—C6	120.07 (18)	H19B—C19—H19C	109.5
C4—C5—H5	120.0	O6—C20—O5	123.31 (18)
C6—C5—H5	120.0	O6—C20—C21	126.38 (19)
C7—C6—C5	119.87 (18)	O5—C20—C21	110.30 (17)
C7—C6—H6	120.1	C20—C21—H21A	109.5
C5—C6—H6	120.1	C20—C21—H21B	109.5
C6—C7—O5	116.25 (17)	H21A—C21—H21B	109.5
C6—C7—C2	121.23 (17)	C20—C21—H21C	109.5
O5—C7—C2	122.49 (16)	H21A—C21—H21C	109.5

N1—C8—C9	120.51 (17)	H21B—C21—H21C	109.5
N1—C8—C13	120.48 (17)	C16—C31—H31A	109.5
C9—C8—C13	118.97 (16)	C16—C31—H31B	109.5
C10—C9—C8	120.62 (16)	H31A—C31—H31B	109.5
C10—C9—H9	119.7	C16—C31—H31C	109.5
C8—C9—H9	119.7	H31A—C31—H31C	109.5
C9—C10—C11	119.92 (16)	H31B—C31—H31C	109.5
O4—S1—N2—C14	54.64 (17)	O3—S1—C11—C10	-145.34 (14)
O3—S1—N2—C14	-178.04 (14)	N2—S1—C11—C10	104.29 (15)
C11—S1—N2—C14	-63.48 (16)	O4—S1—C11—C12	165.08 (13)
O1—C1—C2—C3	-163.29 (18)	O3—S1—C11—C12	34.24 (16)
O2—C1—C2—C3	15.7 (2)	N2—S1—C11—C12	-76.13 (15)
O1—C1—C2—C7	15.2 (3)	C10—C11—C12—C13	-0.6 (3)
O2—C1—C2—C7	-165.75 (17)	S1—C11—C12—C13	179.85 (14)
C7—C2—C3—C4	-1.7 (3)	C11—C12—C13—C8	0.6 (3)
C1—C2—C3—C4	176.85 (17)	N1—C8—C13—C12	178.54 (17)
C2—C3—C4—C5	0.7 (3)	C9—C8—C13—C12	0.6 (3)
C3—C4—C5—C6	0.9 (3)	C16—N4—C14—N3	0.5 (3)
C4—C5—C6—C7	-1.3 (3)	C16—N4—C14—N2	-178.55 (15)
C5—C6—C7—O5	-177.79 (17)	C18—N3—C14—N4	-0.3 (3)
C5—C6—C7—C2	0.2 (3)	C18—N3—C14—N2	178.80 (15)
C20—O5—C7—C6	-115.03 (19)	S1—N2—C14—N4	-8.2 (2)
C20—O5—C7—C2	67.0 (2)	S1—N2—C14—N3	172.64 (13)
C3—C2—C7—C6	1.3 (3)	C14—N4—C16—C17	-0.4 (2)
C1—C2—C7—C6	-177.27 (17)	C14—N4—C16—C31	178.34 (16)
C3—C2—C7—O5	179.18 (16)	N4—C16—C17—C18	0.2 (3)
C1—C2—C7—O5	0.6 (3)	C31—C16—C17—C18	-178.52 (17)
N1—C8—C9—C10	-179.76 (17)	C14—N3—C18—C17	0.0 (2)
C13—C8—C9—C10	-1.8 (3)	C14—N3—C18—C19	178.84 (16)
C8—C9—C10—C11	1.8 (3)	C16—C17—C18—N3	0.0 (3)
C9—C10—C11—C12	-0.6 (3)	C16—C17—C18—C19	-178.74 (17)
C9—C10—C11—S1	178.94 (13)	C7—O5—C20—O6	4.1 (3)
O4—S1—C11—C10	-14.50 (16)	C7—O5—C20—C21	-174.72 (16)

#### Hydrogen-bond geometry (Å, °)

<i>D</i> —H··· <i>A</i>	<i>D</i> —H	H··· <i>A</i>	<i>D</i> ··· <i>A</i>	<i>D</i> —H··· <i>A</i>
N1—H30 <i>A</i> ···O3 <sup>i</sup>	0.88 (2)	2.54 (2)	3.120 (2)	124 (2)
N1—H30 <i>B</i> ···O4 <sup>i</sup>	0.87 (2)	2.40 (2)	3.010 (2)	128 (2)
N2—H31···O1	0.84 (2)	1.94 (2)	2.775 (2)	175 (2)
O2—H32···N3	0.84 (2)	1.90 (2)	2.724 (2)	168 (2)

Symmetry code: (i)  $x-1, -y+1/2, z-1/2$ .

All esds (except the esd in the dihedral angle between two l.s. planes) are estimated using the full covariance matrix. The cell esds are taken into account individually in the estimation of esds in distances, angles and torsion angles; correlations between esds in cell parameters are only used when they are defined by crystal symmetry. An



N2—H31···O1	0.84 (2)	1.94 (2)	2.775 (2)	175 (2)
O2—H32···N3	0.84 (2)	1.90 (2)	2.724 (2)	168 (2)

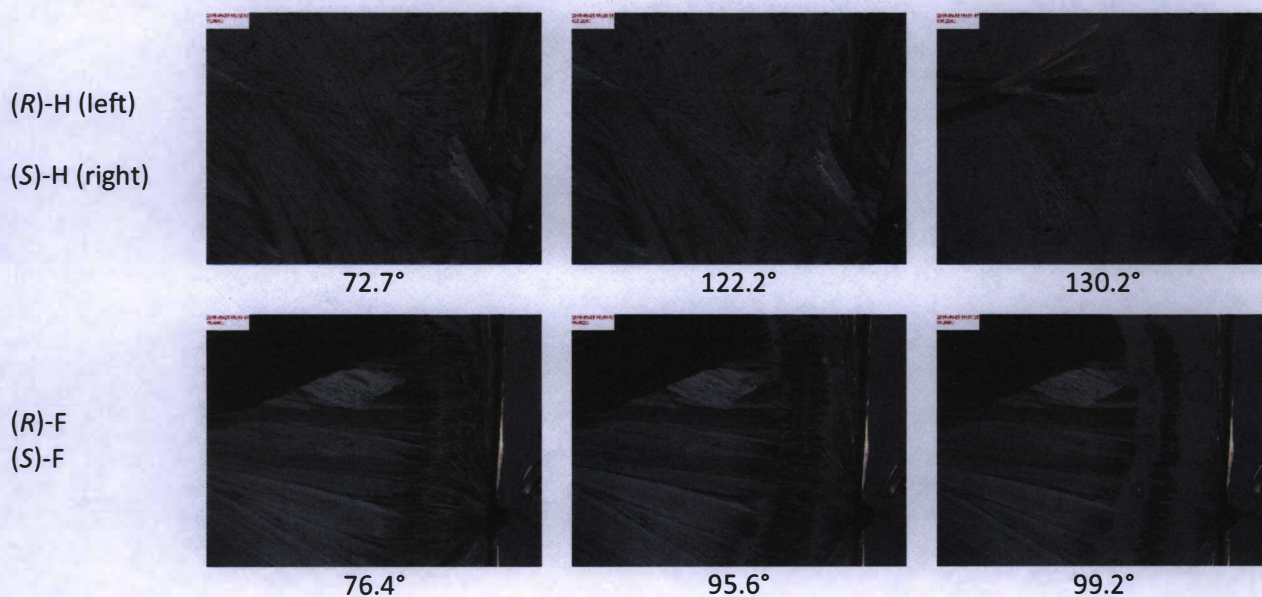
Symmetry code: (i)  $x-1, -y+1/2, z-1/2$ .

All esds (except the esd in the dihedral angle between two l.s. planes) are estimated using the full covariance matrix. The cell esds are taken into account individually in the estimation of esds in distances, angles and torsion angles; correlations between esds in cell parameters are only used when they are defined by crystal symmetry. An approximate (isotropic) treatment of cell esds is used for estimating esds involving l.s. planes.

## S2. Hot-Stage Microscopy

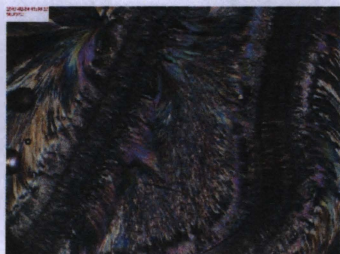
*Table S1: Hot-Stage Images of Racemic and Quasiracemic Pairs*

### Racemic Mixtures





(S)-Cl  
(R)-Cl



90.7°



108.9°



116.7°

(S)-CN  
(R)-CN



110.683°

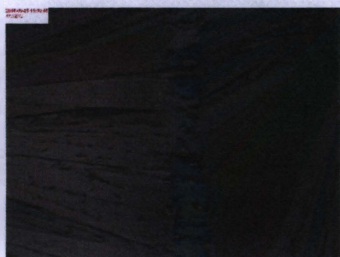


122.640°

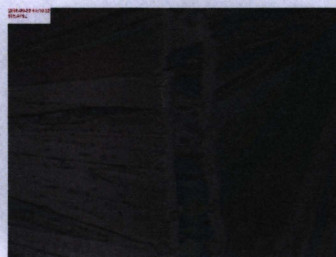


135.214°

(R)-Me  
(S)-Me



77.1°



105.5°

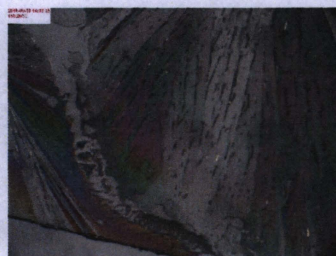


112.3°

(R)-NO<sub>2</sub>  
(S)-NO<sub>2</sub>



114.9°



159.2°



161.1°

(R)-Br  
(S)-Br



100.7°



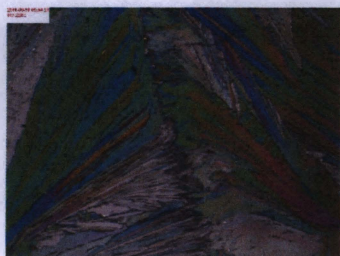
110.5°



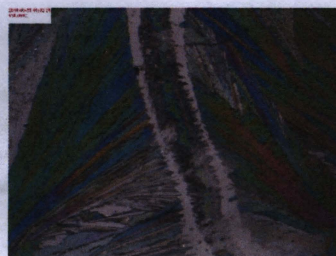
113.1°



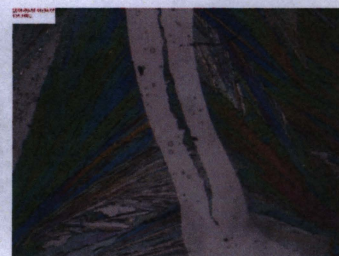
(*R*)-CF<sub>3</sub>  
(*S*)-CF<sub>3</sub>



107.2°

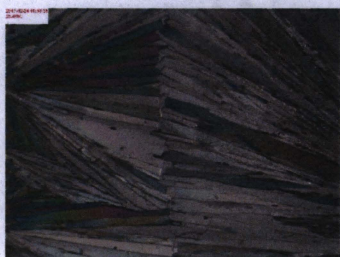


130.1°

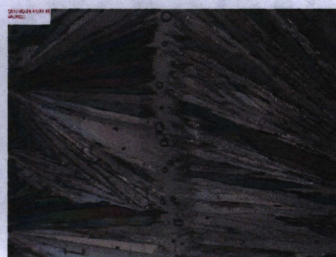


135.2°

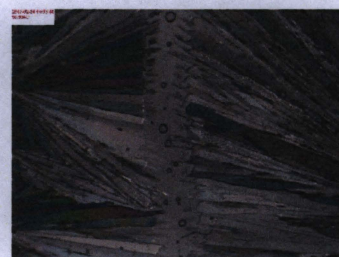
(*S*)-OMe  
(*R*)-OMe



25.5°

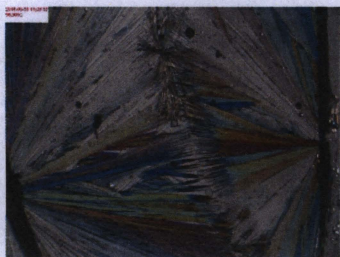


48.1°



50.6°

(*R*)-I  
(*S*)-I



98.5°

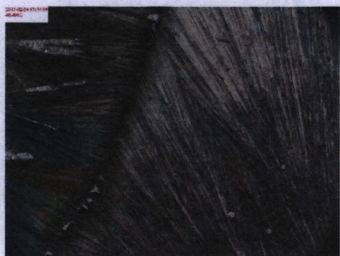


122.4°

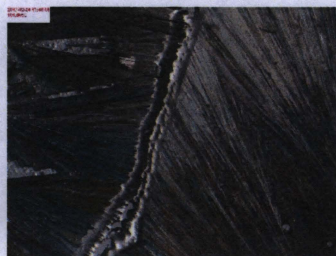


129.8°

(*S*)-Phenyl  
(*R*)-Phenyl



46.4°



101.6°



104.8°

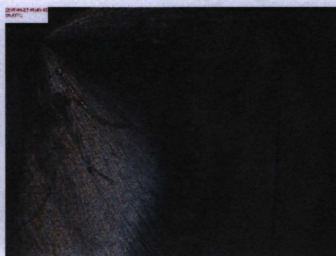
### Hydrogen

(*S*)-H  
(left)



80.8°

(*R*)-F  
(right)



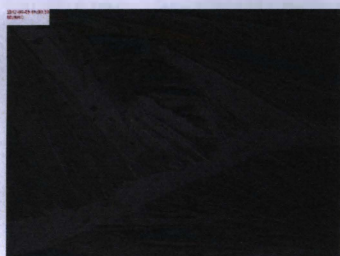
95.8°



110.2°



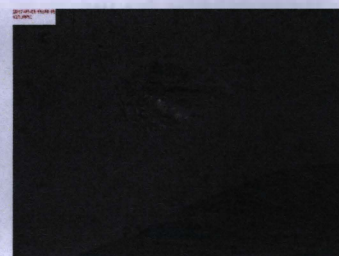
(S)-Cl  
(R)-H



89.6°

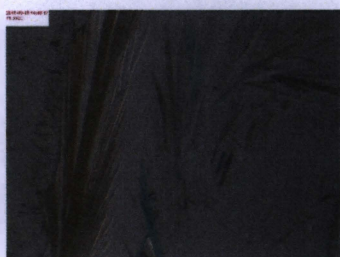


110.3°



123.8°

(S)-H  
(R)-CN



71.3°



98.6°



145.0°

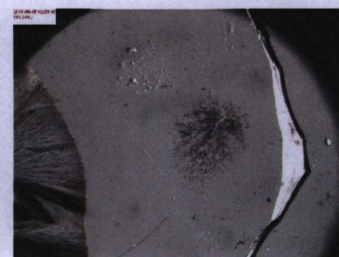
(R)-H  
(S)-Me



75.5°



95.9°



111.1°

(S)-H  
(R)-NO<sub>2</sub>



88.5°

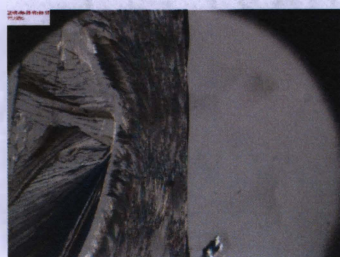


114.3°



127.1°

(R)-H  
(S)-Br



77.1°



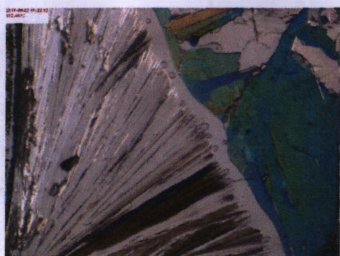
105.4°



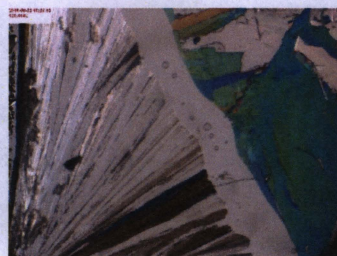
121.9°



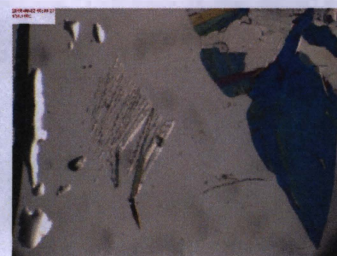
(S)-H  
(R)-CF<sub>3</sub>



102.5°



120.8°

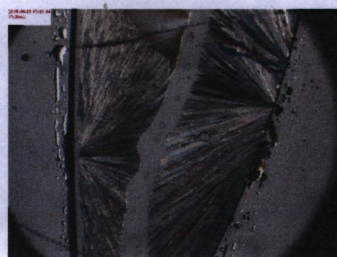


131.1°

(S)-H  
(R)-OMe



45.5°

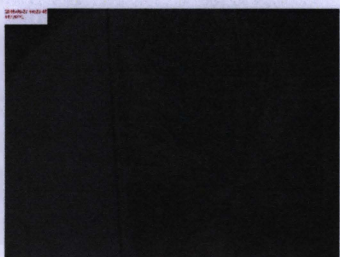


73.9°



78.5°

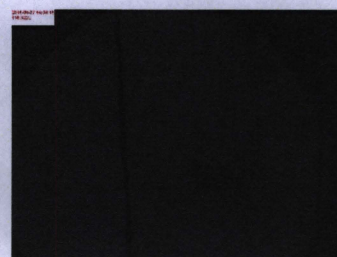
(R)-H  
(S)-I



117.7°



132.2°



138.3°

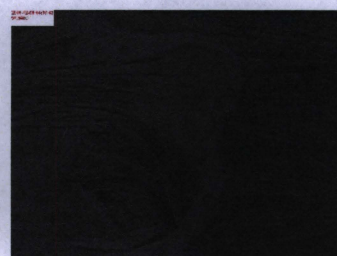
(R)-H  
(S)-Phenyl



50.7°



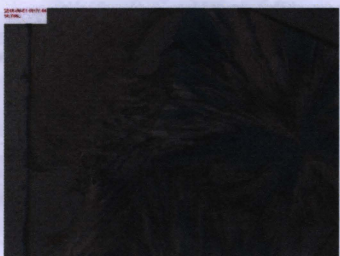
76.8°



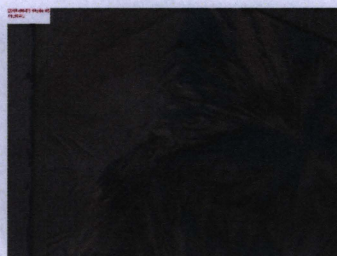
97.5°

### Fluoride

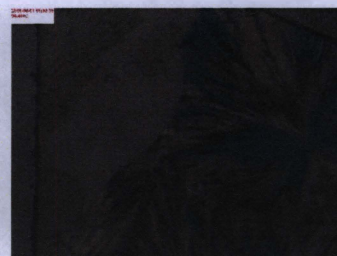
(S)-Cl  
(R)-F



50.8°



71.5°



94.4°



(S)-F  
(R)-CN



43.8°



82.9°



95.0°

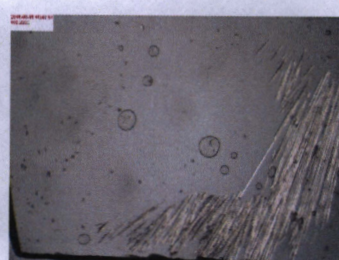
(S)-Me  
(R)-F



77.4°

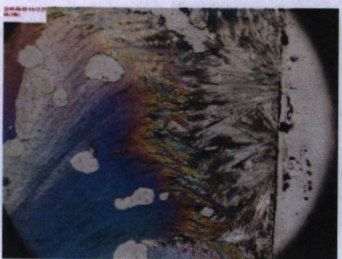


96.5°

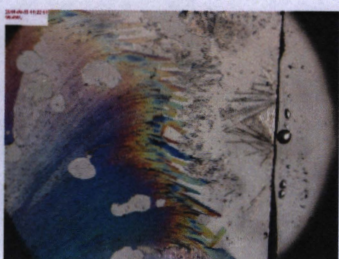


102.2°

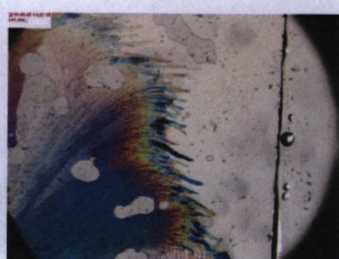
(S)-NO<sub>2</sub>  
(R)-F



80.2°



96.4°



119.8°

(S)-Br  
(R)-F



69.3°



90.8°



98.9°

(S)-CF<sub>3</sub>  
(R)-F



53.1°



91.8°



97.8°



(S)-OMe  
(R)-F



49.9°



61.8°

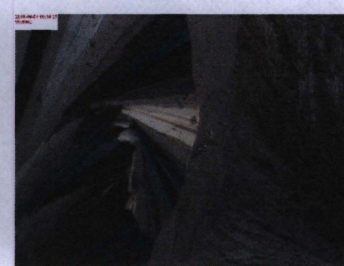


79.5°

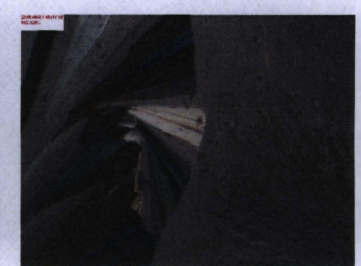
(S)-I  
(R)-F



58.7°

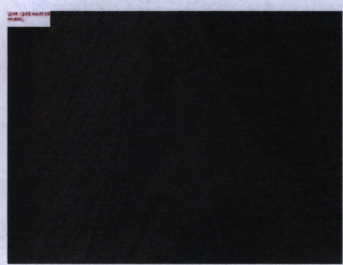


99.7°

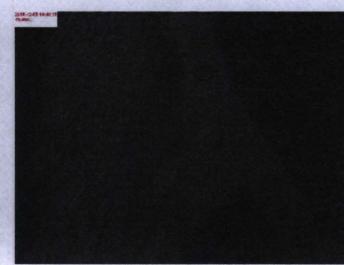


102.5°

(R)-F  
(S)-Phenyl



55.7°



78.5°



103.7°

Chloride

(S)-Cl  
(R)-CN



86.4°



95.0°

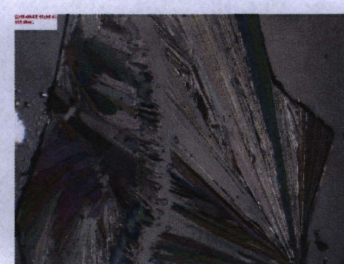


100.1°

(S)-Cl  
(R)-Me



98.7°



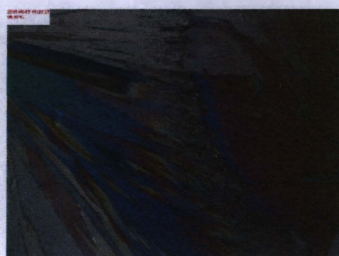
105.6°



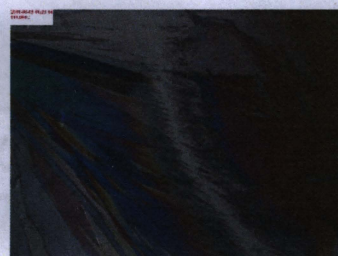
113.3°



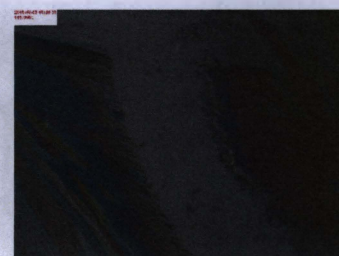
(S)-Cl  
(R)-Nitro



96.5°

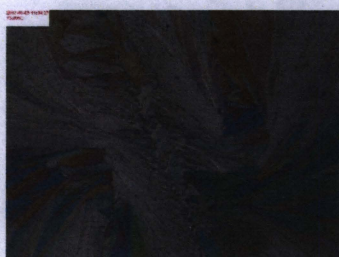


111.1°

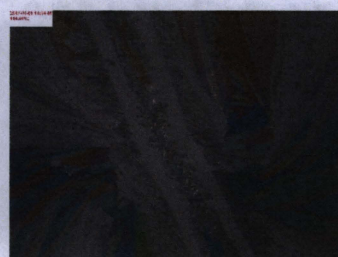


112.0°

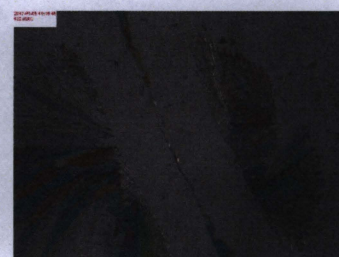
(S)-Cl  
(R)-Br



73.1°



114.4°

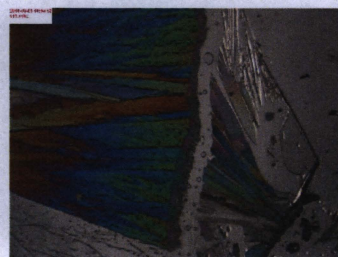


122.0°

(S)-Cl  
(R)-CF<sub>3</sub>



105.6°



113.7°



117.7°

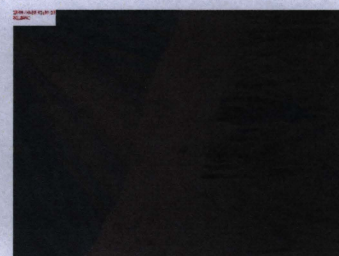
(R)-Cl  
(S)-OMe



50.9°

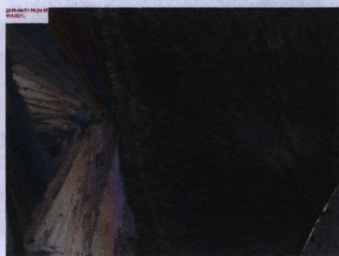


66.3°



82.2°

(S)-I  
(R)-Cl



101.8°



115.5°



118.2°



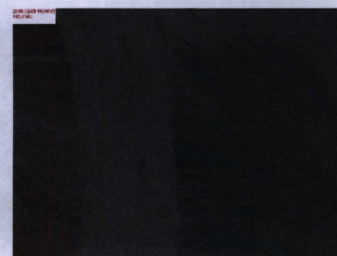
(*R*)-Cl  
(*S*)-Phenyl



63.3°



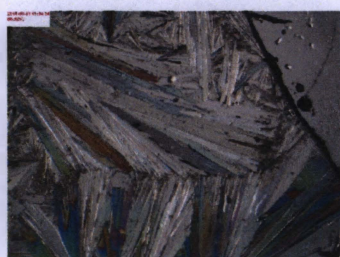
95.2°



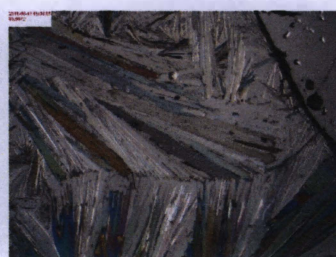
112.1°

**Cyano**

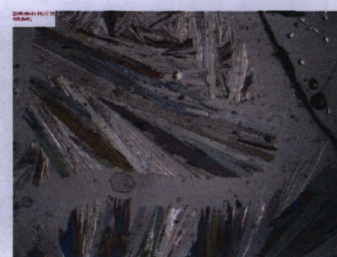
(*S*)-Me  
(*R*)-CN



66.5°

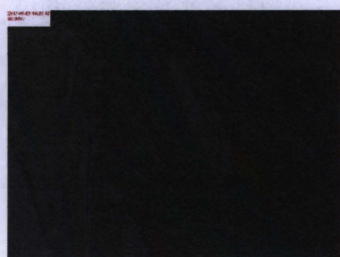


83.7°

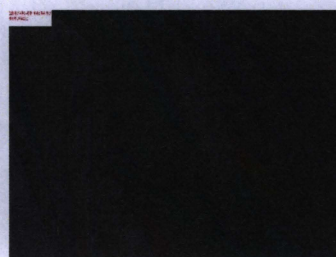


100.6°

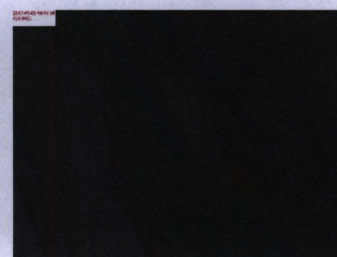
(*R*)-CN  
(*S*)-Nitro



80.9°



109.7°



121.7°

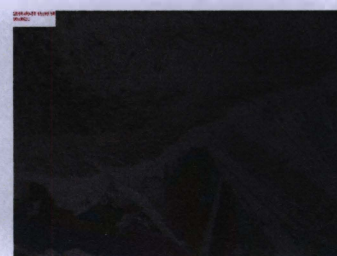
(*S*)-Br  
(*R*)-CN



70.5°

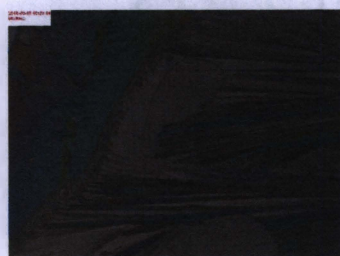


95.2°

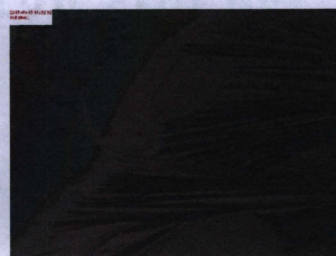


99.1°

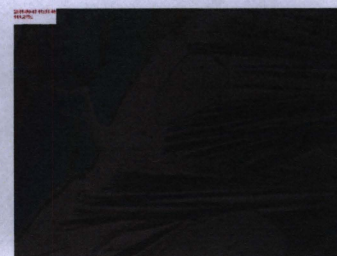
(*S*)-CF<sub>3</sub>  
(*R*)-CN



86.0°



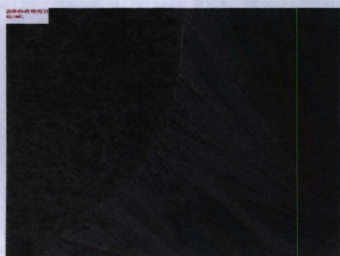
108.6°



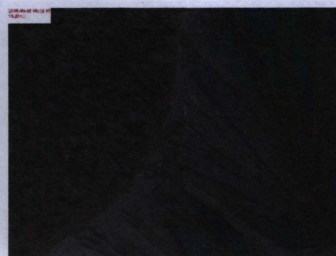
111.3°



(R)-CN  
(S)-OMe



42.1°

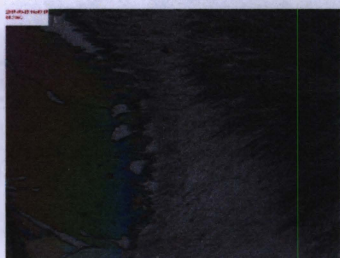


71.2°



83.2°

(S)-I  
(R)-CN



81.2°



104.7°



107.2°

(S)-Phenyl  
(R)-CN



56.9°



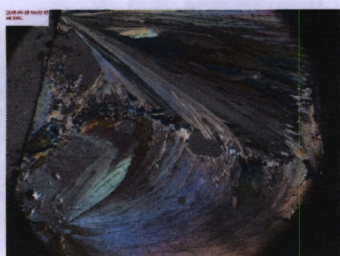
79.2°



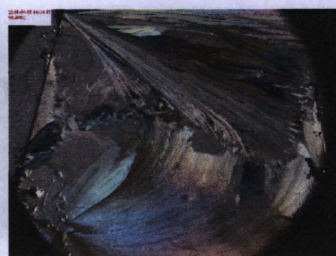
90.5°

Methyl

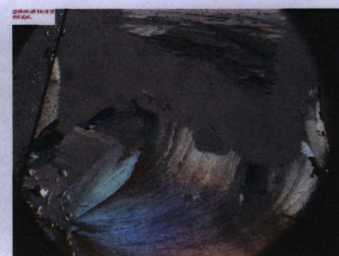
(S)-NO<sub>2</sub>  
(R)-Me



44.5°

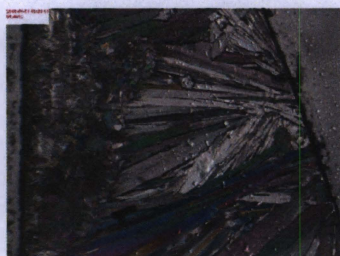


98.5°

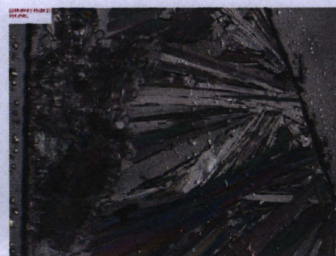


109.8°

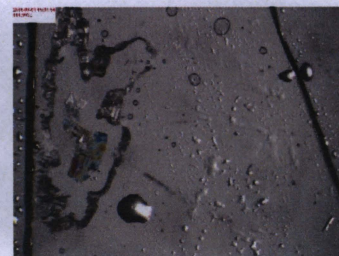
(S)-Br  
(R)-Me



81.4°



101.8°



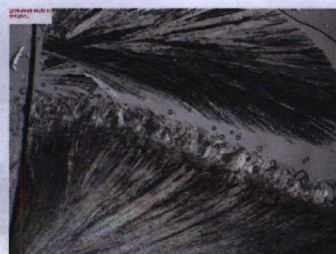
112.0°



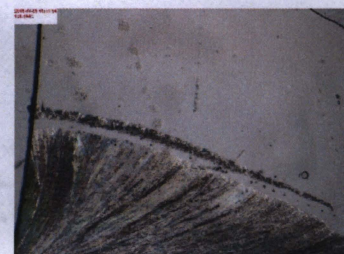
(S)-Me  
(R)-CF<sub>3</sub>



82.4°

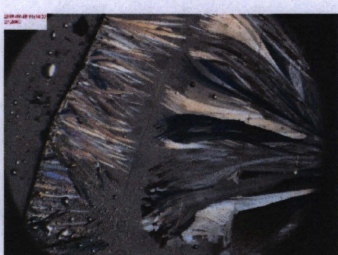


106.3°

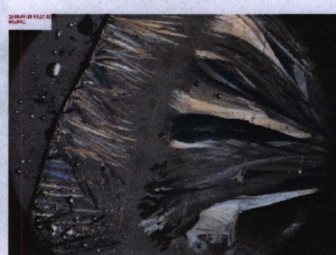


120.2°

(S)-OMe  
(R)-Me



27.3°



63.1°

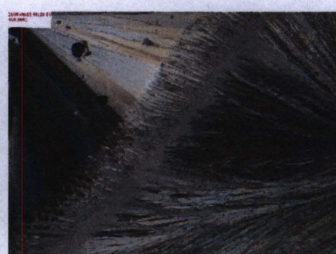


71.8°

(S)-I  
(R)-Me



46.9°



106.6°



121.8°

(S)-Me  
(R)-Phenyl



73.9°



94.9°



108.8°

**Nitro**

(R)-NO<sub>2</sub>  
(S)-Br



105.0°



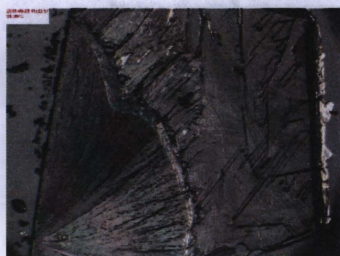
113.6°



123.8°



(S)-NO<sub>2</sub>  
(R)-CF<sub>3</sub>



92.0°

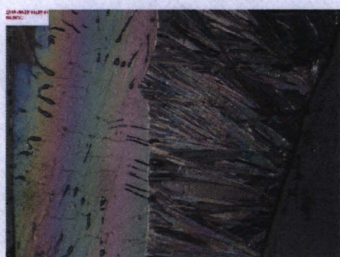


137.7°

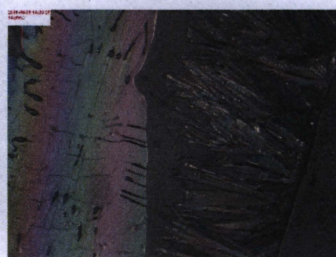


147.8°

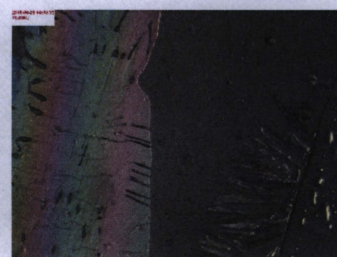
(R)-NO<sub>2</sub>  
(S)-OMe



64.6°



74.1°



78.9°

(R)-NO<sub>2</sub>  
(S)-I



81.3°



118.3°



128.6°

(S)-NO<sub>2</sub>  
(R)-Phenyl



60.4°



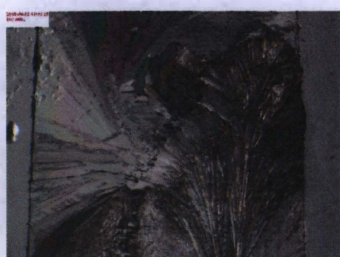
107.0°



113.1°

### Bromide

(S)-Br  
(R)-CF<sub>3</sub>



107.5°



117.6°



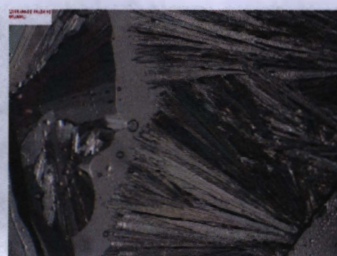
118.8°



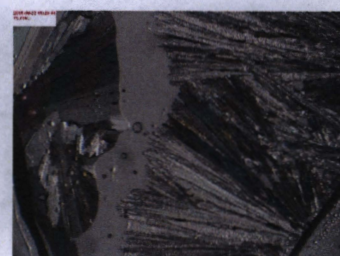
(S)-OMe  
(R)-Br



42.4°



69.1°

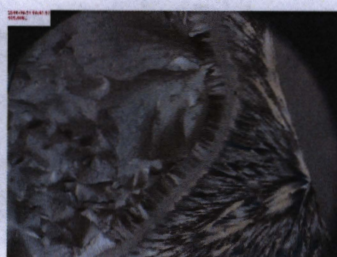


75.7°

(S)-I  
(R)-Br



103.0°



109.8°



112.0°

(S)-Br  
(R)-Phenyl



74.6°



97.1°



111.9°

**Trifluoromethyl**

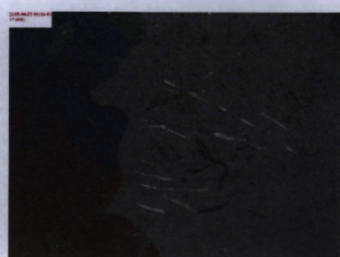
(S)-OMe  
(R)-CF<sub>3</sub>



26.3°

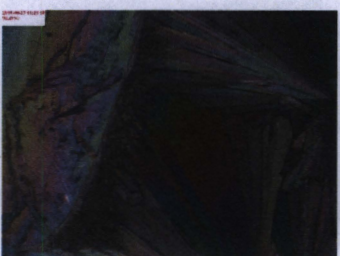


65.4°

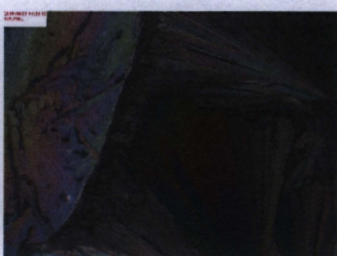


77.1°

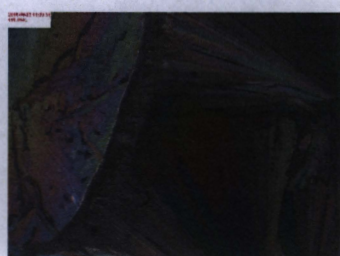
(S)-I  
(R)-CF<sub>3</sub>



92.3°



109.8°



110.8°



(S)-Phenyl  
(R)-CF<sub>3</sub>



69.3°



95.4°



111.3°

**Methoxy**

(S)-OMe  
(R)-I



42.3°

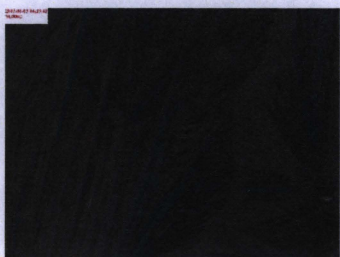


73.1°

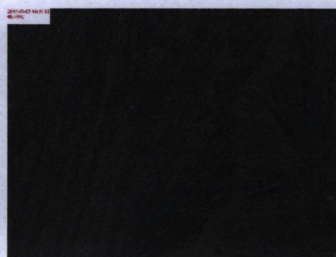


105.5°

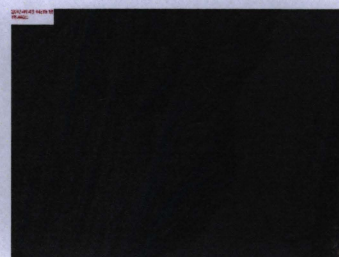
(R)-Phenyl  
(S)-OMe



31.0°



60.2°



78.4°

**Iodide**

(R)-I  
(S)-Phenyl



43.0°



94.6°



111.6°

**Table S2: Hot Stage Images of Same Handed Homochiral Diarylamide Derivatives**

**Hydrogen**



(R)-H (left)  
(R)-F (right)



102.3°

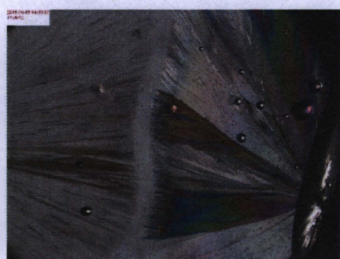


107.4°

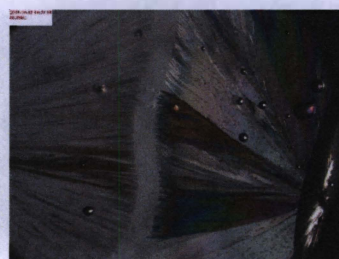


132.1°

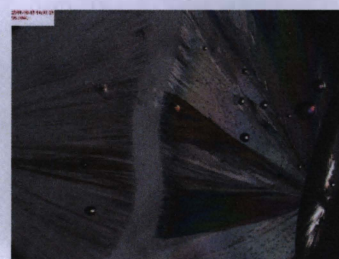
(S)-Cl  
(S)-H



77.0°



88.9°



95.1°

(R)-H  
(R)-CN



86.6°

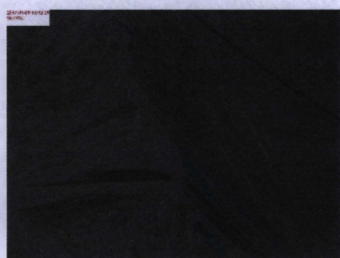


122.5°



130.3°

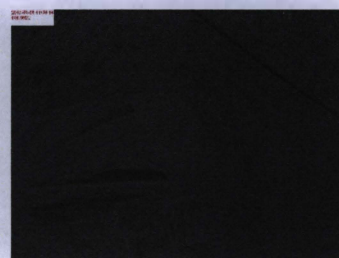
(S)-H  
(S)-Me



90.2°

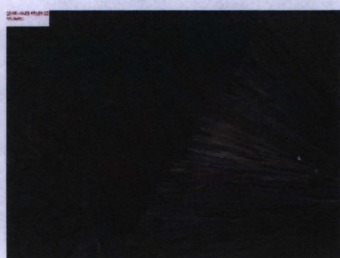


102.4°

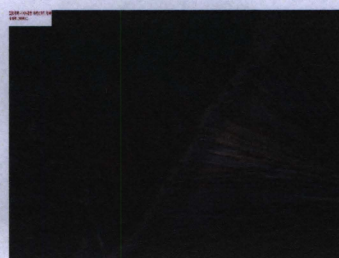


109.0°

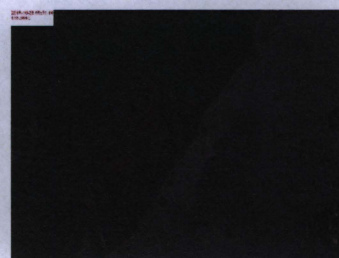
(S)-NO<sub>2</sub>  
(S)-H



93.5°



118.3°



135.4°



(S)-H  
(S)-Br



76.5°



94.9°



123.1°

(S)-H  
(S)-CF<sub>3</sub>



100.9°



120.1°



126.7°

(S)-OMe  
(S)-H



62.2°



78.2°



80.1°

(S)-I  
(S)-H



90.1°



126.4°



132.2°

(R)-Phenyl  
(R)-H



84.0°



107.4°



111.9°

**Fluoride**



(S)-Cl  
(S)-F



65.6°



90.3°

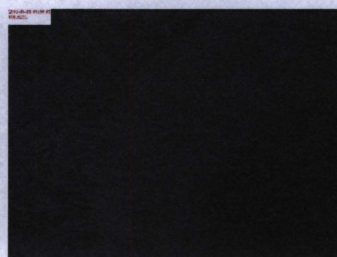


102.9°

(R)-F  
(R)-CN



89.9°



100.5°



102.4°

(S)-Me  
(S)-F



64.4°



87.8°



102.7°

(S)-F  
(S)-NO<sub>2</sub>



72.4°

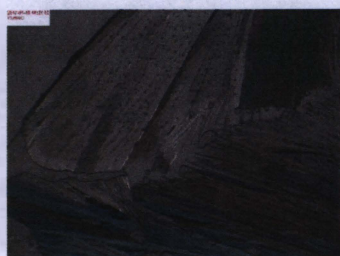


100.3°

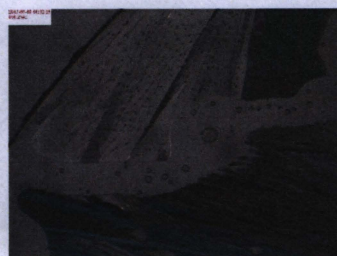


103.2°

(S)-Br  
(S)-F



73.6°



100.2°



103.7°



(S)-F  
(S)-CF<sub>3</sub>



62.4°



97.9°



103.5°

(S)-F  
(S)-OMe



55.1°



75.6°



78.3°

(S)-F  
(S)-I



91.3°



97.7°



103.6°

(R)-Phenyl  
(R)-F



75.9°



88.2°



102.8°

**Chloride**

(R)-Cl  
(R)-CN



78.5°



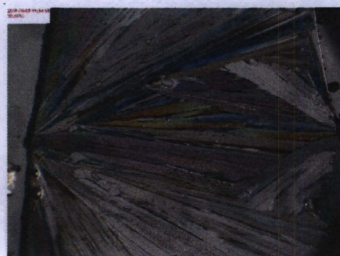
113.7°



119.3°



(S)-Cl  
(S)-Me



99.4°



103.5°



110.9°

(S)-NO<sub>2</sub>  
(S)-Cl



82.2°



122.6°



166.3°

(R)-Cl  
(R)-Br



112.7°



119.3°



121.0°

(S)-CF<sub>3</sub>  
(S)-Cl



110.2°

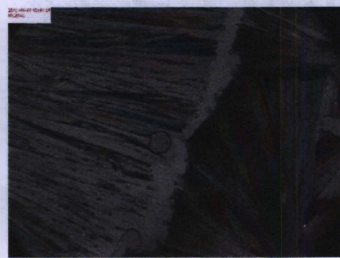


119.8°



122.4°

(S)-OMe  
(S)-Cl



63.3°



78.4°



78.0°



(R)-I  
(R)-Cl



63.4°



94.1°



122.2°

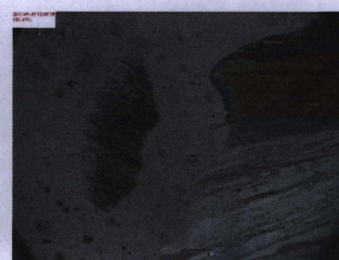
(R)-Phenyl  
(R)-Cl



71.4°



104.2°



112.4°

**Cyano**

(R)-Me  
(R)-CN



86.2°



109.1°

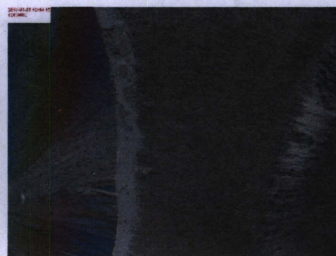


111.3°

(R)-NO<sub>2</sub>  
(R)-CN



66.9°

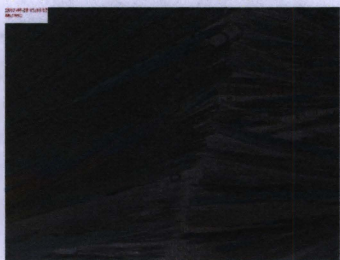


126.1°



136.2°

(R)-Br  
(R)-CN



86.2°



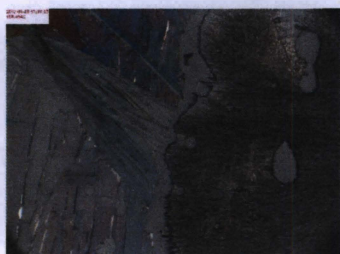
101.8°



122.2°



(R)-CF<sub>3</sub>  
(R)-CN



106.5°



126.2°



134.9°

(R)-OMe  
(R)-CN



54.2°



75.6°

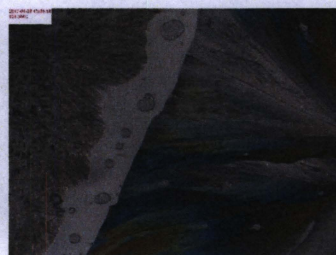


78.1°

(R)-CN  
(R)-I



84.0°



121.4°



135.4°

(R)-Phenyl  
(R)-CN



78.6°



107.3°



111.8°

Methyl

(S)-NO<sub>2</sub>  
(S)-Me



66.9°



104.1°



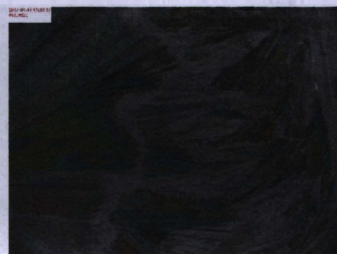
111.0°



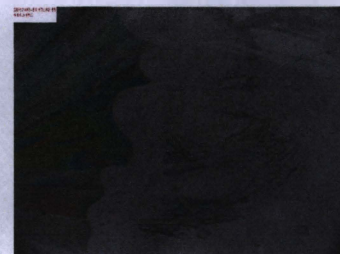
(S)-Br  
(S)-Me



81.3°



103.0°



111.1°

(R)-CF<sub>3</sub>  
(R)-Me



84.6°



100.9°



102.7°

(S)-OMe  
(S)-Methyl



63.5°



77.0°



79.0°

(R)-I  
(R)-Me



60.2°



101.3°



110.5°

(R)-Phenyl  
(R)-Me



84.1°



104.3°



110.7°

Nitro



(S)-NO<sub>2</sub>  
(S)-Br



101.0°



122.0°



169.0°

(S)-NO<sub>2</sub>  
(S)-CF<sub>3</sub>



101.6°



140.3°



143.1°

(S)-NO<sub>2</sub>  
(S)-OMe



47.5°



74.7°



79.0°

(S)-NO<sub>2</sub>  
(S)-I



86.2°



120.8°



137.0°

(R)-NO<sub>2</sub>  
(R)-Phenyl



74.9°



109.7°



112.5°

**Bromide**



(R)-CF<sub>3</sub>  
(R)-Br



93.3°



120.8°



121.8°

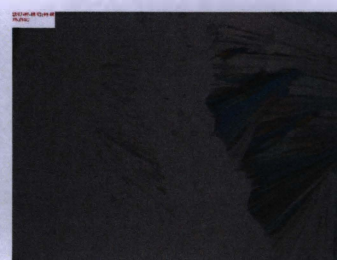
(S)-OMe  
(S)-Br



61.3°

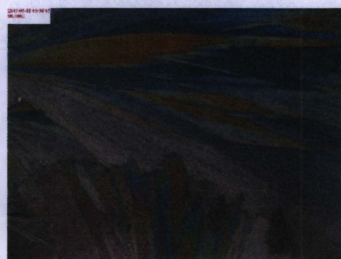


76.1°

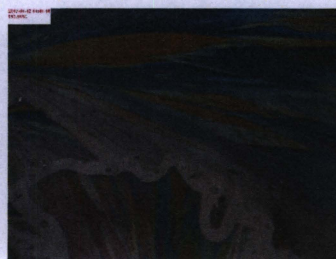


78.7°

(S)-I  
(S)-Br



96.2°



113.5°



121.4°

(S)-Br  
(S)-Phenyl



85.2°



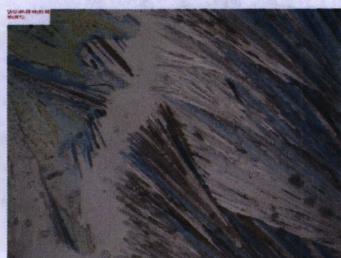
106.6°



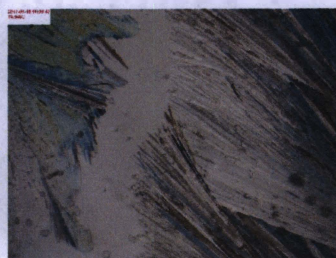
109.6°

**Trifluoromethyl**

(S)-CF<sub>3</sub>  
(S)-OMe



59.1°



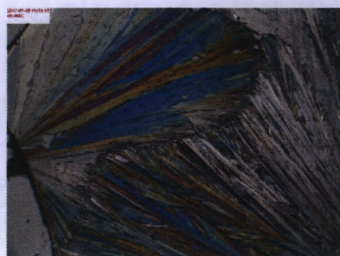
74.5°



77.5°



(S)-I  
(S)-CF<sub>3</sub>



89.5°



119.3°

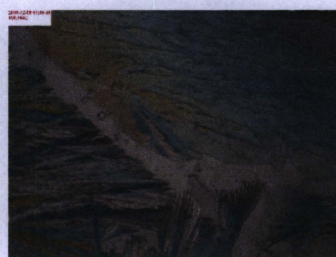


139.3°

(R)-CF<sub>3</sub>  
(R)-Phenyl



69.3°



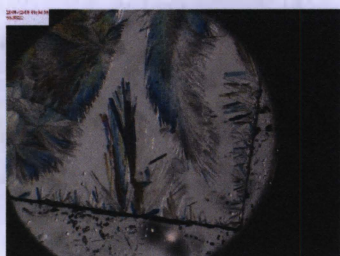
100.2°



111.9°

**Methoxy**

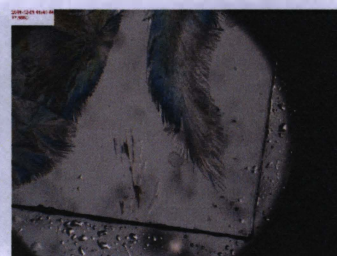
(S)-I  
(S)-OMe



53.8°

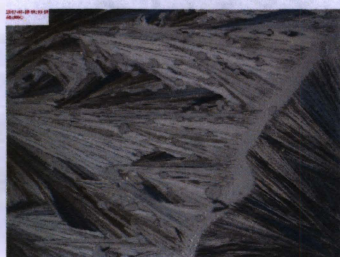


69.9°



77.6°

(R)-OMe  
(R)-Phenyl



46.1°



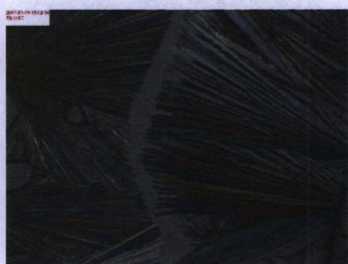
73.1°



78.0°

**Iodide**

(R)-Phenyl  
(R)-I



79.1°



106.5°



111.4°



### S3. X-ray Crystallography - Powder Diffraction

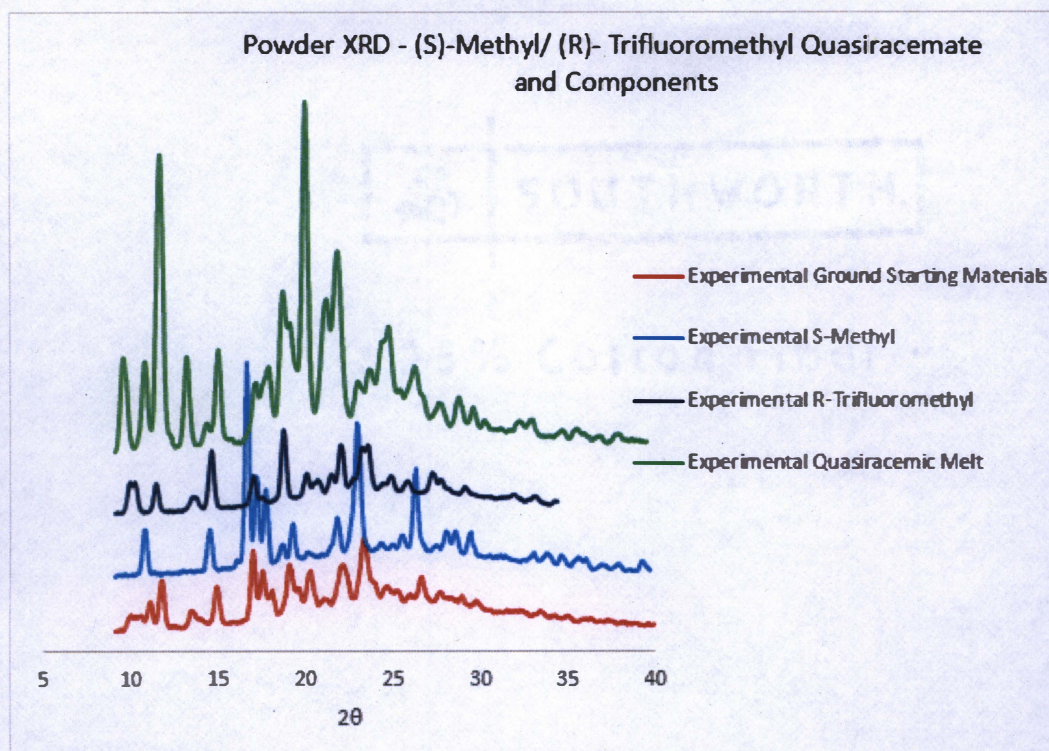


Figure S.19: Powder XRD of (S)-CH<sub>3</sub>/(R)-Br Quasiracetam and Related Components.



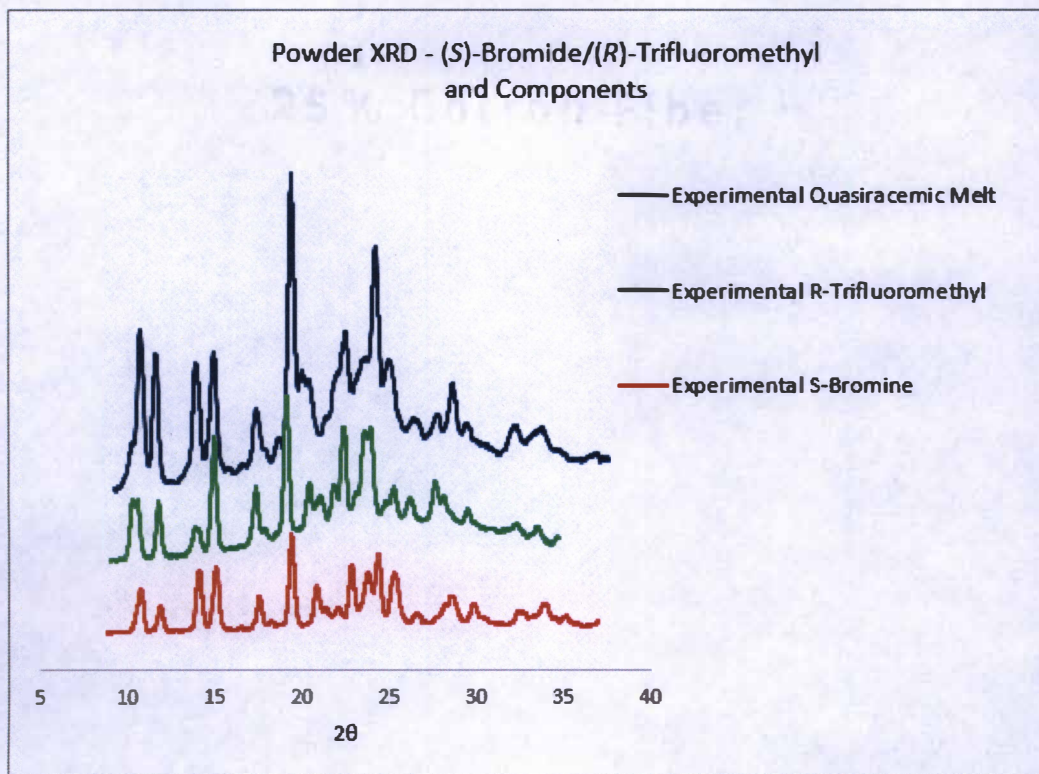


Figure S.20: Powder XRD of (S)-Br/(R)-CF<sub>3</sub> Quasiracemate and Related Components.

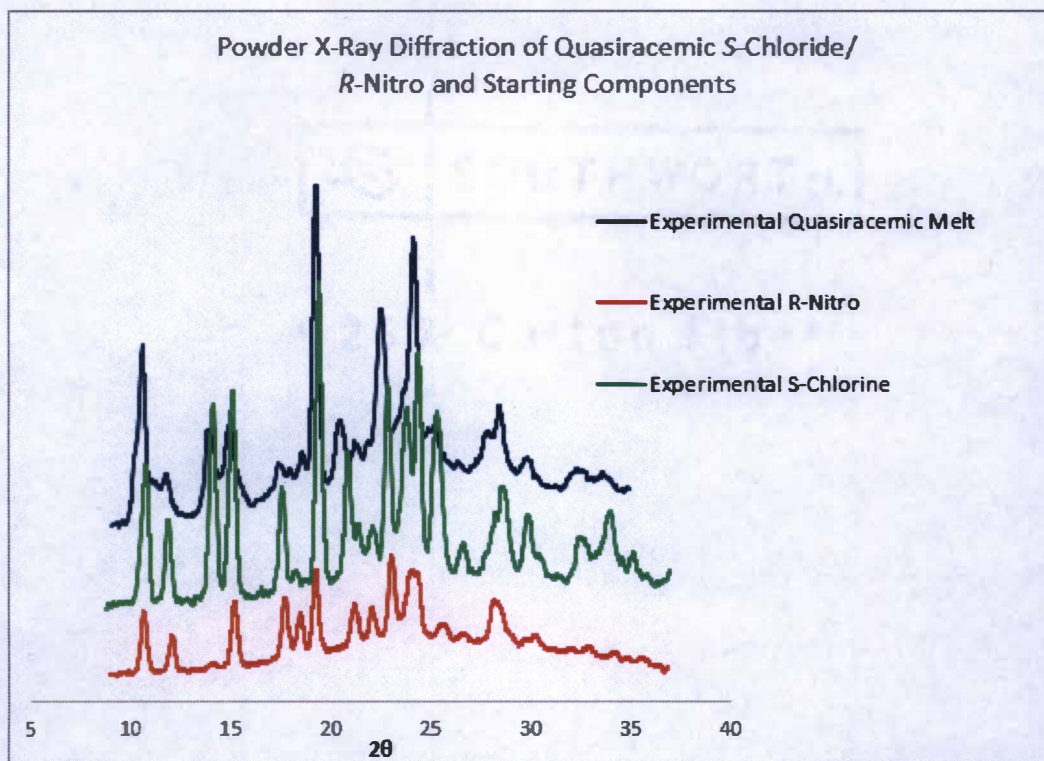


Figure S.21: Powder XRD of (S)-Cl/(R)-NO<sub>2</sub> Quasiracemate and Related Components.



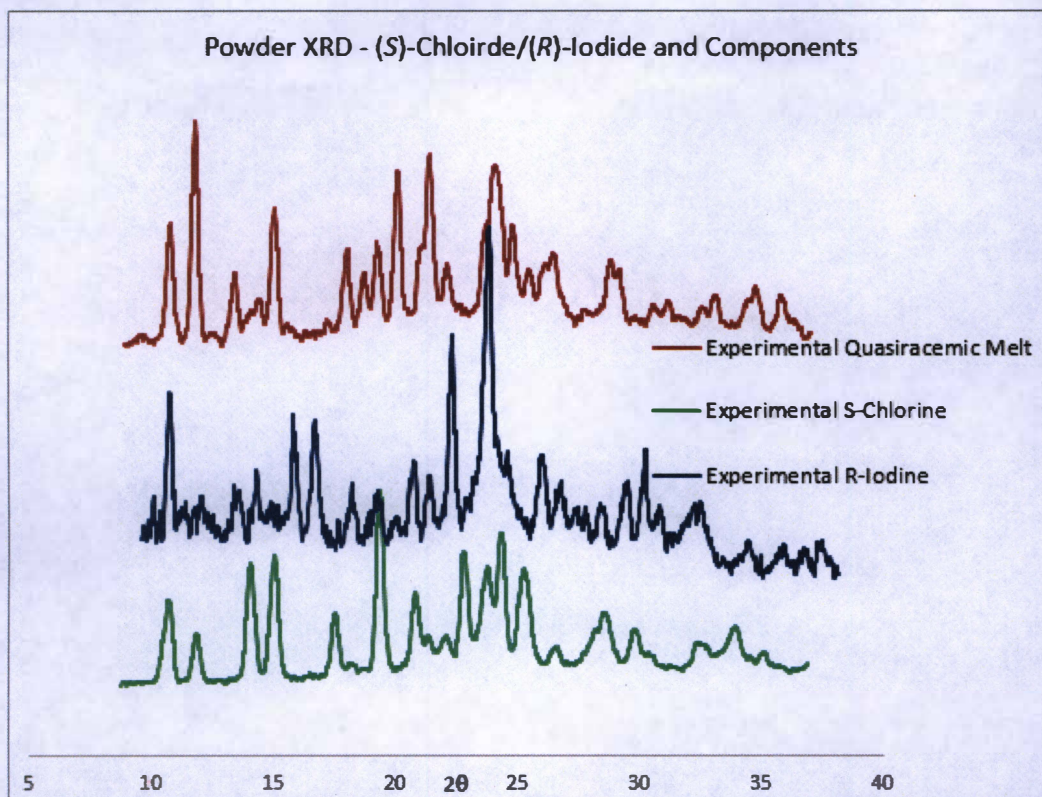


Figure S.22: Powder XRD of (S)-Cl/(R)-I Quasiracemate and Related Components.

303 SOUTH WORTH

25% CARBON FIBER



#### S4. Single Crystal X-ray Diffraction

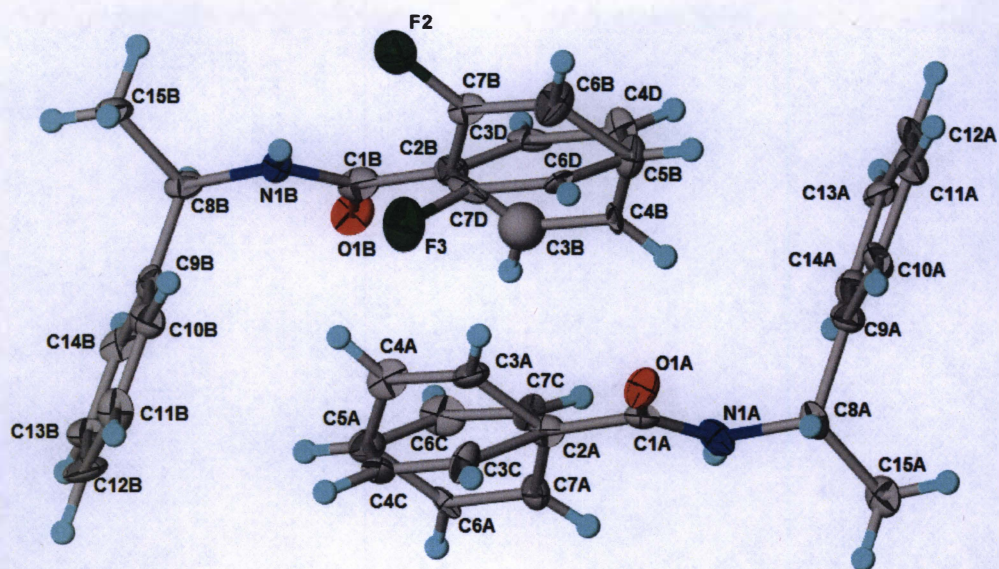


Figure S.23: Crystal Structure of *N*-(2-Fluoro)/*N*-2-(benzoyl)methylbenzylamine Quasiracemate Showing Thermal Parameters (50% Thermal Ellipsoids).

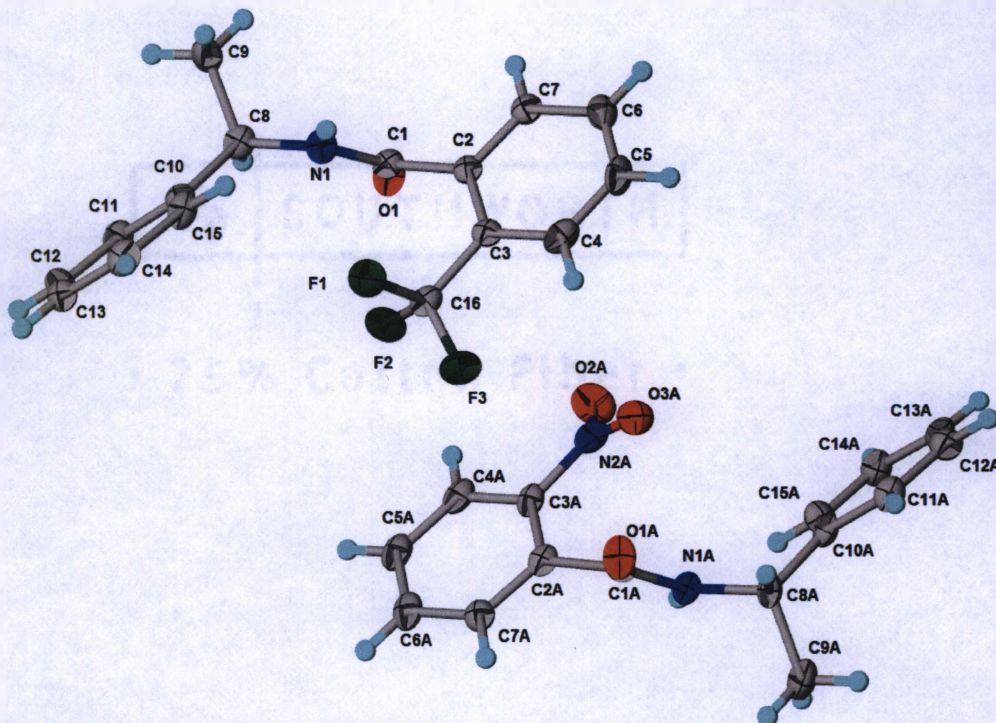


Figure S.24: Crystal Structure of *N*-(2-Trifluoro)/*N*-2-(Nitrobenzoyl)methylbenzylamine Quasiracemate Showing Thermal Parameters (50% Thermal Ellipsoids).



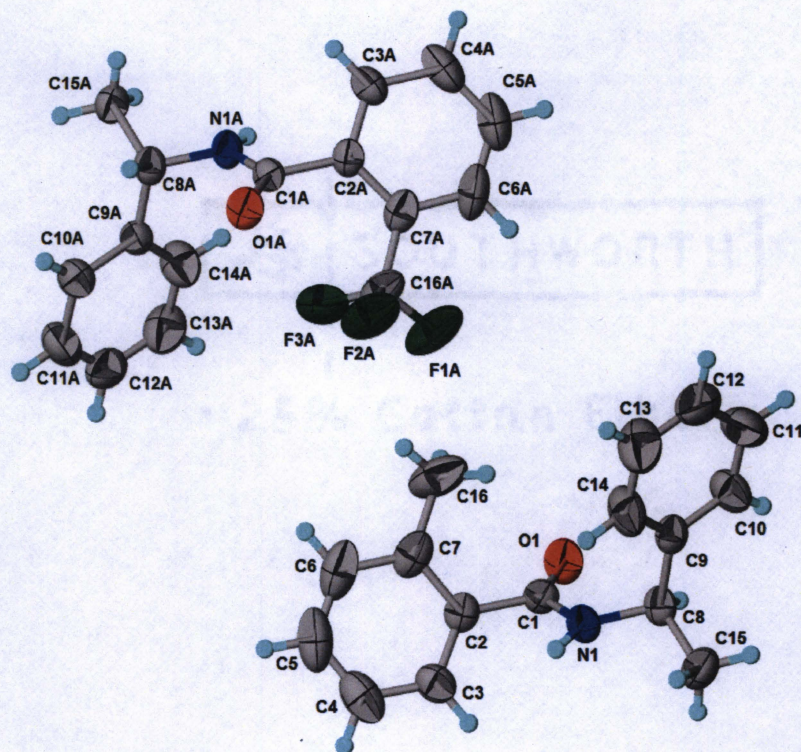


Figure S.25: Crystal Structure of *N*-(2-Trifluoro)/*N*-2-(Methylbenzoyl)methylbenzylamine Quasiracemate Showing Thermal Parameters (50% Thermal Ellipsoids).

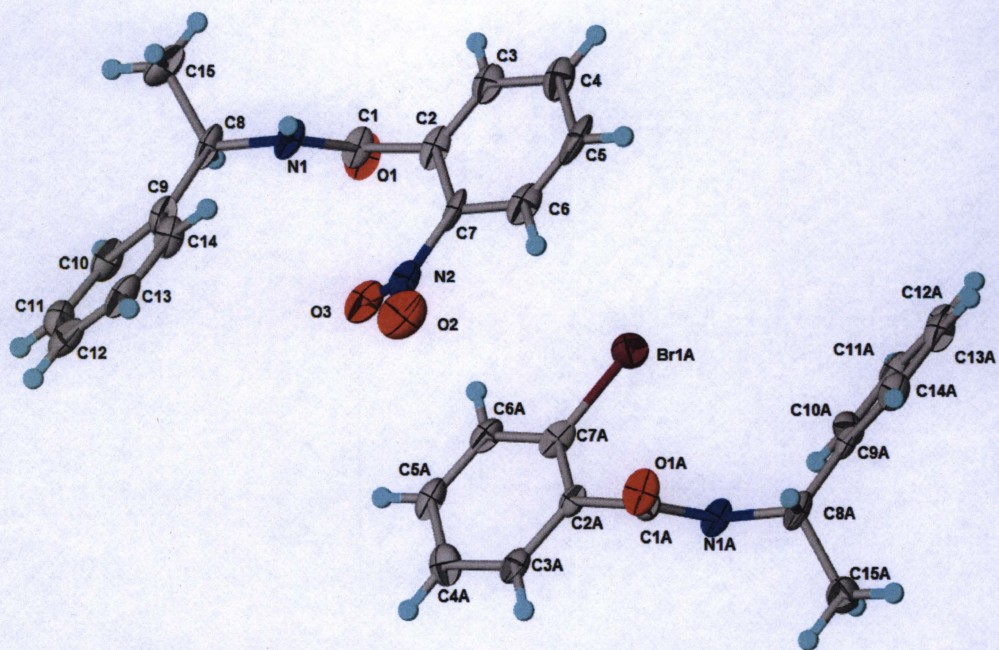
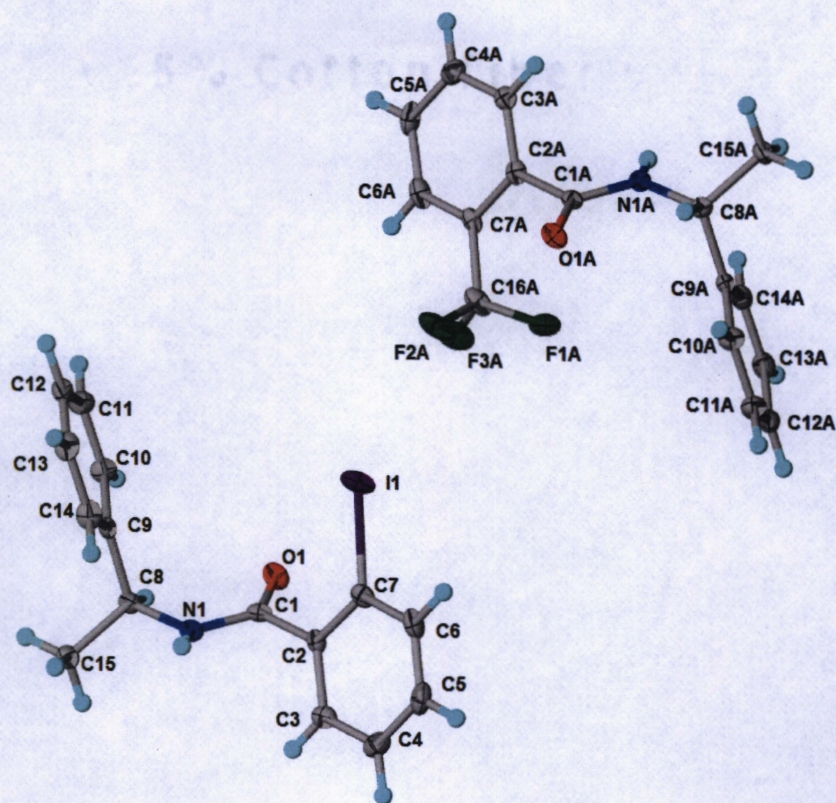


Figure S.26: Crystal Structure of *N*-(2-Nitro)/*N*-2-(Bromobenzoyl)methylbenzylamine Quasiracemate Showing Thermal Parameters (50% Thermal Ellipsoids).





*Figure S.27: Crystal Structure of N-(2-Trifluoro)/N-2-(Iodobenzoyl)methylbenzylamine Quasiracemate Showing Thermal Parameters (50% Thermal Ellipsoids).*

Table S3: Crystallographic data for diarylamide quasiracemates.

	(R)-Cl/(S)Br <sup>1</sup>	(±)-Br <sup>1</sup>	(S)-H/(R)-F	(S)-NO <sub>2</sub> /(R)-CF <sub>3</sub>
<b>Crystal data</b>				
CCDC deposit no.	LUNQIU	LUNQEQ	1534590	1534591
Empirical formula	C <sub>30</sub> H <sub>28</sub> BrClN <sub>2</sub> O <sub>2</sub>	C <sub>15</sub> H <sub>14</sub> NOBr	C <sub>30</sub> H <sub>14</sub> FN <sub>2</sub> O <sub>2</sub>	C <sub>31</sub> H <sub>28</sub> F <sub>3</sub> N <sub>3</sub> O <sub>3</sub>
Crystal System, space group	Monoclinic <i>P2</i> <sub>1</sub> (no. 4)	Orthorhombic <i>Pbca</i> (no. 61)	Triclinic <i>P1</i> (no. 1)	Monoclinic <i>P2</i> <sub>1</sub> (no. 4)
<i>M</i> <sub>r</sub>	563.90	304.18	468.55	563.56
<i>a</i> , Å	8.7790(8)	9.4207(7)	5.3540(2)	8.3035(14)
<i>b</i> , Å	17.699(2)	16.361(1)	8.3824(4)	9.6853(13)
<i>c</i> , Å	9.4652(9)	18.348(2)	13.8585(7)	17.333(3)
$\alpha$ , deg	90	90	96.477(3)	90
$\beta$ , deg	108.391(8)	90	93.829(3)	101.057(9)
$\gamma$ , deg	90	90	105.841(3)	90
<i>V</i> , (Å <sup>3</sup> )	1395.6(2)	2828.0(4)	591.42(5)	1368.0(4)
<i>Z</i> , <i>Z'</i>	2, 1	8, 1	1, 1	2, 1
<i>D</i> <sub>calc</sub> (g cm <sup>-3</sup> )			1.316	1.368
$\mu$ (mm <sup>-1</sup> ), rad. type			0.705, Cu <i>K</i> $\alpha$	0.882, Cu <i>K</i> $\alpha$
<i>F</i> <sub>000</sub>			248	588
temp (K)			100(2)	100(2)
Crystal form, color			plate, colorless	plate, colorless
Crystal size, mm			0.39 x 0.07 x 0.07	0.26 x 0.01 x 0.03
<b>Data collection</b>				
Diffractometer			Bruker Apex II	Bruker Apex II
<i>T</i> <sub>min</sub> / <i>T</i> <sub>max</sub>			0.653/0.753	0.591/0.753
No. of refls. (meas., uniq., and obs.)			13271/3785/2730	20018/4899/3797
<i>R</i> <sub>int</sub>			0.0760	0.0992
$\vartheta$ <sub>max</sub> (°)			68.25	68.22
<b>Refinement</b>				
<i>R</i> / <i>R</i> <sup>2</sup> <sub><math>\omega</math></sub> (obs data)			0.0668/0.1661	0.0616/0.1599
<i>R</i> / <i>R</i> <sup>2</sup> <sub><math>\omega</math></sub> (all data)			0.0946/0.1886	0.0787/0.1708
<i>S</i>			1.045	1.061
No. of refls.			3785	4899
No. of parameters			406	380
$\Delta\rho$ <sub>max/min</sub> (e·Å <sup>-3</sup> )			0.638/-0.204	0.341/-0.350
<i>flack</i>			-0.1(4)	0.23(15)



Table S3: Crystallographic data for diarylamide quasiracemates. (Continued)

	(R)-CH <sub>3</sub> /(S)-CF <sub>3</sub>	(R)-NO <sub>2</sub> /(S)-Br	(R)-CF <sub>3</sub> /(S)-I	(S)-OMe
<b>Crystal data</b>				
CCDC deposit no.	1534592	1534593	1534594	1534589
Empirical formula	C <sub>32</sub> H <sub>31</sub> F <sub>3</sub> N <sub>2</sub> O <sub>2</sub>	C <sub>30</sub> H <sub>28</sub> BrN <sub>3</sub> O <sub>4</sub>	C <sub>31</sub> H <sub>28</sub> F <sub>3</sub> IN <sub>2</sub> O <sub>2</sub>	C <sub>16</sub> H <sub>17</sub> NO <sub>2</sub>
Crystal System, space group	Monoclinic P2 <sub>1</sub> (no. 4)	Monoclinic P2 <sub>1</sub> (no. 4)	Orthorhombic P2 <sub>1</sub> 2 <sub>1</sub> 2 <sub>1</sub> (no. 19)	Orthorhombic P2 <sub>1</sub> 2 <sub>1</sub> 2 <sub>1</sub> (no. 19)
<i>M<sub>r</sub></i>	532.59	574.46	644.45	255.30
<i>a</i> , Å	8.7183(13)	8.2953(5)	9.4943(2)	5.8757(10)
<i>b</i> , Å	18.007(2)	9.5761(5)	16.1705(4)	14.464(2)
<i>c</i> , Å	9.5051(11)	17.2423(9)	18.3454(5)	15.887(3)
<i>α</i> , deg	90	90	90	90
<i>β</i> , deg	106.811(8)	101.342(3)	90	90
<i>γ</i> , deg	90	90	90	90
<i>V</i> , (Å <sup>3</sup> )	1428.4(3)	1342.92(13)	2816.52(12)	1350.2(4)
<i>Z</i> , <i>Z'</i>	2, 1	2, 1	4, 1	4, 1
<i>D<sub>calc</sub></i> (g cm <sup>-3</sup> )	1.572	1.421	1.520	1.256
<i>μ</i> (mm <sup>-1</sup> ), rad. type	0.748, Cu <i>Kα</i>	2.420, Cu <i>Kα</i>	9.367, Cu <i>Kα</i>	0.661, Cu <i>Kα</i>
<i>F<sub>000</sub></i>	560	592	1296	544
temp (K)	100(2)	100(2)	100(2)	100(2)
Crystal form, color	plate, colorless	plate, colorless	plate, colorless	block, colorless
Crystal size, mm	0.44 x 0.17 x 0.10	0.15 x 0.11 x 0.03	0.15 x 0.15 x 0.10	0.31 x 0.15 x 0.06
<b>Data collection</b>				
Diffractometer	Bruker Apex II	Bruker Apex II	Bruker Apex II	Bruker Apex II
<i>T<sub>min</sub></i> / <i>T<sub>max</sub></i>	0.591/0.753	0.587/0.753	0.532/0.753	0.669/0.753
No. of refls. (meas., uniq., and obs.)	20723/5088/3596	20609/4825/3810	43195/5159/4723	5676/2162/1911
<i>R<sub>int</sub></i>	0.0734	0.1097	0.0765	0.0381
<i>θ<sub>max</sub></i> (°)	68.20	68.25	68.23	68.22
<b>Refinement</b>				
<i>R</i> / <i>R</i> <sup>2</sup> <sub>ω</sub> (obs data)	0.0515/0.1446	0.0737/0.1536	0.0277/0.0582	0.0371/0.0852
<i>R</i> / <i>R</i> <sup>2</sup> <sub>ω</sub> (all data)	0.0712/0.1662	0.0967/0.1652	0.0328/0.0612	0.0435/0.0893
<i>S</i>	1.073	1.088	1.004	1.060
No. of refls.	5088	4825	5159	2162
No. of parameters	363	351	362	178
<i>Δρ<sub>max/min</sub></i> (e·Å <sup>-3</sup> )	0.157/-0.172	1.047/-0.821	0.624/-0.507	0.172/-0.161
<i>flack</i>	0.0(2)	0.10(2)	-0.005(3)	0.0(2)



Table S4: Hydrogen Bond Parameters for Diarylamide Quasiracemate Structures.

Compound	D-H...A	D-H (Å)	H...A (Å)	D...A (Å)	D-H...A (°)
(S)-H/(R)-H	N1A-H1A...O1A <sup>i</sup>	0.87(3)	2.33(3)	3.143(6)	156(5)
	N1B-H1B...O1B <sup>ii</sup>	0.87(3)	2.32(3)	3.122(7)	154(5)
(S)-NO <sub>2</sub> /(R)-CF <sub>3</sub>	N1-H1...O1 <sup>iii</sup>	0.86(3)	2.02(3)	2.870(6)	170(9)
	N1A-H1A...O1A <sup>iv</sup>	0.86(3)	2.02(3)	2.855(6)	164(6)
(R)-CH <sub>3</sub> /(S)-CF <sub>3</sub>	N1A-H1A...O1 <sup>v</sup>	0.85(2)	2.08(3)	2.911(5)	164(4)
	N1-H1...O1A <sup>vi</sup>	0.87(2)	2.11(3)	2.923(5)	156(5)
(R)-NO <sub>2</sub> /(S)-Br	N1-H1...O1 <sup>vii</sup>	0.85(3)	1.97(4)	2.802(11)	166(12)
	N1A-H1A...O1A <sup>viii</sup>	0.84(2)	2.06(3)	2.871(11)	164(10)
(R)-CF <sub>3</sub> /(S)-I	N1-H1...O1A <sup>v</sup>	0.82(3)	2.15(3)	2.946(5)	163(5)
	N1A-H1A...O1 <sup>ii</sup>	0.84(2)	2.13(3)	2.948(5)	164(4)
(S)-OMe	N1-H1...O2 <sup>v</sup>	0.883(19)	1.94(2)	2.669(3)	139(3)

Symmetry codes: (i)  $x-1, y, z$ ; (ii)  $x+1, y, z$ ; (iii)  $-x, y-0.5, -z$ ; (iv)  $-x+1, y+0.5, -z+1$ ; (v)  $x, y, z$ ; (vi)  $x, y, z-1$ ; (vii)  $-x+1, y-0.5, -z$ ; (viii)  $2-x, 0.5+y, 1-z$

## S5. $^1\text{H}$ NMR Overlays

(*S*)-Cl/(*R*)-Br Quasiracemate

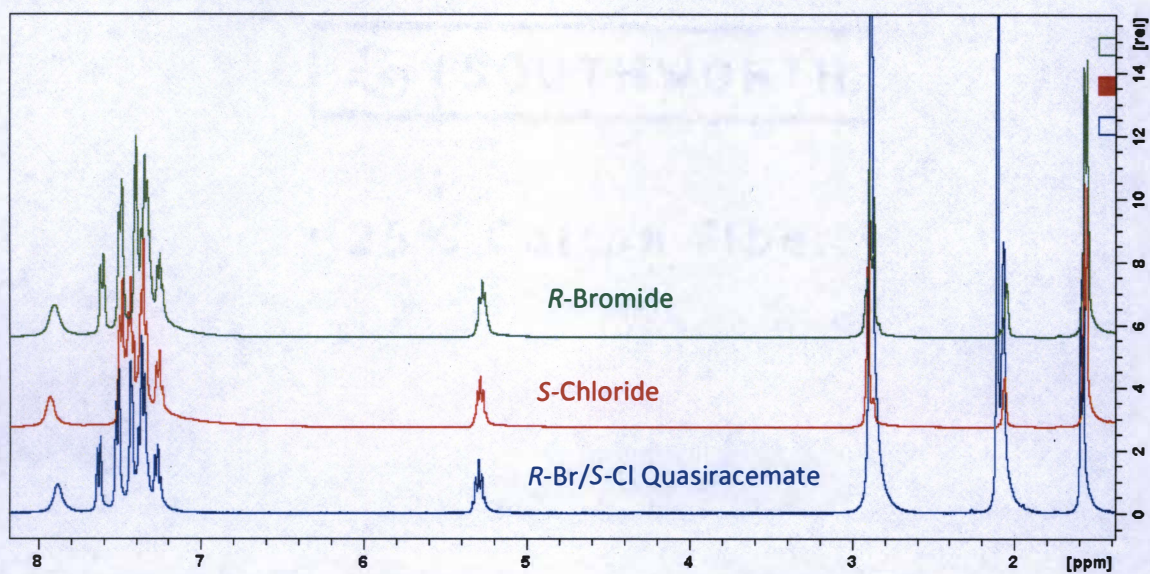


Figure S.28:  $^1\text{H}$  NMR Overlays of the *S*-Cl/*R*-Br Quasiracemate System.

(*S*)- $\text{NO}_2$ /(*R*)- $\text{CF}_3$  Quasiracemate

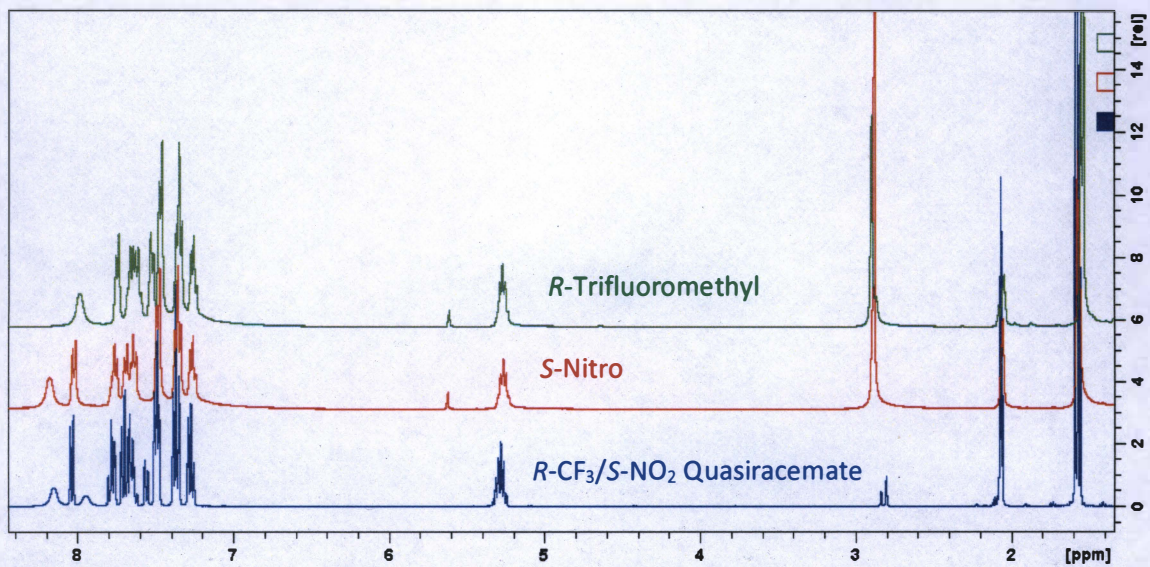


Figure S.29:  $^1\text{H}$  NMR Overlays of the *S*- $\text{NO}_2$ /*R*- $\text{CF}_3$  Quasiracemate System.



(S)-Br/(R)-CF<sub>3</sub> Quasiracemate

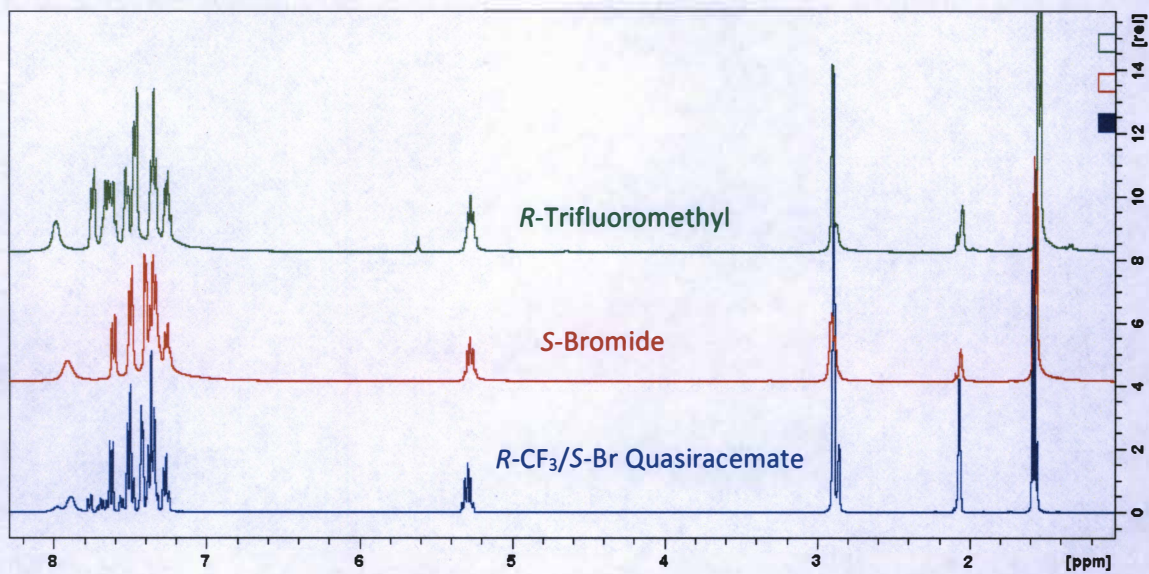


Figure S.30: <sup>1</sup>H NMR Overlays of the S-Br/R-CF<sub>3</sub> Quasiracemate System.

(S)-Cl/(R)-I Quasiracemate

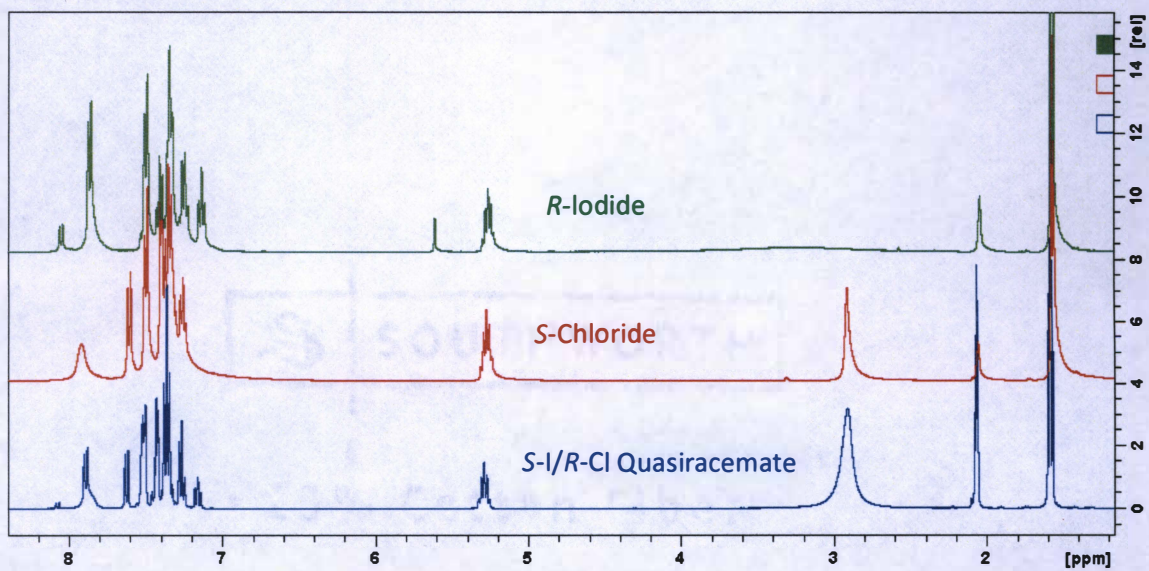


Figure S.31: <sup>1</sup>H NMR Overlays of the S-Cl/R-I Quasiracemate System.

## S6 – Functional Group and Chemical Framework Volume and Surface Area Comparisons

Functional group volume and surface area approximations were taken from previously reported values.<sup>1,2</sup> The following table provides percent increases of the volume and surface areas corresponding to both functional group and the 2-substituted diarylamide molecular frameworks.

### Volume Comparisons

Table S5: Functional Group Volume Comparison

Group Volume (Å <sup>3</sup> )												
5.9	H											
7.8	F	32.2										
19.6	Cl	232.2	151.3									
21.0	CN	255.9	169.2	7.1								
23.3	CH <sub>3</sub>	294.9	198.7	18.9	11.0							
23.2	NO <sub>2</sub>	293.2	197.4	18.4	10.5	-0.4						
27.6	Br	367.8	253.8	40.8	31.4	18.5	19.0					
28.9	CF <sub>3</sub>	389.8	270.5	47.4	37.6	24.0	24.6	4.7				
32.6	OCH <sub>3</sub>	452.5	317.9	66.3	55.2	39.9	40.5	18.1	12.8			
34.6	I	486.4	343.6	76.5	64.8	48.5	49.1	25.4	19.7	6.1		
82.9	C <sub>6</sub> H <sub>5</sub>	1305.1	962.8	323.0	294.8	255.8	257.3	200.4	186.9	154.3	139.6	
		H	F	Cl	CN	CH <sub>3</sub>	NO <sub>2</sub>	Br	CF <sub>3</sub>	OCH <sub>3</sub>	I	C <sub>6</sub> H <sub>5</sub>

Table S6: Diarylamide Molecular Volume Comparison

Diarylamide Molecular Volume (Å <sup>3</sup> )												
221.9	H											
223.8	F	0.9										
235.6	Cl	6.2	5.3									
237.0	CN	6.8	5.9	0.6								
239.3	CH <sub>3</sub>	7.8	6.9	1.6	1.0							
239.2	NO <sub>2</sub>	7.8	6.9	1.5	0.9	0.0						
243.6	Br	9.8	8.8	3.4	2.8	1.8	1.8					
244.9	CF <sub>3</sub>	10.4	9.4	3.9	3.3	2.3	2.4	0.5				
248.6	OCH <sub>3</sub>	12.0	11.1	5.5	4.9	3.9	3.9	2.1	1.5			
250.6	I	12.9	12.0	6.4	5.7	4.7	4.8	2.9	2.3	0.8		
298.9	C <sub>6</sub> H <sub>5</sub>	34.7	33.6	26.9	26.1	24.9	25.0	22.7	22.0	20.2	19.3	
		H	F	Cl	CN	CH <sub>3</sub>	NO <sub>2</sub>	Br	CF <sub>3</sub>	OCH <sub>3</sub>	I	C <sub>6</sub> H <sub>5</sub>

## Surface Area Comparisons

Table S7: Functional Group Surface Area Comparison

Group Surface Areas ( $\text{\AA}^2$ )											
6.8	H										
12.1	F	77.9									
29.0	Cl	326.5	139.7								
32.2	CN	373.5	166.1	11.0							
33.4	CH <sub>3</sub>	391.2	176.0	15.2	3.7						
37.0	NO <sub>2</sub>	444.1	205.8	27.6	14.9	10.8					
37.1	Br	445.6	206.6	27.9	15.2	11.1	0.3				
37.3	CF <sub>3</sub>	448.5	208.3	28.6	15.8	11.7	0.8	0.5			
40.1	OCH <sub>3</sub>	489.7	231.4	38.3	24.5	20.1	8.4	8.1	7.5		
45.0	I	561.8	271.9	55.2	39.8	34.7	21.6	21.3	20.6	12.2	
94.9	C <sub>6</sub> H <sub>5</sub>	1295.6	684.3	227.2	194.7	184.1	156.5	155.8	154.4	136.7	110.9
	H	F	Cl	CN	CH <sub>3</sub>	NO <sub>2</sub>	Br	CF <sub>3</sub>	OCH <sub>3</sub>	I	C <sub>6</sub> H <sub>5</sub>

Table S8: Diarylamide Surface Area Comparison

Diarylamide Molecular Surface Areas ( $\text{\AA}^3$ )											
302.8	H										
308.1	F	1.8									
325.0	Cl	7.3	5.5								
328.2	CN	8.4	6.5	1.0							
329.4	CH <sub>3</sub>	8.8	6.9	1.4	0.4						
333.0	NO <sub>2</sub>	10.0	8.1	2.5	1.5	1.1					
333.1	Br	10.0	8.1	2.5	1.5	1.1	0.0				
333.3	CF <sub>3</sub>	10.1	8.2	2.6	1.6	1.2	0.1	0.1			
336.1	OCH <sub>3</sub>	11.0	9.1	3.4	2.4	2.0	0.9	0.9	0.8		
341.0	I	12.6	10.7	4.9	3.9	3.5	2.4	2.4	2.3	1.5	
390.9	C <sub>6</sub> H <sub>5</sub>	29.1	26.9	20.3	19.1	18.7	17.4	17.4	17.3	16.3	14.6
	H	F	Cl	CN	CH <sub>3</sub>	NO <sub>2</sub>	Br	CF <sub>3</sub>	OCH <sub>3</sub>	I	C <sub>6</sub> H <sub>5</sub>



## S.7 References

- (1) Gavezzotti, A. *J. Am. Chem. Soc.* **1983**, *105* (16), 5220–5225.
- (2) Gavezzotti, A. *J. Am. Chem. Soc.* **1985**, *107* (4), 962–967.